

Analysis of Proteins Involved in Chlorophyll Catabolism:
The impact of Chlorophyllase and Water Soluble Chlorophyll Protein on
the reduction of undesirable pigments in crop plants

DISSERTATION

zur Erlangung des akademischen Grades
doctor rerum naturalis
(Dr. rer. nat.)
im Fach Biologie

eingereicht an der
Mathematisch-Naturwissenschaftlichen Fakultät I
der Humboldt-Universität zu Berlin

von
Master of Genetics, Sridevi Damaraju

Präsident der Humboldt-Universität zu Berlin
Prof. Dr. Dr. h.c. Christoph Marksches

Dekan der Mathematisch Naturwissenschaftliche Fakultät I
Prof. Dr. Lutz-Helmut Schön

Gutachter
Prof. Dr. Bernhard Grimm
PD. Dr. Heiko Lockstein
PD. Dr. Kurt Zoglauer

Tag der mündlichen Prüfung: 11- June-2010

TABLE OF CONTENTS

ABBREVIATIONS	1
ZUSAMMENFASSUNG	3
ABSTRACT	5
 1 INTRODUCTION	 7
1.1 Chlorophyll – the Green Power	7
1.2 Green seed problem	8
1.3 Minimising the Green Seed problem	9
1.4 Chlorophyll catabolism	10
1.4.1 Chlorophyllase	13
1.4.1.1 Localization of Chlase in the chloroplasts	13
1.4.1.2 Enzymatic kinetics of Chlase	14
1.4.1.3 Molecular properties of the genes encoding Chlase in different plant species	18
1.4.1.4 Post translational regulation of Chlase expression and activity	24
1.4.1.5 Functional roles of Chlase in plants	24
1.4.2 Significance of others enzymes in Chl catabolism	24
1.4.3 Water Soluble Chlorophyll Protein (WSCP)	26
1.4.3.1 Classification of WSCPs	26
1.4.3.1.1 Class I WSCPs	26
1.4.3.1.2 Class II WSCPs	27
1.4.3.2 Molecular and functional aspects of WSCPs	28
1.4.3.3 Pigment binding and photoprotective function of WSCPs	30
1.4.3.4 Functions of WSCPs in plant system	34
 2 AIM	 35
 3 MATERIALS	 37
3.1 Plasmid DNA	37
3.2 Oligonucleotides	37
3.3 Organisms	37
3.4 Antibodies	37
3.5 Chemicals and material	38
3.6 Equipments	39
3.7 Glass and Plastic ware	39
3.8 Kits, Substances, Enzymes and Buffers	39
3.9 Solutions and buffers	40
 4 METHODS	 46
4.1 Reverse transcription	46
4.2 Polymerase chain reaction	46
4.3 Overexpression of Chlase in <i>E. coli</i>	46
4.4 Protein purification and antibody production	47
4.5 Agarose gel electrophoresis	47
4.6 SDS-PAGE analysis	48
4.7 Western blot Analysis	48
4.8 <i>In vitro</i> enzyme activity assays	48
4.8.1 Extraction of Chl for enzyme assays	49
4.8.2 Conversion of Chl to Phe	49
4.8.3 Enzyme assays of Chlase	50

4.8.4	Coupled assays with Chlase and WSCP	53
4.9	Production and analysis of transgenic tobacco plants	53
4.9.1	Propagation of sterile tobacco plants	53
4.9.2	Transformation of tobacco plants	54
4.10	Plant growth and treatment regimes	55
4.11	Analysis of transgenic tobacco plants	55
4.11.1	Genomic DNA isolation from plants	55
4.11.2	Initial screening of plants by PCR	56
4.11.3	Total RNA isolation from plants	56
4.11.4	Radioactive labelling of probes	56
4.11.5	Southern blot analysis	57
4.11.6	Northern blot analysis	57
4.11.7	Protein extraction from plants	58
4.11.7.1	From Chlase overexpressor plants	58
4.11.7.2	From WSCP overexpressor plants	58
4.11.8	Selection of Chlase overexpressor plants based on the functional activity of protein <i>in vitro</i>	59
4.11.9	Isolation and fractionation of chloroplasts from Chlase overexpressor plants	59
4.11.10	Experiments on Chlase overexpressor plants	60
4.11.11	Experiments on WSCP overexpressor plants	60
4.11.12	Analysis of pigments from transgenic tobacco plants	61
4.11.12.1	Estimation of steady state levels of Chl and Chlide <i>a</i>	61
4.11.12.2	NCC extraction and quantification	62
4.11.12.3	Determination of Pchlde Content	62
4.11.12.4	Determination Chl catabolite levels in Chlase overexpressor plants due to <i>in vitro</i> activity of recombinant CcChlase	62
4.11.13	Determination of ALA-synthesizing capacity	63
4.11.14	Chl fluorescence experiments of WSCP overexpressor plants	63
4.11.15	Estimation of peroxidase activity in WSCP overexpressor plants	64
4.11.16	Statistical analysis	65
5	RESULTS	66
5.1	Chlorophyllase	66
5.1.1	<i>CcCHLASE</i> (Chlase gene from <i>Citrus clementii</i>) as transgene	66
5.1.2	Purification of His-CcChlase for production of antiserum against Chlase	66
5.1.3	<i>In vitro</i> enzyme activity assays of recombinant His-CcChlase protein	68
5.1.3.1	Enzymatic activity of His-CcChlase protein	69
5.1.3.2	Optimization of temperature and pH for His-CcChlase activity	72
5.1.3.3	Effect of reaction time on enzyme activity of His-CcChlase	73
5.1.3.4	Effect of acetone concentration on His-CcChlase activity	74
5.1.3.5	Effect of substrate concentration on His-CcChlase activity	75
5.1.3.6	Effect of protein concentration on His-CcChlase activity	75
5.1.3.7	Substrate specificity of His-CcChlase	76
5.1.3.8	Effect of phytol concentration on His-CcChlase activity	78
5.1.3.9	His-CcChlase activity on thylakoid membranes	79
5.1.3.10	Effect of various metal ions on His-CcChlase activity	79
5.1.3.11	Effect of reagents that modify the functional groups on His-CcChlase activity	80
5.1.3.12	Effect of oil concentration on His-CcChlase activity	81

5.1.3.13	Optimization of different extraction solutions in the oil assays for maximal Chlide recovery.....	81
5.1.3.14	Activity of His-CcChlase on Pheophytin as substrate.....	83
5.1.3.15	Activity of His-CcChlase on Chl in oils at different stages of oil refining	84
5.1.4	Tobacco as a model for development of transgenic plants.....	85
5.1.5	Production and preliminary analysis of transgenic tobacco plants overexpressing <i>CcCHLASE</i>	85
5.1.6	Estimation of copy number of <i>CcCHLASE</i> in Chlase overexpressor lines	89
5.1.7	Analysis of T1 generation of transgenic plants overexpressing <i>CcCHLASE</i> ..	89
5.1.7.1	Transcript levels of <i>CcCHLASE</i> in the Chlase overexpressor plants	90
5.1.7.2	CcChlase activity is resided in the membrane fraction of chloroplasts.....	91
5.1.7.3	CcChlase activity from the leaves of various developmental stages demonstrated by <i>in vitro</i> activity assays.....	92
5.1.7.4	Accumulation of higher amounts of Chl catabolites in Chlase overexpressor plants during 80% acetone extraction method	94
5.1.7.5	Steady state levels of green coloured pigments and NCC contents in T1 generation of Chlase overexpressor lines.....	95
5.1.7.6	ALA synthesising capacity of Chlase overexpressor plants.....	108
5.2	Water Soluble Chlorophyll Protein (WSCP).....	109
5.2.1	Cloning, characterization and expression of WSCP in <i>E. coli</i>	109
5.2.2	<i>In vitro</i> assays to test the function of WSCP	111
5.2.3	Production of transgenic tobacco plants overexpressing <i>Cau-WSCP-35</i>	112
5.2.4	Selection of WSCP overexpressor candidate lines.....	113
5.2.5	Estimation of copy number of <i>WSCP</i> transgene in WSCP overexpressor lines.....	114
5.2.6	Analysis of T1 generation of WSCP overexpressor plants	115
5.2.6.1	Functional role of <i>Cau-WSCP-35</i> during Chl degradation seen as leaf senescence	115
5.2.6.2	Measurements of Chl precursors like Pchlide in WSCP overexpressor plants	119
5.2.6.3	Expression levels of WSCP protein during drought stress.....	122
5.2.6.4	Determination of phototolerance mechanism in WSCP overexpressor plants.....	123
6	DISCUSSION.....	134
6.1	Choice of <i>Citrus Chlase</i> as transgene.....	134
6.1.1	<i>CcCHLASE</i> was expressed as His-CcChlase and used for antibody production.....	134
6.1.2	Enhanced <i>in vitro</i> Chl hydrolysis by His-CcChlase proved its Chlase activity	135
6.1.2.1	His-CcChlase exhibits an optimal activity at 40°C and pH 8.0	137
6.1.2.2	Effect of incubation time on His-CcChlase activity	138
6.1.2.3	Increased acetone concentration minimises the His-CcChlase activity ..	139
6.1.2.4	Substrate – Enzyme interaction	139
6.1.2.5	Effect of enzyme concentration on His-CcChlase activity.....	140
6.1.2.6	Specificity of His-CcChlase towards Chl <i>a</i> and Chl <i>b</i>	141
6.1.2.7	Inhibitory effect of Phytol on His-CcChlase activity	142
6.1.2.8	His-CcChlase activity on thylakoid membranes clarifies how Chl was stabilized in thylakoid membranes	142
6.1.2.9	Inactivation of His-CcChlase by metal ions	143

6.1.2.10	Functional groups involved	144
6.1.2.11	Increase in oil concentration leads to reduced His-CcChlase activity.....	144
6.1.2.12	Selection of different extraction solutions other than acetone to recover more Chlide during oil processing	145
6.1.2.13	His-CcChlase also hydrolyses Phe	147
6.1.2.14	His-CcChlase activity in oils during different phases of oil processing..	147
6.1.3	Need for transgenic rapeseed plants with increased <i>CcCHLASE</i> expression	148
6.1.4	Overexpression of <i>CcCHLASE</i> in tobacco did not impart phenotypic and morphological differences to the plants.....	149
6.1.5	PCR and <i>in vitro</i> enzyme activity measurements confirmed the presence of <i>CcCHLASE</i> transgene in the Chlase overexpressor plants.....	150
6.1.6	Southern blot confirmed the stable integration of <i>CcCHLASE</i> transgene in the Chlase overexpressor plants	151
6.1.7	Characterization of T1 generation of Chlase overexpressor plants.....	152
6.1.7.1	Northern blot analysis confirmed the presence of <i>CcCHLASE</i> transcripts in the overexpressor lines	152
6.1.7.2	CcChlase activity was retained in the membrane fraction of chloroplasts.....	153
6.1.7.3	Young leaves of the Chlase overexpressor lines retained higher <i>in vitro</i> CcChlase activity	153
6.1.7.4	Recombinant CcChlase protein remains active in 80% acetone seen as higher amounts of Chl catabolites in the leaf pigment extracts	155
6.1.7.5	Absolute acetone minimised the <i>in vitro</i> production of Chlide <i>a</i>	156
6.1.7.6	Steady state levels of Chl and Chlide <i>a</i> and NCC contents in Chlase overexpressor lines during senescence	156
6.1.7.7	Chlase overexpressor plants did not show any differences in ALA synthesizing capacity	164
6.2	Importance of WSCP in plant metabolism.....	164
6.2.1	<i>Cau-WSCP</i> as transgene	165
6.2.2	Isolation and expression of WSCP from cauliflower	165
6.2.3	WSCP did not aid in enhanced Chlase mediated Chl hydrolysis <i>in vitro</i>	166
6.2.4	WSCP overexpressor plants did not show any phenotypical differences with respect to WT tobacco	166
6.2.5	Presence of <i>Cau-WSCP-35</i> in WSCP overexpressor plants was confirmed by PCR and western blot	167
6.2.6	Copy number of <i>Cau-WSCP-35</i> transgene in WSCP overexpressor plants..	168
6.2.7	Presence of recombinant <i>Cau-WSCP</i> did not enhance the Chl breakdown pathway <i>in vivo</i>	168
6.2.8	WSCP acts as a repository for Chl precursors <i>in vivo</i>	169
6.2.9	WSCP: A stress induced protein in plants.....	170
6.2.10	Photoprotective function of recombinant <i>Cau-WSCP-35</i> protein.....	171
7	CONCLUSIONS	177
7.1	Chlorophyllase.....	177
7.2	Water Soluble Chlorophyll Protein	178
8	REFERENCES	179

LIST OF FIGURES

Fig. 1: Structure of Chl <i>a</i> molecule.....	7
Fig. 2: Green seeds.....	9
Fig. 3: Schematic representation of Chl degradation pathway occurring in senescent chloroplasts.....	11
Fig. 4: Detailed reaction mechanism of the Chl degradation pathway	11
Fig. 5: Alignment of aa sequences of Chlases isolated from different plant sources	21
Fig. 6: Alignment of all known aa sequences of WSCPs and drought and salt stress induced proteins from various plant sources	30
Fig. 7: Overall structure of tetrameric WSCP-Chl complex and Chl-binding cavity	32
Fig. 8: Schematic representation of measurements of Chl fluorescence	64
Fig. 9: SDS-PAGE and western blot analysis of recombinant and purified His-CcChlase	67
Fig. 10: SDS-PAGE and western blot analysis of recombinant and purified His-CcChlase along with total protein extract from <i>Citrus</i> and tobacco leaves ...	68
Fig. 11: Recombinant His-CcChlase activity demonstrated by phase separation assay	69
Fig. 12: Enzyme assays of Chlase performed with different cellular fractions of <i>E. coli</i> containing His-CcChlase	70
Fig. 13: Enzyme assays of His-CcChlase performed with crude soluble fractions of <i>E. coli</i> , purified His-CcChlase and bacterial soluble fractions containing empty pQE80 vector.....	71
Fig. 14: Effect of pH on stability and activity of His-CcChlase.....	73
Fig. 15: Effect of increased acetone concentration on His-CcChlase activity.....	74
Fig. 16: Effect of increased substrate concentration on hydrolytic activity of His-CcChlase.....	75
Fig. 17: Effect of enzyme concentration on His-CcChlase activity.	76
Fig. 18: Substrate specificity of His-CcChlase on Chl <i>a</i>	77
Fig. 19: Substrate specificity of His-CcChlase on Chl <i>b</i>	78
Fig. 20: Effect of phytol on hydrolytic activity of His-CcChlase.....	78
Fig. 21: His-CcChlase activity with varied concentrations of Chl in thylakoid membranes.....	79
Fig. 22: Changes in specific activities of His-CcChlase based on oil concentration.....	81
Fig. 23: Extraction capacity of hexan/acetone mixture to retain Chlide formed in the reaction	82
Fig. 24: Extraction of Chlide in a buffer-ethanol system at different pH	83
Fig. 25: Activity of His-CcChlase demonstrated in oils at various stages of refining	84
Fig. 26: Phenotypic representation of Chlase overexpressor lines compared to WT tobacco plants	86
Fig. 27: Agarose gel electrophoresis of PCR amplification of the <i>CcCHLASE</i> transgene of Chlase overexpressor lines	87
Fig. 28: Southern blot analysis of genomic DNAs isolated from Chlase overexpressor and WT tobacco plants	89
Fig. 29: Gel electrophoresis of total RNA samples and northern blot analysis of transcript levels of <i>CcCHLASE</i> from WT and Chlase overexpressor plants.	90
Fig. 30: Gel electrophoresis of total RNA samples and northern blot analysis of transcript levels of <i>NtCHLASE</i> from WT and Chlase overexpressor plants	91
Fig. 31: Enzymatic activity of CcChlase from young, mature and senescent leaf samples of plants grown under normal growth conditions and plants incubated in dark chamber for 5 days	93
Fig. 32: Amounts of Chls, Chlide <i>a</i> and Pheide <i>a</i> from both WT and Chlase overexpressor lines during extraction of pigments in 80% acetone	95

Fig. 33: Steady state levels of Chl and Chlide <i>a</i> from both WT and Chlase overexpressor plants	97
Fig. 34: Chlide <i>a</i> /Chl ratios from leaf samples of WT and Chlase overexpressor plants...	98
Fig. 35: Analysis of NCCs from leaves of different developmental stages of normally grown WT and Chlase overexpressor lines	98
Fig. 36: Analysis of NCCs from leaves of different developmental stages from dark incubated WT and Chlase overexpressor lines.....	101
Fig. 37: ALA synthesising capacity measured in young and mature leaves from WT and Chlase overexpressor plants.	109
Fig. 38: Sequence homology of truncated protein sequence of WSCP plasmid clones 49 and 35 with reference <i>Cau-WSCP</i> protein	110
Fig. 39: SDS-PAGE and western blot analysis of recombinant and purified MBP-WSCP	111
Fig. 40: Coupled assays performed using recombinant His-CcChlase and WSCP proteins with Chl	112
Fig. 41: Phenotypic representation of WSCP overexpressor plants compared to WT tobacco plants	113
Fig. 42: Agarose gel electrophoresis of PCR amplified fragments of <i>Cau-WSCP-35</i> transgene of WSCP overexpressor lines	114
Fig. 43: Western blot analysis of total soluble protein fractions from WT and WSCP overexpressor lines	114
Fig. 44: Southern blot of genomic DNAs isolated from the WSCP overexpressor and WT tobacco plants.....	115
Fig. 45: Western blot analysis of young, mature and senescent leaf samples of the WSCP overexpressor lines	116
Fig. 46: Western blot of total soluble protein extracts containing recombinant <i>Cau-WSCP-35</i> from all leaves of line 40	116
Fig. 47: Western blot analysis of native WSCP protein from cauliflower leaves	117
Fig. 48: Steady state levels of Chls analysed from leaf pigment extracts of different age groups from WT and WSCP overexpressor lines.....	118
Fig. 49: Chl and Chlide <i>a</i> amounts analyzed from pigment extracts of leaf material of different age groups of WT and WSCP overexpressor lines.....	119
Fig. 50: Pchlide levels estimated in WT tobacco and WSCP overexpressor lines during the course of ALA feeding experiments	120
Fig. 51: Amounts of Pchlide in etiolated seedlings of WT and WSCP overexpressor lines	121
Fig. 52: Protein expression pattern of <i>POR</i> (protochlorophyllide oxidoreductase) and <i>Cau-WSCP-35</i> in etiolated seedlings of WT tobacco and WSCP overexpressor plants	121
Fig. 53: Western blot analysis of soluble protein extracts of drought stressed leaf samples from WT tobacco and WSCP overexpressor lines	122
Fig. 54: SDS-PAGE analysis of protein extracts of leaf samples from leaves exposed to drought stress from WT tobacco and the WSCP overexpressor lines.....	122
Fig. 55: Determination of xanthophyll cycle pigment levels from WT and WSCP overexpressor plants	124
Fig. 56: Xanthophyll cycle pigments from both WT and WSCP overexpressor leaves exposed to different light intensities	126
Fig. 57: Estimation of free peroxide radicals formed due to <i>in vitro</i> peroxidase activity in WT and WSCP overexpressor leaves on exposure to high light intensities ...	128
Fig. 58: Estimation of free peroxide radicals generated <i>in vivo</i> in WT and WSCP overexpressor plants	129

Fig. 59: Chl fluorescence measurements with WT and WSCP overexpressor plants - short-term light stress.....	131
Fig. 60: Chl fluorescence measurements with WT and WSCP overexpressor plants - long-term light stress.....	133

LIST OF TABLES

Table 1: Molecular characteristics of the Chlase genes identified so far from different plant species.	23
Table 2: Classification and properties of WSCPs.	33
Table 3: List of conditions and parameters chosen to study the functional activity of recombinant His-CcChlase protein <i>in vitro</i>	52
Table 4: Growth conditions adapted for regeneration of transgenic plants	55
Table 5: List of various experiments done with WT and Chlase overexpressor plants	60
Table 6: Experimental design to analyze the <i>in vivo</i> functional activity of overexpressed Cau-WSCP-35 protein in WSCP overexpressor plants	61
Table 7: Effect of reaction time on His-CcChlase-catalysed hydrolytic activity on Chl..	74
Table 8: Extent of Chl hydrolysis as a result of increased protein concentration	76
Table 9: Metal ion effect on hydrolytic activity of His-CcChlase	80
Table 10: Effects of application of various functional group modifying reagents on the hydrolytic activity of His-CcChlase.....	80
Table 11: Chlide extraction using water-linoleate mixture.....	82
Table 12: Hydrolytic activity of His-CcChlase on Phe and Chl as substrates	84
Table 13: Specific activities of Chlase protein isolated from both WT and Chlase overexpressor lines.....	88
Table 14: Enzyme activity of recombinant CcChlase protein present in chloroplastic fractions of leaves from Chlase overexpressor and WT tobacco plants	92
Table 15: Steady state levels of Chl and Chlide isolated from leaf material harvested from control, normal incubated and dark incubated leaves from both WT and Chlase overexpressor lines for 5 days	100
Table 16: Steady state levels of Chls and Chlide <i>a</i> (from WT and Chlase overexpressor plants) after induction of senescence by methyl jasmonate and ACC.....	103
Table 17: Amounts of NCCs quantified after senescence inducing experiments using methyl jasmonate and ACC in both WT and Chlase overexpressor plants	104
Table 18: Steady state levels of green coloured pigments from both WT and Chlase overexpressor plants in response to salt stress	105
Table 19: Steady state levels of Chls and Chlide <i>a</i> in WT and Chlase overexpressor plants in response to water deficit.....	106
Table 20: NCCs amounts after stress experiments (drought and salt) in WT and Chlase overexpressor plants.....	108

ABBREVIATIONS

aa	amino acid
ATP	adenosine triphosphate
APS	ammonium persulfate
ALA	amino levulinic acid
<i>A. tumefaciens</i>	<i>Agrobacterium tumefaciens</i>
BAP	6-Benzylaminopurine or benzyl adenine
BSA	Bovine serum albumin
β-ME	β-mercaptoethanol
cDNA	complementary DNA
CaMV	Cauliflower mosaic virus
Chlase	Chlorophyllase
Chl	Chlorophyll
Chlide <i>a</i>	Chlorophyllide <i>a</i>
DAB	3, 3'-Diaminobenzidine
DEPC	Diethyl pyrocarbonate
DNA	Deoxyribonucleic acid
DNase	Deoxyribonuclease
dH ₂ O	distilled water
DMSO	Dimethyl sulfoxide
dNTP	Deoxyribonucleotide triphosphates
DTT	Dithiothreitol
EDTA	Ethylenediaminetetraacetic acid
<i>E. coli</i>	<i>Escherichia coli</i>
EtBr	Ethidium bromide
FCC	fluorescent Chl catabolites
gFW	gram fresh weight
g	Gram
h	Hours
HPLC	High performance liquid chromatography
IAE	Iodoacetamide
IPTG	Isopropylthiogalactoside
Kbp	kilobase pairs
kDa	kilodaltons
L	Litre
mg	milli gram
μg	micro gram
μl	micro litre
μmol	micromol
min	Minutes
M	Molar
MOPS	3-(N-morpholino)propanesulfonic acid
MS	Murashige and Skoog basal medium
mRNA	messenger RNA

nmol	Nanomol
NAA	Naphthalene acetic acid
NCC	non-fluorescent colourless Chl catabolites
NEM	N-ethylmaleimide
<i>N. tabacum</i>	<i>Nicotiana tabacum</i>
N ₂	Nitrogen
O/N	overnight
O.D.	optical density
PAO	Phaeophorbide a oxygenase
PCR	polymerase chain reaction
Pchl _{ide}	Protochlorophyllide
Pheide a	Phaeophorbide a
Phe	Pheophytin
PMSF	Phenylmethanesulfonyl fluoride
POR	NADPH:protochlorophyllide oxidoreductase
PVPP	Polyvinyl polypyrrolidone
q _N	non-photochemical quenching of Chl fluorescence
RNA	Ribonucleic acid
RNase	Ribonuclease
RT	room temperature
RTase	reverse transcriptase
RCCR	red chlorophyll catabolite reductase
rpm	rotations per minute
ROS	reactive oxygen species
s	seconds
SD	Standard deviation
SDS	sodium dodecyl sulfate
SDS-PAGE	sodium dodecyl sulfate-polyacrylamide gel electrophoresis
SE	Standard error
TEMED	N, N, N', N'-tetramethyl ethylene diamine
TLC	Thin-layer chromatography
Tris	Tris(hydroxymethyl)aminomethane
TX-100	Triton X-100
x g	Gravitational force
WT	wild type

ZUSAMMENFASSUNG

Die vorliegende Doktorarbeit enthält Untersuchungen ausgewählter Aspekte des Chlorophyllabbauweges mit dem Ziel, das “Green seed problem” in *Brassica napus* (Raps) einzudämmen. Im Mittelpunkt der Arbeit stehen bestimmte Aspekte der Regulierung des Chlorophyllstoffwechselweges. Es wurden Experimente mit transgenen Tabakpflanzen durchgeführt, die zwei Proteine des Chlorophyllabbauweges überexprimieren, die Chlorophyllase (Chlase) und das wasserlösliche Chlorophyllprotein (WSCP).

Chlase ist das Hauptenzym, welches den Anfangsschritt des Chlorophyllabbaus katalysiert. Es wurde das Chlase Gen aus *Citrus clementii* verwendet. Eine Chlase cDNA Sequenz, welches das reife Protein ohne plastidäres Transitpeptid kodiert, wurde im *E.coli* System als His-markiertes CcChlase Protein exprimiert. Die löslichen Bakterienextrakte, welche His-CcChlase enthalten, wurden auf ihre *in-vitro* Chlase Aktivität bei verschiedenen Substratkonzentrationen, pH-Werten, Ölkonzentrationen und in verschiedenen Puffersystemen untersucht. Darüber hinaus wurde die katalytische Aktivität des rekombinanten Proteins im Rapsöl in verschiedenen Stadien des Raffinerieprozesses untersucht. In allen Aktivitätstests war das rekombinante Protein in der Lage, Chl zu Chlide zu hydrolysieren. Die löslichen Extrakte von Bakterien, die His-CcChlase exprimieren, wurden mittels Ni-NTA Affinitätschromatographie gereinigt. Das aufgereinigte CcChlase Protein wurde auch nach seiner *in-vitro* Aktivität untersucht. Anschließend wurde das Chlase Gen unter Kontrolle des CaMV 35S Promoters mit Hilfe des *Agrobacterium*-vermittelten Gentransfers in Tabakpflanzen eingebracht. Die Analyse von Tabakpflanzen wurde der samenspezifischen Chlase-Expression in Raps auf Grund der einfacheren Anzucht und größerer Erträge von Blattmaterial vorgezogen. Mehr als 95% der erzeugten Chlase-exprimierenden transgenen Linien zeigten höhere Chlase Aktivitäten, was sich durch Akkumulation höherer Katabolitmengen, im Vergleich zu Wildtyp Tabakpflanzen, ausdrückte. Die höhere Chlase Aktivität wurde in den Membranen der Chloroplasten gefunden, die aus den transgenen Pflanzen isoliert wurden. Die funktionale Aktivität der transgenen CcChlase wurde an drei ausgewählten transgenen Linien (T1 Generation) unter verschiedenen Seneszenz- und Stressbedingungen untersucht. Das Enzym war selbst unter ungünstigen Trockenheits- und Salzangelbedingungen katalytisch aktiv. Dies wurde durch das Vorhandensein erhöhter *steady-state* Chlide Gehalte in den transgenen Linien im Vergleich zum Wildtyp bewiesen. Die Anwendung von Seneszenz-induzierenden Wirkstoffen wie Ethylen und Methyljasmonat verstärkten

die Seneszenzerscheinungen in Blättern und führten zu erhöhter Umwandlung von Chl zu Chlase und dadurch höheren *steady-state* Chlide-a Gehalten in den transgenen Linien.

Zusätzlich wurde vorgeschlagen, dass WSCPs eine Rolle in der Blattseneszenz und für Lichtschutzmechanismen spielt. Das WSCP Gen aus Blumenkohl wurde als Transgen ausgewählt. Die Gensequenz von WSCP, die das reife Protein ohne Transitpeptid kodiert, wurde in *E. coli* als Fusionsprotein mit dem Maltose bindenden Protein (MBP) exprimiert. Kombinierte Assays für rekombinante WSCP und His-CcChlase zeigten keine verstärkte *in-vitro* Aktivität von Chlase bei Vorhandensein von WSCP. Transgene Tabakpflanzen, die unter Kontrolle des 35S Promoters das WSCP Gen überexprimieren wurden mit *Agrobacterium*-vermittelter Transformation generiert. Die detaillierte Analyse der Proteinexpression und Pigmentgehalte zeigte, dass die Überexpression von WSCP nicht den Chl Abbauweg *in-vivo* verstärkt. Die Akkumulation höherer Pchlde-Gehalte in WSCP Überexprimierern bestätigte die Rolle von WSCP als Speichermolekül von Chlorophyllvorstufen. Obwohl die WSCP-Überexprimierer keine signifikanten Unterschiede bei der Messung der Chl-Fluoreszenz zeigten, ergaben sich signifikant geringere Zeaxanthin-Gehalte und auch geringere Peroxidase-Aktivitäten selbst unter hohen Lichtintensitäten von 700 - 900 $\mu\text{mol photonen m}^{-2} \text{s}^{-1}$. Diese Ergebnisse bestätigen die Lichtschutzfunktion von WSCP.

Die Ergebnisse der hier präsentierten Arbeit halfen bei der Analyse einiger Aspekte des Chl-Abbauweges und verwandter Prozesse und sind von großer Bedeutung für die Ölsamenindustrie, die Landwirtschaft und den Gartenbau, da dadurch die Steigerung und Verringerung des Chlorophyllabbaus kontrolliert werden kann. Allgemein kann das Verständnis der Kontrolle des Chl-Abbaus helfen, neue und bessere Studien zur Kontrolle des Chl-Abbaus in Samen durchzuführen. Dies würde das Vermeiden von photoreaktiven Verschmutzungen mit Chl-Derivaten erleichtern, was eine Steigerung des ökonomischen Nutzens von biologischen Produkten zur Folge hätte.

Schlagworte: Chlorophyllabbau, Chlorophyllase, Chlorophyllide, WSCP, Xanthophyll, Transgene Tabakpflanzen, Green-seed problem

ABSTRACT

The present doctoral thesis contains investigations of some facets of the chlorophyll (Chl) catabolic pathway with a special intention to curtail the “Green seed problem” in *Brassica napus* (rapeseed). The work focuses on certain aspects of regulation of Chl catabolism. Experiments were performed with transgenic tobacco plants overexpressing two proteins in the Chl degradation pathway viz., the Chlorophyllase (Chlase) and the Water Soluble Chlorophyll Protein (WSCP).

Chlase is the principal enzyme, which catalyses the initial step of the Chl catabolic pathway. The Chlase gene from *Citrus clementii* was chosen as transgene. The Chlase cDNA sequence encoding the protein without transit peptide was expressed in *E. coli* as His-tagged CcChlase protein. The bacterial soluble extracts containing His-CcChlase were analyzed for the functional activity in vitro in the presence of varying substrate concentrations, different pH, different oil concentrations and buffer extraction systems. Furthermore, the recombinant protein was tested for its catalytic activity in rapeseed oil obtained from different stages of oil refinement. In all the functional tests, the recombinant protein was able to efficiently hydrolyse Chl to Chlide. The bacterial soluble extracts containing His-CcChlase were purified using Ni-NTA affinity chromatography and the purified CcChlase protein was also tested for its activity in vitro. Subsequently, the Chlase cDNA sequence (coding for the protein with transit peptide) under the control of a CaMV 35S promoter was introduced into tobacco plants using *Agrobacterium*-mediated transformation. Analysis of tobacco plants was preferred in contrast to seed specific expression of Chlase in rapeseed plants, due to the easy propagation and availability of higher amounts of leaf material from tobacco. More than 95% of the produced Chlase overexpressor lines were found to possess higher activities of Chlase, which was indicated by accumulation of higher amounts of catabolites in comparison to wild type (WT) tobacco plants. Presence of higher Chlase activity was confirmed in the membrane fractions of chloroplasts isolated from the overexpressor plants. The functional activity of the transgene CcCHLASE was analysed by subjecting three selected Chlase overexpressor lines (T1 generation) to various senescence and stress conditions. The enzyme was found to be catalytically active even under adverse conditions of drought and salt stress. This was evident from the presence of increased steady state levels of Chlide a in the overexpressor lines compared to the WT tobacco plants. Application of senescence promoting agents like ethylene and methyl jasmonate enhanced senescence conditions of the leaves leading to

increased accessibility of Chlase to Chl and in turn higher steady state levels of Chlide a in the overexpressor lines.

In addition, WSCP was proposed to play a role in leaf senescence and photoprotective mechanism of plants. The WSCP gene from cauliflower was chosen as transgene. The cDNA sequence of WSCP coding for the protein without transit peptide was expressed in *E. coli* as a fusion protein with maltose binding protein (MBP) tag. Coupled assays of recombinant WSCP and His-CcChlase demonstrated no enhanced in vitro activity of Chlase in the presence of WSCP indicating no active participation of WSCP in Chl breakdown. Transgenic tobacco plants overexpressing WSCP (protein with transit peptide) under the control of 35S promoter were generated using *Agrobacterium*-mediated transformation. Detailed analysis of protein expression and pigment contents concluded that overexpression of WSCP does not enhance the Chl catabolic pathway in vivo. Accumulation of higher levels of Pchlide in WSCP overexpressor plants confirmed the role of WSCP as a storage molecule of Chl precursors. Although, the WSCP overexpressor plants did not show significant differences in Chl fluorescence measurements, they had significantly lower zeaxanthin levels and peroxidase activity even at high light intensities of 700 – 900 $\mu\text{mol photons m}^{-2} \text{ s}^{-1}$. These results confirm a photoprotective function of WSCP.

Results from the present study helped for the analysis of certain aspects of the Chl degradation pathway and related processes, which could be of great use to the oil industry, for agriculture and horticulture by controlling both increase and decrease of Chl breakdown. In general, understanding of the control of Chl breakdown could assist in improved and emerging studies on the control of Chl degradation in seeds. This would further enhance the easy removal of the photoreactive contaminants of Chl derivatives resulting in an increase of the commercial value of biological products.

Keywords: Chlorophyll degradation pathway, Chlorophyllase, Chlorophyllide, WSCP, Xanthophyll, Transgenic Tobacco plants, Green-seed problem

1 INTRODUCTION

1.1 Chlorophyll – the Green Power

Chlorophyll (Chl) is the green coloured photosynthetic pigment found in algae, cyanobacteria and in the leaf tissue of plants. It is the most abundant naturally occurring pigment in the biosphere. Chl belongs to the class of cyclic tetrapyrroles with four interconnected pyrrole rings (chlorine ring) and Mg^{+2} ion in the centre. In turn, the chlorine ring has several side chains along with a long phytol side chain. Various forms of Chl differing in side chains attached to chlorine ring (*viz.*, Chl *a*, Chl *b*, Chl *c* and Chl *d*) exist in nature, of which Chl *a* is the abundant form (Fig. 1).

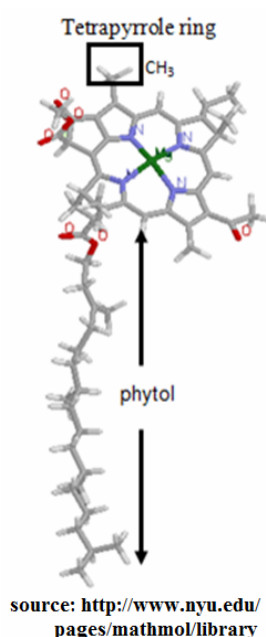


Fig. 1 : Structure of Chl *a* molecule

Chl is central in the light-dependent process of photosynthesis and critical for sustenance of plant life. On the other hand, light-absorbing properties of this pigment could also result in phototoxicity of its anabolic as well as catabolic metabolites. The biosynthesis, accumulation and degradation of Chl are associated with chloroplast development, photomorphogenesis and chloroplast-nuclear signalling (reviewed in Eckhardt et al., 2004). More than one billion tons of Chl are biosynthesized and degraded every year (Matile et al., 1996). Since biosynthesis and breakdown of Chl occur throughout plant development, their coordinated regulation is necessary to prevent any accumulation of intermediate compounds that can potentially damage plant tissue. While Chl anabolism is relatively well studied, Chl catabolism has not been the focus of research until recently.

The natural phenomenon of Chl catabolism (degreening) occurs mostly during leaf senescence, fruit ripening, and seed maturation. In addition, Chl breakdown is also observed during natural turn over of Chl, which is affected by environmental factors such as excess light (Prasil et al., 1992; Andersson and Barber, 1996), extreme temperatures and water storage (Goldschmidt, 2001). While excessive light causes photoinhibition, extreme temperatures cause cell death and both instances witness a dramatic increase in Chl breakdown. Regulation of Chl catabolism in plants has commercial benefits in food and agriculture industry. For example, retardation of Chl breakdown increases shelf life of green leaves and may increase the cereal yield. On contrary, senescence perceived as acceleration of catabolism, enhances ripening of crop products. Likewise, “**Green seed problem**” of rapeseed (*Brassica napus*) that has been a huge commercial problem for oil industry can be dealt through regulation of Chl catabolism. Therefore, the identification of genes associated with Chl breakdown contributes to understanding of function and control of Chl catabolism.

1.2 Green seed problem

B. napus is commonly called as oil rapeseed. The produce of this crop is widely used as animal feed, cooking oil and bio-diesel. The leading producers of this crop are the European Union, Canada, America, Australia, China and India. In Canada, the oil is termed as Canola or LEAR (Canadian oil low acid, Low Erucic Acid Rapeseed). Rapeseed is the crop of choice in winter (September to June) providing good coverage of soil, and limiting nitrogen run-off. Seeds contain more than 40% oil as against 18% for soy oil, which is the second widely used oil crop. Rapeseed oil is one of the nutritionally healthy edible oils containing omega-3 fatty acids and a very low saturated fatty acid content (Sodergreen et al., 2001).

Quality of rapeseed oil depends largely on the time of harvest, seed storage, and protein, lipid and Chl contents. Normally, Chl pigments in the rapeseeds are steadily broken down during maturation giving black seeds, but low temperatures and excess precipitation or early frost could interfere with the ripening of seeds resulting in high proportion of green seeds (Fig. 2a & b) (Johnson-Flanagan et al., 1990; McGregor et al., 1999). Extracted with oil, Chl in green seeds interferes with the subsequent oil processing causing oxidation, rancidity and a reduced shelf life of oil (Levadoux et al., 1987; Kalmokoff et al., 1988; Singh and Chuaqui, 1991). External addition of Chl or Chl breakdown analogues during oil bleaching confirmed the reduced stability of rapeseed oil (Tautorius and Low, 1993;

Rammurthy and Low, 1995). This is mainly due to the photooxidant properties of Chl catabolites. Studies done by Bonham-Smith et al. (2006) using non-lethal freezing stress showed an increased retention of Chl in mature rapeseeds.

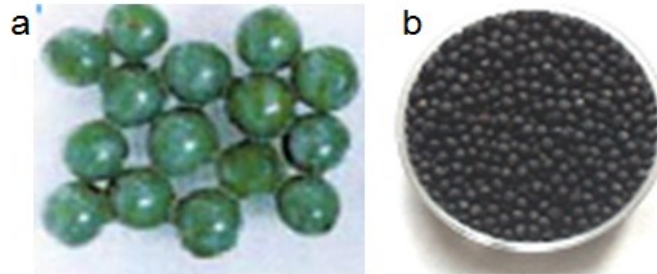


Fig. 2: Green seeds (a) produced by *B. napus* instead of the normal black seed (b) when the plants are exposed to low temperatures and precipitation conditions.

1.3 Minimising the Green Seed problem

Attempts to curtail the economic losses of Green seed problem focussed on improving both at industrial level (oil-processing methods) and at plant level (agricultural produce).

At industrial level

- 1) Enzymatic degradation of Chl during refining (Levadoux et al., 1987; Kalmokoff et al., 1988), but had little success.
- 2) Use of both physical and chemical methods to remove Chl from extracted seed oil such as adsorption technology (Singh and Chuaqui, 1991), which is very expensive.
- 3) Of late, a cost-effective process was developed to remove Chl from canola oil by a bleaching method using mineral acids like H_3PO_4 and H_2SO_4 [reported reduction from 30 ppm to < 0.01 ppm (Bahmaei et al., 2005)].

At plant level

In the absence of germplasm from *Brassica* species with low seed Chl content, plant researchers focussed on generating transgenic plants against conventional breeding techniques.

- 1) Production of genetically modified *B. napus* (canola) plants with *Lhcb*-antisense RNA expression, inhibiting the synthesis of a light-harvesting Chl binding protein of the photosystem II antenna complexes. Studies showed decreased Chl contents in mature seeds and suppression of renewed pigment synthesis following frost (Johnson-Flanagan et al., 1999).

- 2) Generation of transgenic *B. napus* plants with altered Chl synthesis by the expression of an antisense gene against glutamate 1-semialdehyde aminotransferase (GSAAT) (Tsang et al., 2003). This approach showed decreased levels of Chl in ripening seeds. These seeds did not show any effect in the growth and development and were fully viable.

In addition to these, various other studies indicated that genetic approaches through gene alteration techniques appear to alleviate the Green seed problem. It may be surmised that residual Chl content in *Brassica* seeds is due to delayed or faulty Chl catabolism. However, Chl catabolism that ought to have slowed down causing Green seed problem was not studied. Hence development of transgenic plants that overexpress genes in Chl catabolism would give better insight into Green seed problem.

1.4 Chlorophyll catabolism

Chl catabolism occurs in senescent chloroplasts (gerontoplasts). Degradation of Chl occurs at two stages – before (early stage) and after (late stage) cleavage of the tetrapyrrole macrocyclic ring (reviewed in Hörtensteiner, 2006). Normally, early steps are common in all plants, followed by species-specific modifications of Chl breakdown products (reviewed in Takamiya et al., 2000). The breakdown products of early stage are greenish, and those of the late stage are colourless. Finally, ATP-dependent transport systems mediate the transfer of catabolites from gerontoplasts to vacuoles (Fig. 3).

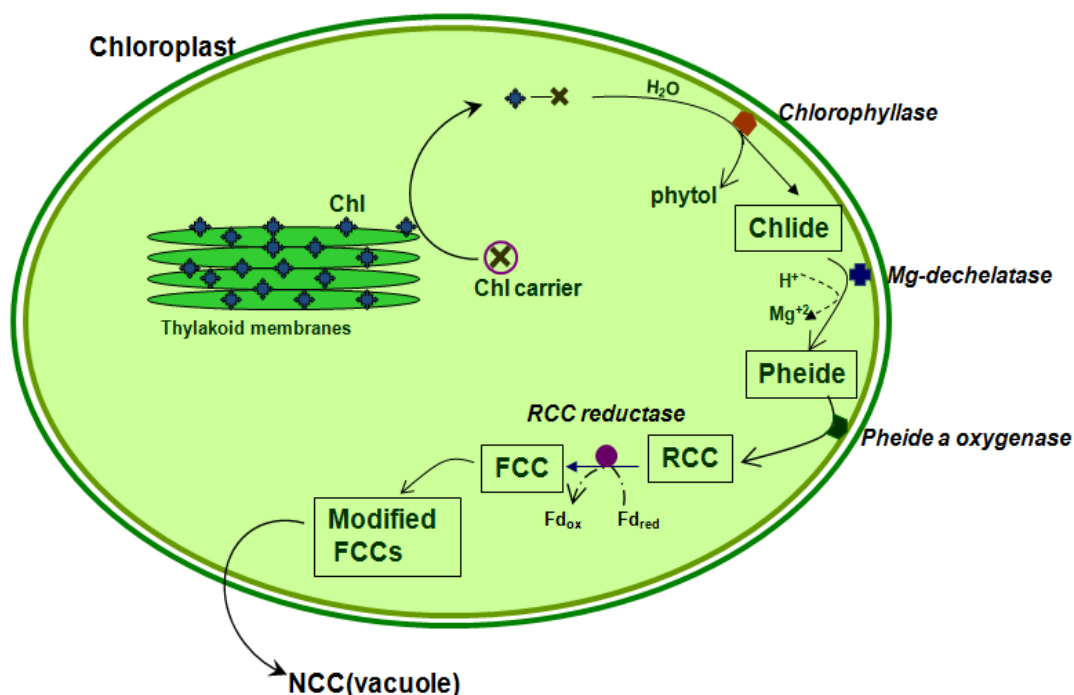


Fig. 3: Schematic representation of Chl degradation pathway occurring in senescent chloroplasts.

Chl breakdown pathway can be classified as Type I and Type II reactions (Brown et al., 1991) (Fig. 4).

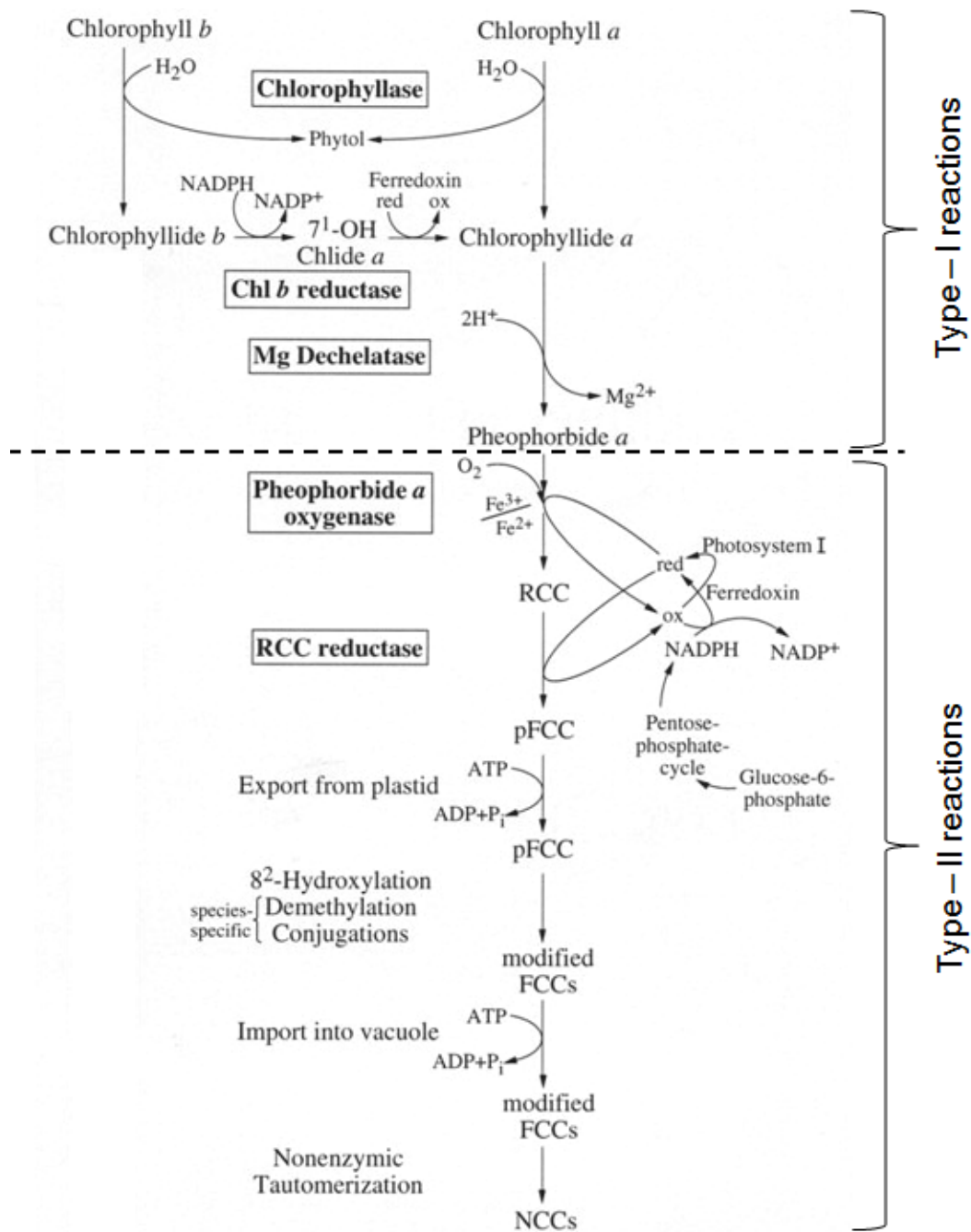


Fig. 4: Detailed reaction mechanism of the Chl degradation pathway showing the enzymes and cofactors involved in each step (Brown et al., 1991).

Type I reactions modify the Chl molecule retaining the macrocyclic conjugation and the products are pigments. The steps involved are

- Dephytylation (removal of phytol residue in the ring IV) of Chl *a* to Chlorophyllide *a* (Chlide *a*) catalysed by the enzyme Chlorophyllase (Chlase),
- Removal of Mg^{+2} from the macrocycle by displacement with 2H^{+} (dechelation) mediated by Mg-dechelating substance and
- Some modifications that are probably specific for plant species resulting in the formation of Pheophorbide (Pheide) *a*.

Type II reactions follow type I reactions, which involve cleavage of the macrocyclic ring, destruction of pigment character and eventual recycling of its elements. The steps involved are

- Cleavage of the Pheide *a* by pheophorbide *a* oxygenase (PAO) to form red Chl catabolite (RCC).
- RCC is converted to primary fluorescent Chl catabolite (pFCC) by the action of red Chl catabolite reductase (RCCR).
- pFCC is further modified to FCC (fluorescent Chl catabolite) and transported into vacuole in the form of non-fluorescent Chl catabolite (NCC).

The later stage is thus essential for degreening of leaf tissue and therefore determines Chl degradation in leaf senescence and fruit ripening.

WSCP aids in transport of Chl?

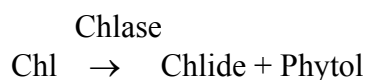
The spatial separation of Chl and Chlase in the chloroplasts necessitates a mediator to remove and transport the Chl molecule to the site of action of Chlase. Water Soluble Chlorophyll Protein (WSCP; denoted as ⊗ in Fig. 3) present in the stromal fraction of the chloroplasts has been attributed to mediate this Chl transport function (Matile et al., 1997; Hörtensteiner, 2004). However, this hypothesis of WSCP as a carrier protein needs experimental validation and may provide a better understanding of Chl catabolism.

While Chl catabolism is a complex process involving series of reactions, we presume that Chlase and WSCP are candidate genes for transgenic studies that could enhance the Chl breakdown.

1.4.1 Chlorophyllase

Chlorophyllase (chlorophyll-chlorophyllido hydrolase, Chlase; EC 3.1.1.14), is the first enzyme in the Chl-degradation pathway (Amir-Shapira et al., 1987; Matile et al., 1999). Chlase exists in ferns, mosses, brown & red algae, diatoms and higher plants. Chlase principally catalyzes hydrolysis of Chl. Depending on the reaction conditions; Chlase may also play a role in esterification and transesterification of Chlide in the presence of primary alcohols (Michalski et al., 1988).

Wilstatter and Stoll (1913) discovered Chlase and proposed that Chl catabolism starts with the removal of phytol side chain from Chl by Chlase. Based on the enzyme kinetics of Chlase in the acetone powders of *Citrus* leaves, the reaction



follows a first order kinetics (Garcia et al., 1980). The conversion of Chl *b* to 7-hydroxymethyl Chl *a* is the primary and obligatory catalytic step of Chl degradation and is mediated by Chl *b* reductase (schematically represented in Fig. 4) (Folly and Engel, 1999; Scheumann et al., 1999).

Activity of Chlase correspond with lower Chl levels in senescing leaves, fruit ripening with ethylene (Kura-Hotta et al., 1987; Trebitsh et al., 1993) and unfavourable environmental conditions like drought stress (Majumdar et al., 1991). Presence of Chlase also in pre-senescent leaves, greened tissues, and during periods of increased Chl synthesis (normal green leaves and developing fruits) suggest a role in Chl turnover and homeostasis (Tanaka et al., 1982; Minguez-Mosquera and Gallardo-Guerrero, 1996). Chlase proteins from different higher and lower plants, algae show significant homology, indicating a common structural feature of hydrolases and esterases.

1.4.1.1 Localization of Chlase in the chloroplasts

Chlase is a hydrophobic protein localised in the envelope membranes of chloroplasts (Brandis et al., 1996; Matile et al., 1997). Chlase under normal conditions is in an inactive form in the membrane and its activity is modulated by membrane environment (Hudak et al., 2005). Senescence-induced changes in the thylakoid organization leads to activation of Chlase in chloroplasts that subsequently breaks down Chl (reviewed in Takamiya et al., 2000). Although some reports speculated about different cellular locations (Terpsta, 1981;

Tsuchiya et al., 1997; review, Takamiya et al., 2000), it is not very likely that Chlase isoforms are located outside plastids.

Localisation of Chlase in plant cells has been successfully demonstrated through gene isolation, cloning and functional assays. Initial studies showed intracellular localisation (plastid type) of Chlase in *Citrus* species (Jacob-Wilk et al., 1999). Recently, fluorescence imaging techniques revealed a specific localisation of Chlase in chloroplast membranes of *Ginkgo biloba* and *Citrus* species (Okazawa et al., 2006; Harpaz-Saad et al., 2007; Shemer et al., 2008). In *Arabidopsis*, Chlase isoforms viz., *AtCLH1* and *AtCLH2* localise in cytosol (Schenk et al., 2007) and plastids (Tsuchiya et al., 1999) respectively. This extra plastidial localisation of *AtCLH1* (cytosolic) was in concordance with the assumption of Takamiya et al. (review, 2000) and points to a novel Chl catabolism pathway in vacuoles, distinct from that in plastids. Further, Schenk et al. (2007) envisaged that there exists alternate Chlases having motifs common to lipases or lipolytic enzymes, rendering these enzymes Chlase-like hydrolytic activity. These enzymes and their encoding genes can perhaps be identified on the basis of their relation to senescence-related Chl breakdown *in vivo*.

Chlase proteins display an N-terminal transit peptide, similar to other chloroplast proteins, indicating a transport function to chloroplasts. Contrary to this, an N-terminal deletion mutant (*CHLASEAN*, lacking the first 21 residues of a transit peptide sequence) successfully translocated into chloroplasts, giving rise to a speculation of an alternate function for the Chlase N-terminus signal sequence. This assumption gains credence from the increased activity of *CHLASEAN* under low light conditions compared to *CHLASE1*-expressing plants suggesting regulatory elements in the amino terminal region of the protein (Harpaz-Saad et al., 2007).

1.4.1.2 Enzymatic kinetics of Chlase

Enzymatic studies of Chlase in plants showed that its activity is associated with Chl-lipoprotein complexes and requires an organic solvent for *in vitro* activity (Ardao and Vennesland, 1960; Klein and Vishiniac, 1961; Holden, 1961). Chlase isolated from various marine algae and plants showed similar activity (Barrett and Jeffrey, 1964). Studies on Chlase isolated from *Ailanthus altissima* showed active hydrolysis of Chl *a* and *b*, Pheophytin (Phe) *a* and *b*. However, protochlorophyll *a* and 4-vinyl protochlorophyll *a* were not hydrolyzed and were competitive inhibitors (Mc Feeters et al., 1971). Since the

early 1980's, Chlase from marine algae and plants has been the focus of enzyme kinetics studies.

From algae

Reaction kinetics of Chlase protein isolated from the algae *Chlorella protothecoides* and *Phaodactylum tricornatum* was studied extensively because of its industrial importance. Most of the research was aimed at minimising deleterious effects of residual Chl in the Canola oil production. The reaction mechanisms of Chlase were optimised with the following parameters.

Effect of nature of organic solvent

Chlase isolated from *P. tricornatum* showed an improved catalytic activity in the presence of various organic solvents (acetone, ethanol and propanol) using either monophasic or biphasic systems (Khamessan et al., 1995a & b). Use of selected organic solvents in the reaction medium improved the solubility of Chlase and Chl and influenced the hydrolytic activity of the enzyme.

Effect of Mg^{+2} , lipids, reducing agents and detergents

Chlase isolated from *P. tricornatum* in both soluble and membranous forms showed enhanced activity by addition of divalent cations like Mg^{+2} along with reducing agents such as DTT and ascorbate. Similarly addition of Triton X-100 (TX-100) solubilised the chloroplast membranes, increasing the Chlase activity (Terpstra, 1980). Addition of negatively charged membrane lipids like phosphatidylglycerol (PG) inactivated the enzyme, but addition of Mg^{+2} reversed the process (Lambers and Terpstra, 1985). On the other hand, activity of the enzyme was markedly enhanced by addition of various membrane lipids (phosphatidylcholine, phosphatidylglycerol, and β -carotene) to the reaction medium (Khalyfa et al., 1995).

Effect of inhibitors and activators

Phytol, a byproduct of Chl hydrolysis, showed non-competitive inhibitory effect on Chlase by binding at a different site from the substrate, Chl (Khamessan et al., 1994). Various chemicals like diisopropyl fluorophosphates (DFP) and iodoacetamide (IAE) inhibited the catalytic activity of Chlase *in vitro* (Kermasha et al., 1992; Khalyfa et al., 1995). Comparative analysis of the effects of various surfactants on Chlase hydrolytic activity in

organic water system identified Span 85 (a surfactant) to increase the Chlase activity (Khamessan and Kermasha, 1996).

Effect of pH and temperature

Chlase isolated from *P. tricornatum* showed an increased activity even at a higher pH of 8.0 and 45°C (Kermasha et al., 1992; Arriagada-Strodtz et al., 2007).

Effect of type of substrate and enzyme concentration

Partially purified Chlase enzyme from *P. tricornatum* was assayed for its hydrolytic activity on Chl and Phe in the reaction medium and the optimum substrate concentrations were determined (Khamessan et al., 1993; Samaha and Kermasha, 1997a & b; Yi et al., 2006). Hydrolytic activity of Chlase was affected by varying the amount of protein fraction in the assay (Khamessan et al., 1995a; Bitar et al., 2004).

Effect of oil concentration

Hydrolytic activity of partially purified Chlase from *P. tricornatum* in a refined-bleached-deodorized canola oil (RBD) model system was investigated in various assay systems. It was found that presence of 10% oil in the micellar system containing Span 85 and polysorbate 80 decreased V_{max} values of Chlase activity by 6.2 and 9.6 times, respectively (Kermasha and Khamessan, 2001).

Similarly, the activity of purified Chlase from *C. protothecoides* was measured at various conditions of temperature, substrate concentration and other parameters (Shioi et al., 1980).

Based on all the above data, it is imperative to choose a reaction system for large scale processing in oil industry that can maintain maximum Chlase activity even under higher oil concentration, temperature and other reaction conditions.

From plant sources

Although enzyme kinetics studies from algae gave sufficient insight into the activity of Chlase, certain aspects like fruit ripening and various stress factors can only be understood from description of Chlase activities of higher plants. Chlase enzyme has been isolated and purified from different plant species like olive, *Capsicum*, *Citrus* etc., and assayed for its physical and chemical properties *in vitro* by various research groups.

Chlase activity and reaction kinetics during fruit ripening

Ethylene, a fruit ripening agent, increased the activity of Chlase in Calamondin fruits, while AgNO₃, an antagonist of ethylene reversed the effect (Purvis, 1980). Accumulation of Chl breakdown products in the fruit peels of ethylene-treated oranges showed that the hormone promoted degreening of fruits (Gray et al., 1997). Chlase activity was monitored at different stages of ripening in various cultivars of *Capsicum*. The red cultivar showed increased Chlase activity during maturation and ripening, which correlated to the decreased Chl amounts, while the green cultivar showed maximum activity only during later ripening stages (Hornero-Me'ndez and Mí'nguez-Mosquera, 2002).

However, in few cases like ethylene-treated *Citrus unshiu* fruits and olives, Chlase activity remained unchanged even with decreased amounts of Chl during fruit ripening. This was due to peroxidase-mediated Chl breakdown in the presence of H₂O₂ (Shimokawa and Uchida, 1992; Roca and Mí'nguez-Mosquera, 2003).

Enzyme kinetics of Chlase isolated from olive fruits showed that the enzyme has higher affinity for Chl *b* than Chl *a* (Mí'nguez-Mosquera et al., 1994). In olives, presence of Chlase throughout their developmental cycle i.e., during both Chl synthesis and degradation was demonstrated by the presence of small amounts of Chlide *a* and *b* during Chl biosynthesis and fruit ripening (Mí'nguez-Mosquera and Gallardo-Guerrero, 1996). Enzyme activity of Chlase from *Capsicum* fruits was studied in terms of substrate specificity, pH and temperature optimum. In addition, effects of various metal ions and functional group modifying agents on Chlase activity were analysed (Hornero-Me'ndez and Mí'nguez-Mosquera, 2001).

Chlase activity during leaf senescence

Chlase initiates Chl degradation and an enhanced Chlase activity is supposed to be associated with leaf senescence. Many plants show such an increased activity, correlating with loss of Chl (Shimokawa, 1981; Gong and Mattheis, 2003). In contrast, a decreased Chlase activity with a loss of Chl was reported in soybean leaves (Majumdar et al., 1991) and no correlation was reported in *Arabidopsis* (Todorov et al., 2003a).

Chlase activity at various stages of leaf senescence in plants like parsley, tobacco, wheat, and tomato revealed a decreased enzyme activity with a decrease in Chl content from young to senescent leaves. On the other hand, in plants like melia and nasturtium, the

activity was high through out the period of senescence even when most of the Chl has disappeared (Ben-Yaarkov et al., 2006).

However, senescence promoted by ethylene treatment did not always affect the Chlase activity *in vivo*. Radish seedlings did not show any Chlase activity in ethylene-treated radish cotyledons. The Chl *a* present in the senescent cotyledons was degraded by a Chl *a*-bleaching peroxidase, which was enhanced by ethylene (Adachi et al., 1996). Increased peroxidase activity seen during Chl degradation tends to stimulate the process of senescence in post-harvest horticultural plants (Yamauchi et al., 2004).

Chlase activity during various kinds of stress

Stress conditions such as drought, salt and low oxygen are usually associated with impairment of chloroplast membrane structure, and results in an increased Chlase activity (Mihailovic et al., 1997). In a study, wild type (WT) and non-yellowing mutant leaves of snap bean subjected to low oxygen (0.5% O₂) showed a retarded Chl degradation with no effect on Chlase activity and accumulation of Chlide *a* and *b* (Fang et al., 1998). However, no change in Chlase activity was observed during drought conditions in soybean leaves, although a significant rise in the specific activity of the enzyme was seen in water stressed leaves (Majumdar et al., 1991).

In addition to the above-mentioned work, extensive research was performed to assess the molecular and functional properties of the enzyme *in vitro* by cloning the *Chlase* gene and characterising the encoded protein from different plant species like *Citrus*, *Arabidopsis*, *Ginkgo*, *Triticum* and others.

1.4.1.3 Molecular properties of the genes encoding Chlase in different plant species

From *Citrus* species

Chlase protein was first extracted and purified by gel-filtration from plastid fractions of fruit peels of ethylene treated orange (*Citrus sinensis* L. osbeck valencia). The purified heated protein had a molecular weight of 35 kDa (Trebitsh et al., 1993). The cDNA sequence coding for Chlase (termed as *CHLASE1*) was identified and cloned from Valencia orange which encoded a protein of 329 amino acids (aa). The calculated molecular mass of precursor protein of *CHLASE1* was 35 kDa. The protein expressed in *E. coli* successfully catalyzed the breakdown of Chl *in vitro* (Jacob-Wilk et al., 1999). Mass spectrometry of the protein bands (cut from acrylamide gel) of the putative and mature

forms of *CHLASE1* from ethylene-treated *Citrus limon* fruit peels confirmed the molecular weight as 35 kDa and 33 kDa respectively (Shemer et al., 2008).

From *Chenopodium album*

Two major Chlases (*CaCLH1* and *CaCLH2*), purified from acetone powders of mature leaves of *C. album*, were estimated to have molecular masses of 41.3 and 40.2 kDa by SDS-PAGE. Enzyme kinetics and K_m values of these two Chlases were similar. Their N-terminal aa sequences were almost identical except for a deletion in the tenth aa residue in one of the Chlases (Tsuchiya et al., 1997). The *CaCLH* cDNA was cloned in *E. coli* and activity was measured *in vitro* (Tsuchiya et al., 1999). The *CaCLH* contained a signal peptide typical for uptake of the protein into the endoplasmic reticulum (ER), and has no signal sequence for ER retention. The *CaCLH* shared 37% homology with *AtCLH1* (coronatine induced *AtCOR1*).

From *Arabidopsis thaliana*

Two Chlase homologues were identified from *A. thaliana* viz., *AtCLH1* and *AtCLH2*. *AtCLH1* was first identified as a gene induced by coronatine which was up regulated in *Arabidopsis* leaves by methyl jasmonate and wounding (*ATHCOR1*) (Benedetti et al., 1998). However, methyl jasmonate had no effect on the second isoform, i.e., *AtCLH2*, also identified and cloned from *Arabidopsis*. Between *AtCLH1* and *AtCLH2*, the transit peptide sequence of the latter was typical for chloroplast localisation, while for *AtCLH1* the subcellular localisation was obscure. The soluble protein extracts of *E. coli* overexpressing *ATHCOR1*, was shown to possess Chlase activity *in vitro*. Increased amounts of Chlide *a* without a substantial change in total amount of extractable Chl were found in WT and *coil* plants overexpressing *ATHCOR1* compared to antisense *coil* mutants of *Arabidopsis* (Benedetti and Arruda, 2002). *In vitro* activity assays performed with both *AtCLH1* and *AtCLH2* showed that *AtCLH2* required higher amounts of detergent and acetone for its activity. Based on RNAi experiments of *AtCLH2*, it was concluded that *AtCLH2* behaves *in vivo* similar to *AtCLH1*. Protein expression profiles of *AtCLH1* and *AtCLH2* in different plant organs in response to dark treatment indicated their distinct functions in *Arabidopsis* (Liao et al., 2007).

Gene silencing of *AtCLH1* by RNAi led to failure of Chl degradation in *Arabidopsis* plants after tissue damage in response to *Erwinia carotovora*. Exposure of the mutants to high light caused an elevated accumulation of reactive oxygen species (ROS), suggesting an

active role of *AtCLH1* in damage control after tissue injury and plant defence pathway (Kariola et al., 2005). However, non-localisation of *AtCLH1* and *AtCLH2* in chloroplasts (detailed in section 1.4.1.1) and senescence studies with their double knockout mutants did not support specific Chlase function in Chl catabolic pathway. This led to a speculation that these two genes were not involved in senescence related Chl breakdown in *Arabidopsis* leaves (Schenk et al., 2007). In this context, another protein termed as Pheophytin-pheophorbide hydrolase (Pheophytinase - PPH), a chloroplast-located and senescence-induced hydrolase was identified in *Arabidopsis*. PPH specifically dephytylates the Mg-free Chl pigment, Pheophytin *a* (Phe *a*), yielding Pheide *a*. *Arabidopsis* mutants deficient in PPH (*pph-1*) were unable to degrade Chl during senescence and exhibited a stay-green phenotype. Furthermore, *pph-1* accumulated Phe during senescence. Hence, an alternative sequence of early Chl catabolic reactions was proposed with removal of Mg most likely preceding dephytylation: Chl / Phe *a* / Pheide *a* (Schelbert et al., 2009).

From *Gingko biloba*

Yellowing of leaves during autumnal senescence and the role of Chlase was studied in *G. biloba*. The cDNA encoding Chlase in *G. biloba* (*GbCLH*) was cloned and the expression of *GbCLH* was analysed during the yellowing of the leaves. Expression levels of *GbCLH* were highest in green leaves and very low during the process of leaf yellowing, suggesting a role of *GbCLH* in Chl homeostasis rather than Chl breakdown in *Gingko* (Tang et al., 2003). The recombinant GbCLH protein was tested for its *in vitro* activity and showed that it hydrolyses Chl *a* and Phe *a* more rapidly than Chl *b* and Phe *b* (Okazawa et al., 2006).

From wheat (*Triticum aestivum*)

Chlase gene was also cloned from wheat. The encoded protein acts as a dimeric protein exhibiting both hydrolase and carboxylesterase (*p*-nitrophenyl (PNP)-butyrate, PNP-decanoate, and PNP-palmitate) activities in the plant. Sequence analysis of the protein indicated its soluble nature with no membrane-spanning region (Arkus et al., 2005). A high purification assay system was developed using immobilised recombinant wheat Chlase protein to study the enzyme kinetics which led to a better insight into *in vitro* activity of a cloned recombinant plant protein (Arkus and Jez, 2006).

From broccoli (*Brassica oleracea* var. *Italica*)

Three Chlase genes were identified and cloned from broccoli to study the phenomenon of post harvest yellowing in the florets. They were termed as *BoCLH1*, *BoCLH2* and *BoCLH3*

of which only the transcript levels of *BoCLH1* were detected during yellowing. The effect of *BoCLH1* in leaf yellowing was proved by RNAi constructs of the gene which resulted in slower yellowing of the florets. The delay in yellowing lasted only for a couple of days and suggested that other proteins than Chlase are involved in post harvest yellowing of broccoli. However, this effect was absent when RNAi constructs of *BoCLH2* and *BoCLH3* were transformed into the florets (Chen et al., 2008).

Lipase motif is conserved in all *Chlase* genes

All of the cloned Chlases contained their putative respective transit peptides at the N-terminus, but the aa sequences differed considerably. Deduced aa sequences of these Chlases (*CHLASE1*, *AtCLH1*, *AtCLH2*, *CaCLH1* and *CaCLH2*) had several common characteristics. Active site of Chlase shows a lipase motif [ATP-GTP-binding motif (P-loop)] containing a conserved serine residue. Various site-directed mutants of *CaCLH* in the conserved regions (Ser162, Asp191 and His262) have revealed that these residues are vital for the Chlase activity (Tsuchiya et al., 2003). Lack of a membrane-spanning region in these Chlases (judging from their hydropathy profiles) suggests that the Chlases cloned to date are not intrinsic membrane proteins. This might be one reason why most Chlases are easily extracted from algal cells or acetone powder of higher plants with an aqueous or dilute detergent solution.

Derived from all available *Chlase* gene sequences of various plants, their aa sequences were aligned to assess the homology between the individual proteins. A homology of 30 - 40% among all the Chlase proteins and the presence a conserved serine residue within the serine lipase motif, which is very essential for the hydrolytic activity of the protein, is shown in Fig. 5.

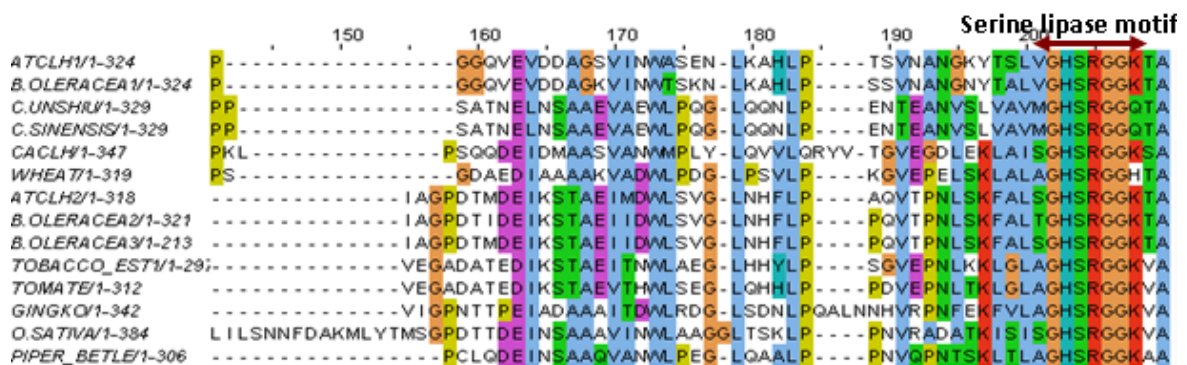


Fig. 5: Alignment of aa sequences of Chlases isolated from different plant sources. The conserved lipase motif is shown as the dark arrowed line (serine is seen at 204 position in the picture).

The possible intracellular target site was predicted for all Chlases using the proteomic software. Experimental evidence was given for a few of them recently (for Chlase from *Citrus* species, *Ginkgo* and *Arabidopsis*). A brief summary of these results along with molecular weight of the proteins and isoelectric points is given as Table 1.

Plant	Predicted target	Experimental evidence	MW (kDa)	pI
<i>Arabidopsis thaliana</i> <i>AtCLH1</i> (coronatine induced) <i>AtCLH2</i>	Cytoplasmic Plastids	Cytosol (Schenk et al., 2007)	34.8 34.9	5.75 6.98
<i>Chenopodium album</i> (<i>CaCLH</i>)	Endoplasmic reticulum		38.7	8.88
<i>Citrus sinensis</i> (<i>CsCHLASE</i>)	Chloroplasts	Chloroplasts (Harpaz-Saad et al., 2007; Shemer et al., 2008)	35.2	6.53
<i>Citrus unshiu</i> (<i>CuCHLASE</i>)	Chloroplasts		35.2	6.16
<i>Ginkgo biloba</i> (<i>GbCLH</i>)	Chloroplasts	Chloroplasts (Okazawa et al., 2006)	37.1	7.14
<i>Oryza sativa</i>	Endoplasmic reticulum		39.6	6.88
<i>Piper betle</i>	Cytoplasmic		33	6.3
<i>Nicotiana tabacum</i> (<i>NtCLH</i>) EST	Chloroplasts		34.4	6.78
<i>Lycopersicum esculentum</i>	Chloroplasts		34	7.3
<i>Triticum aestivum</i>	Cytoplasm		33.8	6.13
<i>Brassica oleracea</i> var. <i>italica</i> <i>BoCLH1</i> <i>BoCLH2</i> <i>BoCLH3</i>	Cytoplasm Chloroplasts Cytoplasm		34.6 35.2 23	5.71 6.25 5.93

Table 1: Molecular characteristics of the Chlase genes identified so far from different plant species.

1.4.1.4 Post translational regulation of Chlase expression and activity

Rate-limiting function of Chlase enzyme indicates a possibility for its post-translational regulation in Chl catabolism. While some reports support this view (Matile et al., 1997 & 1999; Jacob-Wilk et al., 1999), other reports contradict the rate-limiting nature of Chlase in Chl catabolism (Minguez-Mosquera and Gallardo-Guerrero, 1996; Fang et al., 1998).

Using deletion mutants for *Citrus CHLASE* (*CHLASEAN*; N-terminal 21 aa deletion), Harpaz-Saad et al. (2007) proved the rate-limiting nature of Chlase. Authors showed that deletion mutants displayed extensive Chl breakdown in both tobacco protoplasts and squash leaves in comparison to full-length *CHLASE* constructs. More so, *CHLASEAN*-expressing squash leaves displayed a dramatic chlorotic phenotype in plants grown under low-intensity light and exhibited a lesion-mimic phenotype under normal light. This phenotype was surmised to be due to accumulation of Chlide, a photodynamic Chl breakdown product (Harpaz-Saad et al., 2007). This work shows that Chlase has indeed regulatory domains and is controlled via post-translational regulation.

1.4.1.5 Functional roles of Chlase in plants

Chlase plays a unique role in plant metabolism. In summary, various aspects of the activity of Chlase are as follows:

1. Chlase catalyses the first key regulatory step in Chl catabolism thereby aiding in regeneration of micronutrients for continuous synthesis of Chl in the plants.
2. Chlase is essential during senescence processes, which are crucial for crop improvement by increasing the economical yield of crops.
3. Chlase might stimulate the senescence process in plants, regulated by hormones such as ethylene.
4. It participates in the defence pathway of plants in response to various pathogen attacks leading to production of decreased levels of ROS.
5. Climatic changes can be responsible for triggering the degradation of Chl.

1.4.2 Significance of others enzymes in Chl catabolism

The second step in Chl degradation is the removal of central Mg^{+2} ion from Chlide *a* to yield Pheide *a*. In higher plants and algae, this reaction is considered to be catalysed by an enzyme termed Mg-dechelataase (Shioi et al., 1991; Vicentini et al., 1995). This enzyme can remove Mg^{+2} *in vitro*, not only from Chlide but also from an artificial dephytylated

substrate Chlorophyllin (Suzuki and Shioi, 2002). They have isolated a protein of 20 kDa termed as MCS (Mg chelating substance) from *C. album* which exhibited Mg-releasing activity with Chlorophyllin but not native substrate, Chlide.

Further conversion of Pheide *a* (macrocycle cleavage) into RCCs is catalyzed by PAO (an envelope membrane Fe-dependent monooxygenase enzyme) which results in loss of green colour. PAO is highly specific for Pheide *a*, while Pheide *b* inhibits the activity in a competitive manner (reviewed in Hörtensteiner, 2006). This explains that NCCs identified so far are exclusively derived from Chl *a*. The expression of PAO is restricted to senescent tissues (reviewed in Eckhardt et al., 2004). In *Arabidopsis*, the gene for PAO was identified as *Accelerated cell death 1* (*Acd1*) encoding a protein (AtPAO) and its activity was proved *in vitro* (Pruz'inska' et al., 2003). Another PAO orthologue was reported from maize known as *lethal leaf spot 1* (*LLS1*) (Gray et al., 2002). Both *Acd1* and *LLS1* belong to a small family of structurally related but functionally distinct Rieske-type oxygenases (Gray et al., 2004). Knockout mutants of both *LLS1* and *Acd1* retained Chl during dark induced senescence with no accumulation of colourless Chl catabolites and showed a light-dependent cell death phenotype of leaves due to deposition of Pheide *a* (Pruz'inska' et al., 2003 & 2005).

The generation of pFCCs from Pheide *a* is catalysed by RCC reductase (RCCR) stereospecifically reducing the C20/C1 double bond of RCC, resulting in the formation of two possible C1 stereoisomers of pFCCs (pFCC1 or pFCC2) (Rododni et al., 1997). The presence of an additional protein termed as RCC forming factor (RFF) was suggested to act along with PAO in RCC formation (Pruz'inska' et al., 2005). RCCR is a soluble chloroplastic protein, identified as *Accelerated cell death 2* (*Acd2*) in *Arabidopsis* (Wüthrich et al., 2000). Normally the protein localizes to chloroplasts but in response to stress partially locates to mitochondria (Mach et al., 2001; Yao et al., 2004; Yao and Greenberg, 2006). *RCCR/ACD2* is a single-copy gene in *Arabidopsis* (*At4g37000*) and constitutively expressed during all phases of leaf development (Pruz'inska' et al., 2005). Similar to *Arabidopsis* PAO knockouts, the *Acd2* mutants also showed light-dependent cell death phenotype due to accumulation of photodynamic RCCs and singlet oxygen species (Pruz'inska' et al., 2007).

After export from the chloroplasts, the pFCCs are modified by reactions reminiscent of detoxification processes widely occurring in plants (Kreuz et al., 1996). The pFCCs are

hydroxylated and following species-specific modifications (Kräutler, 2003; review, Hörtensteiner, 2006), result in FCCs which are imported into vacuole by a primary active transport process (Hinder et al., 1996). Finally, FCCs are converted to their respective NCCs by nonenzymatic tautomerization, catalyzed by the acidic vacuolar sap (Oberhuber et al., 2003). Structure analysis of NCCs from different plant species has revealed that, with one exception, they are all derived from Chl *a* (Kräutler, 2003; Müller et al., 2006).

1.4.3 Water Soluble Chlorophyll Protein (WSCP)

Catalysis of Chl by Chlase necessitates transport of Chl from its location in thylakoid membranes to the site of action of Chlase i.e., chloroplast envelope. WSCP is predicted to be such a putative transporter, whose role as Chl binding protein facilitates Chl degradation (represented as ⊗ in Fig. 1). WSCPs were reported from *Brassicaceae*, *Polygonaceae*, *Chenopodiaceae*, and *Amaranthaceae* families (Murata et al., 1971; Takamiya, 1973).

1.4.3.1 Classification of WSCPs

The WSCPs in the plants are classified into two types based on their photo-convertibility,

- a) *Chenopodium* type – Class I and
- b) *Brassica* type – Class II.

Class-I unlike Class-II, show a drastic change in absorption spectrum on exposure to visible light. Sequence homology shows differences in their N-terminus aa sequences (Kamimura, 1997).

1.4.3.1.1 Class I WSCPs

The first WSCP protein identified was a Class I type, isolated from *C. album* and designated as CP668 (Chl protein 668), based on its absorption maxima at 668 nm (Yakushiji et al., 1963). The protein is photosensitive and changes its absorption spectrum from 668 to 743 nm upon irradiation to visible light in the presence of molecular oxygen. The native and irradiated Chl-WSCP complexes show both Chl *a* and *b* and lack carotenoids (Takamiya et al., 1963 & 1968). Flash experiments proved involvement of a triplet state of Chl *a* as an intermediate during photoconversion and production of ROS. Reconstitution of CP668 apoprotein with Chl molecules also showed photoconversion and a higher content of Chl *a* compared to Chl *b* (Chl *a/b* = 6.2) (Oku and Tomita, 1975). CP668 found in *Atriplex*, *Polygonum* and *Amaranthus* weighs 78 kDa, with Chl *a:b* in the

ratio of 6:1 (Takamiya, 1973). CP668 localises more in stems compared to leaves and prominent in younger parts compared to older parts of the plant.

1.4.3.1.2 Class II WSCPs

The WSCP proteins belonging to this class does not exhibit any change in their photo convertibility on exposure to light. They are classified into two subtypes based on their Chl *a/b* ratios with ratios being 1:1 or 2:1 or 4:1 (reviewed in Satoh et al., 2001). Studies on this class of WSCPs indicated their role in photosynthesis because of their water-solubility, low Chl content, and stress-induction.

Class IIA WSCPs

Class IIA WSCP was first purified from cauliflower (*Brassica oleracea var botrys*) (Murata et al., 1971; Nishio and Satoh, 1997) and later from various plants like wild mustard (Murata and Murata, 1971), brussels sprouts (Kamimura et al., 1997), turnip, and Japanese radish (Shinashi et al., 2000). The holo-WSCPs of most *Brassica* species are tetramers (Satoh et al., 1998) possessing higher content of Chl *a* (Chl *a/b* = 6.3 - 10) but no carotenoids (Murata and Murata, 1971; Murata et al., 1971; Kamimura, 1997). CP673 (Chl protein 673) (brussels sprouts) contained one molecule of Chl in the tetramer which is the lowest content of Chl in the WSCPs so far determined (Kamimura, 1997). All class IIA WSCPs have identical maximum red absorption wavelength and possess Chl *a* and *b* components in 4:1 ratio (Sugiyama and Murata, 1978; Satoh et al., 1998; Shinashi et al., 2000).

Class IIB WSCPs

A Class IIB WSCP, first reported in *Lepidium virginicum* has a Chl *a/b* ratio of 1:1 or 2:1 with the ratio varying depending on the growth habitat of plant (Murata et al., 1980; Itoh et al., 1982). Murata et al. (1980) isolated the protein as CP661 (Chl protein 661) which showed an absorption wavelength at 661 nm with a Chl *a/b* ratio of 1. Subsequently, the same protein complex was isolated at different absorption maximum of 663 nm (CP663 – Chl protein 663) with a Chl *a/b* ratio of 1.6 – 1.9 (Murata and Ishikawa, 1981). The CP663 isolated from different organs of the plant exhibited different Chl *a/b* binding ratios. The WSCP from *Lepidium* was also a tetramer with a molecular weight of 78 - 80 kDa (Murata and Ishikawa, 1981; Itoh et al., 1982) bound to four Chl molecules indicating that each subunit of the tetramer possessed one Chl molecule. The isoelectric point of the WSCP was determined to be 4.2 - 4.5.

1.4.3.2 Molecular and functional aspects of WSCPs

The current knowledge about WSCP is mostly from work done on the Class II type proteins. Most of the research articles refer to Class II as just ‘WSCP’ without mentioning the type. In the present context, WSCP would refer only to class II, unless otherwise mentioned.

WSCPs from different plant species bind Chl *a* and *b* in different ratios. The WSCP proteins share homology with various stress related proteins like BnD22 (oil seed rape) and P22 (radish). Some members of the WSCP family are inducible after drought and heat stress as well as leaf detachment. For instance, WSCP from oil seed rape has dual functions; as BnD22, a drought stress induced protein and as a 19 kDa protease inhibitor protein termed as Trypsin Inhibitor protein (TI). The transcripts of BnD22 and TI are higher during nitrogen recycling from mature leaves to young leaves, which could be important for retardation of senescence. In nitrogen starvation and methyl jasmonate treatment, BnD22 and TI activity are induced, delaying the initiation of senescence. This indicates a protective function of WSCP in younger tissues from adverse conditions by maintaining metabolism (protein integrity and photosynthesis). Also the protein contributes to better utilisation of recycled nitrogen from sources and sustains sink growth of the plants (Desclos et al., 2008).

The N-terminal aa sequence of WSCP was deduced for the first time for CP673 (brussels sprouts), with a molecular weight of 78 kDa (pI – 4.7) consisting of three or four subunits of 22 kDa each. The protein complex is extremely heat stable, homologous to BnD22 and P22 and contain signature motif of Kunitz type protease inhibitor family ([LIVM]-x-D-x-[EDNTY]-[DG]-[RKHDENQ]-x-[LIVM]-x(5)-Y-x-[LIVM]) but does not inhibit any protease, such as chymotrypsin and trypsin (Kamimura et al., 1997). Similarly, the cauliflower WSCP accumulates during wounding and water deficiency of leaves (Nishio and Satoh, 1997).

WSCP from Cauliflower

An insight into the functional properties of WSCP was obtained from molecular cloning of the corresponding gene from cauliflower (Satoh et al., 1998). The protein sequence encoded by the *Cau-WSCP* cDNA sequence contained 19 aa residues for a transit peptide and 199 aa residues for the mature form of WSCP. The protein showed a homology of 94% to BnD22 and 51% to P22. The mature protein (22 kDa) was overexpressed in *E. coli*

as a maltose binding protein (MBP) fusion protein. *In vitro* reconstitution experiments using spinach thylakoid membranes, confirmed that MBP-WSCP could form tetramers similar to native protein. The protein had a higher affinity towards Chl *a* than Chl *b* as seen from the change in Chl *a/b* ratio from 2.89 to 2.41 indicating a possible removal of Chl *a* from the spinach thylakoid membranes. This led to a prediction that WSCP plays a role in the Chl degradation process by transporting the Chls from thylakoid membrane-protein complexes to the site of Chlase (Matile et al., 1997). Same authors also predicted a role of WSCP in organisation of photosynthetic apparatus during acclimation of plants to various light environments based on its Chl binding capacity and the removal of Chl from thylakoid membranes (Matile et al., 1997). Reports indicate that the signal peptide in the native protein play a role in sorting the protein through ER (Satoh et al., 1998), similar to that in BnD22 (Downing et al., 1992).

WSCP from Japanese radish (*Raphanus sativus* L. var. *Hortensis*)

Crystallisation of WSCP from the main veins of Japanese radish, determined the molecular structure of the protein (Shinashi et al., 2000). The protein showed 92% homology with the WSCP of *Lepidium*. The cDNA coding for *Raphanus*-WSCP encodes a protein of 24 kDa. Presence of a signal peptide sequence in the cDNA indicates transportation of the protein to the ER. Another isoform of *Raphanus*-WSCP was also identified which was similar to the P22 protein (Satoh et al., 2002). Both the proteins retained the conserved signature motif of Kunitz type protease inhibitor family and their N-terminal and C-terminal sequences are identical to that of *Cau*-WSCP.

WSCP from kale (*Brassica oleracea* L. var. *Acephala*)

Two isoforms for WSCP protein were crystallised from the leaves of kale, which showed 95% homology to each other. Out of the two allelic forms, one (Q8H0F0) is identical to the *Cau*-WSCP throughout the C-terminal sequence and the other (Q8H0E9) differed slightly (Horigome et al., 2003). The mature monomeric kale-WSCP (Q8H0F0) has a molecular mass of 18.8 kDa. The *kale*-WSCP protein was similar to WSCP protein of rapeseed (BnD22) and cauliflower (*Cau*-WSCP), and undergoes a posttranslational cleavage at the C-terminal region in the mature protein. This C-terminal region is not the signal peptide sequence but suggested to play a role in protein targeting towards a specific cellular component (Ilami et al., 1997; Satoh et al., 1998).

WSCP from barley

A WSCP homologue was isolated from etiolated barley seedlings (*Hordeum vulgare*) exposed to light for 2 h and termed as free Chl binding protein (*FCBP/hv-WSCP*) (Reinbothe et al., 2004). This protein was expressed as a precursor protein of 27 kDa and after import into the chloroplasts, a 22 kDa mature protein remained in the outer envelope of barley etioplasts. Import of the precursor protein was light dependent and inducible when the isolated plastids were fed with 5-aminolevulinic acid (ALA). The FCBP protein exhibited the function of a putative Chlide carrier protein during the disintegration of putative PORA+PORB complex (holochrome) and transition of protochlorophyllide (Pchlde) to Chlide.

Sequence homology of a stretch of aa residues derived from the protein sequences of known WSCPs and related stress induced proteins from various plant sources is given in the following figure (Fig. 6).

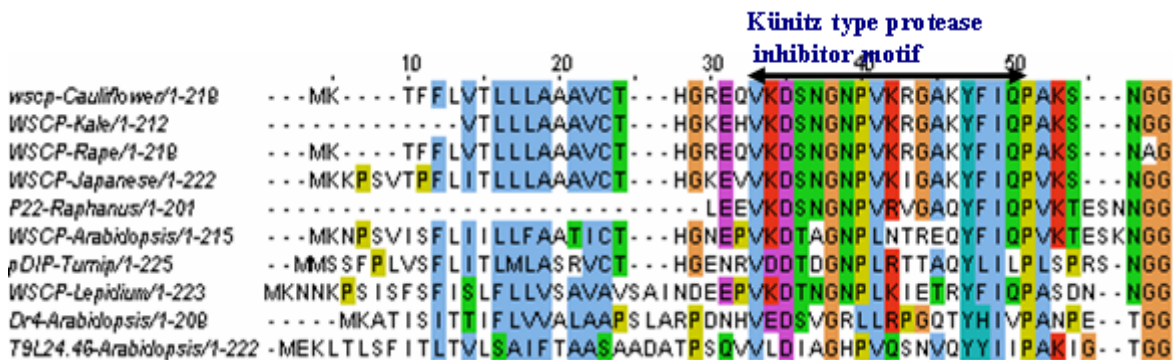


Fig. 6: Alignment of all known aa sequences of WSCPs and drought and salt stress induced proteins from various plant sources. The conserved motif of the Kunitz type protease inhibitor family is indicated by the thick bar in the picture.

1.4.3.3 Pigment binding and photoprotective function of WSCPs

WSCP forms oligomers by binding to Chl molecules. This was evident from the *in vitro* reconstitution experiments of MBP-WSCP and Chl where in the formation of MBP-WSCP-Chl complexes were visualized by Chl fluorescence. The fluorescence was visible only in the case of tetrameric and hexameric complexes, but not in the dimeric and trimeric forms. Based on the amount of protein subunits per complex and Chl, the stoichiometry was calculated to be 2 Chls per tetramer, as in the case of the native WSCP. However, the WSCP-Chl complexes did not show any carotenoids (Satoh et al., 1998). This is in contrary to the fact that all Chl or bacteriochlorophyll (BChl) containing complexes were found to contain carotenoids, which aid in the prevention of Chl-induced photooxidation. This process is facilitated by rapid quenching of energy derived from both the Chl triplet

and oxygen singlet – excited states (due to excitation of Chl molecules in solution) by carotenoids, which are of great importance to plants in protecting them from photoinhibition.

Schmidt et al. (2003) explained the prevention of photooxidation in WSCP-Chl complexes lacking in carotenoids, based on the levels of singlet oxygen species in comparison to unbound Chl molecules. The spin-trap EPR measurements showed that the extent of singlet oxygen species formation was four times lower in native and recombinant WSCP complexes, compared to the unbound Chls. This increasing photostability of WSCP-pigment complexes was confirmed by *in vitro* fluorescence measurements of the irradiated reconstituted pigment-protein complexes. The recombinant WSCP-Chl complexes showed a reduction in Chl fluorescence of 50% compared to 90% in unbound Chls (Schmidt et al., 2003).

Experiments were also performed to check if Chl derivatives can form complexes with WSCPs apart from Chl. His-Cau-WSCP protein extracts were used in the reconstitution experiments and no tetramerisation of the protein was seen when thylakoid membranes containing higher amounts of carotenoids were employed. However, the protein could oligomerise in the presence of BChl. The central metal ion (Mg^{+2}) and phytol group of Chl were essential for pigment binding and tetramer formation, which was not seen when Phe *a* and Chlide *a* and *b* were employed in reconstitution experiments. However, the process was restored when Zn^{2+} was inserted into Phe *a* (Schmidt et al., 2003).

A possible photoprotective function of WSCP in the absence of quenching by carotenoids against photo oxidation was proposed by Horigome et al. (2007) by analysing the crystal structure of WSCP-Chl complex from *Lepidium virginicum* (Virginia pepper weed) (Fig. 7). As seen from Fig. 7, Chl molecules were attached to the molecular surface of protein monomers indicating a minor contribution of pigment molecules to protein folding mechanism. Chl binding of WSCP solely depends on a co-ordination bond between the carbonyl oxygen of Pro-36 and the central Mg^{+2} ion of Chl molecule whose absence in Phe *a* makes binding to WSCP impossible (Schmidt et al., 2003). This co-ordination bond might help in the necessary removal of Chl molecule from thylakoid membranes by WSCP. Each monomeric WSCP binds one Chl molecule forming a hydrophobic cavity in the centre of the tetramer, and the hydrophobic interaction among the four phytol chains might aid in tetramerisation of WSCP which is not possible with Chlide. Also the absence

of a central metal ion makes it inaccessible to molecular oxygen and inhibits the production of ROS (Drzewiecka-Matuszek et al., 2005).

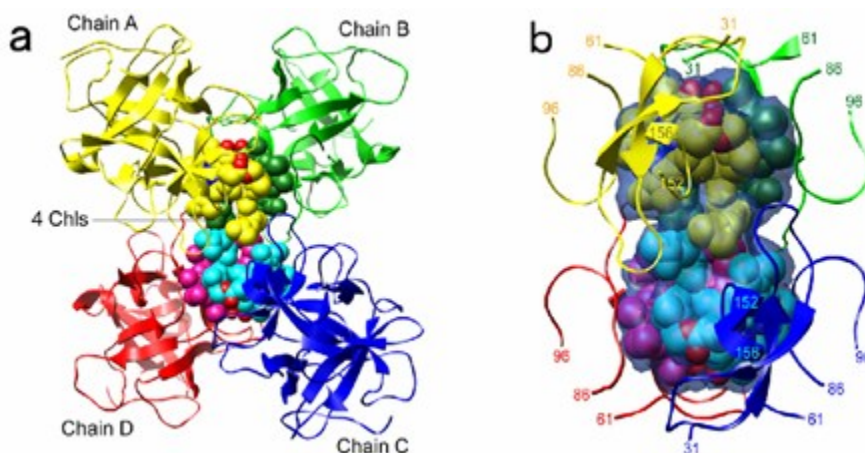


Fig. 7: Overall structure of the tetrameric WSCP-Chl complex and Chl-binding cavity. *a*, the protein moiety (WSCP) is shown in a ribbon model and Chl molecules in a Corey-Pauling-Koltun model. The four monomers are shown in *yellow*, *green*, *blue*, and *red*. The principal dimers are the pairs of chains A and B and chains C and D. *b*, the hydrophobic cavity enclosing the four Chl molecules is shown as a *blue transparent surface*. The residues of 31 - 61, 86 - 96, and 152 - 156 of each WSCP monomer are shown (Horigome et al., 2007).

Dissipation of light-induced excitation energy of Chl in the hydrophobic cavity of WSCP could partly be due to the partial emission of fluorescence by the Chl molecules in the WSCP complex (Sugiyama and Murata, 1978; Satoh et al., 1998). Also quenching could possibly be due to 1) a sequence of electron exchanges between Chl molecules and the nearby aromatic residues (Trp - 90 and Trp - 154) and 2) energy transfer between the Chl molecules in the Chl dimers formed in the tetrameric complex leading to energy dissipation by fluorescence quenching. The above reasons could positively account for the photoprotective function of WSCP.

Based on all the available information regarding the WSCPs, its properties have been summarised in the following table (Table 2).

	Class I	Class IIA	Class IIB
Genus	<i>Chenopodium</i> <i>Atriplex</i> <i>Amaranthus</i> <i>Polygonum</i>	<i>Brassica</i> <i>Raphanus</i>	<i>Lepidium</i>
Photoconversion upon illumination	Yes	No	No
Prominent absorption peak Before illumination	668 nm (CP668)	673 - 674 nm	661 nm (CP661) 663 nm (CP663)
After illumination	740 - 743 nm	No change	No change
Molecular mass in native conditions	78 kDa	76 - 80 kDa	76 kDa
Molecular mass in denaturing conditions	16 kDa	20 - 24 kDa	16/22 kDa
Chl <i>a/b</i> ratio	6.2	6-10	CP661 - 1.0 CP663 - 1.5 - 1.7
Number of Chls per complex	7	1 – 4	4
Subunit composition	Unknown	Tetramer	Tetramer
Sequence homology	Not known	Drought induced proteins and proteinase inhibitors	Drought induced proteins and proteinase inhibitors

Table 2: Classification and properties of WSCPs.

1.4.3.4 Functions of WSCPs in plant system

The WSCPs are hydrophilic proteins found in plants and assumed to play various roles in plant metabolism and development.

1. It has been proposed that WSCP acts as a carrier molecule of Chl from thylakoid membranes to the site of action of Chlase for initiating the process of Chl degradation in the chloroplasts.
2. It could serve as a repository for Chl derivatives during light-induced chloroplast development and Chl biogenesis.
3. The WSCPs are homologous to stress-induced proteins and are induced by drought, heat and leaf detachment. They decrease the proteinase activity in leaves and delay senescence.
4. Moreover, a photoprotective role was proposed to WSCP due to the inhibition of the formation of ROS on exposure to light.
5. WSCP can serve as a model to understand pigment-pigment and pigment-protein interactions in the pigment-protein complexes.
6. It might well be that WSCP protects the plants from adverse conditions by nitrogen recycling and improving nitrogen use efficiency.

2 AIM

Scientific interest of the present work is focussed on studies of Chl degradation pathway at biochemical and molecular levels.

The “Green seed problem” of rapeseed can be attributed to deregulation of Chl catabolism and could be tackled by analysing the key enzymes in the Chl catabolic pathway. This could be achieved by

1. Cloning the genes involved in Chl catabolism,
2. Analysis of their gene products for Chl degradation and
3. Characterization of transgenic tobacco plants with expression of these proteins to understand the role of the enzymes *in vivo*. These findings could be extrapolated to develop ideas to minimise the Chl contents in mature rapeseed.

It is expected that an insight into the mechanism of Chl degradation helps to understand the control of Chl degradation during leaf senescence.

The main goals of this study were:

1. Investigation of regulatory mechanisms in the degradation pathway of Chl in plants.
2. Identification of candidate genes involved in Chl breakdown pathway.
3. Expressing the cDNA sequences of the candidate genes in *E. coli* system and the functional evaluation of their respective proteins by *in vitro* enzymatic studies.
4. Expressing the cDNA sequences of the candidate genes in transgenic tobacco plants and characterising the transgenic lines with respect to phenotype, senescence and various stress conditions.

To achieve the above goals, following strategies were followed:

Chlase and WSCP were the candidate genes for the present study. Chlase was the choice gene, since it initiates Chl catabolism and is widely considered as a rate limiting enzyme in Chl degradation (Tsuchiya et al., 1999). WSCP was chosen because of its predicted role as Chl carrier protein assisting in Chl degradation (Matile et al., 1997).

For Chlase:

1. Characterisation of Chlase from *Citrus* species by expressing *CcCHLASE* in *E. coli* and *in vitro* validation of its functional activity.
2. Optimisation of recombinant His-CcChlase with respect to its reaction kinetics by various *in vitro* enzyme assays, for application of recombinant Chlase during oil refining processes for successful removal of residual Chl in oil.
3. Production of transgenic plants overexpressing CcChlase protein and propagation of positive overexpressor lines.
4. Characterisation of Chlase overexpressor plants at T0 and T1 generation by genetic, molecular and biochemical methods, in order to analyse the physiological and regulatory aspects of the transgene in Chl catabolism and during various stress conditions.

For WSCP:

1. Expression of the *Cau-WSCP* cDNA sequence in *E. coli* and assaying the functional aspects of the recombinant protein *in vitro*.
2. Production of transgenic tobacco plants overexpressing Cau-WSCP protein and propagation of positive overexpressor lines.
3. Characterisation of WSCP overexpressor plants at T0 and T1 generation by genetic, molecular and biochemical methods, in order to analyse the regulatory and functional properties of the transgene during Chl synthesis and degradation and high light stress.

3 MATERIALS

3.1 Plasmid DNA

The following plasmid DNA containing respective cDNA sequences were used for the present study.

pMALC2 (Amp^r)

pQE80 (Amp^r)

pCAMBIA3301 (Basta^r)

3.2 Oligonucleotides

For *CcCHLASE*

35S-promoter primer

5' TATCCTTCGCAAGACCCTTCCTC 3'

reverse primer

5' ACAGCTGCAGAATTCGTTAACTTTTACATGAG
TTGTCGTAAGC 3'

For *NtCHLASE* (EST)

Forward primer

5' ACTTCAGACATGGTGATAAGTTACTC 3'

Reverse primer

5' ATCAACTCACTTGATTTCCCTTCC 3'

For *Cau-WSCP*

35S-promoter primer

5' TATCCTTCGCAAGACCCTTCCTC 3'

reverse primer

5' TTCGCGAAGCTTGACTAGTAGAATGGGAACAT
CCTTAG 3'

3.3 Organisms

Bacteria

Escherichia coli - BL21(DE3)pLysS (Novagene, Germany)

Agrobacterium tumefaciens - C58C1 (Larebeke et al., 1984)

Plants

Citrus clementii (fruits and leaves from local market)

Nicotiana tabacum cv. Samsun (SNN) (IPK, Gatersleben)

Brassica oleracea var. botrys (green house grown plants)

3.4 Antibodies

For CcChlase:

Antisera against recombinant CcChlase protein was prepared at the Pineda antikörper service, Berlin, Germany.

For Cau-WSCP:

Antibody against WSCP was a generous gift from H. Satoh, Department of Biomolecular science, Toho University, Chiba, Japan.

3.5 Chemicals and material

Acetic acid, Acetone, Acrylamide, Bisacrylamide, Chloroform, DEPC, dibasic Sodium Phosphate (anhydrous), dibasic Potassium Phosphate, EDTA, Glucose, Glycerol, Hexamine cobaltchloride, Isopropanol, Isoamylalcohol, Levulinic acid, monobasic Sodium Phosphate, monobasic Potassium Phosphate, Petrol ether, Phenol, Potassium acetate, Potassium hydroxide, Sodium Hydroxide, Sterile filters, Sodium carbonate, Trichloro acetic acid, TX-100 (**Carl Roth GmbH, Karlsruhe, Germany**).

Amphoterecin, Ampicillin, 5-ALA, 6-BAP, Bitek agar, Casein hydrolysate, Cephotaxime, IPTG, Kanamycin, MS medium including vitamins, NAA, Rifampicin, Sucrose (**Duchefa, Haarlem, The Netherlands**).

Ammonium persulfate, Ammonium nitrate, Hydrochloric acid, Hydrogen peroxide, Lysozyme, Magnesium chloride, Magnesium sulphate, Manganese chloride, Mercuric chloride, MOPS, Perchloric acid (**Merck, Darmstadt, Germany**).

DMSO, DTT, Formamide, Formaldehyde, β -mercaptoethanol (β -ME), Potassium Chloride, PMSF, PVPP, Sodium Chloride (**Applichem ltd, Darmstadt, Germany**).

Ficoll400, Hybond-N⁺ and nitrocellulose membrane (**Amersham Biosciences, Freiburg, Germany**).

Bacto agar, Bacto tryptone, Yeast extract (**Difco laboratories, Germany**).

Coomassie Brilliant blue (**Fluga AG chemicals, Buchs, Switzerland**).

Bromophenolblue, Glutathione (reduced) (**Serva chemicals, Heidelberg, Germany**).

Di ethyl ether, DAB, Hexane (**Fluka chemicals, Seelze, Germany**).

Agarose (**FMC bio products, Netherlands**).

Ammonium peroxy disulphate (**Ferak GmbH, Berlin, Germany**).

Ethanol, Ethyl acetoacetate, Methanol (**J. T. Baker chemicals**).

Ethidium Bromide (**Sigma chemicals, St. Louis MO, USA**).

Ethephon (**Sigma Aldrich, Steinheim, Germany**).

X-ray films (**Kodak, England**).

Trisure (**Bioline GmbH, Luckenwalde, Germany**).

(α -³²P)dCTP (**Hartmann Analytic, Braunschweig, Germany**).

Phospho imaging plate (**Fujifilm, Düsseldorf, Germany**).

3.6 Equipments

Agarose gel apparatus, Gel dryer, PCR, Thermo cycler, UV transilluminator	Bio Rad
Waterbath	Perbio science
Thermomixer	Eppendorf AG
Vortexer	Vortex Genie
Microfuge	Hetich Zentrifugen
Rotor centrifuge, UV spectrophotometer	Kontron instruments
Shaking incubator (innova 4000)	New Brunswick Scientific
Heating block	Bio San instruments
SDS-PAGE apparatus, Vacuum blotter	Amersham biosciences
Mettler balance	Sartorius instruments
pH meter	Knick instruments
Autoclave	Varioklave
Microwave oven	Severin microwave
Incubator, Growth chamber	Heraeus instruments
HPLC equipment: 717 plus Autosampler, 600 and 600S Controller, HPLC columns, 474 Scanning Fluorescence Detector	Waters
UV-Stratalincer 2400	Stratagene
Homogeniser RTR 2020 (Heidolph), Waring blender 8011-G (Bender and Hobein)	Schütt Labortechnik GmbH
Bioimaging analyser BAS-IPMS 2340	RAYTEST
PAM 2000, FMS2 fluorometer	Hansatech

3.7 Glass and Plastic ware

Centrifuge tubes, Micropipettes, Test tube, Glass flasks, Petriplates.

3.8 Kits, Substances, Enzymes and Buffers

Restriction enzymes and reaction buffers, RNase A1, lysozyme, lambda DNA maker for agarose gel electrophoresis (**New England Biolabs, Schwalbach/Taunus, Germany**).

DNase, 10x DNase buffer, dNTPs, DecaLabel DNA labelling kit, Klenow-Fragment exo⁻, Restriction enzymes and reaction buffers, MgCl₂ (50mM), RevertAidTM M-MuLV Reverse Transcriptase, 5x reverse transcriptase reaction buffer, Taq polymerase and buffer (**Fermentas, St. Leon-Rot, Germany**).

PCR purification kit, SDS-PAGE loading buffer (5x), ProbeQuantTM G-50 micro columns, Protein molecular weight marker (**Amersham Biosciences, Freiburg, Germany**).

Plasmid Mini Prep kit, Gel Extraction kit, **The QIAexpressionistTM** protein purification system (**QIAGEN, Hilden, Germany**).

Chemiluminescence detection kit (for Western blot) (**Applichem ltd, Darmstadt, Germany**).

3.9 Solutions and buffers

Growth media

Following growth media were made in distilled water (dH₂O) to 1 litre and sterilised by autoclaving.

LB medium (For <i>E. coli</i>)	Bactotryptone-10 g, Yeast extract - 5 g, NaCl - 10 g and pH adjusted to 7.0 with NaOH. For solid medium 1.5% of bactoagar was added.
------------------------------------	--

YEB medium (For <i>Agrobacterium tumefaciens</i>)	Casein hydrolysate – 5 g, Yeast extract – 1 g, Sucrose – 5 g and pH adjusted to 7.2 with NaOH. Then MgSO ₄ ·7H ₂ O – 0.685 g and 15 g of bactoagar were added. At the time of use rifampicin -100 mg/L and kanamycin – 50 mg/L were added.
---	--

For tobacco plants

1 MS medium	MS medium including vitamins – 4.41 g, pH adjusted to 5.7 with NaOH and finally 6 g of Bitek agar was added.
-------------	--

Co-cultivation medium	Sucrose – 30 g was added to 1 MS medium. After autoclaving, 0.02 mg/L NAA, 1 mg/L BAP were added.
-----------------------	---

Callus induction medium	MS medium including vitamins – 4.41 g, sucrose – 30 g, pH adjusted to 5.7 with NaOH and 6 g of Bitek agar was added. After autoclaving, 0.5 mg/L NAA, 1 mg/L BAP, 2 mg/L Basta, 5 mg/L Amphoterecin, 50 mg/L Cephotaxime were added.
Regeneration medium	MS medium including vitamins – 4.41 g, sucrose – 30 g, pH adjusted to 5.7 with NaOH and finally 6 g of Bitek agar was added. After autoclaving, BAP, 2 mg/L Basta, 5 mg/L Amphoterecine, 50 mg/L Cephotaxime were added.
Maturation medium	MS medium including vitamins – 4.41 g, sucrose – 30 g, pH adjusted to 5.7 with NaOH and finally 6 g of Bitek agar was added. After autoclaving, 2 mg/L Basta, 5 mg/L Amphoterecine, 50 mg/L Cephotaxime were added.
Rooting medium	MS medium including vitamins – 4.41 g, sucrose – 30 g, pH adjusted to 5.7 with NaOH and finally 6 g of Bitek agar was added. After autoclaving, 2 mg/L Basta was added.

Hormones and antibiotics

Hormones and antibiotics were filter sterilised and stored at -20°C.

Hormone stock Solutions	NAA - 0.5 mg/ml (in ethanol). BAP - 1 mg/ml (in dH ₂ O with few drops of HCl).
Antibiotic stock solutions	Ampicillin - 50 mg/ml in dH ₂ O. Rifampicin - 25 mg/ml in DMSO. Kanamycin - 50 mg/ml in dH ₂ O. Basta (Glufosinate ammonium) - 10 mg/ml in dH ₂ O. Amphoterecine - 5 mg/ml in DMSO. Cephotaxime – 200 mg/ml in dH ₂ O.

Buffers**SDS-Polyacrylamide gel electrophoresis (SDS-PAGE) and western blot analysis:**

All the solutions were made with dH₂O.

10X PAGE buffer (1 L)	30 g Tris-base, 110 g glycine, 10 g SDS
Tris buffer (1.5 M) (1 L)	181.71 g of Tris-base. pH was adjusted to desired value with 2M NaOH and stored at 4°C.
6X SDS-PAGE loading buffer (100 ml)	15 g DTT, 15 g SDS, 1.5 g Bromophenol blue, 50 ml glycerol.
Coomassie staining solution (100 ml)	0.25 g of coomassie brilliant blue R-250, 0.25 g of coomassie brilliant blue G-250 in methanol acetic acid solution (40% methanol and 10% acetic acid). The solution was filtered through Whatman filter paper (Grade 1) to avoid particulate matter.
Destaining solution	10% acetic acid, 40% methanol
Fixative	20% ethanol, 10% glycerol
5X Lamelli-gel loading buffer (50 ml)	25 ml (0.5 M) Tris pH 6.8, 5 g SDS, 25 ml glycerin, 3.87 g DTT, 200 g Bromophenolblue
10X Transfer buffer (1 L)	15.1 g Tris, 72 g Glycine and 0.01 g SDS in dH ₂ O
10X TBS (pH 7.4) (1 L)	15 g of Tris-Base, 88 g of NaCl and pH adjusted to 7.4 with conc. HCl
1X TBST	1 liter of TBS, 0.1% Tween 20
Blocking solution	5 g of milk powder in 100 ml of 1x TBST
Ponceau red solution	0.1% Ponceau S in 5% acetic acid

DNA and RNA electrophoresis:

All the solutions were made with dH₂O.

50X TAE buffer (1 L)	242 g Tris-base, 57.1 g glacial acetic acid, 100 ml 0.5 M EDTA pH 8.0
6X gel loading buffer (100 ml)	0.25% Bromophenolblue, 0.25% Xylene cyanol FF, 15% Ficoll 400, 5X TAE
10X MEN (1 L)	41.86 g of MOPS, 4.1 g of Na-Acetate, 3.72 g of Na ₂ -EDTA and pH adjusted to 7.0 with KOH
RNA gel-loading buffer (150 µl)	10X MEN – 750 µl, formamide – 75 µl, formaldehyde – 26.25 µl, ethidium bromide – 1.5 µl, DEPC water or autoclaved double dH ₂ O – 39.75 µl

Buffers for genomic DNA and RNA isolation:

Extraction solution (100 ml)	350 mM sorbitol – 6.38 g, 100 mM Tris-HCl pH 8.0 – 10 ml from 1M stock solution, 5 mM EDTA pH 8.0 – 1 ml from 0.5 M stock solution
Lysis buffer (100 ml)	200 mM Tris-HCl pH 8.0 – 20 ml from 1M stock solution, 500 mM EDTA – 10 ml from 0.5 M stock solution, 2 M NaCl – 11.69 g, 2% CTAB – 2 g
Sarkosyl (100 ml)	N-lauroyl sarkosin – 5 g, Sodium bisulphite - 0.38 g, PVP – 1 g
Chloroform:Isoamyl alcohol	24 ml of chloroform and 1 ml of isoamyl alcohol (v/v)
RNase A (10 mg/ml)	100 mg of RNase A in 10 ml (10 mM) Na acetate (pH 6.0), mixed thoroughly, boiled for 15 min at 95°C and finally neutralised with 1/100 th volume of 1 M Tris pH 8.0. The solution was stored at -20°C.
DEPC water (1 L) for RNA isolation	1 ml of DEPC in dH ₂ O and kept for continuous shaking for over night (O/N). Autoclaved for 90 min before use.

Buffers for Southern and northern blot analysis:

20X SSC (1 L)	3 M NaCl (175.8 g), 0.3 M $\text{Na}_3\text{C}_3\text{H}_5\text{O}(\text{COO})_3$ (88.2 g) and pH adjusted to 7.0.
Denaturation buffer (1 L)	0.5 M NaOH (20 g), 1.5 M NaCl (88 g).
Renaturation buffer (1 L)	0.5 M Tris-HCl (66.5 g), 1.5 M NaCl (88 g) and pH adjusted to 7.0.
Depurination buffer (1 L)	0.2 M HCl (22.5 ml of 32% stock), 0.85 M NaCl (100 g)
NSEB (1 L) (Hybridisation buffer)	250 mM Sodium Phosphate buffer pH 7.2 (250 ml of 1 M stock), 7% SDS (70 g), 1 mM EDTA (2 ml of 0.5 M pH 8.0), 1% BSA (10 g).
Wash buffer 1 (1 L)	2X SSC (100 ml of 20X SSC stock), 0.2% SDS (2 g)
Wash buffer 2 (1 L)	0.2X SSC (10 ml of 20X SSC stock), 0.2% SDS (2 g)

Solutions for protein extraction (from *N. tabacum*):For Chlase overexpressor plants

Homogenisation buffer	0.1 M Tris pH 7.5, 0.5 M sorbitol, 1 mM DTT, 0.1% BSA, 1 mM PMSF.
Solubilisation buffer	0.1 M Tris pH 7.5, 0.5 M sorbitol, 1 mM PMSF, 0.1% Triton X-100.

For WSCP overexpressor plants

Extraction buffer	20 mM sodium phosphate buffer pH 7.5, 1% PVPP, 0.1% β -ME.
-------------------	--

Solutions for isolation of chloroplasts (from Chlase overexpressor plants):

Grinding buffer (1 L)	0.33 M Sorbitol, 50 mM Hepes-KOH (pH 7.3), 2 mM EDTA and 0.1% BSA
Shock buffer (1 L)	25 mM Hepes-KOH pH 8.4 and 4 mM MgCl_2 .

Solutions for ALA synthesising capacity (from *N. tabacum*):

40 mM ALA 5.25 g of 5-aminolevulinic acid in 20 mM potassium phosphate buffer pH 7.0.

Ehrlich reagent 373 ml acetic acid, 90 ml of 70% perchloric acid and 1.55 g of mercuric chloride. Before use 2 g of p-dimethyl amino benzaldehyde was added for 110 ml of Ehrlich reagent.

Other buffers

Sodium Phosphate buffer chart: Mono and di-sodium salts are prepared as 1 M solutions and mixed in a specific ratio to obtain desired pH, sterilised by autoclaving and stored at RT. Dilutions were made in water and used accordingly.

1 M Na₂HPO₄ (1 L): 141.96 g of anhydrous dibasic sodium phosphate in dH₂O.

1 M NaH₂PO₄.H₂O (1 L): 138 g of monobasic sodium phosphate in dH₂O

pH, 25°C	1 M Na ₂ HPO ₄ (ml)	1 M NaH ₂ PO ₄ (ml)
6.0	120	880
6.6	352	648
7.0	577	423
7.4	774	226
8.0	932	68

Potassium Phosphate buffer chart: Mono and di-potassium salts are prepared as 1 M solutions and mixed in a specific ratio to obtain desired pH, sterilised by autoclaving and stored at RT. Dilutions were made in water and used accordingly.

1 M K₂HPO₄ (1 L): 174.18 g of K₂HPO₄ in dH₂O.

1 M KH₂PO₄: 136.09 g of KH₂PO₄ in dH₂O.

pH, 25°C	1 M K ₂ HPO ₄ (ml)	1 M KH ₂ PO ₄ (ml)
6.8	497	503
7.0	615	385

IPTG: 0.1 M solution in dH₂O, filter sterilised and stored at –20°C.

Lysozyme: 10 g of lysozyme in 1 ml of 25 mM NaHPO₄ (pH 7.4) buffer.

80% acetone: 80 ml of 100% acetone + 20 ml of dH₂O.

100 mM PMSF: 17.4 mg of PMSF in 1 ml of dH₂O.

10 mM KOH: 0.56 g of KOH in 1 L of dH₂O.

10% TX-100: 10 ml of TX-100 in 100 ml of dH₂O.

4 METHODS

4.1 Reverse transcription

The reverse transcription of RNA was done according to Sambrook and Russel, (2001). The desired quantity of RNA (2 µg) was incubated for 5 min at 68°C with an oligo dT primer (T18-Pac) followed by 5 min on ice and gentle spin. The reaction mixture contained 5x reaction buffer, 10 mM dNTPs, RNase inhibitor and finally RTase enzyme. The mixture was given a brief spin and incubated at 42°C for 60 min and the reaction was terminated by incubating the mixture at 70°C for 10 min. The resultant cDNA was used as template for DNA amplification by PCR.

4.2 Polymerase chain reaction (PCR)

The desired genes were amplified by PCR (according to Sambrook and Russel, 2001). Typically, a PCR reaction was set in a 50 µl volume with 100 ng of template DNA, 5 µl of 10x reaction buffer, 200 µM dNTP mix, and 10 pmol of gene specific primers, 2 mM MgCl₂ and 2 - 5 units of Taq Polymerase enzyme. The thermal cycles consisted of an initial denaturation at 94°C for 2 min, followed by 34 cycles of denaturation (94°C for 20 s), annealing (58°C for 40 s) and extension (72°C for 50 s). A final extension of 72°C for 10 min was given to fill-in the protruding ends of newly synthesized PCR products. The resultant amplicons were analysed by agarose gel electrophoresis using a standard DNA molecular weight marker.

4.3 Overexpression of Chlase in *E. coli*

Protein expression of *CcCHLASE* sequence (coding for protein without transit peptide) was performed according to Sambrook and Russel, (2001). *E. coli* (BL21DE3pLysS) containing the plasmid vector with or without the Chlase gene was revived from a frozen stock culture stored at -80°C in 50% glycerol. Frozen cells were revived by scrapping the solid ice in the frozen stock vial with a sterile pipette tip and growing them in 3 ml of liquid LB medium containing 100 mg/L Amp for O/N at 37°C in an orbital shaker at 200 rpm. On the subsequent day, 1 ml of O/N culture was inoculated in 200 ml of LB-Amp medium and grown for 2 - 3 h in an orbital shaker (200 rpm) until an O.D. of 0.6 (A₅₄₀ nm) was reached. An aliquot of 3 ml of culture was centrifuged, and the pellet was frozen at -20°C. This pellet represented the uninduced fraction of culture. The remaining culture was induced for gene expression by addition of IPTG (1.2 mM) and incubated for another 2 - 3 h at 30°C. Finally, the bacterial culture was centrifuged at 5,000 x g for 10 min, and the

pellet was sonicated using 25 mM Na-phosphate buffer pH 7.4, 0.5 mg/ml lysozyme and 0.1% TX-100. Sonicate was centrifuged at 10,000 rpm for 15 min to separate soluble (supernatant) and membrane (pellet) fractions. The soluble fraction was mixed with 87% glycerol and preserved as aliquots at -20°C. Membrane fraction was washed twice with 25 mM Na-phosphate buffer pH 7.4, and resuspended in the same buffer containing 0.1% TX-100 and stored at -20°C until use.

4.4 Protein purification and antibody production

Soluble fractions of *E. coli* overexpressing *CcCHLASE* (His-tag fusion protein) were purified using Ni-NTA resin under native conditions as described by manufacturer (Qiagen) in “**The QIAexpressionist™**” manual. Expression and purification of Chlase was repeated and pure Chlase protein was pooled until an amount of approximately 1 mg was obtained. The obtained pure protein was used for the production of polyclonal antibody in rabbits by Pineda Antikörper Service, Berlin, Germany. Additionally, pure protein was also used to test the functional activity of the protein *in vitro*.

4.5 Agarose gel electrophoresis

Agarose gel electrophoresis was carried out as per Sambrook and Russell, (2001).

For DNA: Appropriate quantity of agarose was dissolved in 1X TAE buffer by boiling in a microwave oven. The molten agarose was cooled to 60°C, Et Br was added (0.5 µg/µl) and poured into the Bio-Rad gel casting tray fitted with a comb. Later, the solidified gel was placed in a horizontal agarose gel electrophoresis tank filled with 1X TAE buffer, comb was removed and DNA samples prepared with gel loading buffer (6X) were loaded into slots and electrophoresed at 80 V for 90 min. After the run was complete, the gel was observed under UV illumination and photographed using a Gel-Doc system.

For RNA: Typically done as above, except that agarose was dissolved in sterile dH₂O and on cooling, 4% of formaldehyde and 10% of 10X MEN were added. For analysis, 10 µg of RNA sample was taken, dissolved in 10 µl of RNA gel loading buffer and heated at 65°C for 5 min to denature the RNA. The solidified gel was placed in a horizontal agarose gel electrophoresis tank containing 1X MEN, precooled RNA samples were loaded and run for initial 30 min at 20 V and for 3 - 4 h at 65 V.

4.6 SDS-PAGE analysis of expressed protein

E. coli cell pellets (uninduced and induced fractions) obtained in section 4.3, were resuspended in 5X SDS-PAGE loading buffer and expression of proteins was analyzed by 12% SDS-PAGE.

Initially, the glass plates for gel electrophoresis were cleansed with isopropanol, sandwiched with a 1 mm spacer and fixed to an Amersham gel casting platform. Resolving gel (12% polyacrylamide, 0.1% SDS, 0.375M Tris-HCl, pH 8.8) was poured between the glass plates leaving 2 - 3 cm from the top space, overlaid with water or isopropanol to avoid air contact and allowed to solidify. After the gel polymerization, isopropanol was poured off and the top of the resolving gel was rinsed with water. This polymerized gel was overlaid with a stacking gel (4% polyacrylamide, 0.1% SDS, 0.125M Tris-HCl, pH 6.8) comb was inserted and allowed to solidify. The gel assembly was then placed in a vertical gel electrophoresis tank filled with running buffer and the wells were rinsed with running buffer. The protein samples contained in loading buffer, were boiled at 95°C (5 min), centrifuged (2 min) and loaded into the wells. Electrophoresis was carried out for 90 min at 120 V and gels were stained with Coomassie Brilliant Blue solution (30 min), destained in destaining solution and fixed in fixative solution. Stained protein bands were viewed under white light.

4.7 Western blot Analysis

Separation of proteins by SDS-PAGE and blotting onto nitro-cellulose membrane was performed using semi-dry western blot transfer protocol (Sambrook et al., 1989). Blotted membranes were incubated with protein specific antibody in blocking solution for either 2 h at RT or O/N at 4°C, followed by washing with 1X TBST buffer (three times, each for 10 min). Later, membranes were incubated for 1 h at RT with a species-specific secondary antibody blocking solution (Horseradish Peroxidase conjugated). Finally stringent washings with 1X TBST (three times, each for 10 min) and 1X TBS (two times, each for 10 min) were done to reduce the background. Signals were visualised using Chemiluminescence detection kit (Applichem Ltd) and detected by exposure to X-ray film.

4.8 *In vitro* enzyme activity assays

Functional enzymatic activity of recombinant proteins (*E. coli* expressed) of Chlase and WSCP was assessed through various *in vitro* assays. Essentially, all experiments were conducted in a reaction volume of 700 µl, containing substrate (Chl dissolved in acetone),

enzyme (soluble *E. coli* extracts with 0.1% TX-100) and 25mM sodium phosphate buffer (pH 7.4).

4.8.1 Extraction of Chl for enzyme assays

For *in vitro* enzyme assays Chl was extracted from spinach leaves according to the following protocol. Leaf material of 10 g, was grounded with mortar-pestle using 30 ml of acetone and 3 ml of petrol-ether. The solution was filtered using a gauze cloth and filtrate was poured in a separating funnel. Ten ml of n-Hexane and 10% (w/v) NaCl solution were added to filtrate and the resulting solution was mixed thoroughly and let to stand for few minutes. As the pigments move to the upper hexane phase, the lower aqueous phase was drained off keeping the top of separating funnel open. The hexane phase was washed with 50 ml of dH₂O for 3 - 4 times by removing the water phase. The hexane phase was dispensed into 1 ml aliquots and dried in a vacuum concentrator. Finally, the pellet was dissolved in acetone and concentration of Chl was calculated by measuring the absorbance of Chl at 663 and 646 nm using a spectrophotometer. The amount of Chl *a* and *b* were calculated independently using the formula (Lichtenthaler, 1983) and depending on the % of acetone used to dissolve the Chl.

100% Acetone

Chl *a* (mg/L) = 11.75. A₆₆₂ - 2.35 A₆₄₅

Chl *b* (mg/L) = 18.61. A₆₄₅ - 3.96 A₆₆₂

Chl *a* or *b* (mg/L)*dilution factor = Chl *a* or *b* in mg/μl

Total Chl content = Chl *a* + Chl *b*

80% Acetone

Chl *a* (mg/L) = 12.21.A₆₆₃ - 2.81. A₆₄₆

Chl *b* (mg/L) = 20.13.A₆₄₆ - 5.03.A₆₆₃

The Chl mixtures were also separated into Chl *a* and Chl *b* by TLC. The pigment mixtures were run on TLC films and the respective separated pigments were scrapped out and dissolved in acetone. The pigment extracts of Chl *a* and Chl *b* were dried under vacuum and checked for their characteristic absorbance spectrum.

4.8.2 Conversion of Chl to Phe

The conversion of Chl mixture to Phe was accomplished by addition of few drops of 10% HCl solution, filter sterilised and stored at -20°C. The absorbance of the obtained Phe was measured at 665 and 653 nm (for Phe *a* and Phe *b* respectively) and the corresponding concentrations were calculated according to Lichtenthaler, (1987).

80% Acetone

$\text{Phe } a = 22.42 A_{665} - 6.81 A_{653}$ $\text{Phe } a \text{ (mg/L)} * \text{dilution factor} = \text{Phe } a \text{ in mg/}\mu\text{l}$

$\text{Phe } b = 40.17 A_{653} - 18.58 A_{665}$ $\text{Phe } b \text{ (mg/L)} * \text{dilution factor} = \text{Phe } b \text{ in mg/}\mu\text{l}$

Total Phe content = $\text{Phe } a + \text{Phe } b$

4.8.3 Enzyme assays of Chlase

***E. coli* expressed CcChlase:** The functional activity of CcChlase protein was assessed *in vitro* in a water-miscible organic solvent system using soluble extracts of *E. coli* containing His-CcChlase as enzyme and spinach Chl as substrate. After a specified time interval, 350 μl of the reaction mixture was added to 1 ml of the organic solvent containing acetone/hexane in 1:1 ratio. Obtained mixtures were centrifuged and respective lower aqueous phases were washed with hexane to remove residual Chl. The amount of Chlide *a* formed was determined by measuring absorbance at 663, 646 and 720 nm and calculated according to Lichtenthaler, (1983). A series of enzyme assays were performed to optimise reaction conditions for CcChlase protein and are listed in Table 3. All the data on enzyme activities were presented as a mean of three independent experiments with standard error (SE) bars.

Parameter	A concentration of 0.1% TX-100 was maintained in all the reactions and the assay mixtures were incubated at a shaker speed of 600 rpm.				
	Chl	Bacterial soluble extract containing 0.1% TX-100	Acetone	Time (min)	Temperature
Effect of detergent	250 μ M	100 μ g	16%	15	35°C
Different cellular fractions (homogenate, soluble, membrane)	250 μ M	100 μ g	16%	15	35°C
With purified CcChlase	250 μ M	100 μ g	16%	10, 20, 30	40°C
Effect of pH and temperature (Soluble protein extracts were isolated using different pH buffers during sonication – 6.0, 6.6, 7.4, 8.0)	250 μ M	100 μ g	16%	15	30°C to 60°C (5°C gradient)
Reaction time	250 μ M	100 μ g	16%	5, 10, 15, 30, 45, 60, 75, 90 and 105	40°C
Effect of acetone concentration	250 μ M	100 μ g	10%, 20%, 34%, 49%, 63%, 78%, and 98%	30	40°C
Effect of substrate concentration	50 μ M to 500 μ M with a gradient of 50 μ M	100 μ g	16%	30	40°C
Effect of protein concentration	250 μ M	Soluble extracts (50 μ g to 400 μ g) at 50 μ g gradient	16%	30	40°C
Substrate specificity	Chl <i>a</i> or Chl <i>b</i> (50 μ M to 500 μ M with a gradient of 50 μ M)	100 μ g	16%	30	40°C
Effect of phytol concentration (0, 2, 4, 6, 8 and 10 μ M)	250 μ M	100 μ g	16%	30	40°C

With thylakoid membranes	Thylakoid membranes on the basis of their Chl contents (50 μ M to 500 μ M with a gradient of 50 μ M)	100 μ g	16%	30	40°C
Effect of metal ions (Mg^{+2} , Mn^{+2} , Cu^{+2} , Zn^{+2} , Co^{+2} , Fe^{+2} and Fe^{+3} at a concentration of 10 μ M each)	250 μ M	100 μ g	16%	30	40°C
Effect of functional groups (IAE, NEM, DTT, and β -ME and used at a concentration of 1 mM)	250 μ M	100 μ g	16%	30	40°C
Effect of oil content	250 μ M	100 μ g	Various oil % in reaction (0, 10, 55, 71.4% of oil in the place of buffer)	15	30 to 60°C
Optimisation of different extraction solvents for Chlide recovery <ul style="list-style-type: none"> • Solvent mixture (hexane: acetone) was used in ratios of 1:1, 3:1 and finally only hexane • series of solutions containing water and sodium linoleate in different ratios (4:1, 3:2, 2:3 and 1:4) • buffer (ranging from pH 2-13)/ethanol extraction system 	250 μ M	100 μ g	71.4% oil	15	55°C
Assays using oil extracted from rapeseeds during different phases of oil refining			55% oil		

Table 3: List of conditions and parameters chosen to study the functional activity of recombinant His-CcChlase protein *in vitro*.

From transgenic plants overexpressing *CcCHLASE*: The *in vitro* enzyme activity of overexpressed CcChlase in transgenic plants was determined by performing the enzyme assays using Chl as substrate and plant protein extracts as source of enzyme. Reaction mixtures (1 ml) contained 250 μ M of Chl, 0.1% TX-100 and 25mM sodium phosphate buffer (pH 7.4). The amount of Chlide formed was determined by measuring absorbance at 663, 646 and 720 nm and calculated according to Lichtenthaler, (1983).

4.8.4 Coupled assays with Chlase and WSCP

The ability of WSCP in promoting the functional activity of Chlase was tested *in vitro*. The chosen cDNA sequences of WSCP (*Cau-WSCP-35* and *Cau-WSCP-49*) were expressed as maltose binding protein-fusion proteins (MBP-Cau-WSCP-35 and MBP-Cau-WSCP-49) in *E. coli*, to obtain soluble protein. All the assays were conducted in a water-miscible organic solvent system (700 μ l) using Chl (250 μ M) as substrate and soluble *E. coli* extracts containing recombinant His-CcChlase (100 μ g) as enzyme. Soluble bacterial protein extracts containing MBP-Cau-WSCP-35 / MBP-Cau-WSCP-49 (100 μ g and 200 μ g) were added to the reaction as source of WSCP. Soluble protein extracts of *E. coli* containing empty plasmids pMALC2 and pQE80 were used as negative controls for WSCP and Chlase. Similarly, soluble extract of *E. coli* containing MBP-Cau-Satoh (100 μ g and 200 μ g concentrations) was taken as positive control. Reactions were carried out for 30 min at 40°C and 600 rpm. After specified time intervals, 300 μ l of the reaction mixture was added to 1 ml of the organic solvent containing acetone/hexane in 1:1 ratio. The mixtures were centrifuged, the lower aqueous phases washed with hexane to remove the residual Chl. The amount of Chlide formed was determined by measuring absorbances at 663, 646 and 720 nm and calculated according to Lichtenthaler, (1983).

4.9 Production and analysis of transgenic tobacco plants

4.9.1 Propagation of sterile tobacco plants

WT tobacco seeds (*Nicotiana tabacum* SNN) were germinated *in vitro* on 1MS medium. The seeds were surface sterilised in Millicepitol (an antiseptic alcoholic solution), washed 3 - 4 times with sterile dH₂O and placed on solid 1MS medium plates without any antibiotic. Further, seedlings were sub-cultured for 3 - 4 weeks to obtain mature plants, which were subsequently used for transformation procedures.

4.9.2 Transformation of tobacco plants

The transgenic plants were produced by *A. tumefaciens* mediated transformations using either sterile tobacco hypocotyls or leaf discs (modified version of Horsch et al., 1985).

Propagation of *A. tumefaciens*: Bacterial host (*A. tumefaciens*) containing the binary vector (pCAMBIA3301) with the transgene (cDNA sequence of *CcCHLASE* or *Cau-WSCP-35* coding for the respective protein with transit peptide under the control of 35S promoter) was revived from a frozen glycerol stock. The transgene constructs contained in *A. tumefaciens* were kindly provided by Dr. Ulrich Eckhardt. Cultures were grown O/N at 28°C, 220 rpm for 16 - 24 h in 10 ml YEB medium with antibiotics (rifampicin and kanamycin at 100 µg/L and 50 µg/L, respectively). Subsequently the culture was centrifuged at 3,000 x g for 10 min; the pellet was resuspended in 10 ml of fresh YEB medium with antibiotics and used for further transformations.

Transformation using leaf discs: The WSCP overexpressor plants were produced using sterile leaf discs. Three weeks old sterile tobacco leaves were cut along the mid rib into 1 cm² pieces under sterile conditions. The leaf discs were placed on a sterile Whatman filter paper wet with liquid MS medium and later incubated in the *Agrobacterium* culture for 2 - 3 min. This allows the bacteria to infect the plant cells. The leaf discs were dried on a sterile Whatman filter paper to remove the excess bacteria and placed on plates containing co-cultivation medium. The plates were covered with aluminium foil (to avoid light) and incubated at 28°C for 3 days to allow the transfer of T-DNA into the plant genome. After 3 days, the leaf discs were cultured on callus induction medium with lower sides of leaves facing the medium to facilitate the nutrient intake from the medium through the pores present on the lower side of the leaf. After callus formation, the calli were placed on regeneration medium for the formation of shoots. Shoots were propagated on maturation medium and subsequently transferred to rooting medium for formation of roots. The resultant transformants were selected for their ability to grow on MS medium containing Basta (Glufosinate ammonium). The mature plants developed were transferred to the green house for further analysis.

Transformation using hypocotyls: Hypocotyls were also employed for the production of Chlase overexpressor plants. Hypocotyls used were from 8 - 10 days old seedlings, which have a high potential for cell division. For this purpose, each seedling was cut above the roots and hypocotyls along with the cotyledons were used for transformations. Hypocotyls

were tapped gently with a needle and were placed in liquid culture of *Agrobacterium* on co-cultivation medium and incubated in dark at 28°C. Rest of the steps followed were similar to that for leaf disc transformation. Table 4, shows a tabular representation of the various steps involved in generation of transgenic plants.

Time required	Type of medium	Conditions	
		Light	Dark
3 days	Co-cultivation		28°C
3 – 4 weeks	Callus induction	16 h 22°C	8 h 20°C
3 – 4 weeks	Regeneration	16 h 22°C	8 h 20°C
3 – 4 weeks	Maturation	16 h 22°C	8 h 20°C
3 – 4 weeks	Rooting	16 h 22°C	8 h 20°C

Table 4: Growth conditions adapted for regeneration of transgenic plants either from sterile leaf discs or hypocotyls.

4.10 Plant growth and treatment regimes

Transgenic and WT tobacco plants were grown in green house at 25°C using 12 h light (150 $\mu\text{mol photons m}^{-2} \text{s}^{-1}$) / 12 h dark cycle. Leaves were harvested from 4 - 6 weeks-old plants, frozen in liquid N₂ and stored at -80°C. All experiments were conducted on T1 generation of primary transformants which were obtained by vegetative propagation.

4.11 Analysis of transgenic tobacco plants

4.11.1 Genomic DNA isolation from plants

Genomic DNA was isolated from leaf extracts as described by Doyle and Doyle, (1990).

This method was based on disruption of plant cell structures using mechanical means without degradation of nuclear material. Addition of CTAB, a cationic detergent, effectively removes co-extracted plant polysaccharides. For this, 100 mg of leaf material in liquid N₂ was ground in a homogeniser to break the cell wall. Extraction solution was made fresh taking extraction buffer (preheated to 65°C), lysis buffer containing CTAB and sarcosyl in the ratio of 1:1:0.4. To the ground sample, 750 μl of prewarmed extraction solution was added, mixed by vortexing and incubated at 65°C for 20 min. To the mixture, 750 μl of chloroform: isoamylalcohol (24:1) was added, mixed by vortexing and centrifuged for 10 min at 10,000 rpm. The clear upper phase was transferred into a new test tube, 30 μl of RNase A was added and incubated for 15 min at 37°C. To the mixture, 750 μl of isopropanol was added, mixed and centrifuged for 5 min at 10,000 rpm. The supernatant was discarded and the pellet was washed twice with 70% ethanol by

centrifuging at 10,000 rpm for 5 min. The pellet was dried at 37°C and dissolved in 30 µl of TE buffer or sterile double distilled water. The resultant genomic DNA was used both for PCR and Southern blot.

4.11.2 Initial screening of plants by PCR

All the transgenic plants produced from the section 4.9.2 were initially screened by PCR for the presence of the transgene. For this, the genomic DNA isolated was diluted in water and PCR was performed as per the section 4.2 for individual transgenic lines with respective primer pairs. The selected positive lines were analysed for the functional aspects of the expressed proteins by various methods.

4.11.3 Total RNA isolation from plants

Total RNA was isolated from the leaf material for all selected plants, using Trisure reagent. Trisure maintains the integrity of the extracted RNA while disrupting the cells and subsequently dissolving cellular components (Chomczynski, 1993).

Leaf material of about 100 mg was homogenised in 1 ml of Trisure reagent, vortexed and incubated at RT for 5 min. Subsequently, 0.2 ml of chloroform was added, shaken vigorously for 15 s and incubated at RT for another 2 - 3 min. This results in separation of the mixture into three phases – pale green phenol-chloroform phase, interphase and upper aqueous phase containing RNA. The samples were centrifuged at 12,000 x g for 15 min at 4°C. The upper phase was taken into a new test tube, and 0.5 ml of isopropanol added and incubated for 10 min at RT. The samples were centrifuged at 12,000 x g for 10 min to pellet the RNA. The pellet was washed two times with 1 ml of 75% ethanol, vortexed and centrifuged at 7,500 x g for 5 min. Finally, the pellet was dissolved in sterile distilled water by incubating for 10 min at 55 - 60°C and stored at -80°C. The samples were used for both cDNA synthesis and northern blot analysis.

4.11.4 Radioactive labelling of probes

Radioactive labelled DNA fragments for Southern and northern blot analysis were generated using DecaLabel kit (Fermentas). Initially, the probes for respective gene sequences were amplified using gene specific primers and respective plasmid constructs. The amplicons were then radio labelled with the help of the kit to be used as probes in subsequent hybridization experiments. This kit uses random primers (decamers) which anneal to denatured template DNA and dNTPs along with α -³²PdCTP were then

incorporated into new DNA strands by Klenow fragment exo^- . Typically, reaction contained a template (PCR purified product) of 50 ng, in 10x reaction buffer, denatured at 95°C and supplied with mixture of dNTPs (dATP, dGTP, dTTP and $\alpha\text{-}^{32}\text{PdCTP}$) and Klenow fragment exo^- . On incubation at 37°C for 1 h, radiolabelled probes were synthesised and later purified using ProbequantTM G-50 micro columns to remove the unlabelled isotope.

4.11.5 Southern blot analysis

Southern blot analysis of transgenic tobacco plants was done (according to Southern, 1975) to determine the number of integration sites of the transgene which in turn helps to estimate the copy number of the transgene. Total genomic DNA was isolated from several independent transgenic lines expressing either *CcCHLASE* or *Cau-WSCP-35*. Southern blot analysis was performed according to Sambrook et al. (1989). Genomic DNA was digested with a 6 base cutting restriction enzyme, either EcoRV or XbaI over 12 h at 37°C. Digested fragments were electrophoretically separated on a 0.8% TAE agarose gel at 25 V O/N, viewed under UV transilluminator and photographed. The gel was washed with denaturation buffer for 30 min and incubated in neutralisation buffer for 30 min. Renaturation of DNA was done by incubating the gel in renaturation buffer for 20 min. The processed gel was blotted and DNA was transferred on to a Hybond-N⁺ membrane by upward capillary transfer technique in the presence of 20X SSC. Crosslinking of DNA to membrane was done in presence of 120 mJ of UV light energy for 30 s. The blotted membrane was prehybridised in NSEB buffer for 1 h at 65°C. Hybridisation of the DNA on the membrane was done with incubation of the corresponding ³²P radiolabelled probe for O/N at 65°C. After hybridisation, the membranes were washed two-times (each 15 min) with wash buffer 1 and repeated using wash buffer 2. The membrane was exposed on a phosphoimaging plate for O/N in an autoradiography cassette and visualised for the presence of transgene with the help of phosphoimager. The method was used for analysis of both Chlase and WSCP overexpressor plants.

4.11.6 Northern blot analysis

Northern blot analysis was done to assess the transcript levels of transgene in transgenic plants. For this purpose, total RNA was extracted as described in section 4.11.3 (Sambrook and Russell, 2001). Ten µg of RNA per sample were electrophoretically separated on a 4% formaldehyde-agarose gel, viewed under the UV transilluminator and photographed. The

electrophoresed gel was blotted and RNA was transferred on to Hybond-N⁺ membrane by upward capillary transfer technique in the presence of 20X SSC. The membrane was cross-linked by using 120 mJ of UV light energy for 30 s. The blotted membrane was prehybridised in NSEB buffer for 1 h at 65°C. Hybridisation of the mRNA on the membrane was done with incubation of the corresponding ³²P radiolabelled probe for O/N at 65°C. After hybridisation, the membranes were washed two-times (each 15 min) with wash buffer 1 and repeated using wash buffer 2. The membrane was exposed on a phosphoimaging plate for O/N in an autoradiography cassette and visualised for the transcript levels of the transgene with the help of phosphoimager.

4.11.7 Protein extraction from plants

4.11.7.1 From Chlase overexpressor plants

Hundred mg of leaf material was ground in liquid N₂ and mixed with 1 ml of homogenisation buffer (from section 3.9). The suspension was vortexed and centrifuged for 5 min at 800 x g to remove debris. The supernatant was further centrifuged for 10 min at 5,000 x g at 4°C to separate soluble and membrane fractions. The supernatant contained all the soluble proteins and the pellet comprised of the crude organellar membrane fraction. The pellet was dissolved in 100 µl of solubilisation buffer, centrifuged at 18,000 rpm for 30 min at 4°C. The collected supernatant contained all the membrane bound proteins. Quantification of proteins in both soluble and membrane fractions was done with Bradford reagent using BSA as standard (Bradford, 1976). Separation of proteins by SDS-PAGE and detection of Chlase protein was done by western blotting using anti-Chlase antibody and horse radish peroxidase conjugated secondary antibody.

4.11.7.2 From WSCP overexpressor plants

Hundred mg of leaf material was ground with liquid N₂ and 400 µl of extraction buffer was added and vortexed. The mixture was filtered through a layer of miracloth to remove cell debris, suspended into a test tube and centrifuged at 13,000 rpm for 1 min. The flow through contained all the soluble proteins and were analysed by SDS-PAGE and western blot using anti-WSCP antibody.

4.11.8 Selection of Chlase overexpressor plants based on the functional activity of protein *in vitro*

The PCR positive Chlase overexpressor lines were analysed for enzymatic activity of Chlase *in vitro* to select the most suitable lines for further experiments. Leaf samples from both WT and overexpressor lines were collected in duplicates, each weighing approximately 100 mg. Samples were ground to powder with liquid N₂ and used for pigment and protein extraction. For pigment extraction, 1 ml of ice cold 80% acetone was added and incubated at RT with shaking (500 rpm) for 30 min. Samples were centrifuged and pigment extracts were separated into Chl and Chlide phases by addition of equal volume of n-hexane. Both the phases were measured spectrophotometrically at 663 nm, 646 nm and 720 nm and pigment amounts were calculated according to Lichtenthaler, (1983). Total protein was extracted from the second set of samples according to section 4.11.7.1 and quantified by Bradford assay. Transgenic lines were selected based on amounts of Chlide produced mg protein⁻¹ min⁻¹.

4.11.9 Isolation and fractionation of chloroplasts from Chlase overexpressor plants

Chloroplasts were isolated from WT and Chlase overexpressor lines according to Gualberto et al. (1995). Before isolation of chloroplasts, plants were kept in dark for one day to avoid accumulation of starch grains in the chloroplasts. Isolation procedure was performed at low temperatures and dark conditions.

Fully expanded top leaves (approximately 20 g) were harvested and ground with 100 ml of cold grinding buffer using a Waring blender set at 70% power by three bursts of 5 s each. The homogenate was filtered through two layers of 0.95 µm nylon mesh into precooled polycarbonate centrifuge tubes. Chloroplasts were pelleted by centrifugation at 3,000 x g for 5 min and supernatant was discarded. The chloroplast pellet was gently resuspended in same buffer (with out BSA) with a fine brush. Volume of the suspension was increased to 30 ml and transferred to sterile Corex tubes. The chloroplasts were pelleted at 3,000 x g for 5 min and lysed by hypotonic shock (to separate subsequently stromal and thylakoid fractions), centrifuged and the pellet was resuspended in shock buffer and incubated on ice for 10 min. The suspension was centrifuged at 40,000 x g for 20 min to yield soluble a stromal fraction and a pellet of total chloroplast fraction. The pellet fraction was washed twice and dissolved in shock buffer with 0.1% TX-100. Both soluble and membrane fractions were analysed for functional activity of the recombinant protein.

4.11.10 Experiments on Chlase overexpressor plants

To assess the *in vivo* functional activity of the recombinant CcChlase protein in the Chlase overexpressor plants, various stress experiments were performed and steady state levels of the green coloured pigments were analyzed. The experimental approach was represented in the following Table 5. All the experiments were performed thrice for statistical significance.

Phenomenon	Experimental conditions
Senescence	
Natural senescence	Samples were (100 mg each) were collected from leaves of all developmental stages i.e., young, mature and senescent.
Artificial or induced senescence	
Dark incubation of leaves	Leaves kept in 12 h light / 12 h dark conditions for 5 days and leaves in continuous dark for 5 days.
Treatment with ACC (precursor of ethylene)	Leaf discs kept in water as control and in 3 mM ACC for 24 and 48 h
Methyl jasmonate treatment	Leaf discs kept in water as control and in methyl jasmonate (25 mg/L) for 24 and 48 h
Induction of abiotic stress	
Drought stress	One leaf kept in water as control and other leaf without water for 30 h in a petridish
Salt stress	One leaf kept normal tap water as control and other leaves in 0.5 M NaCl for 2 days.

Table 5: List of various experiments done with WT and Chlase overexpressor plants to analyze the functional activity of recombinant CcChlase *in vivo*.

4.11.11 Experiments on WSCP overexpressor plants

Various experiments were performed to evaluate the functional role of WSCP during plant development and are given in Table 6. All the experiments were performed thrice and the results are represented as mean values with standard error bars.

Phenomenon	Experimental conditions
Senescence	
Natural senescence	Samples were (100 mg each) were collected from leaves of all developmental stages i.e., young, mature and senescent.
Artificial or induced senescence	
Dark incubation of leaves	Leaves kept in 12 h light/12 h dark conditions for 5 days and leaves in continuous dark for 5 days
Etiolating of seedlings	Seed from both WT and T1 generation of WSCP overexpressor plants were taken and germinated in dark and maintained for one week to obtain etiolated seedlings
Induction of abiotic stress	
Drought stress	One leaf kept in water as control and other leaf without water for 30 h in a petridish
Light stress	Detached leaves of both WT and WSCP overexpressor plants exposed to various light intensities ranging from 100 to 1000 $\mu\text{mol photons m}^{-2} \text{s}^{-1}$.

Table 6: Experimental design to analyze the *in vivo* functional activity of overexpressed Cau-WSCP-35 protein in WSCP overexpressor plants.

4.11.12 Analysis of pigments from transgenic tobacco plants

4.11.12.1 Estimation of steady state levels of Chl and Chlide *a*

Steady state levels of Chl and its green coloured catabolite Chlide *a* were quantified in transgenic plants by HPLC. For this, 100 mg of leaf tissue was taken, homogenised in liquid N₂, and 1.5 ml of ice cold 99% acetone (with 10 μM KOH) was added. Samples were vortexed and immediately centrifuged at 13,000 rpm, 4°C for 2 min. Supernatants were collected in separate test tubes (extracts 1). The pellets were again resuspended with 1.5 ml of ice cold 99% acetone (with 10 μM KOH) by vortexing, and incubated on ice for 5 min. Samples were centrifuged at 13,000 rpm, 4°C for 2 min. Supernatants were collected into separate test tubes (extracts 2). Both the extracts (1 and 2) from all samples were measured for their Chl and Chlide *a* contents by HPLC. The amounts were determined by measuring the fluorescence emission spectrum in acetone fractions between 600 and 700 nm. The excitation wavelength was 430 nm. Amounts of the steady state levels of either Chl or Chlide *a* were calculated as the sum of either Chl or Chlide *a* in both the extracts (1 and 2).

4.11.12.2 NCC extraction and quantification

The non fluorescent Chl catabolites (NCC) in Chlase overexpressor plants were determined according to protocol given by Berghold et al. (2004).

One hundred mg of leaf material was ground in liquid N₂ and 400 µl of buffer 1 (20% 0.5 M Tris-HCl, pH 8.0 + 80% methanol) was added and vortexed. Samples were centrifuged for 2 min at 13,000 rpm and supernatants were transferred into new test tube tubes. To each supernatant, 150 µl of buffer 2 (50 mM potassium-phosphate buffer pH 7.0) was added and NCCs were measured by HPLC. The amounts were determined by measuring the fluorescence emission spectrum in the fractions between 350 and 750 nm and excitation wavelength was 320 nm.

4.11.12.3 Determination of Pchlde Content

For the Pchlde determination, samples were fixed for 2 min using steam and ground in acetone/0.1N NH₄OH (9/1, v/v) using mortar and pestle. Suspensions were centrifuged at 5,000 x g for 5 min and supernatants were collected. Carotenoids in etiolated seedlings and Chls in green samples were removed by washing the collected supernatant with an equal volume of hexane. Relative amounts of Pchlde were determined by measuring the fluorescence emission spectrum in acetone fractions between 600 and 700 nm. The excitation wavelength was 435 nm. No correction for Mg-ProtoMME was needed, as its fluorescence at 635 nm under excited at 435 nm was only 1.3% of that observed at 595 nm when excited at 420 nm.

4.11.12.4 Determination Chl catabolite levels in Chlase overexpressor plants due to *in vitro* activity of recombinant CcChlase

Formation of Chl catabolites other than Chlide *a* due to the presence of recombinant CcChlase protein in the overexpressor plants was assayed *in vitro*. Approximately, 100 mg of material was harvested from leaves of various developmental stages and homogenised in liquid N₂, and 0.5 ml of ice cold 80% acetone (with 10 µM KOH) was added. Samples were vortexed and kept at -20°C for 1 h. Samples were centrifuged at 13,000 rpm, RT for 5 min. Supernatants were collected in separate test tubes. The pellets were again resuspended with 0.5 ml of ice cold 80% acetone (with 10 µM KOH) by vortexing and incubated again for 1 h at -20°C. The process was repeated till colourless pellets were obtained. All the supernatants were pooled and measured for their Chl, Chlide *a* and Pheide *a* contents by HPLC.

4.11.13 Determination of ALA-synthesizing capacity

ALA synthesising capacity of transgenic plants was determined according to the protocol of Mauzerall and Granick, (1956).

Three hundred mg of leaf material was taken and incubated in 20 mM potassium phosphate buffer pH 7.0 containing 40 mM levulinic acid (ALA) under light for 6 h. Leaf discs were dried on a paper towel and ground to powder using liquid N₂. To the leaf powder, 1 ml of 20 mM potassium phosphate buffer pH 6.8 was added, vortexed and centrifuged at high speed for 3 min. Supernatants were taken in aliquots of 400 µl, 200 µl and 100 µl and made up to a volume of 400 µl with 20 mM potassium phosphate buffer pH 6.8. To each aliquot, 100 µl of ethylacetoacetate was added, boiled for 10 min at 100°C and kept on ice for 5 min. Five hundred µl of modified Ehrlich reagent was added to each sample, vortexed and centrifuged for 5 min at high speed and absorbance of supernatants were measured at 553nm, 525 nm and 600 nm. The same protocol was followed for plotting a standard curve for ALA taking ALA concentrations from 1 to 100 µg/ml and measuring absorbance at 553 nm, 525 nm and 600 nm. ALA synthesising capacity of the transgenic and WT plants was calculated as µg/gFW based on the standard curve.

4.11.14 Chl fluorescence experiments of WSCP overexpressor plants

The changes in Chl fluorescence in WSCP overexpressor plants on exposure to high light were monitored using a pulse amplitude modulated fluorometer (PAM) (FMS2, Hansatech). Both WT and transgenic WSCP overexpressor plants were grown in the green house as described in section 4.10 and kept in dark 1 h prior to the experiment. Maximum photochemical efficiency of PSII in the dark-adapted state, $F_v / F_m = (F_m - F_0) / F_m$, was measured in all selected lines. Actinic light was supplemented with a high intensity white light source equipped with a 75-W tungsten halogen lamp and delivered via a separate fibre optic connected to the leaf-disc chamber. The actinic light intensity used was 900 µmol photons m⁻² s⁻¹. Measurements were made with two different periods of light stress: short term (6 min) and long term (50 min).

Determination of the Chl fluorescence was a measure for the intactness of PSII. After an initial saturating light pulse, high continuous light was applied for 50 min. Every 10 min, a saturating light pulse was given. After the continuous light was turned off, three saturating light pulses were given every 1 min (Fig. 8). Maximum PSII quantum yield (F_v / F_m) was determined in dark-adapted leaves. After initial chlorophyll fluorescence yield (F_0) was

determined in low modulated measuring light, a 0.8 s pulse of saturating white light ($> 8000 \mu\text{mol photons m}^{-2} \text{s}^{-1}$) was applied to obtain maximum Chl fluorescence yield (F_m) and the F_v / F_m (F_v , the variable Chl fluorescence yield, defined as $F_m - F_o$). Steady-state fluorescence levels (F_s') and maximum Chl fluorescence levels (F_m') during exposure to $900 \mu\text{mol photons m}^{-2} \text{s}^{-1}$ illumination were measured. Actual quantum yield of PSII electron transport (Φ_{PSII}) was calculated as $(F_m' - F_s') / F_m'$. Three individual plants were taken for each selected line (WT and WSCP overexpressor plants) and measurements were repeated twice.

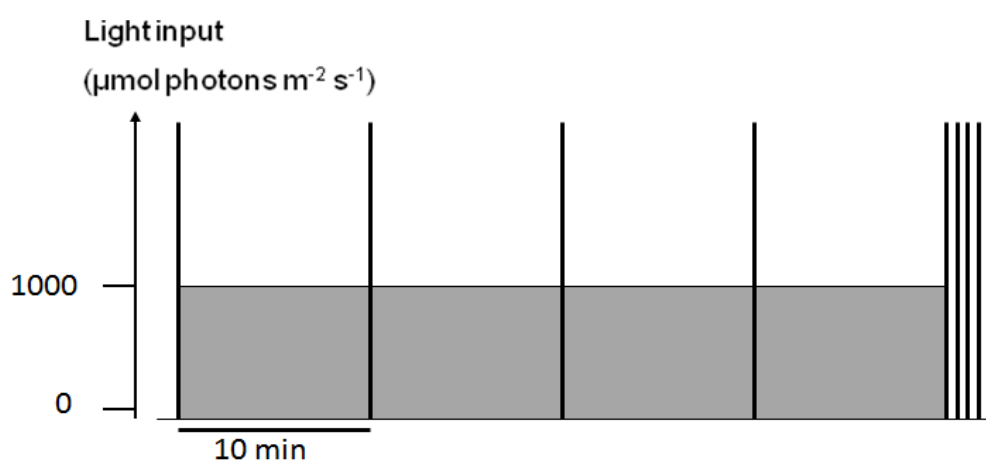


Fig. 8: Schematic representation of measurements of Chl fluorescence using a PAM for 60 min light stress.

4.11.15 Estimation of peroxidase activity in WSCP overexpressor plants

The levels of ROS in terms of peroxide radicals formed as a result of peroxidase activity were measured by using 3, 3'-Diaminobenzidine (DAB).

Detached leaves were taken from both WT and WSCP overexpressor plants and placed under a high light intensity for 4 h. Approximately, 100 mg of fresh leaves were taken from both WT and WSCP-synthesising transgenic plants, homogenised in 1 ml of 10 mM Tris pH 6.5 containing 0.2% Tween 20. Homogenates were vortexed and centrifuged at 13,000 rpm and 4°C for 5 min. Supernatants were collected in separate test tubes and protein contents were quantified by Bradford assay. To 790 μl of buffer, 10 μl of protein extract and 200 μl of 1 mg/ml DAB were added. Absorbance at 330 nm of was recorded as control and 10 μl of 30% H_2O_2 was added as substrate for peroxidase. Absorbances at 330 nm were measured for a period of 2 min with a time interval of 2 s. The results were demonstrated as absorbance/ μg protein and were means of three independent experiments.

The method was repeated at various light intensities ranging from 300 to 700 $\mu\text{mol photons m}^{-2} \text{s}^{-1}$.

4. 11.16 Statistical analysis

All the experiments were performed thrice and the values obtained represent the means of individual data along with their error bars. T-test and F-test were performed using Microsoft excel and the data denoted with * ($p < 0.05$) indicate the significant statistical differences between WT and overexpressor plants.

5 RESULTS

5.1 Chlorophyllase

5.1.1 *CcCHLASE* (Chlase gene from *Citrus clementii*) as transgene

The *CcCHLASE* cDNA sequence inserted in pQE80 (*E. coli* expression vector) was taken as starting material for the present study. This coding sequence was previously cloned from *C. clementii* fruit peels (Damaraju, 2003) and found to be more than 95% homologous to the published cDNA sequence of *CHLASE1* (reference gene) of *C. sinensis* (Jacob-Wilk et al., 1999). The deduced aa sequence of *CcCHLASE* retained the signature motif of serine lipases similar to *CHLASE1* (Fig. 5, section 1.4.1.3). The *CcCHLASE* cDNA sequence cloned into pQE80 was 924 bp long (308 aa; 33 kDa) and lacked the coding sequence for a putative transit peptide. Expression of the recombinant CcChlase protein was optimised in the *E. coli* host, BL21DE3pLysS strain (section 4.3), to obtain the recombinant protein in the soluble bacterial fraction (Damaraju, 2003). The obtained protein contained a N-terminal His-tag and analysis by SDS-gel electrophoresis (Fig. 9) confirmed the calculated molecular weight as approximately 35 kDa (33 kDa CcChlase and approximately 2 kDa of 6XHis-tag).

5.1.2 Purification of His-CcChlase for production of antiserum against Chlase

Antiserum was raised in rabbits against purified recombinant His-CcChlase to analyse the expression of CcChlase protein in Chlase overexpressor tobacco plants. To achieve this, the *CcCHLASE* cDNA (in pQE80) was initially expressed in *E. coli* (BL21DE3pLysS), and the obtained soluble bacterial extracts were purified using Ni-NTA metal affinity chromatography (Qiagen). Pure native His-CcChlase protein was eluted with 250 mM imidazole buffer and was visualised as a single band of size 35 kDa in the coomassie stained gel (lane 6, Fig. 9). Western blot analysis employing an anti-His antibody (lanes, 10, 11 and 12, Fig. 9) confirmed the presence of His-CcChlase in soluble and insoluble fractions of bacterial lysates, as well as in the eluted fraction.

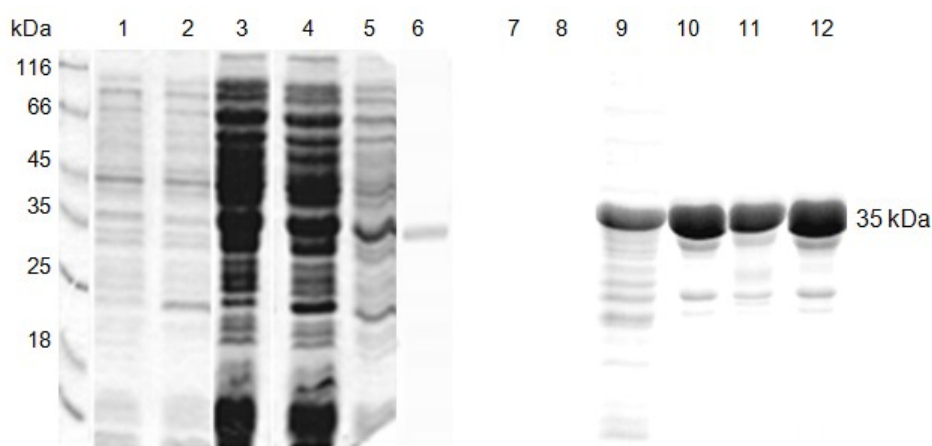


Fig. 9: Coomassie staining of SDS-PAGE (lanes 1 – 6) and western blot analysis (lanes 7 – 12) of recombinant and purified His-CcChlase:
 lane 1, a soluble protein extract of *E. coli* containing empty pQE80 vector (10 µg);
 lane 2, an uninduced fraction of *E. coli* lysate before inducing the expression of *CcCHLASE* with IPTG (10 µg),
 lane 3, total cellular lysate of *E. coli* after inducing the expression of *CcCHLASE* with IPTG (20 µg),
 lane 4, a soluble protein extract of *E. coli* containing His-CcChlase (20 µg),
 lane 5, an insoluble fraction of the sonicated induced culture of *E. coli* containing His-CcChlase (20 µg).
 lane 6, purified His-CcChlase from a soluble protein extract of *E. coli* using Ni-NTA agarose (0.5 µg),
 lane 7, a soluble protein extract of *E. coli* containing empty pQE80 vector as negative control for anti-His antibody,
 lane 8, protein extract of uninduced fraction of *E. coli* before inducing the expression of *CcCHLASE* with IPTG as control for the absence of recombinant protein,
 lane 9, Anti-His tag antibody detected the His-CcChlase as 35 kDa protein band from total cellular lysates (2 µg) of lane 3,
 lane 10, a soluble fraction of lane 4 (2 µg) showing the His-CcChlase protein,
 lane 11, an insoluble fraction of lane 5 (2 µg) showing the His-CcChlase protein,
 lane 12, an immune-reacting band of purified His-CcChlase (0.5 µg) using anti-His antibody.

His-CcChlase from various Ni-NTA purifications was pooled to obtain an amount of 1 mg/ml and supplied to an antibody production company named Pineda Antikörper Service, Berlin, Germany. The anti-serum obtained from rabbits after 60 days of immunisation was used as a source for anti-CcChlase polyclonal antibodies. The antibody solution was tested by western blot against bacterial soluble extracts containing His-CcChlase and total protein extracts of *Citrus* leaves. The antiserum recognised the CcChlase protein in both bacterial soluble extracts containing His-CcChlase (35 kDa; Fig. 10, lanes 10 -12) and *Citrus* leaf extracts (33 kDa; Fig. 10, lanes 12). In another experiment, the antiserum also detected an immune-reacting band of 33 kDa size protein in WT tobacco plants (Fig. 10, lane 14) and also in Chlase overexpressor plants (Fig. 10, lanes 15 and 16). Hence, the use of the anti-

CcChlase antibody has limitations in screening of the CcChlase protein in the overexpressor plants.

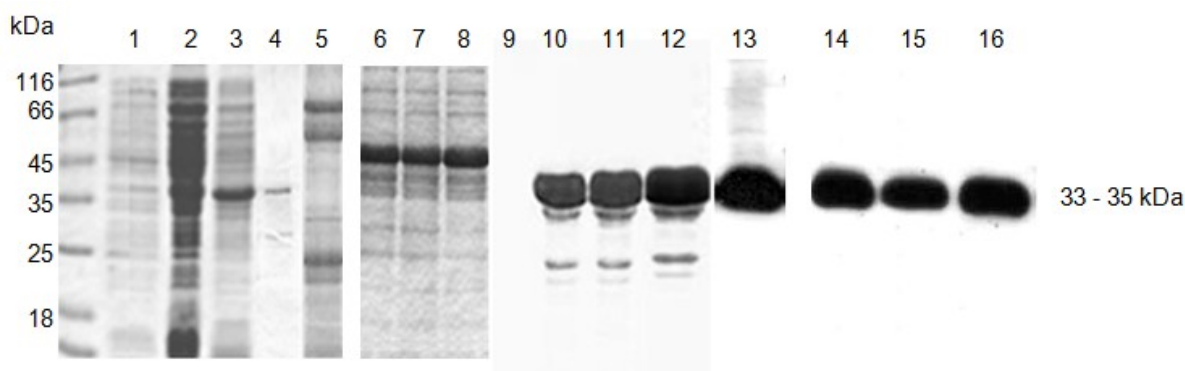


Fig. 10: Coomassie stained SDS-PAGE (lanes 1 – 8) and western blot analysis (lanes 9 – 16) of recombinant and purified His-CcChlase along with total protein extract from *Citrus* and tobacco leaves.

- lane 1, a soluble protein extract of *E. coli* containing empty pQE80 vector (20 µg);
- lane 2, total cellular lysate of *E. coli* containing His-CcChlase (10 µg),
- lane 3, a soluble protein extract of *E. coli* containing His-CcChlase (20 µg),
- lane 4, purified His-CcChlase from soluble protein extract of *E. coli* using Ni-NTA agarose (0.3 µg),
- lane 5, total protein extract from *Citrus* leaves taken as positive control (20 µg)
- lane 6, total protein extract from WT tobacco leaves (20 µg)
- lanes 7 & 8, total protein extract from transgenic tobacco plants overexpressing *CcCHLASE* (20 µg)
- lane 9, soluble protein extract of *E. coli* containing empty pQE80 vector as negative control for anti-His-CcChlase antibody with no detection of protein,
- lane 10, His-CcChlase detected as 35 kDa protein from total cellular extract of *E. coli* (2 µg),
- lane 11, soluble extract (2 µg) of lane 3,
- lane 12, immune-reacting band of purified His-CcChlase (0.3 µg),
- lane 13, *Citrus* leaf total protein extract (20 µg of lane 5) showed Chlase protein (without transit peptide) with a expected size of 33 kDa.
- lane 14, WT tobacco leaf total protein extract (20 µg of lane 6) showed the presence of an immune reacting band of 33 kDa similar to that seen in *Citrus* leaf extracts.
- lanes 15 & 16, total leaf protein extract of a Chlase overexpressing line (20 µg of lanes 7 & 8) showed the presence of an immune reacting band of 33 kDa (similar to *Citrus* and also to WT tobacco as seen in lane 14).

5.1.3 *In vitro* enzyme activity assays of recombinant His-CcChlase protein

In vitro assays were performed to analyse the functional activity of His-CcChlase expressed in *E. coli* system. Enzyme activity was measured by the ability of His-CcChlase to catalyze Chl breakdown, forming Chlide. All the assays were conducted in a water-miscible organic solvent reaction system containing buffer and acetone. Enzyme activity of Chlase was given as the amount of Chlide formed in the reaction (nmol hydrolysed Chl) or as specific activity (nmol hydrolysed Chl mg protein⁻¹ min⁻¹). All the results indicate the mean values ± SE bars of three independent experiments.

5.1.3.1 Enzymatic activity of His-CcChlase protein

A pilot experiment was designed to obtain a quantitative proof that His-CcChlase present in *E. coli* extracts has indeed Chlase activity. Crude lysates obtained after sonication of induced bacterial cultures containing His-CcChlase were assayed for their enzyme activity as described in section 4.8.3. Following the experiment, phase separation of Chl and Chlide in the assay mixtures was carried out using acetone/hexane (1:1). Two controls were included - crude lysate from *E. coli* containing an empty vector (pQE80 without *CcCHLASE*), and a buffer control (without protein). As shown in Fig. 11, sample 3 demonstrated a clear phase separation of Chlide from Chl, indicating the hydrolysis of Chl by His-CcChlase present in the whole cellular lysates of *E. coli*.

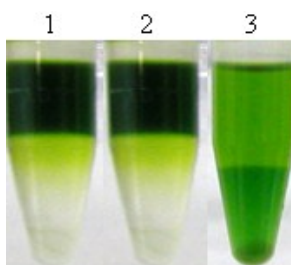


Fig. 11: Recombinant His-CcChlase activity demonstrated by phase separation assay.
Control reaction with no enzyme (only buffer and Chl),
Control reaction with a crude protein extract of *E. coli* containing an empty pQE vector after incubation with Chl for 15 min,
Crude enzyme extract of an *E. coli* strain harbouring the pQE80-*CcCHLASE* vector after incubation with Chl for 15 min.

As Chlase is a membrane protein of chloroplasts, use of detergents and organic solvents during extraction facilitates easy withdrawal of the protein into the soluble phase. Hence during the process of sonication of induced bacterial cultures, 0.1% TX-100 was added to accumulate more recombinant Chlase protein in the soluble fraction. Additionally, presence of a detergent in the reaction medium enhanced the catalytic activity of the enzyme *in vitro* (Benedetti and Arruda, 2002). In order to see the effect of TX-100 on the catalytic activity of CcChlase, assays were done with or without TX-100 in the assay mix. It was observed that addition of 0.1% TX-100 to the protein extracts increased enzyme efficiency of His-CcChlase up to three times. Chlide production in the presence of TX-100 was 8.75 ± 1.23 nmol hydrolysed Chl mg protein⁻¹ min⁻¹ in comparison to an assay without TX-100 yielding 3.06 ± 1.45 nmol mg protein⁻¹ min⁻¹ Chlide. Hence, all *in vitro* assays were carried using 0.1% TX-100 in the reaction mixture (Table 3, section 4.8.3).

Chlase, which contain the conserved serine lipase motif (Tsuchiya et al., 1999), was supposed to be inhibited by serine protease inhibitors such as PMSF in the reaction mixture. PMSF reacts irreversibly and specifically with active serine residues in serine proteases. Hence, the assay reaction was titrated using varying amounts of PMSF to determine its inhibitory effect on Chlase. The protein amount used in the assays was 100 μg (bacterial crude extracts containing His-CcChlase) and PMSF concentration varied between 1 mM to 5 mM. It was observed that PMSF concentration up to 1.5 mM had no effect on Chlase activity, while higher amounts (> 2 mM) inhibited the enzyme activity. Therefore, to minimize the problems of protein degradation during preparation, an amount of 1.2 mM PMSF was added to all the protein extracts.

Comparative analysis of Chlase activity in various cellular fractions of *E. coli* was done to select the most suitable fraction for subsequent enzyme assays. Accordingly, induced cultures of *E. coli* containing His-CcChlase were fractionated into membrane and soluble fractions as described in section 4.3. These two fractions along with an aliquot of the crude lysate from the same culture were assayed for their respective Chlase activity on Chl. As shown in Fig. 12, it was evident that cellular homogenates which contained both soluble and membrane fractions, showed higher activity. However between soluble and insoluble fractions, the former retained higher activity compared to the insoluble fraction.

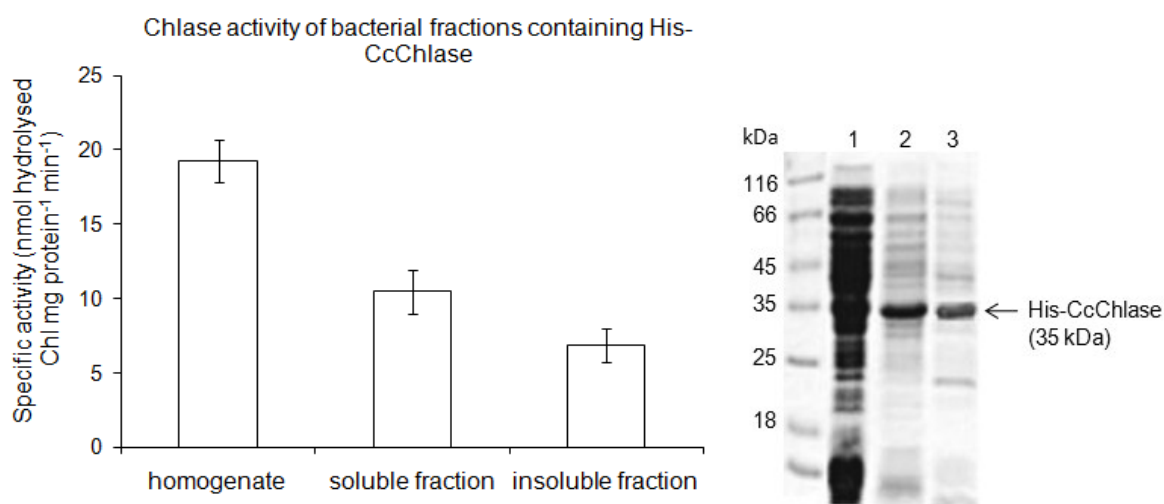


Fig. 12: Enzyme assays of Chlase performed with different cellular fractions of *E. coli* containing His-CcChlase (soluble, insoluble and cellular homogenate - each 100 μg). Specific activity of the enzyme was given as mean \pm SE values of three independent experiments. The protein content of respective cellular fractions used in the assays was presented in a coomassie-stained gel (right panel); lane 1 – homogenate (20 μg), lane 2 - soluble fraction (20 μg) and lane 3 - insoluble fraction (20 μg). The recombinant His-CcChlase protein was seen as a 35 kDa protein band.

Similarly, enzyme activities were also compared between Ni-NTA purified His-CcChlase and crude soluble *E. coli* extracts containing His-CcChlase. As described in Table 3, section 4.8.3, bacterial soluble extract containing unpurified His-CcChlase and purified His-CcChlase (100 μ g each) was assayed using 250 μ M of Chl substrate. Crude soluble extracts of *E. coli* containing empty vector (pQE80 without *CcCHLASE*) were included as control. As shown in Fig. 13, activity of crude soluble extract was nearly 5 times higher, compared to that of a purified protein fraction. The amount of Chl hydrolysed by the action of the crude soluble extract of *E. coli* containing His-CcChlase was higher in the first 10 min. In the next 10 min (i.e., by 20 min), the increase was a little more than 50% of that seen in the initial 10 min. With increase in the reaction time from 20 to 30 min, no big difference was observed in the amount of Chl hydrolysed in the reaction. The soluble bacterial extracts containing empty pQE vector did not show any hydrolysis of Chl and served as a good negative control. Since soluble bacterial extracts containing His-CcChlase gave better results in terms of activity compared to purified protein (Fig. 13), all further assays were performed with soluble extracts of *E. coli*.

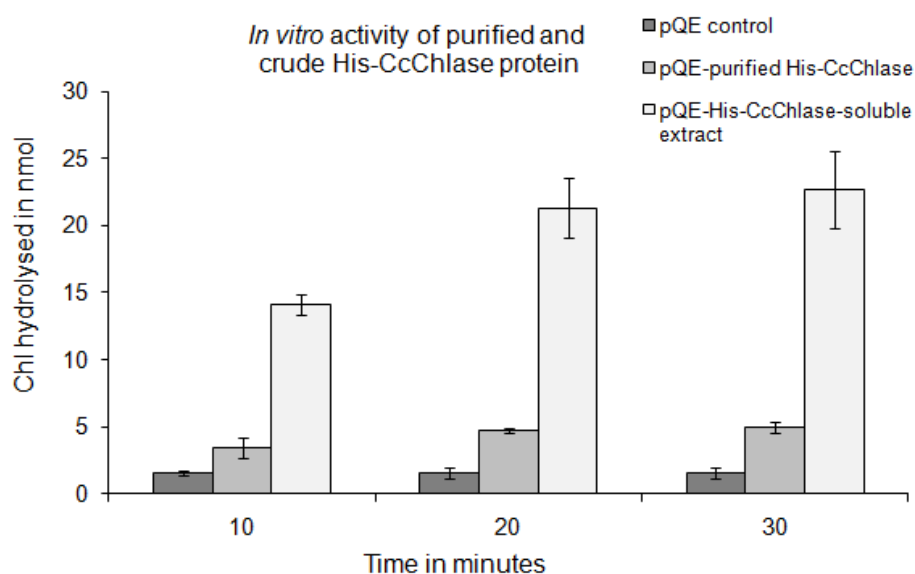


Fig. 13: Enzyme assays of His-CcChlase performed with crude soluble fractions of *E. coli*, purified His-CcChlase and bacterial soluble fractions containing empty pQE80 vector (each 100 μ g). The given values represent the means \pm SE values of three independent experiments. The protein contents in each fraction for comparison can be viewed in Fig. 10 of section 5.1.2.

Based on the above preliminary experiments, soluble *E. coli* fractions containing His-CcChlase with 1.2 mM PMSF and 0.1% TX-100 were used for the subsequent enzyme assays. All the assays were performed as mentioned in Table 3, section 4.8.3, optimising reaction conditions with respect to pH, reaction temperature, incubation time, presence of

metal ions and functional group modifying reagents in the reaction. Further, in view of a possible industrial application of Chlase protein, some parameters, like different oil concentrations and oil from various stages of rapeseed oil refinement, were also determined. Usually, definite amount of substrate (250 μ M of Chl) and enzyme (100 μ g of bacterial soluble extracts containing His-CcChlase) were used in all the assays. But in the assays performed to determine the enzyme kinetic parameters such as K_m and V_{max} , the amounts of substrate and enzyme were varied accordingly.

5.1.3.2 Optimization of temperature and pH for His-CcChlase activity

The activity of enzymes strongly depends on changes in temperature and pH. Temperature affects the activation energy of the catalytic reaction and also the thermal stability of enzyme and substrate. Similarly, pH of the medium controls the ionization state of charged aa residues in the protein, and thus affects the enzymatic activity. Therefore activity of soluble *E. coli* extracts containing His-CcChlase was measured as a function of pH and temperature. To accomplish this, *E. coli* cultures containing His-CcChlase were sonicated and extracted using sodium phosphate buffers of varying pH (section 3.9). These extracts contained in pH specific sodium phosphate buffers were used for the assays.

As shown in Fig. 14, optimal temperature for His-CcChlase activity was in the range between 40°C to 50°C depending on the pH of the buffer. It was observed that enzyme activity in high pH buffers (pH 7.4 and 8.0) was higher at 40°C and declined gradually with an increase in temperature. On the other hand, enzyme activity in low pH buffers (pH 6.0 and 6.6) showed relatively a gradual increase in enzyme activity with a high activity at 50°C. Overall, a pH of 7.4 or 8.0 and a temperature of 40°C were found to be optimal for His-CcChlase activity, since these conditions showed high enzyme activity.

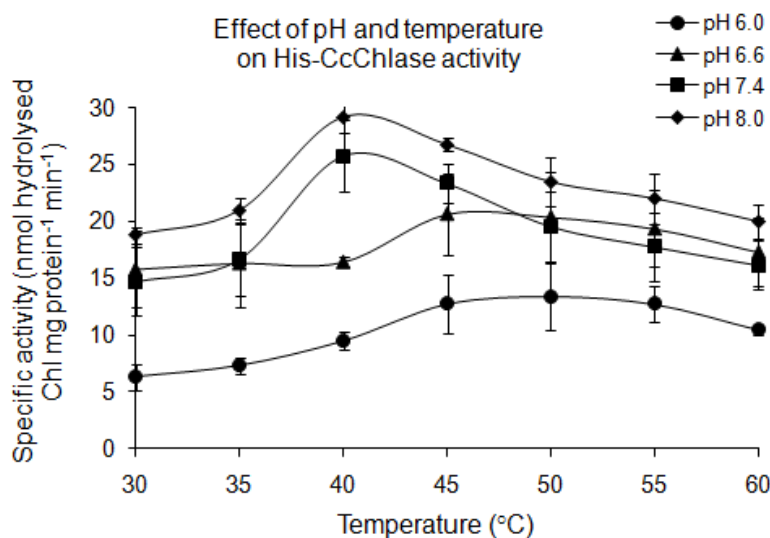


Fig. 14: Effect of pH on stability and activity of His-CcChlase. Specific activity was expressed as nmol hydrolysed Chl mg protein⁻¹ min⁻¹. Higher activity of His-CcChlase was recorded at 40°C using buffers of pH 7.4 and 8.0.

5.1.3.3 Effect of reaction time on enzyme activity of His-CcChlase

To estimate the reaction time required to attain maximum hydrolytic activity of Chlase, assays were performed by varying the incubation times of the reaction. Objective of the experiment was to examine the efficiency of the enzyme in terms of its continuous activity, and whether inhibition or inactivation/degradation of Chlase would reduce the enzyme activity with time.

The results in Table 7 show percentage of residual Chl after hydrolysis with His-CcChlase for specified incubation time period. It was observed that an incubation time of 5 min resulted in nearly 4.4% of Chl hydrolysis, as denoted by 95.6% of residual Chl. Increasing the reaction time to 30 min resulted in 10% Chl hydrolysis. Further increase in time showed only a marginal 1.4% increase in the amounts of Chl hydrolysis between 30 min and 105 min. Based on this experiment, it could be said that the activity of Chlase was observable up to 30 min, with highest during the first 5 min. This may be explained by the higher availability of the substrate to the enzyme in the initial 5 min. The decrease in Chl hydrolysis after 30 min might be due to presence of excess substrate in the reaction mixture compared to enzyme content or decrease in the stability of the enzyme. The specific activity of the enzyme was higher in the first 5 min of the reaction and decreased gradually with increasing time period.

Reaction time (min)	Residual Chl (%)	Specific activity (nmol hydrolysed Chl mg protein ⁻¹ min ⁻¹)
5	95.6	21
10	94.2	14
15	92.0	13
30	90.0	8
45	89.8	4
60	89.4	3
75	89.1	2.4
90	88.7	2
105	88.6	1.6

Table 7: Effect of reaction time on His-CcChlase-catalysed hydrolytic activity on Chl in a water-miscible organic solvent system. About 10% of Chl hydrolysis was reached in 30 min of reaction time. The amount of Chl present in the reaction before start of the reaction was taken as 100% to calculate the % of subsequent Chl hydrolysis.

5.1.3.4 Effect of acetone concentration on His-CcChlase activity

Acetone was the choice for solubilising Chl, because of its good solubility and low toxicity compared to other solvents like methanol, hexane, chloroform, *n*-propanol. An assay was designed to determine the effect of acetone on the activity of His-CcChlase, by varying the acetone content from 10 to 98% (vol/vol) in a water-miscible organic solvent system.

The results in Fig. 15 show that specific activity of His-CcChlase was more or less similar between 10 - 38% of acetone, differing marginally by 1.5 fold. Higher acetone content (> 40%) resulted in a steady fall of enzyme activity, with almost no activity at 80 - 98% acetone. Higher quantity of acetone precipitates proteins (enzyme) in the reaction mix and therefore, has an inhibitory effect on Chlase activity.

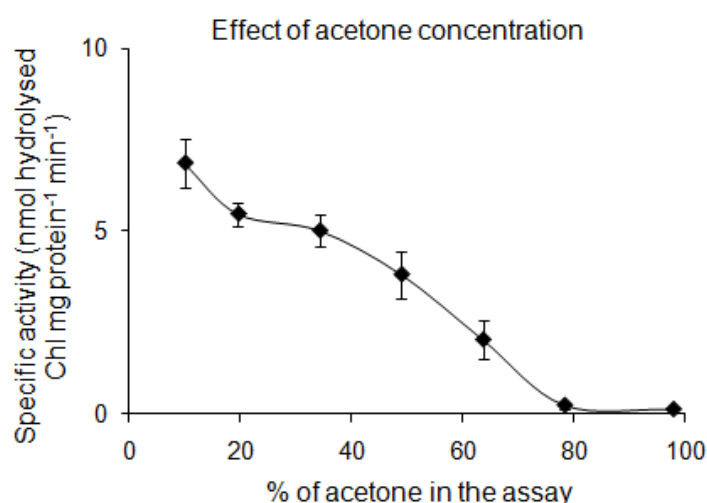


Fig. 15: Effect of increased acetone concentrations on His-CcChlase activity. The activity was given in terms of specific activity of the enzyme (nmol hydrolysed Chl

mg protein⁻¹ min⁻¹). Increased acetone amounts in the assays decreased the activity of His-CcChlase.

5.1.3.5 Effect of substrate concentration on His-CcChlase activity

Rate of enzymatic reaction depends on substrate concentration. At a constant enzyme concentration, lower substrate levels could be a limiting factor, while a higher substrate level saturates the reaction and does not enhance the reaction. Hence it is critical to determine the V_{max}, which is the maximum velocity achieved, when the enzyme is saturated with substrate. Accordingly, an assay was designed for a stepwise increase of 50 μ M substrate (Chl) content from 50 to 500 μ M. The obtained results (Fig. 16a) plotted as a graph exhibit a typical Michaelis-Menten kinetics as the amount of product (Chlide) increased with subsequent increase in substrate concentration.

Fig. 16b shows a Lineweaver-Burk plot with reciprocal of velocity (1/V on Y-axis) versus reciprocal of substrate (1/S on X-axis) using non linear regression analysis. The determined K_m value of Chlase was 272.3 nmol/ml Chl indicating the substrate concentration to achieve half of the enzyme's maximum velocity. V_{max} (rate of the reaction), was calculated from the plot and found to be 39.6 nmol hydrolysed Chl mg protein⁻¹ min⁻¹.

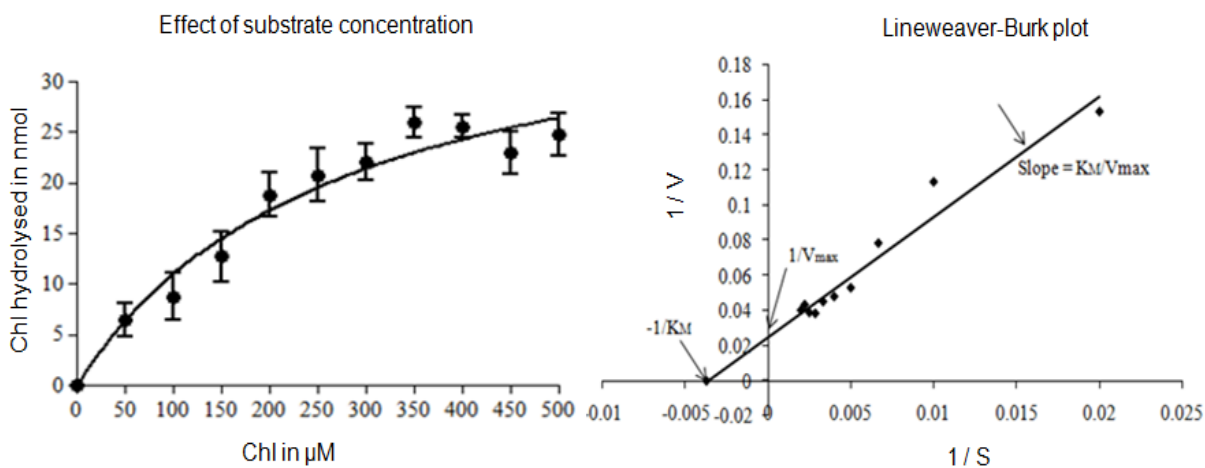


Fig. 16: a) Effect of increased substrate concentration on hydrolytic activity of His-CcChlase. b) Lineweaver-Burk plot of effect of substrate concentration on hydrolytic activity of His-CcChlase.

5.1.3.6 Effect of protein concentration on His-CcChlase activity

This assay was designed to study the effect of increasing enzyme concentration on Chlase catalysed hydrolysis, keeping the amount of substrate (250 μ M of Chl) and incubation time period (30 min) constant. The results (Table 8) show that an increase in enzyme concentration from 50 - 400 μ g, increased the amount of Chl hydrolysed by almost 5 times.

soluble extract containing His-CcChlase (μg)	% of Chl hydrolysis in 30 min
50	3.3
100	5.3
150	6.6
200	8.1
250	9.7
300	11.4
350	13.2
400	14.3

Table 8: Extent of Chl hydrolysis as a result of increased protein concentration in the assay mixture with defined substrate concentration ($250 \mu\text{M}$) and reaction time (30 min). The protein amounts in the reaction medium varied from 50 - 400 μg with a gradient of 50 μg .

Based on Lineweaver-Burk graph ($1/V$ vs $1/S$) using non-linear regression analysis, K_m and V_{max} values were calculated and found to be 242.3 nmol/ml of Chl and 46.9 nmol hydrolysed Chl $\text{mg protein}^{-1} \text{ min}^{-1}$ respectively (Fig. 17).

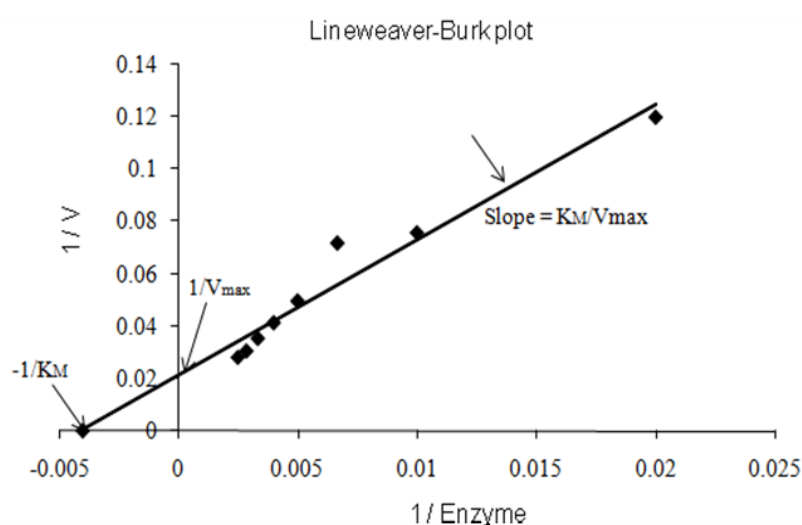


Fig. 17: Lineweaver-Burk plot: Effect of enzyme concentration on His-CcChlase activity.

5.1.3.7 Substrate specificity of His-CcChlase

As it is well known that Chlase easily catalyses Chl *a* than Chl *b*, activity of recombinant His-CcChlase was tested to assess the affinity of the enzyme to the substrate. The substrate used was either purified Chl *a* or Chl *b* (as described in section 4.8.1) taken in various concentrations (from 50 - 500 μM with increasing gradient of 50 μM).

Initially, Chl *a* was checked for its affinity on Chlase and the K_m and V_{max} were calculated. It was observed that the amount of Chl hydrolysed increased exponentially up to 250 μM and then remained stationary (Fig. 18a). Based on Lineweaver-Burk graph ($1/V$ vs $1/S$) using non-linear regression analysis, K_m and V_{max} values were calculated and found to be 148.9 nmol/ml of Chl *a* and 25.9 nmol hydrolysed Chl mg protein⁻¹ min⁻¹ respectively (Fig. 18b).

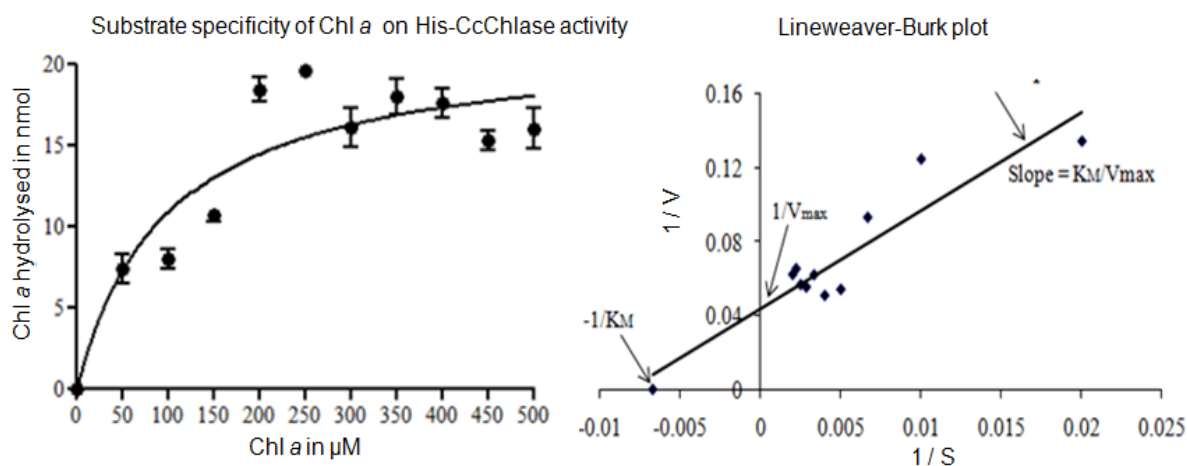


Fig. 18: a) Substrate specificity of His-CcChlase: Activity of Chlase on Chl *a*.
b) Lineweaver-Burk plot: Substrate specificity of Chl *a* on hydrolytic activity of His-CcChlase.

Similarly, enzyme activity of His-CcChlase was also tested with increasing concentrations of Chl *b* as shown in Fig. 19a. Amount of Chlase activity recorded a steep increase at 50 μM and continued to show a gradual increase until 250 μM of Chl *b* substrate concentration. Later on, even an addition of higher amounts of substrate did not influence the enzyme activity to a larger extent. K_m and V_{max} values were calculated based on Lineweaver-Burk graph ($1/V$ vs $1/S$) using non linear regression analysis, and found to be 48.9 nmol/ml of Chl *b* and 24.8 nmol hydrolysed Chl mg protein⁻¹ min⁻¹ respectively (Fig. 19b).

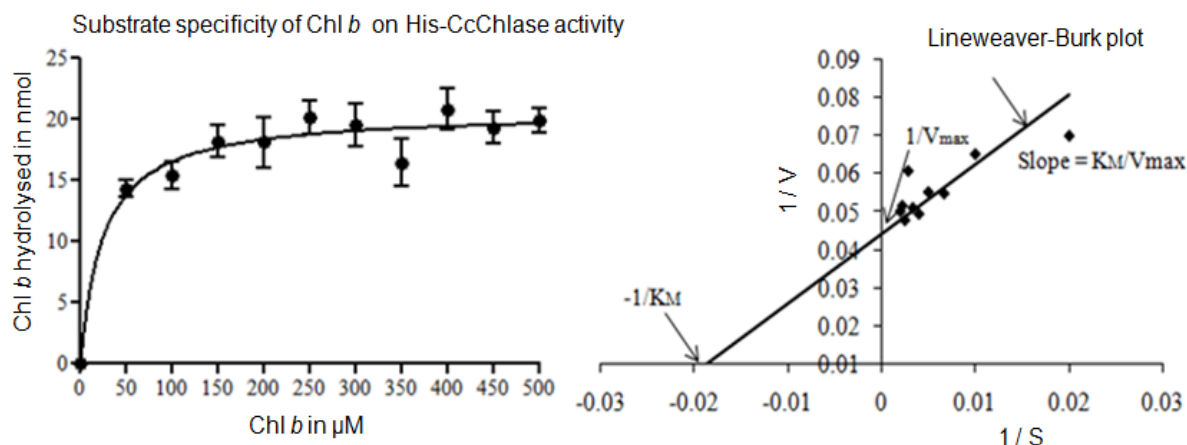


Fig. 19: a) Substrate specificity of His-CcChlase on Chl *b*.
b) Lineweaver-Burk plot: Substrate specificity of Chl *b* on His-CcChlase activity.

5.1.3.8 Effect of phytol concentration on His-CcChlase activity

Phytol, a byproduct of Chl hydrolysis has a non-competitive inhibitory effect on Chlase. Therefore, assays were designed to study the inhibitory effect of increasing concentrations of phytol on the catalytic activity of His-CcChlase. Phytol was added at concentrations of 0, 2, 4, 6, 8 and 10 μM in the reaction. The results confirmed the inhibitory effect of phytol on Chlase activity, as seen from a reduction in Chlide amounts in the reaction mixture. Phytol at a concentration of 10 μM almost inhibited Chlase activity resulting a meagre 0.4% of Chlide, as against 28% Chlide in the absence of phytol (Fig. 20a). A Lineweaver-Burk graph was plotted with 1/V (Y-axis) and phytol concentration (X-axis) using non linear regression analysis (Fig. 20b). The K_i value for phytol was determined to be 5.4 $\mu\text{M}/\text{ml}$ and V_{max} of Chlase was 34.8 nmol hydrolysed Chl $\text{mg protein}^{-1} \text{ min}^{-1}$ respectively.

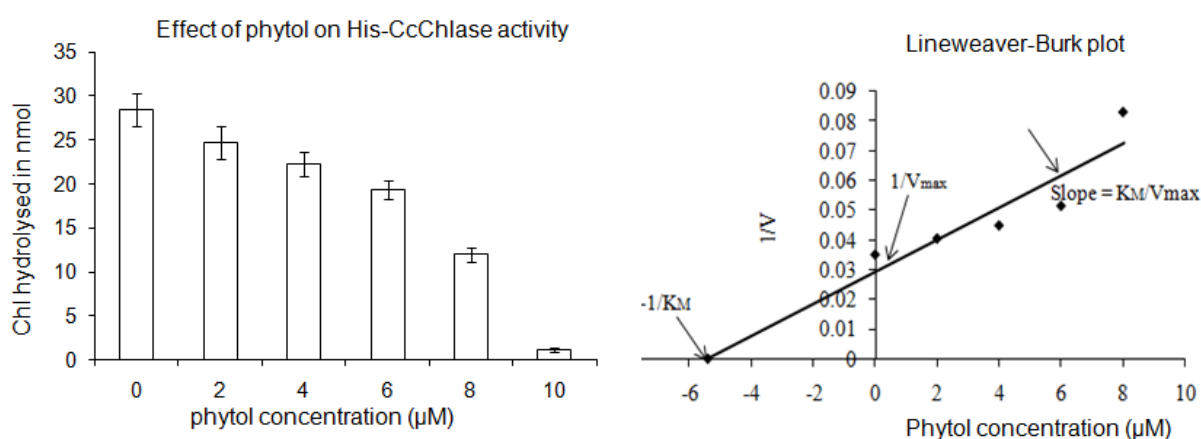


Fig. 20: a) Effect of phytol on hydrolytic activity of His-CcChlase. b) Lineweaver-Burk: Effect of increasing phytol concentration on His-CcChlase activity.

5.1.3.9 Chlase activity on thylakoid membranes

Chlase, being an intrinsic membrane protein (Matile et al., 1997), was tested for its activity on Chl localized in thylakoid membranes. Thylakoid membranes were applied to the assay in amounts based on their Chl concentrations, from 50 to 500 μM with a stepwise gradient of 50 μM . The amount of enzyme was kept constant i.e., 100 μg of bacterial soluble extracts containing His-CcChlase in all the reactions irrespective of substrate concentration. Results shown in Fig. 21a indicate that Chlide amounts increased steadily with an increase in Chl concentration. The Lineweaver-Burk graph was plotted with $1/V$ (Y-axis) and $1/S$ (X-axis) using non linear regression analysis (Fig. 21b). The K_m value determined was 259.9 nmol/ml of Chl. V_{max} was calculated to be 54.8 nmol hydrolysed Chl $\text{mg protein}^{-1} \text{ min}^{-1}$ respectively.

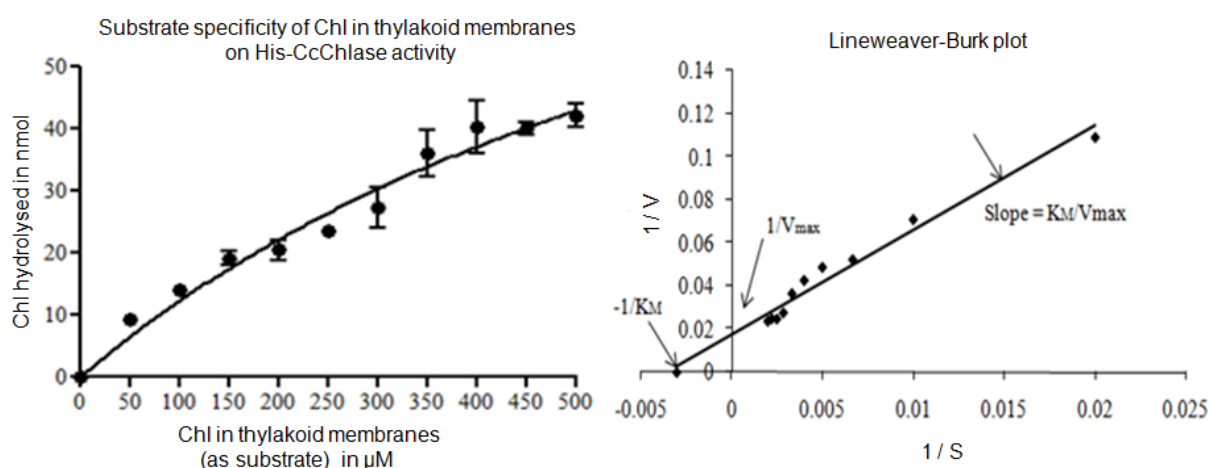


Fig. 21: a) His-CcChlase activity with varied concentrations of Chl in thylakoid membranes. b) Lineweaver-Burk plot: Effect of increasing concentration of Chl in thylakoid membranes on hydrolytic activity of His-CcChlase.

5.1.3.10 Effect of various metal ions on His-CcChlase activity

The effect of various metal ions (Mg^{+2} , Mn^{+2} , Cu^{+2} , Zn^{+2} , Co^{+2} , Fe^{+2} and Fe^{+3} at a concentration of 10 μM each) on enzyme activity of His-CcChlase was studied. The enzyme solution was incubated with the respective metal ion for 4 h at 4°C prior to assay. In parallel, enzyme with no metal ion incubation was used as control.

Metal ion	Inactivation (%)
Control	100
Mg ⁺²	23 ± 2
Mn ⁺²	76 ± 1
Cu ⁺²	67 ± 2
Zn ⁺²	64 ± 4
Co ⁺²	65 ± 3
Fe ⁺²	71 ± 1
Fe ⁺³	43 ± 2

Table 9: Metal ion effect on hydrolytic activity of His-CcChlase in a water-miscible organic solvent system. The amount of Chl hydrolysed in control reaction (without metal ion) was taken as 100%. A subsequent decrease in Chlide amounts produced due to the presence of the respective metal ion in the reaction was given as % of inactivation of His-CcChlase by the metal ion.

The results shown in Table 9 indicate that addition of metal ions in the reaction mix had an inhibitory effect on Chlase activity, resulting in lesser amounts of Chlide. Of all the metal ions studied, Mg⁺² and Fe⁺³ had a relatively lower inhibitory effect on His-CcChlase.

5.1.3.11 Effect of reagents that modify the functional groups on His-CcChlase activity

Various reagents with modifying effects on functional groups were reported for their capacity to alter the activity of His-CcChlase *in vitro* (Hornero-Mendez and Minguez-Mosquera, 2001). The reagents selected were IAE, NEM, DTT, and β-ME and used at a concentration of 1 mM. Enzyme aliquots were pre-incubated with the respective reagents for 4 h at 4°C and enzyme incubated without any reagent was taken as control. As shown in Table 10, DTT and β-ME had an enhancing effect. On contrary, IAE and NEM had a slightly inhibitory effect.

Reagent	Activity (%)
Control	100
IAE	88 ± 6
NEM	78 ± 1
DTT	128 ± 6
β-ME	135 ± 9

Table 10: Effects of application of various functional group modifying reagents on the hydrolytic activity of His-CcChlase in a water-miscible organic solvent system. The amount of Chl hydrolysed in control reaction (absence of reagent) was taken as 100%. Based on the Chlide amounts produced in the reaction due to the presence of respective reagent, the % of activity exhibited by His-CcChlase was given in the table.

5.1.3.12 Effect of oil concentration on His-CcChlase activity

It was of great interest to determine the activity of His-CcChlase in a water-miscible organic solvent system, by adding different percentages of oil. These assays were designed to examine the applicability of recombinant Chlase for use during oil processing from green rapeseeds in the oil processing industry to reduce Chl content in the mature rapeseeds. Assay parameters maintained were mentioned in Table 3, section 4.8.3.

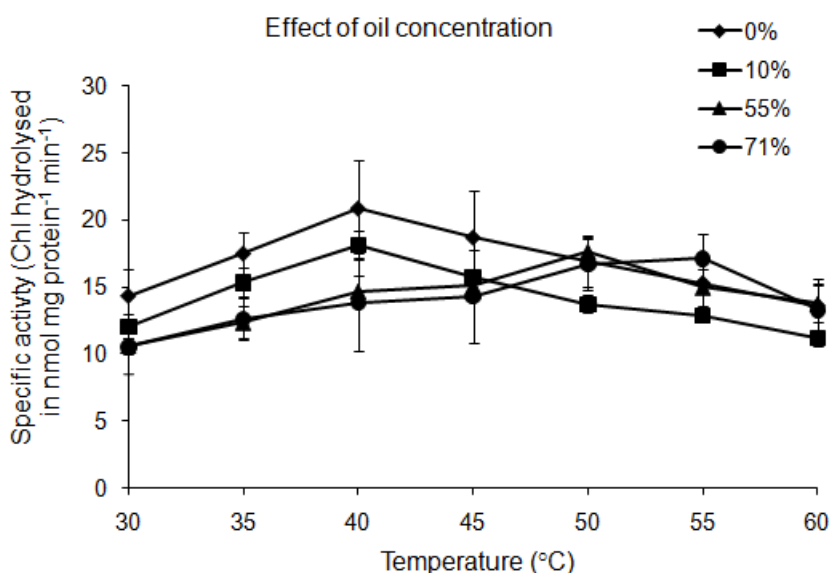


Fig. 22: Changes in specific activities of His-CcChlase based on oil concentration in the reaction medium.

As shown in Fig. 22, it was evident that an increase in the oil proportion of the reaction mixture resulted in a decreased Chlase activity. It was observed that 10% oil in the assay resulted in 16% reduction in enzyme activity. Similarly, 55% and 71% oil in the reaction resulted in a decrease in enzyme activity by 26% and 34% respectively. A significant aspect of this assay was the functional activity of His-CcChlase even in the reaction mixture with 71% oil. It was observed that optimal catalytic activity of His-CcChlase was at 40°C in case of 0% and 10% oil concentration in the assays. But with 55% and 71% oil containing assays, the optimal activity was recorded at 55°C.

5.1.3.13 Optimization of different extraction solutions in the oil assays for maximal Chlide recovery

Acetone, the most commonly used organic solvent for Chlide recovery in *in vitro* Chl hydrolysis experiments, has certain limitations in oil industry. Presence of even trace amounts of acetone could lead to turbidity of oil during storage and hence alternate extraction solvents are used for enzymatic hydrolysis. To analyse and compare the

efficiency of other organic solvents, like hexane and ethanol, in Chlide recovery with acetone, assays were designed accordingly. In addition, fatty acid like sodium linoleate was also analysed for its capacity of Chlide recovery as suggested by oil industry (PPM – Pilot Pflanzenöltechnologie Magdeburg e. V, Magdeburg, Germany). The assays contained Chl dissolved in oil, and subjected to His-CcChlase hydrolysis. Resultant Chlide was recovered after phase separation using one of the above mentioned extraction solvents.

Experiments containing either hexane alone or in combination with acetone (hexane:acetone in 1:1 and 3:1 ratios) as solvent mixture, showed that extraction of Chlide was higher in the presence of acetone compared to hexane alone (Fig. 23).

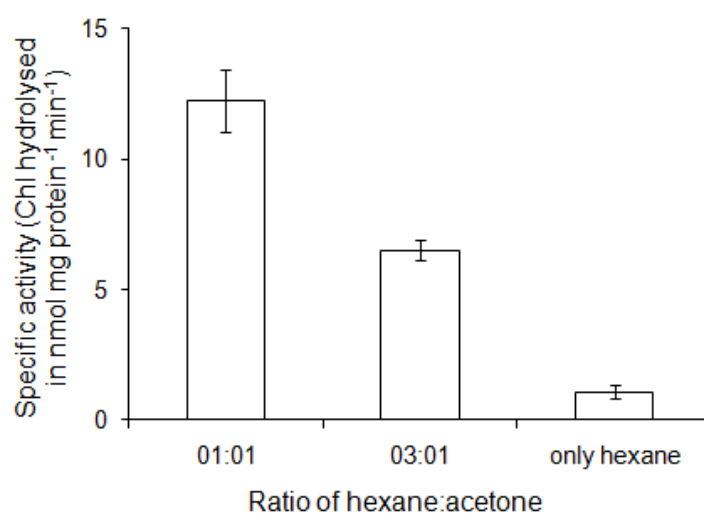


Fig. 23: Extraction capacity of hexan/acetone mixture (different ratios - 1:1, 3:1 and finally only hexane) to retain Chlide formed in the reaction.

Similarly, sodium linoleate was analysed for its efficiency in extracting Chlide after phase separation, using a series of solutions containing water and sodium linoleate in different ratios. The results are summarized in Table 11.

Water:0.1 M sodium linoleate	Chl hydrolysed in nmol mg protein ⁻¹ min ⁻¹
Only water control	5.3 ± 1
4:1	8.2 ± 0.6
3:2	9.7 ± 0.37
2:3	12.1 ± 0.9
1:4	14.4 ± 0.2

Table 11: Chlide extraction using water-linoleate mixture (in the ratios of 4:1, 3:2, 2:3, and 1:4).

An increase in the linoleate ratio relative to water in the phase extraction mixture resulted in higher amounts of Chlide which accumulated in the aqueous phase during the assays. Comparison of the extraction method of water-linoleate (1:4) with that of hexane/acetone (1:1) from Fig. 23, show that the linoleate mixture can be used successfully instead of hexane/acetone, as similar amounts of Chlide were deposited in both the cases.

A different extraction approach of Chlide was examined using a buffer/ethanol system. The Chlide extraction capacity was tested at different pH and was compared to the previous hexane/acetone extraction system. Using the buffer (ranging from pH 2 - 13)/ethanol extraction system (Fig. 24), highest amounts of Chlide were collected in the aqueous phase at pH 8.

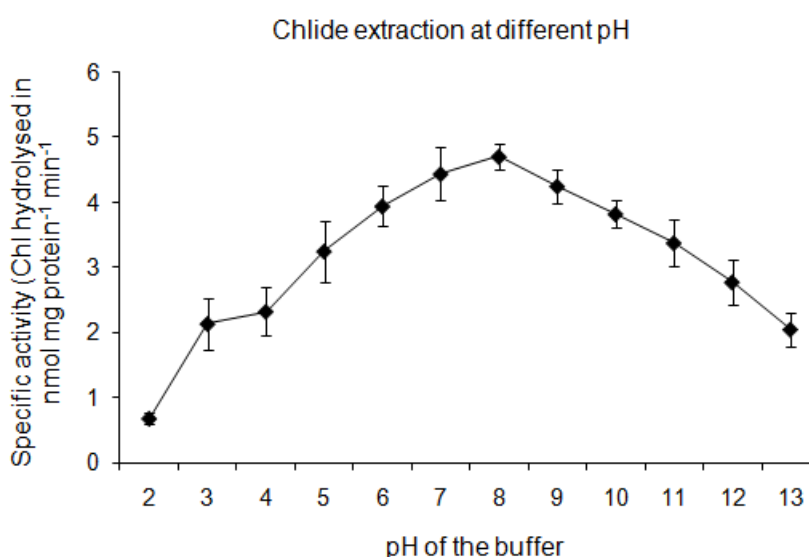


Fig. 24: Extraction of Chlide in a buffer-ethanol system at different pH (2 to 13).

From the above pH extraction method, it was observed that deposition of Chlide into the aqueous phases was possible using a buffer/ethanol system. With an increase in pH of the buffer from 2 to 8, the amount of Chlide deposited reached maximum and a further increase in pH resulted in lower deposition of Chlide in the aqueous phase. Even then, the amounts of maximum Chlide extracted at pH of 8.0 were much lower to those obtained by using either a hexane/acetone (1:1) system or a water-linoleate mixture (3:2, 2:3, and 1:4).

5.1.3.14 Activity of His-CcChlase on Pheophytin as substrate

Pheophytin (Phe), a byproduct of Chl catabolism was produced during the oil processing and acts as a prooxidant leading to reduced stability of oil (Tautorus and Low, 1992). Hence, the presence of Phe in oil should be minimized to account for increased stability of

oil. The present experiment was done to estimate the catalytic activity of Chlase on Phe, when it was subjected as substrate to the catalytic reaction.

Assays were carried out as mentioned in Table 3 (section 4.8.3) using both Phe and Chl as substrates for His-CcChlase. The results were summarized in Table 12. Although, the hydrolytic activity of His-CcChlase was less in case of Phe in comparison to Chl, addition of Chlase to Phe in the oil resulted in formation of Pheide *a* confirming the catalytic activity of Chlase on Phe.

With Chl as substrate (250 μ M)	Chlide <i>a</i> in nmol mg protein ⁻¹ min ⁻¹ - 16 ± 2.3
With Phe <i>a</i> as substrate (250 μ M)	Pheide <i>a</i> in nmol mg protein ⁻¹ min ⁻¹ - 10.2 ± 0.6

Table 12: Hydrolytic activity of His-CcChlase on Phe and Chl as substrates. The amount of substrate was 250 μ M and the enzyme concentration in the assay was 100 μ g of bacterial soluble extracts containing His-CcChlase.

5.1.3.15 Activity of His-CcChlase on Chl in oils at different stages of oil refining

Enzyme assays were also performed using oil at different stages of refinement to check whether the soluble extracts containing recombinant His-CcChlase can decrease the Chl content of rapeseed oil which was supplemented in a pilot fermenting device to prove the concept. The results clearly showed that addition of soluble extracts containing recombinant His-CcChlase can reduce the Chl in refined oil (Fig. 25).

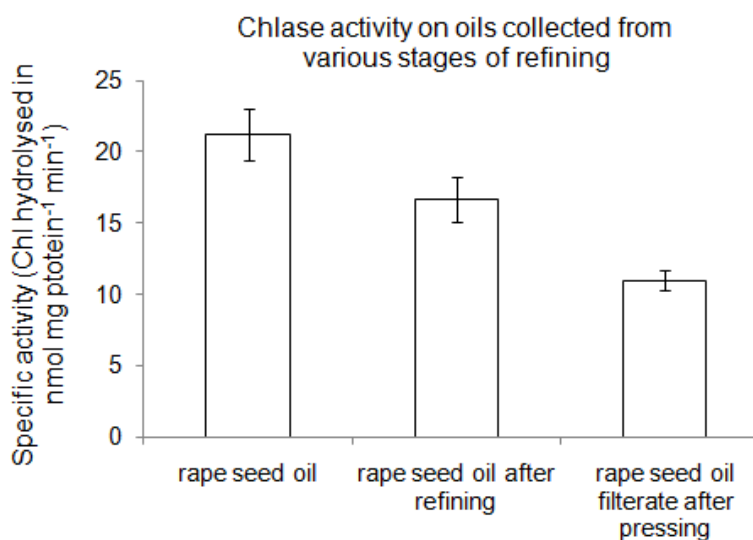


Fig. 25: Activity of His-CcChlase demonstrated in oils at various stages of refining. Chl was dissolved in the oils and taken as substrate (250 μ M) and 100 μ g of soluble extracts containing His-CcChlase was taken as source of enzyme.

The above data has industrial importance to calculate the economical benefit for the production of high quality rapeseed oil.

5.1.4 Tobacco as a model for development of transgenic plants

Primary focus of the study was to analyse the effect of Chlase overexpression on Chl catabolism in transgenic plants during plant development and also during various stress conditions. Accordingly, efforts were made to study Chlase overexpression in *B. napus*, which would give insight into Chl catabolism in mature rapeseeds. *CcCHLASE* gene was cloned under seed-specific promoter of *B. napus* and a modified protocol of De Block et al. (1989) was followed for *A. tumefaciens* mediated transformation of hypocotyl explants of *B. napus*.

However, a low callus formation efficiency (less than 5%) and very poor recovery of shoot regeneration shifted the focus to tobacco plants. Choice of tobacco as a model plant has many advantages: easy growth, established methods for plant regeneration, transformation and physiological and genetical analyses. Also the availability of large biomass and ease of scale-up (million seeds per plant) makes tobacco as an ideal model plant.

5.1.5 Production and preliminary analysis of transgenic tobacco plants overexpressing *CcCHLASE*

To study the physiological and biochemical function of Chlase in plant metabolism, transgenic tobacco plants overexpressing *CcCHLASE* (coding for protein with transit peptide) under the control of 35S promoter were produced. In total, 60 Chlase overexpressor lines were produced according to the method described in section 4.9.2. All the Chlase overexpressor lines shared similar visible phenotype with the WT plants (in terms of leaf morphology and colour, plant height, etc). It was expected that the transgenic plants with overexpressed Chlase protein produce higher amounts of Chlide in leaves compared to WT, which will be present as free pigment in the cells. This extra Chlide was expected to impart photodynamic damage to the plant leading to a necrotic phenotype unlike the WT plants. But such a cell-death phenotype was not seen in the leaves of the Chlase overexpressor plants and found to display the same green pigmentation as the WT tobacco leaves (Fig. 26).



Fig. 26: Phenotypic representation of Chlase overexpressor lines compared to WT tobacco plants. No macroscopic change was observed between the Chlase overexpressor lines and WT plants in all aspects of plant growth and development.

As no phenotypical differences were observed between the Chlase overexpressor lines, all the lines were initially screened by PCR and subsequently by *in vitro* Chlase assays to shortlist candidate lines for their functional evaluation of *CcCHLASE* in Chl catabolism and regulation.

PCR of genomic DNAs isolated from Chlase overexpressor and WT tobacco plants

PCR was performed in order to ascertain the presence of the transgene (*CcCHLASE*) in the Chlase overexpressor plants. Genomic DNA was isolated from the leaf samples of all the 60 Chlase overexpressor plants and screened by PCR for the presence of *CcCHLASE* sequence using gene specific primers as described in materials and methods (section 3.2). The expected size of the amplicon was 1100 bp, and includes the 3' end of the 35S promoter and the complete cDNA sequence of *CcCHLASE*. Genomic DNA from WT leaf samples was taken as control to rule out any non-specific amplification from tobacco genomic DNA. A negative control (without template DNA) was also included in the PCR-reaction assays. Similarly, a positive control i.e., plasmid DNA of binary vector pCAMBIA3301 containing the *CcCHLASE* sequence was also included in the reaction. Amplicons were analysed by agarose gel-electrophoresis and a PCR product of 1100 bp, corresponding to *CcCHLASE* transgene was observed in 55 of 60 DNA samples of Chlase overexpressor lines. An agarose gel picture of PCR samples of different Chlase overexpressor lines along with WT tobacco was shown in Fig. 27.

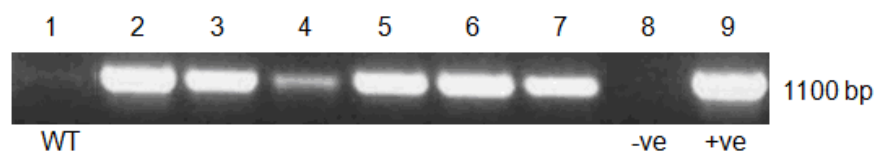


Fig. 27: Agarose gel electrophoresis of PCR amplification of the *CcCHLASE* transgene of Chlase overexpressor lines. The samples WT and –ve (water) control did not show any amplification while the overexpressor samples (2, 3, 4, 5, 6, and 7) showed amplification of a DNA fragment corresponding to the foreign Chlase sequence similar to + ve control (plasmid DNA of binary vector pCAMBIA3301 containing the *CcCHLASE* sequence).

Determination of *in vitro* activity of recombinant Chlase from overexpressor plants during pigment extraction using 80% acetone

Since the antibody against CcChlase cross-reacted with proteins of WT tobacco (Fig. 10, lane 14, section 5.1.2.), an alternative criterion was chosen to analyse the expression of *CcCHLASE* in the overexpressor lines. As overexpression of Chlase gene was expected to result in higher levels of Chlide in overexpressor lines than in WT plants, all the PCR-positive overexpressor lines were tested for *in vitro* activity of the enzyme and compared to WT plants.

In the research group, extraction of pigments from plant tissue was done by using 80% acetone. However, excessive Chlase activity as in the overexpressor lines was still detectable in 80% acetone which hydrolyses Chl *in vitro*. Therefore, for rough initial estimation of transgenic Chlase activity in the tobacco lines, the extraction method was modified by incubating the leaf pigments extracts in 80% acetone for 30 min on ice. The method was performed for both Chlase overexpressor and WT tobacco plants and the pigments were quantified based on spectrophotometric measurements. The calculated Chlide amounts reflected the *in vitro* Chlase activity but not steady state levels of Chlide in the leaf tissue. Based on the amounts of Chlide produced in the samples, the *in vitro* enzyme activity of Chlase was given in terms of specific activity (nmol hydrolysed Chl mg protein⁻¹ min⁻¹).

It was found that more than 97% of the tested Chlase overexpressor plants showed higher Chlase activities than WT tobacco plants (Table 13). Based on the obtained specific activities of recombinant CcChlase protein, the overexpressor plants were grouped in to three classes a) with low to moderate activity b) with higher activity and c) with almost no activity i.e., similar to WT tobacco plants.

WT tobacco and Chlase overexpressing lines	Chlase activity (nmol hydrolysed Chl mg protein ⁻¹ min ⁻¹)	WT tobacco and Chlase overexpressing lines	Chlase activity (nmol hydrolysed Chl mg protein ⁻¹ min ⁻¹)
WT1	0.07 ± 0.01	WT2	0.08 ± 0.01
a) with low to moderate activity			
1	3.21 ± 0.06	2	0.25 ± 0.02
3	0.18 ± 0.01	4	2.22 ± 0.21
5	0.17 ± 0.01	6	3.07 ± 0.28
7	1.77 ± 0.01	8	1.86 ± 0.31
9	2.97 ± 0.25	10	1.37 ± 0.16
11	0.58 ± 0.53	14	0.53 ± 0.04
15	0.66 ± 0.06	16	2.66 ± 0.24
17	3.48 ± 0.31	18	0.16 ± 0.01
20	1.43 ± 0.07	21	2.97 ± 0.22
22	2.97 ± 0.27	23	3.54 ± 0.13
27	3.04 ± 0.23	28	4.88 ± 0.43
29	0.18 ± 0.01	31	3.21 ± 0.27
32	5.11 ± 0.46	33	4.10 ± 0.37
35	0.74 ± 0.06	37	1.06 ± 0.06
38	5.57 ± 0.50	41	4.78 ± 0.44
42	5.34 ± 0.49	44	4.58 ± 0.42
48	3.64 ± 0.02	49	3.64 ± 0.33
50	1.16 ± 0.15	54	1.14 ± 0.11
59	1.69 ± 0.16	60	0.33 ± 0.03
b) higher activity			
13	8.78 ± 0.78	34	11.70 ± 1.06
36	10.24 ± 0.93	38	9.56 ± 0.06
43	8.43 ± 0.77	46	12.06 ± 1.11
47	15.46 ± 1.46	51	13.13 ± 1.19
52	21.4 ± 1.95	56	23.09 ± 2.01
57	11.60 ± 1.06	58	15.92 ± 1.45
c) almost no activities (similar to WT)			
12	0.07 ± 0.01	19	0.12 ± 0.02
25	0.08 ± 0.03	26	0.10 ± 0.01
30	0.04 ± 0.03		

Table 13: Specific activities (nmol hydrolysed Chl mg protein⁻¹ min⁻¹) of Chlase protein isolated from both WT and Chlase overexpressor lines under described assay conditions. The values represent means ± standard deviation (SD) obtained from three independent measurements.

From these overexpressor plants, 15 plants were selected to estimate the copy number of the transgene. Selected lines were 7, 9, 11, 17, 38, 48, 49 and 50 (from group a - with

lesser Chlase activity) and 13, 34, 36, 46, 51, 52 and 56 (group b - with higher Chlase activity).

5.1.6 Estimation of copy number of *CcCHLASE* in Chlase overexpressor lines

Southern blot analysis was performed to determine the copy number of *CcCHLASE* transgene (i.e., the number of insertions of T-DNA into the chromosomal DNA of tobacco) in the selected T0 lines mentioned in section 5.1.5.

Genomic DNA was isolated from leaf material of both WT and the selected 15 Chlase overexpressor lines, digested O/N with the EcoRV restriction enzyme, which does not cut in the transgene, but twice in the T-DNA, and Southern blot was performed. Hybridization was carried out using a ^{32}P dCTP labelled PCR product of *CcCHLASE* (obtained as per section 4.11.4 using pCAMBIA3301 vector construct containing *CcCHLASE*).

The obtained result (Fig. 28) showed that all the overexpressor lines have one copy of *CcCHLASE* transgene, except that the line 13 has four copies. The WT tobacco plants served as good negative controls and did not show any hybridisation signal.

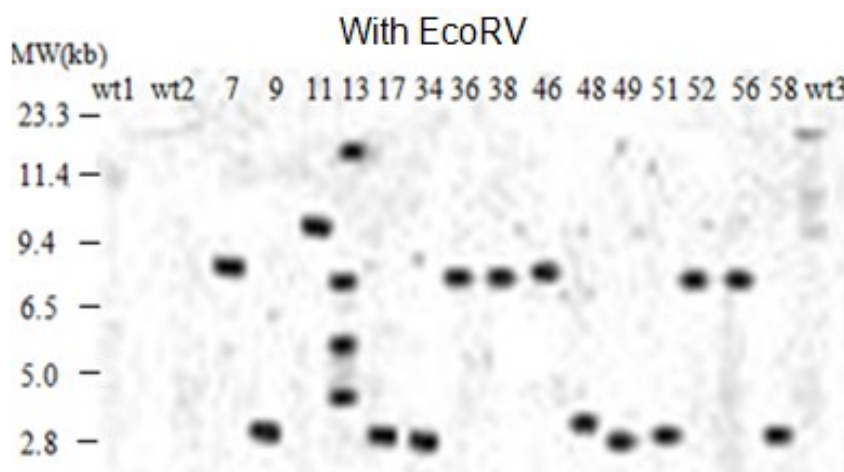


Fig. 28: Southern blot analysis of genomic DNAs isolated from selected 15 Chlase overexpressor and WT tobacco plants demonstrating integration of the *CcCHLASE* gene. Twenty μg of EcoRV digested tobacco genomic DNA was hybridized with radio-labelled *CcCHLASE* probe. The negative control (wt1 and wt2) contained EcoRV digested DNA isolated from untransformed plants. Hybridization signals represent the copy number of *CcCHLASE* in the overexpressor lines.

5.1.7 Analysis of T1 generation of transgenic plants overexpressing *CcCHLASE*

Three Chlase overexpressor lines (46, 51 and 52) were chosen from Table 13 (lines with higher Chlase activity) for further study. Seeds of these three lines were propagated to

yield seedlings of the T1 generation, and their WT progenies were eliminated by selection using Basta. These selected lines and WT were grown under normal light/dark conditions and used for subsequent studies.

5.1.7.1 Transcript levels of *CcCHLASE* in the Chlase overexpressor plants

The transcript levels of *CcCHLASE* in the Chlase overexpressor plants were analysed to confirm that the higher Chlase activity found in these plants correlated with the expression and activity of the *CcCHLASE* transgene and its encoded protein.

Transcript levels of *CcCHLASE* in the overexpressor plants were analysed by northern blot hybridization. Total RNA samples extracted from young leaves of both WT and Chlase overexpressor lines according to section 4.11.3 were blotted onto a nitrocellulose membrane by capillary transfer. Hybridization was carried out with a radio-labelled PCR product of *CcCHLASE* (obtained as per section 4.11.4 using a pCAMBIA3301 vector construct containing *CcCHLASE*). The presence of hybridisation signals for *CcCHLASE* transcripts confirmed the transcriptional activity of the transgene that were absent in WT samples (Fig. 29b). Fig. 29a shows the presence of 28S and 18S subunits in all of the RNA samples and indicates loading of similar quantities of total RNA.

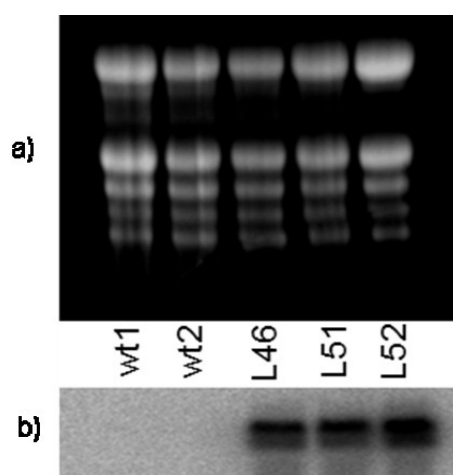


Fig. 29: a) Gel electrophoresis of total RNA samples extracted from young leaves of WT and Chlase overexpressor plants prior to blotting for northern hybridization. b) Northern blot analysis of transcript levels of *CcCHLASE* from WT and Chlase overexpressor plants.

The transcript levels of the native *Chlase* gene from tobacco (*NtCHLASE*) were analysed by the similar method except that hybridization was carried out with a radio-labelled PCR product of *NtCHLASE* (obtained as per section 4.11.4 using a pZero-I vector construct

containing *NtCHLASE*). The presence of signals for *NtCHLASE* transcripts confirmed that the transcriptional activity of the native gene was not affected by the presence of transgene in the Chlase overexpressor lines. The transcript levels were similar in both WT and Chlase overexpressor plants in all stages of leaf development (Fig. 30b). Fig. 30a showed similar quantities of RNA.

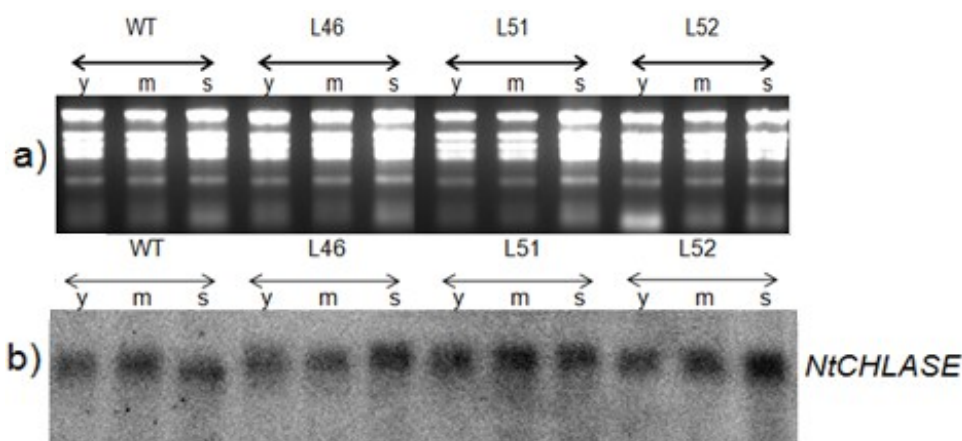


Fig. 30: a) Equal loading of RNA samples on the gel. b) Northern blot analysis of transcript levels of *NtCHLASE* from WT and Chlase overexpressor plants. The samples are denoted as y (young), m (mature) and s (senescent) representing various leaf developmental stages.

5.1.7.2 CcChlase activity resided in the membrane fraction of chloroplasts

Chlase is an intrinsic membrane protein of chloroplasts (Matile et al., 1997). Hence, to confirm the existence of CcChlase activity in the membrane fraction of chloroplasts, *in vitro* activity assays were performed using the soluble stroma and membrane protein fractions of the chloroplasts.

While the previous results of Table 13 (section 5.1.5) were done using entire membrane protein fractions of the leaf tissue, the present assays were done using the protein fractions isolated from the stroma and membrane components of chloroplasts as a source of Chlase. These fractions were tested for their hydrolytic activity with externally supplied Chl as substrate.

Extraction and fractionation of the chloroplasts was done according to section 4.11.9 from both WT and selected Chlase overexpressor lines (lines 46, 51 and 52) and protein fractions were used for the assays (as in section 4.8.3). Results in Table 14 show more activity in membrane fractions than in soluble fractions for all the three lines, confirming

that CcChlase protein resided in the membrane fractions of chloroplasts. The overexpressor lines exhibited almost 5 - 6 times more Chlase activity than WT tobacco plants.

Protein fractions from chloroplasts		Specific activity (nmol hydrolysed Chl mg protein ⁻¹ min ⁻¹)
WT	Soluble	1.33 ± 0.02
	Membrane	4.14 ± 0.32
L46	Soluble	4.52 ± 0.04
	Membrane	25.51 ± 1.41
L51	Soluble	3.72 ± 0.12
	Membrane	23.12 ± 1.23
L52	Soluble	6.14 ± 0.24
	Membrane	31.44 ± 2.51

Table 14: Enzyme activity of recombinant CcChlase protein present in chloroplastic fractions of leaves from Chlase overexpressor and WT tobacco plants. The enzyme activity was given as specific activity (nmol hydrolysed Chl mg protein⁻¹ min⁻¹) and the given values represent means ± SD of three individual experiments.

5.1.7.3 CcChlase activity from the leaves of various developmental stages demonstrated by *in vitro* activity assays

After confirming the Chlase activity in the overexpressor lines, experiments were performed to look into its activity during leaf senescence. Plants (overexpressor lines and WT tobacco) were grown in normal light/dark conditions and in continuous darkness for 5 days. Leaf material (young, mature and senescent) was collected from all the plants and total membrane protein extracts were isolated and subjected to enzyme activity assays by using Chl as substrate (section 4.8.3). It was assumed that dark conditions promote senescence.

Results shown in Fig. 31a and b demonstrate the changes in CcChlase activity in plants grown in normal day/light and complete dark conditions. Obtained data show approximately 25% reduction of Chlase activity in dark grown plants compared to plants grown in normal day-light conditions. In both conditions i.e., light/dark and complete dark, young (y) leaves of the Chlase overexpressor lines showed more Chlase activity than in mature (m) and senescent (s) leaves. Similar phenomenon was also observed in WT tobacco plants.

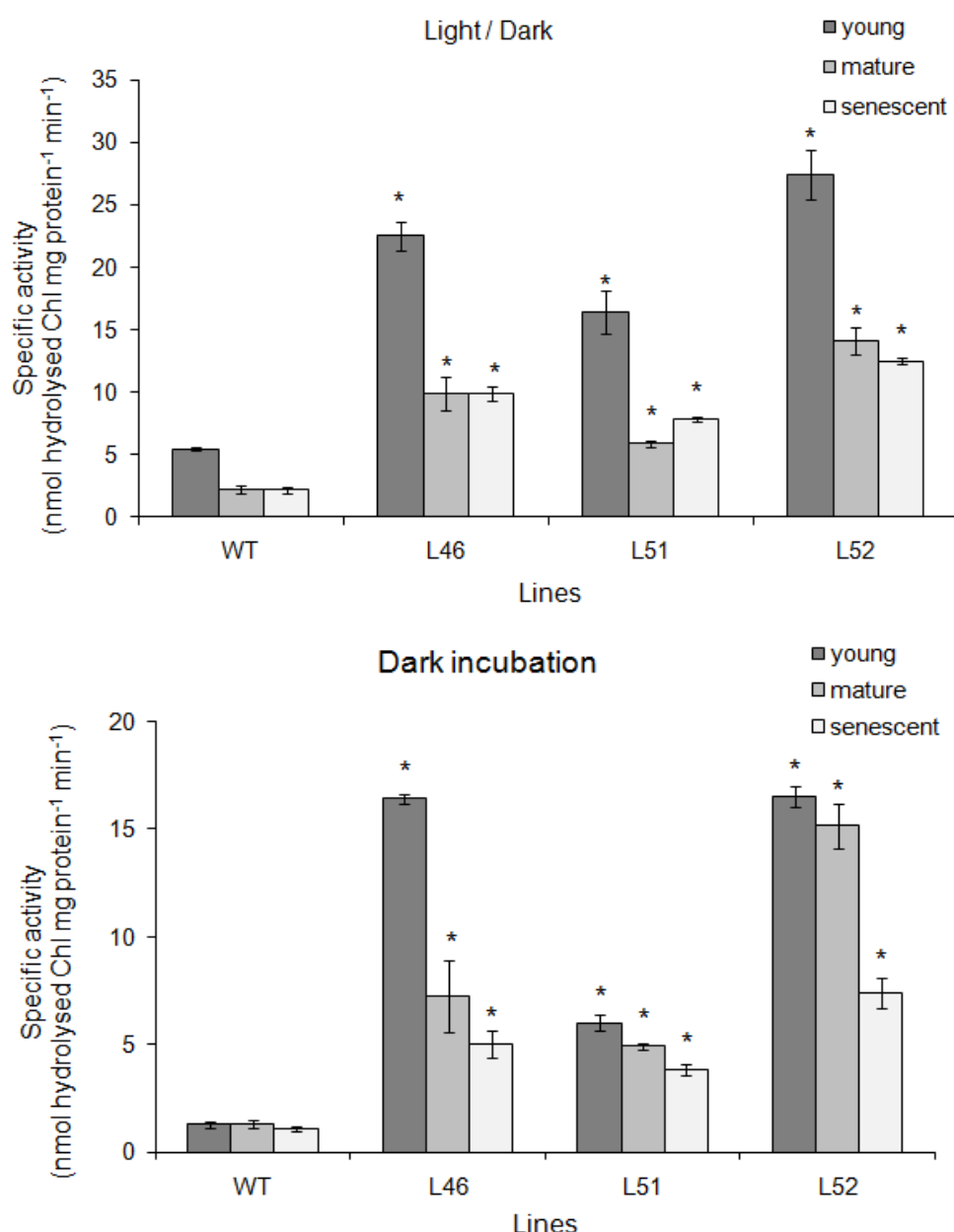


Fig. 31: a) Enzymatic activity of CcChlase from young, mature and senescent leaf samples of plants grown under normal growth conditions in the greenhouse. b) Enzymatic activity of Chlase from young, mature and senescent leaf samples of plants incubated in dark chamber for 5 days. Membrane protein extracts isolated from the given fresh weight samples were used and the specific activities were calculated as nmol hydrolysed Chl mg protein⁻¹ min⁻¹. The calculated results represent mean values \pm SD from three independent experiments ($n = 3$). The difference between WT and Chlase overexpressor plants was given as * for $p < 0.05$ as calculated from F-test and T-test.

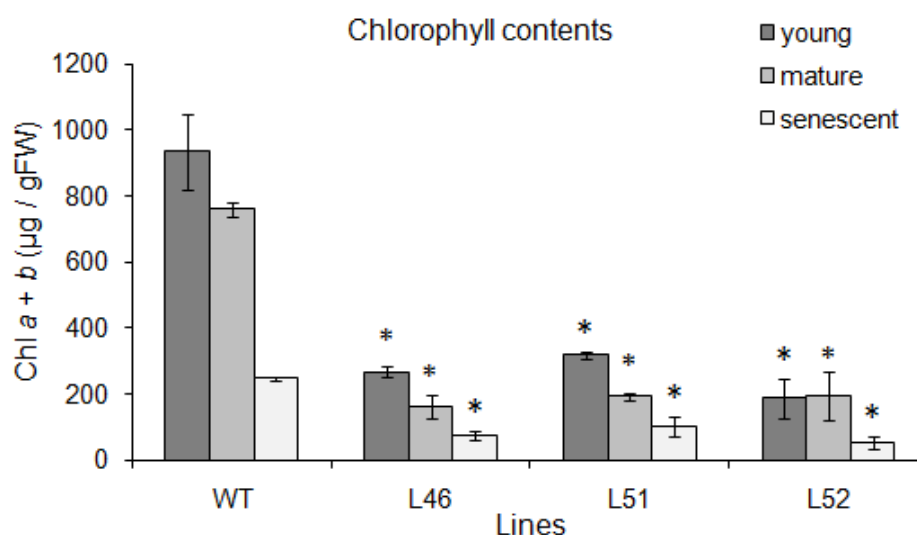
Among the three Chlase overexpressor lines, line 52 showed higher Chlase activity under both light/dark and dark conditions irrespective of leaf age in the order of $y > m > s$. In line 51, the protein extracts from senescent leaf samples showed higher Chlase activity compared to mature leaves in light/dark conditions. But when line 51 grew in dark

conditions, the order of decreasing CcChlase activity was similar to line 52, i.e., $y > m > s$. In line 46, the mature and senescent leaves showed similar Chlase activity under normal light/dark conditions, but in dark, the order followed $y > m > s$. Overall, a 5-fold increase in Chlase activity was observed in the overexpressor lines compared to WT and was attributed to activity of CcChlase protein.

5.1.7.4 Accumulation of higher amounts of Chl catabolites (Chlide *a* and Pheide *a*) in Chlase overexpressor plants during 80% acetone extraction method

Derived from Table 13, it was evident that incubation of leaf pigment extracts in 80% acetone on ice led to considerable accumulation of Chlide seen in the form of increased specific activity of CcChlase in the overexpressor lines compared to WT tobacco plants. Furthermore, the *in vitro* assays shown in Fig. 31a and b demonstrated higher CcChlase activity in young leaves compared to mature and senescent leaves. To corroborate the above results, pigment extractions were initially performed from leaves of WT and selected overexpressor lines using 80% acetone according to the method described in section 4.11.12.4. The differences and the specificity of this experiment in comparison to results of Table 13 and Fig. 31 was to analyse the *in vitro* accumulation of Chlide *a* and Pheide *a* in 80% acetone during extraction.

A huge deposition of almost 20 fold more Chlide *a* and Pheide *a* was observed in the 80% acetone extracts of overexpressor lines compared to WT tobacco plants (Fig. 32). These data indicate the durability or indestructibility of recombinant CcChlase in the overexpressor lines, reflecting the potent activity of CcChlase in the overexpressor lines and were consistent with the *in vitro* enzyme assays in Fig. 31 a and b.



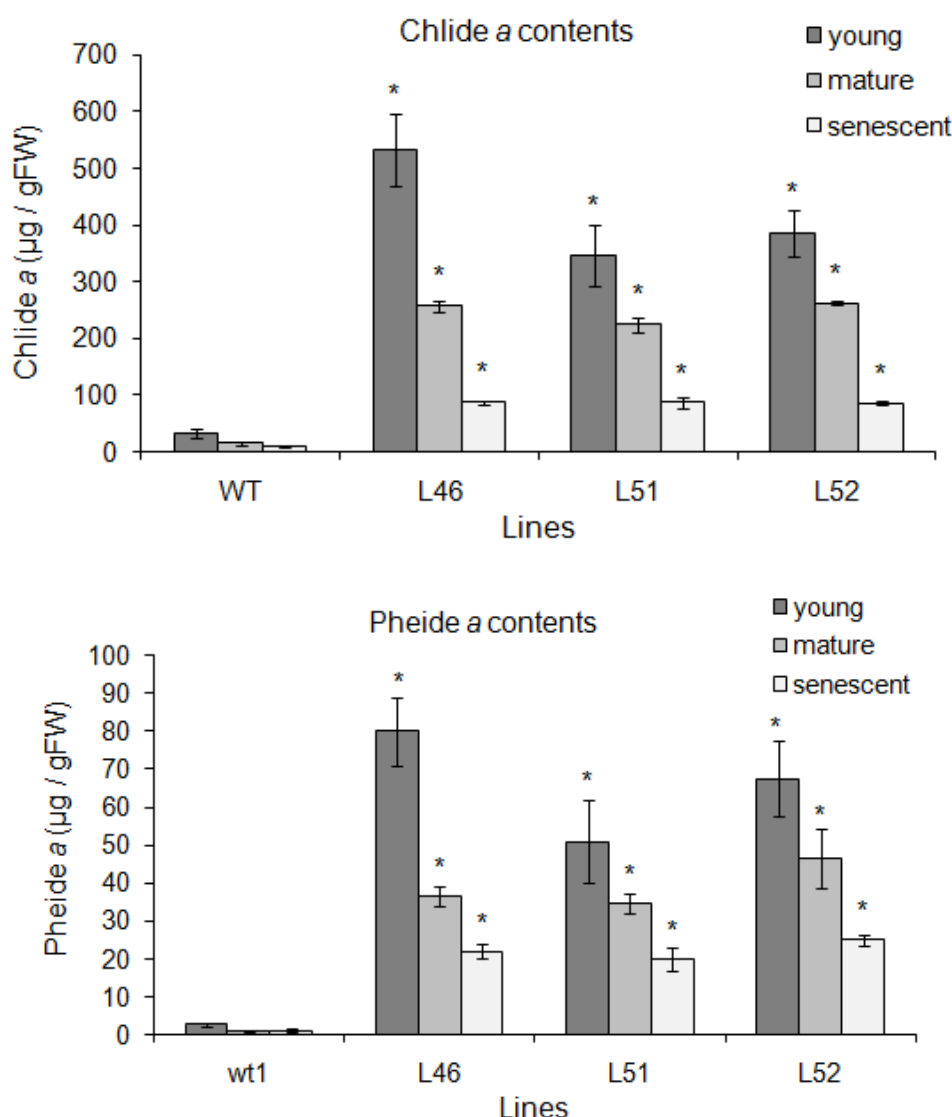


Fig. 32: Amounts of Chl (*a+b*), Chlide *a* and Pheide *a* from both WT and Chlase overexpressor lines, which accumulate during extraction of pigments in 80% acetone. Pigments were quantified (µg/gFW) after extraction from leaves of different developmental stages [young (y), mature (m) and senescent (s)]. Higher levels of Chlide *a* and Pheide *a* were detected in Chlase overexpressor lines than in WT and follows the order $y > m > s$. The calculated results represent mean values \pm SD from three independent experiments ($n = 3$). The difference between WT and Chlase overexpressor plants was given as * for $p < 0.05$ as calculated from F-test and T-test.

5.1.7.5 Steady state levels of green coloured pigments and NCC contents in T1 generation of Chlase overexpressor lines

The steady state levels of Chlide *a* in the leaf tissues would give an account of *in vivo* CcChlase activity. The results from Fig. 32 did not allow distinction between deposition of steady state levels of Chlide *a* in the overexpressor lines and accumulation of Chlide *a* as a result of CcChlase activity during pigment extraction using 80% acetone. It was an unexpected finding that the recombinant *Citrus* Chlase (CcChlase) protein overexpressed

in transgenic plants could not be completely inactivated in 80% acetone while the activity of the native tobacco Chlase of WT was negligible.

Therefore, the extraction method was modified by substituting 80% acetone with absolute acetone (99% acetone) to exclude the possibility of persistent Chlase activity in the pigment samples extracted in 80% acetone. Absolute acetone (> 99%) was used to make sure that all the protein was precipitated so that no more Chlase activity (section 5.1.3.4) was seen in the samples and the results obtained showed genuine *in vivo* pigment levels (steady state levels) of Chl and Chlide *a*. In addition, the end products of Chl breakdown, the colourless non-fluorescent catabolites (NCCs) (Brown et al., 1991), were estimated in plants as a measure of the completion of Chl catabolism.

Chl catabolism occurs mostly during ageing of leaves from young to senescent. This natural senescence process mostly depends on age, but can also be regulated by hormones like ethylene and methyl jasmonate, environmental factors like dark adaptation and stress. Experimentally, leaf senescence can also be induced either by hormonal treatment or by varying the environmental conditions. In the present study, an effort was made to induce senescence in WT and CcChlase overexpressor plants by these agents in order to evaluate the functional activity and stability of the recombinant CcChlase protein *in vivo* during senescence and stress.

At various stages of leaf development (from young to senescent leaves) as a course of natural senescence phenomenon

Total pigments were extracted from young, mature and senescent leaves (described in section 4.11.12.1) and analysed by HPLC for the steady state levels of both substrate (Chl) and product (Chlide *a*) from the three Chlase overexpressor lines (46, 51 and 52) and WT tobacco plants.

The results (Fig. 33) showed higher amounts of Chl in the WT in comparison to the overexpressor lines. The steady state levels of Chlide *a* were higher in the Chlase overexpressor lines compared to negligible levels in WT tobacco plants (Fig. 33). This difference between WT and Chlase overexpressor tobacco plants indicated the enhanced Chl breakdown due to the presence of overexpressed CcChlase protein in the overexpressor lines. Slightly lower levels of Chl in the overexpressor lines were accounted to higher levels of Chlide *a*. A ratio of Chlide *a* to Chl would give a measure of *in vivo*

Chlase activity. This ratio (Fig. 34) was observed only in Chlase overexpressor lines and none in WT tobacco plants due to negligible levels of Chlide *a*. The ratio of Chlide *a* to Chl in the overexpressor lines was of the following decreasing order, young (y) < mature (m) < senescent (s), leaves respectively.

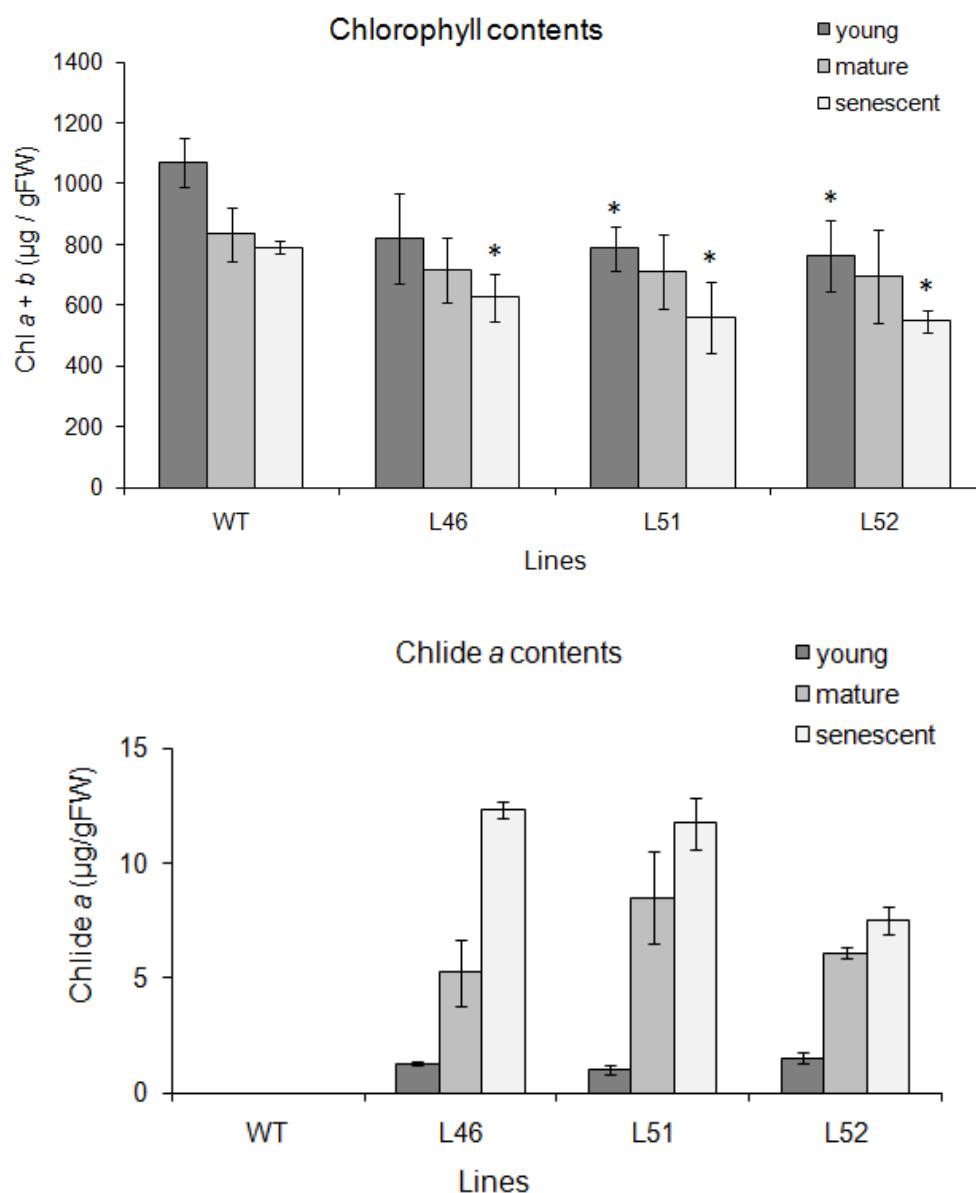


Fig. 33: Steady state levels of Chl (*a+b*) and Chlide *a* from both WT and Chlase overexpressor plants. Pigments were quantified as µg/gFW after extraction from leaves of different developmental stages (young, mature and senescent). Chlide *a* levels were detected only in Chlase overexpressor lines but not in WT tobacco plants and follows the order y < m < s. The calculated results represent mean values ± SD from three independent experiments (n = 3). The difference between WT and Chlase overexpressor plants was given as * for p < 0.05 as calculated from F-test and T-test.

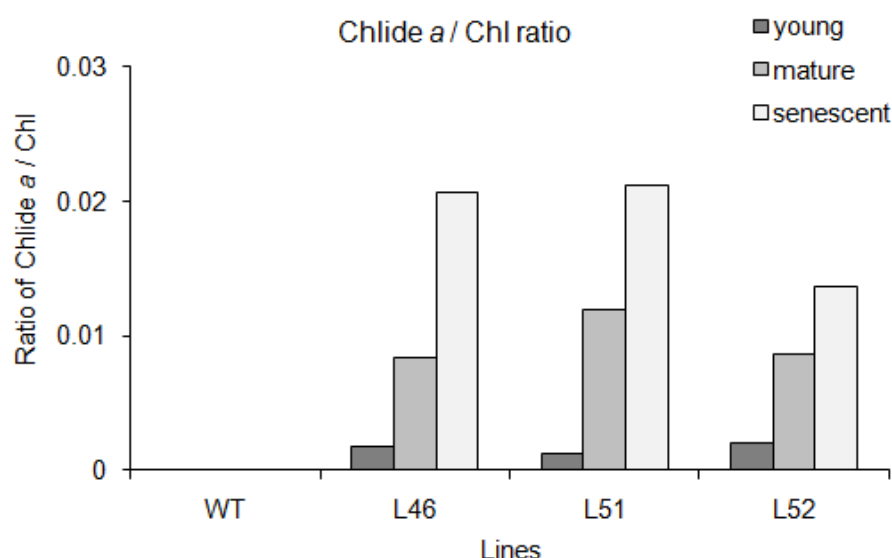


Fig. 34: Chlide *a*/Chl ratios calculated from leaf samples of WT and Chlase overexpressor plants. The ratios follow the order $y < m < s$ with the amount of Chlide *a* being lowest in young leaves. Absence of ratios in WT leaf samples indicate the absence of Chlide *a* steady state levels in WT tobacco plants.

Determination of NCCs levels from young, mature and senescent leaves of both WT tobacco and Chlase overexpressor lines was done as described in section 4.11.12.2. The results plotted on a graph (Fig. 35) showed that significant differences were not seen in the levels of NCCs in WT and Chlase overexpressor tobacco plants. Levels of NCCs were found to be higher in senescent leaves of all plants.

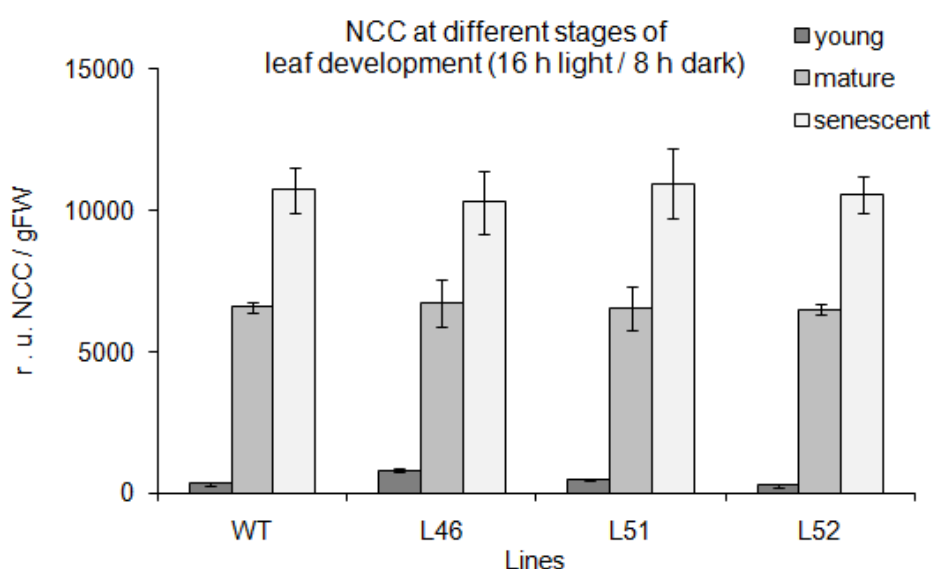


Fig. 35: Analysis of non-fluorescent Chl catabolites from leaves of different developmental stages collected from normally grown WT and Chlase overexpressor lines. As the HPLC factors for the quantification of NCCs were unavailable, the amounts of NCCs were given in relative units (r. u.).

Promotion of senescence in leaves

Induction of senescence by additional longer dark incubation and application of plant hormones like methyl jasmonate and ethylene was widely used (dark incubation of detached parsley leaves - Ben-Yaakov et al., 2006; methyl jasmonate treatment of *Arabidopsis* leaves – Kariola et al., 2005; and exposure of fruits to ethylene - Jacob-Wilk et al., 1999). Therefore, to evaluate the accumulation of steady state levels of Chlide *a* during various senescence conditions, both WT tobacco and Chlase overexpressor lines were subjected to different treatments as listed in Table 5, section 4.11.10.

Dark incubation of detached leaves

Leaves of similar age were selected from both WT tobacco and Chlase overexpressor lines and samples were harvested before start up (0 h) and at the end of the experiments (12 h light/12 h dark – 5 days and complete darkness - 5 days). After pigment extraction using 99% acetone, steady state levels of both Chls (Chl *a* and *b*) and Chlide *a* were quantified by HPLC.

The obtained results in Table 15 showed that Chlide *a* levels were not detected in WT tobacco plants. Data also revealed that the Chl amounts showed a gradual decline with dark incubation and also in detached leaves. The higher steady state levels of Chlide *a* in Chlase overexpressing plants compared to non-detectable amounts in WT clearly reflect the increased hydrolytic activity of recombinant CcChlase.

As shown from Table 15, the amounts of total Chl in overexpressor plants were nearly 12 – 15% lower compared to WT tobacco leaves (taken as 100%) at 0 h (i.e., start of experiment). On incubation of the detached leaves under 12 h light/12 h dark for 5 days, the residual Chl amounts were 91% in WT and 87 - 89% in overexpressor plants compared to their 0 h values. This indicated a decrease in Chl amounts by 10% in WT and 11 - 13% in the overexpressor lines compared to 0 h. Induced senescence by incubation of the detached leaves in continuous dark for 5 days led to a decrease of Chl amounts by 23% in WT compared to the 0 h samples and in overexpressor lines was about 24%.

		Total Chl ($\mu\text{g/gFW}$)	Chlide <i>a</i> ($\mu\text{g/gFW}$)	% of Chl compared to WT	% of residual Chl compared to the value of 0 h sample	Chl/Chlide <i>a</i> ratio
Control leaf (0 h)	WT1	1158 \pm 46	0	100		-
	L46	984 \pm 39*	7.5 \pm 1.2	85		131
	L51	1009 \pm 37*	5.8 \pm 0.9	87		173
	L52	985 \pm 31*	3.7 \pm 0.6	85		266
Detached leaf in 12h light /12 h dark for 5 days	WT1	1051 \pm 42	0		91	-
	L46	866 \pm 53*	8.3 \pm 0.7		88	104
	L51	901 \pm 22*	6.5 \pm 0.4		89	138
	L52	858 \pm 60*	4.4 \pm 0.4		87	195
Detached leaf in complete darkness for 5 days	WT1	890 \pm 49	0		77	-
	L46	745 \pm 36*	6.4 \pm 1.0		76	116
	L51	764 \pm 32*	5.7 \pm 0.9		76	134
	L52	749 \pm 37*	3.9 \pm 0.6		76	192

Table 15: Steady state levels of Chl and Chlide isolated from leaf material harvested from control, normal incubated and dark incubated leaves from both WT and Chlase overexpressor lines. The calculated results represent mean values \pm SD from three independent experiments ($n = 3$). The difference between WT and Chlase overexpressor plants was given as * for $p < 0.05$ as calculated from F-test and T-test.

No steady state levels of Chlide *a* were found in WT leaves irrespective of dark or light/dark incubation along with control (0 h) leaves. In the leaves of Chlase overexpressors, the Chlide *a* amounts increased by 10 - 20% on light/dark incubation for 5 days compared to the 0 h samples. But dark incubation of the leaves for the same period of time, led to a fall in the Chlide *a* amounts by 5 - 15% compared to 0 h in the leaves. This decrease might be due to a) lower availability of Chl as substrate b) continuous turnover of Chl in the leaf tissue or c) continuous degradation of Chlide *a* to the subsequent catabolites.

The ratio of Chl/Chlide *a* could not be determined in WT under any of the experimental conditions (0 h, 12 h light/12 h dark for 5 days and complete darkness for 5 days) due to the absence of steady state levels of Chlide *a*. In comparison, Chlase overexpressor lines due to their inherent Chlide *a* steady state levels demonstrated Chl/Chlide *a* ratios under all tested conditions. It was observed that Chl/Chlide *a* ratios were higher at 0 h in all the three Chlase overexpressor lines. In lines 51 and 52, the ratio of Chl to Chlide *a* was slightly higher in the 12 h light/12 h dark (for 5 days) conditions in comparison to that seen after complete dark incubation for 5 days. But in line 46, the ratio was higher in complete dark incubation conditions (for 5 days) compared to the 12 h light/12 h dark (5 days) conditions.

The amounts of end products of Chl catabolism (NCCs) were also quantified from both WT and Chlase overexpressor lines incubated under continuous dark conditions for two weeks. The results (Fig. 36) showed that no significant differences were observed in the NCC contents between WT and Chlase overexpressor plants even upon dark incubation.

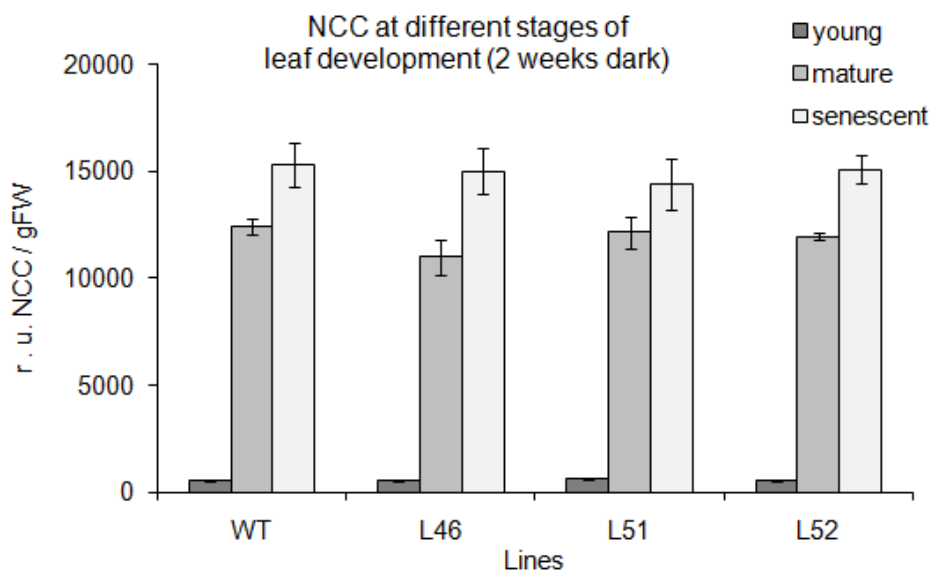


Fig. 36: Analysis of non fluorescent Chl catabolites from leaves of different developmental stages collected from dark incubated WT and Chlase overexpressor lines. As the HPLC factors for quantification of NCCs were unavailable, the amounts of NCCs were given in relative units (r. u.)

As shown in Fig. 36, amounts of NCCs increased drastically with incubation of plants under dark. Comparing Fig. 35 and 36, it was evident that mature and senescent leaves showed a marked increase in NCC levels on dark incubation, while young leaves contained similar low NCC levels irrespective of the incubation conditions.

Role of senescence promoting agents (ethylene and methyl jasmonate)

Leaves of similar age were selected from both WT and Chlase overexpressor lines, leaf discs were harvested and senescence was induced using either methyl jasmonate or ACC (precursor in the synthesis of ethylene) as given in section 4.11.10. Samples were collected before and at the end of the experiment and pigments were measured by HPLC. The quantified amounts of steady state Chl and Chlide *a* levels were documented in Table 16.

Chlide *a* levels were found to be significantly higher in Chlase overexpressor lines compared to WT tobacco plants. The amounts of Chlide *a* were increased in the first 24 h of incubation of leaf discs with respective reagents and declined in the next 24 h. The

initial rise in steady state levels of Chlide *a* was due to the accelerated Chl degradation promoted by ACC and methyl jasmonate by which the substrate presumably became more accessible to Chlase to catalyse the hydrolysis of Chl. No steady state levels of catabolite were detected in WT and served as good control for the presence of recombinant CcChlase protein in overexpressor plants. However, the decrease in Chlide *a* levels during the next 24 h might be due to conversion of Chlide *a* to the immediate catabolites in the pathway.

With methyl jasmonate: The total Chl amounts in the overexpressor lines were nearly 15 – 25% lower in comparison to the WT tobacco leaf samples at 0 h (start-up of the experiment). Incubation of the leaf discs in methyl jasmonate for 24 h led to a decrease of Chl amounts by 13% in WT and 10 – 14% in the overexpressor lines. Prolonged incubation of the leaf discs in the reagent for 48 h showed a fall of Chl amounts by 21% in WT and 13 – 15% in the overexpressor lines (Table 16). The ratio of Chl/Chlide *a* was observable only in overexpressor lines due to the presence of steady state levels of Chlide *a* which were absent in WT. This ratio was observed to be lower during the incubation for 24 h with reagent, but increased during prolonged incubation of 48 h.

With ACC: The total Chl amounts in the overexpressor lines were nearly 18 – 20% lower in comparison to the WT tobacco leaf samples at 0 h (start-up of the experiment). Incubation of the leaf discs in ACC for 24 h resulted in the decrease of Chl amounts by 14% in WT and by 13 – 21% in the overexpressor lines. But prolonged incubation of the leaf discs in the reagent showed a fall in Chl amounts by 30% in WT and 19 – 28% in the overexpressor lines (Table 16). Though higher ratios of Chl/Chlide *a* were seen at 0 h in all the overexpressor lines, after 24 h there was a drastic decrease in the ratios due to the presence of higher amounts of Chlide *a*. But incubation of 48 h showed higher Chl to Chlide *a* ratios compared to 24 h in all the overexpressor samples.

		Total Chl ($\mu\text{g/gFW}$)	Chlide <i>a</i> ($\mu\text{g/gFW}$)	% of Chl compared to WT	% of residual Chl compared to value of the 0 h sample	Chl/Chlide <i>a</i> ratio
Induction of senescence by Methyl jasmonate (3 mM)						
Before starting the experiment (0 h)	WT	1315 \pm 20	0	100		-
	L46	985 \pm 10*	4.5 \pm 1.0	75		219
	L51	1120 \pm 25*	2.3 \pm 0.5	85		487
	L52	1000 \pm 8*	3.2 \pm 0.9	76		313
After 24 h of incubation	WT	1150 \pm 40	0		87	-
	L46	884 \pm 7*	18 \pm 1.2		90	49
	L51	1000 \pm 18	14 \pm 3.4		89	71
	L52	860 \pm 35*	15 \pm 1.6		86	57
After 48 h of incubation	WT	1035 \pm 8	0		79	-
	L46	860 \pm 30*	3.8 \pm 0.2		87	226
	L51	950 \pm 7	3.1 \pm 0.1		85	306
	L52	850 \pm 43*	2.3 \pm 0.1		85	369
Induction of senescence by ACC (3 mM)						
Before starting the experiment (0 h)	WT	1259 \pm 48	0	100		-
	L46	1003 \pm 53*	4.5 \pm 0.7	80		223
	L51	1032 \pm 55*	3.1 \pm 0.3	82		333
	L52	1020 \pm 20*	3.5 \pm 0.9	80		291
After 24 h of incubation	WT	1086 \pm 46	0		86	-
	L46	871 \pm 12*	19.3 \pm 1.2		87	45
	L51	871 \pm 9*	12.6 \pm 1.1		84	69
	L52	803 \pm 45*	16.5 \pm 1.9		79	49
After 48 h of incubation	WT	885 \pm 44	0		70	-
	L46	718 \pm 21*	9.1 \pm 0.8		72	79
	L51	834 \pm 16	5.7 \pm 1.5		81	146
	L52	801 \pm 11*	4.4 \pm 1.3		79	182

Table 16: Steady state levels of Chls and Chlide *a* (from WT and Chlase overexpressor plants) after induction of senescence by methyl jasmonate and ACC. The calculated results represent mean values \pm SD from three independent experiments ($n = 3$). The difference between WT and Chlase overexpressor tobacco plants was given as * for $p < 0.05$ as calculated from F-test and T-test.

Incubation of leaf discs in both ACC and methyl jasmonate did not show any significant changes in the NCCs contents between the WT and Chlase overexpressor tobacco plants (Table 17).

Promotion of senescence			NCC (r. u./gFW)
Methyl jasmonate (3 mM)	Before starting the experiment (0 h)	WT	3180 ± 42
		L46	3180 ± 30
		L51	3065 ± 67
		L52	3114 ± 54
	After 24 h of incubation	WT	3245 ± 40
		L46	3181 ± 62
		L51	3110 ± 88
		L52	3112 ± 76
	After 48 h of incubation	WT	3124 ± 28
		L46	3171 ± 47
		L51	3041 ± 72
		L52	3000 ± 80
ACC (3 mM)	Before starting the experiment (0 h)	WT	4480 ± 56
		L46	4451 ± 72
		L51	4445 ± 46
		L52	4388 ± 23
	After 24 h of incubation	WT	4485 ± 61
		L46	4466 ± 40
		L51	4457 ± 75
		L52	4421 ± 46
	After 48 h of incubation	WT	4477 ± 35
		L46	4398 ± 79
		L51	4419 ± 62
		L52	4397 ± 53

Table 17: No significant differences in the amounts of NCCs quantified after senescence inducing experiments using methyl jasmonate and ACC in both WT and Chlase overexpressor plants. The calculated results represent mean values ± SD from three independent experiments (n = 3). The difference between WT and Chlase overexpressor plants was given as * for $p < 0.05$ as calculated from F-test and T-test.

Abiotic stress conditions

Activity of Chlase was correlated to lower Chl levels during unfavourable conditions of drought and heat stress (Majumdar et al., 1991). In this context, experiments were performed to estimate the steady state levels of Chl and Chlide *a* in the Chlase overexpressor lines.

Detached leaves were taken from both WT and selected T1 lines (lines 46, 51 and 52) and subjected to various kinds of stress conditions like drought and salt. Stress conditions were provided to the leaves as listed in section 4.11.10 and quantification of pigments (using 99% acetone) was done from samples harvested from leaves after the specified experiment.

Salt stress

The results (Table 18) showed that, even at a high concentration of salt (0.5 M NaCl), the overexpressor lines retained higher Chlase activity compared to WT tobacco plants. This was indicated by accumulation of high Chlide *a* levels in the Chlase overexpressor lines.

As incubation of the leaf in salt solution led to its decreased size, the amounts of Chl and Chlide *a* were calculated on the fresh weight basis, which was taken before the start of the experiment. This procedure excludes the assessment of elevated amounts of pigments per unit fresh weight which was altered during the salt stress experiments due to water loss as a result of change in osmotic potential.

Salt stress		Total Chl ($\mu\text{g/gFW}$)	Chlide <i>a</i> ($\mu\text{g/gFW}$)	% of Chl compared to WT	% of residual Chl compared to the value of 0 h sample	Chl/Chlide <i>a</i> ratio
Control leaf (0 h)	WT	1120 \pm 44	0	100		-
	L46	1006 \pm 20*	2.1 \pm 0.1	90		480
	L51	1030 \pm 40	2.6 \pm 0.2	92		396
	L52	1010 \pm 20*	2.3 \pm 0.1	91		439
Leaf in water for 2 days	WT	900 \pm 50	0		80	-
	L46	735 \pm 25*	7.2 \pm 0.5		73	102
	L51	775 \pm 42	5.5 \pm 0.3		75	141
	L52	745 \pm 75*	6.7 \pm 0.7		74	111
Leaf in 0.5 M NaCl for 2 days	WT	890 \pm 40	0		79	-
	L46	565 \pm 17*	1.0 \pm 0.5		56	565
	L51	605 \pm 35	2.7 \pm 0.4		59	224
	L52	675 \pm 30*	2.1 \pm 0.2		67	321

Table 18: Steady state levels of green coloured pigments from both WT and Chlase overexpressor plants in response to salt stress. The calculated results represent mean values \pm SD from three independent experiments ($n = 3$). The difference between WT and Chlase overexpressor plants was given as * for $p < 0.05$ as calculated from F-test and T-test.

The amounts of Chl decreased after 48 h of incubation in water or salt solution compared to 0 h (start-up of the experiment) for both WT and Chlase overexpressor lines (Table 18). The Chlase overexpressor lines showed reduced Chl contents and increased Chlide *a* levels compared to WT. In the control samples (leaves in water for 2 days), the residual Chl amounts in WT were 80% and in the overexpressor lines 73 - 75% in comparison to values of the 0 h samples. This indicated a decrease of Chl contents by 20% in WT and 25 - 27% in the overexpressor lines in the control leaves. After 48 h of salt stress, the residual

amount of Chl was higher in WT (79%) than in overexpressor plants (56 - 67%) with a reduction of Chl content by 21% in WT and 33 - 44% in overexpressor leaves.

The ratios of Chl/Chlide *a* were higher in all the overexpressor lines at 0 h compared to that seen in the pigment extracts of leaf samples collected from leaves incubated for two days in water (Table 18). This could be due to enhanced Chl breakdown in water control leaves. Except line 46, the other two lines 51 and 52 showed a lower Chl/Chlide *a* ratio in the salt stressed leaves in comparison to the 0 h samples. Also the ratios in salt stressed leaves were higher than those seen in water control leaves. This could be due to accelerated conversion of Chlide *a* to its subsequent catabolites.

Drought stress

The calculated results (Table 19) demonstrated the presence of Chlide *a* in both control and drought stress samples. Estimation of steady state levels of green coloured pigments showed that even under water deficiency or drought stress of 30 h, the recombinant CcChlase enzyme could efficiently hydrolyse Chl.

Drought stress		Total Chl ($\mu\text{g/gFW}$)	Chlide <i>a</i> ($\mu\text{g/gFW}$)	% of Chl compared to WT	% of residual Chl content compared to value of the 0 h sample	Chl/Chlide <i>a</i> ratio
Control leaf (0 h)	WT	1185 \pm 19	0	100		-
	L46	968 \pm 20*	9.3 \pm 3.1	90		104
	L51	998 \pm 32*	13.5 \pm 1.4	92		74
	L52	922 \pm 67*	11.2 \pm 1.5	91		82
Leaf in water for 30 h	WT	1045 \pm 15	0		88	-
	L46	847 \pm 52*	12.4 \pm 1.3		87	68
	L51	861 \pm 16*	18 \pm 2.2		86	49
	L52	807 \pm 30*	14.9 \pm 1.8		87	54
Leaf in petri dish without water for 30 h	WT	953 \pm 18	0		80	-
	L46	771 \pm 18*	6.4 \pm 2.6		80	120
	L51	784 \pm 43*	5.0 \pm 1.6		79	157
	L52	735 \pm 21*	7.6 \pm 2.0		80	97

Table 19: Steady state levels of Chls and Chlide *a* in WT and Chlase overexpressor plants in response to water deficit. The calculated results represent mean values \pm SD from three independent experiments ($n = 3$). The difference between WT and Chlase overexpressor plants was given as * for $p < 0.05$ as calculated from F-test and T-test.

As the cell size shrinks due to drought conditions in the leaves, the pigment amounts were calculated on the fresh weight basis taken at 0 h (start-up of the experiment) to exclude the

possibility of more amount of pigment in unit fresh weight due to water loss. A decrease in Chl amounts was observed in both WT and Chlase overexpressor lines after 30 h of incubation of leaves in water or without water compared to 0 h. The Chlase overexpressor lines showed reduced Chl contents and increased Chlide *a* levels compared to WT. In leaves kept in water for 30 h, the residual Chl amount was 88% in WT and 86 – 87% in the overexpressor lines in comparison to 0 h. These data indicated a decrease of Chl contents by 12% in WT and 13 - 14% in the overexpressor lines in the water control leaves. After 30 h of water deficiency, the residual amount of Chl was almost similar in both WT (80%) and the overexpressor lines (79 – 80%) with a reduction in Chl content by 20% in WT and 20 - 21% in overexpressor leaves.

The ratios of Chl/Chlide *a* were higher in the leaf samples collected at 0 h compared to the ratios observed in samples collected from leaves incubated in water for 30 h. The ratios calculated from pigment samples of leaves exposed to water deficiency stress were higher in comparison to that seen at 0 h and 30 h water control due to the presence of lower Chlide *a* amounts in the drought stressed leaves.

The end products of Chl degradation (NCCs) were quantified under both drought and salt stress conditions in both WT and Chlase overexpressor lines. There was an increase in the level of NCCs of stressed samples compared to control samples. But no significant difference in their amounts was observed between WT and Chlase overexpressor plants (Table 20).

Stress phenomenon			NCC (r. u./gFW)
Salt stress	Before starting the experiment (0 h)	WT	4047 ± 75
		L46	4131 ± 56
		L51	4059 ± 68
		L52	4125 ± 76
	After 48 h of leaf incubation in water	WT	5061 ± 84
		L46	5134 ± 73
		L51	4951 ± 81
		L52	5036 ± 51
	After 48 h of leaf incubation in 0.5 M NaCl	WT	6052 ± 94
		L46	6063 ± 85
		L51	5973 ± 77
		L52	5951 ± 83
Drought stress	Before starting the experiment (0 h)	WT	4510 ± 49
		L46	4522 ± 85
		L51	4585 ± 52
		L52	4488 ± 85
	After 30 h of leaf incubation in water	WT	5248 ± 83
		L46	5118 ± 59
		L51	5071 ± 87
		L52	5159 ± 52
	After 30 h of leaf incubation without water	WT	7411 ± 67
		L46	7275 ± 67
		L51	7254 ± 81
		L52	7236 ± 92

Table 20: No significant differences were seen in the NCCs amounts after stress experiments (drought and salt). The calculated results represent mean values ± SD from three independent experiments (n = 3). The difference between WT and Chlase overexpressor plants was given as * for $p < 0.05$ as calculated from F-test and T-test.

5.1.7.6 ALA synthesising capacity of Chlase overexpressor plants

δ -aminolevulinic acid (ALA or 5-aminolevulinic acid) is the first committed compound in the Chl synthesis pathway and its production is the rate limiting step on synthesis of Chl. As the Chlase overexpressor plants possessed higher levels of Chlide compared to WT, experiments were performed to analyse if there exist any differences in the rate of production of ALA between the plants. Leaf discs of both young and mature leaves of WT and overexpressor plants were incubated with 40 mM ALA for a specified time interval and the ALA synthesizing capacity was measured as described in section 4.11.13. The obtained results were graphically represented in Fig. 37.

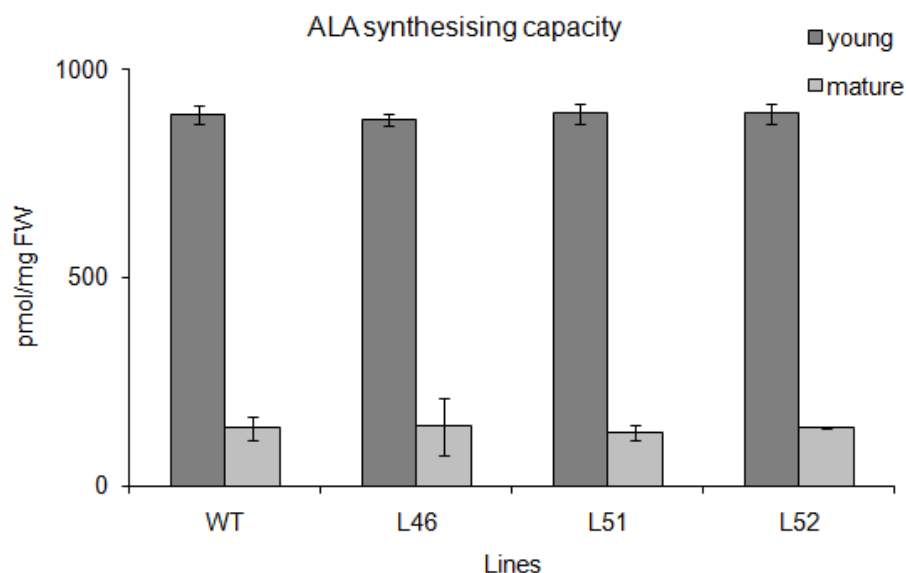


Fig. 37: ALA synthesising capacity measured in young and mature leaves collected from WT and Chlase overexpressor plants.

It was seen that no differences were observed in the ALA production rate between WT and Chlase overexpressor plants. The young leaves exhibited higher levels of ALA synthesizing capacity (~ 10 times) than the mature leaves. Hence, it appeared that overexpression of *CcCHLASE* did not alter the ALA production rate in the Chlase overexpressor plants.

5.2 Water Soluble Chlorophyll Protein (WSCP)

The present study assessed the functional role of WSCP in various processes of plant metabolism, like Chl catabolism, response to stress and ability to store pigments. Experiments were designed to characterise the WSCP protein through expression studies in *E. coli* and in transgenic tobacco plants. Efforts were also made to understand the capacity of WSCP to promote photoprotective mechanisms in plants.

5.2.1 Cloning, characterization and expression of WSCP in *E. coli*

The reference *WSCP* gene sequence selected for the present study was from cauliflower (*Cau-WSCP*) (Satoh et al., 1998). A bacterial expression clone containing the cDNA sequence coding for *Cau-WSCP* protein without the putative transit peptide region was obtained from Dr. Ulrich Eckhardt. Two cDNA sequences (plasmid clones 49 and 35) showed > 98% homology with the reference *Cau-WSCP* sequence (Fig. 38). Each cloned sequence was 597 bp long and encoded a protein of 22 kDa (199 aa long) similar to the reference *Cau-WSCP* protein (Satoh et al., 1998). Both the deduced aa sequences of *Cau-*

WSCP-35 and *Cau-WSCP-49* retained the signature motif of Kunitz type protease inhibitor family similar to the reference protein (Fig. 38).

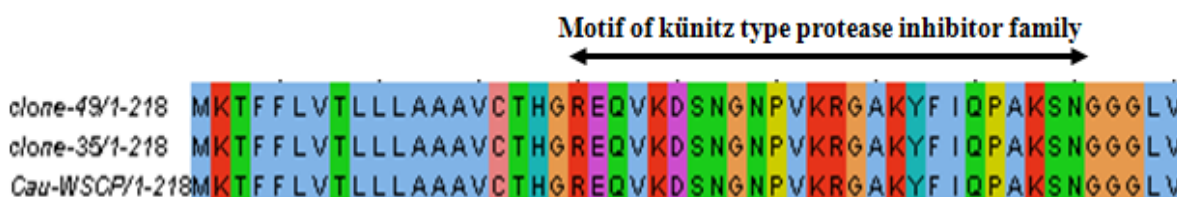


Fig. 38: Sequence homology of truncated protein sequence of WSCP plasmid clones 49 and 35 (*Cau-WSCP-35* and *Cau-WSCP-49*) with reference *Cau-WSCP* protein (Sato et al., 1998). The conserved kunitz type protease inhibitor motif was represented by the black arrow mark.

Comparison between the *Cau-WSCP-35* and *Cau-WSCP-49* deduced aa sequences revealed a single substitution of a conserved aa residue (glycine in the place of glutamic acid, at 108 position) in *Cau-WSCP-49* protein. The aa sequence of *Cau-WSCP-35* was identical to the published sequence (Sato et al., 1998).

Protein expression of *Cau-WSCP-35* and *Cau-WSCP-49* (in the form of MBP-WSCP) was maximum in BL21DE3pLysS strains of *E. coli* at 30°C, after two hours of induction time and with 0.8 mM IPTG. The recombinant protein was found to be accumulated more abundantly in the soluble fractions than in the membrane fractions of *E. coli*. Western blot analysis of the soluble and insoluble fractions of *E. coli* cultures expressing either *Cau-WSCP-35* or *Cau-WSCP-49* along with the positive control (*Cau-MBP-WSCP-Sato*) was shown in Fig. 39. Recombinant WSCP was detected using an anti-*Cau-WSCP* antibody.

As shown in Fig. 39, the recombinant proteins *Cau-WSCP-35* and *Cau-WSCP-49* were detected to be 66 kDa. The molecular mass was similar to that of MBP-*Cau-WSCP* (Sato et al., 1998). The expression of MBP-WSCP was equal in both soluble (Fig. 39, lanes 8 and 10) and insoluble fractions (Fig. 39, lanes 9 and 11) of *E. coli*. Therefore, soluble extracts of *E. coli* containing MBP-WSCP encoded by both sequences (*Cau-WSCP-35* and *Cau-WSCP-49*) were taken for the *in vitro* activity assays.

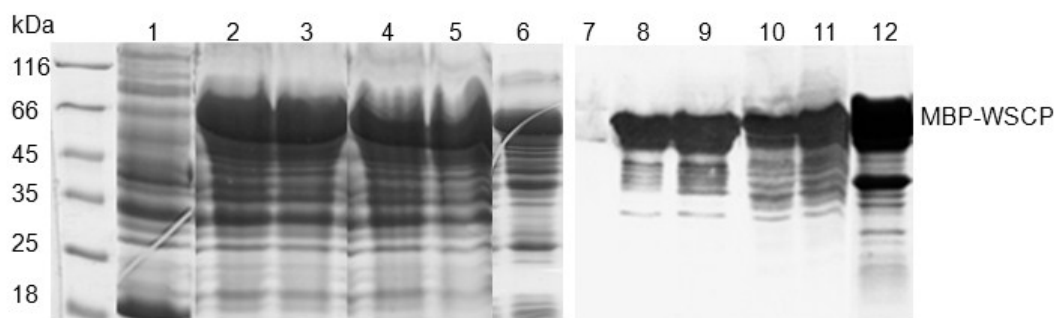


Fig. 39: SDS-PAGE and western blot analysis of recombinant and purified MBP-WSCP

- lane 1, a soluble protein extract of *E. coli* containing empty pMALC2 vector (20 µg)
 lane 2, a soluble protein extract of *E. coli* after inducing the expression of *Cau-WSCP-35* with IPTG (20 µg). Addition of IPTG induced a prominent band corresponding to 66 kDa (indicated as MBP-WSCP) due to a fusion protein of MBP (44 kDa) and WSCP (22 kDa)
 lane 3, an insoluble fraction of the induced culture of *E. coli* containing *Cau-WSCP-35* broken with sonication (20 µg)
 lane 4, a soluble protein extract of *E. coli* after inducing the expression of *Cau-WSCP-49* with IPTG (20 µg)
 lane 5, an insoluble fraction of the induced culture of *E. coli* containing *Cau-WSCP-49* (20 µg)
 lane 6, a soluble fraction of *E. coli* containing *Cau-MBP-WSCP-Satoh* as positive control (10 µg).
 lane 7, a soluble protein extract of *E. coli* containing empty pMALC2 vector as negative control for anti-*Cau-WSCP* antibody with no detection of protein,
 lane 8, *Cau-MBP-WSCP-35* detected as 22 kDa protein band from soluble extracts (2 µg) of lane 2,
 lane 9, an insoluble fraction of lane 3 (2 µg) showing the *Cau-MBP-WSCP-35* protein,
 lane 10, *Cau-MBP-WSCP-49* detected as 66 kDa protein band from soluble extracts (2 µg) of lane 4,
 lane 11, an insoluble fraction of lane 5 (2 µg) showing the *Cau-MBP-WSCP-49* protein,
 lane 12, an immune-reacting band of *Cau-WSCP-Satoh* (2 µg) from soluble protein extracts. Protein detection was feasible by using anti-*Cau-WSCP* antibody.

5.2.2 *In vitro* assays to test the function of WSCP

As WSCP was regarded as a transport protein of Chl to the site of Chlase (Matile et al., 1997), experiments were done to investigate whether the addition of WSCP protein extracts during *in vitro* Chlase activity tests enhances the process of Chl breakdown. The capacity of WSCP to promote the Chlase activity was assessed in terms of Chlide formed in the reaction.

The assays were conducted in a water-miscible organic solvent system as per section 4.8.3. The reaction mixtures contained Chl, bacterial soluble extracts containing His-CcChlase and MBP-Cau-WSCP-35/MBP-Cau-WSCP-49. Soluble extracts of *E. coli* containing empty plasmids pMALC2 and pQE80 were used as negative controls for WSCP and

Chlase. Also the assays were done with soluble extracts of *E. coli* containing MBP-Cau-WSCP-Satoh. Obtained results are illustrated in Fig. 40, which showed that the hydrolytic activity of Chlase was not altered by presence of WSCP in the reaction.

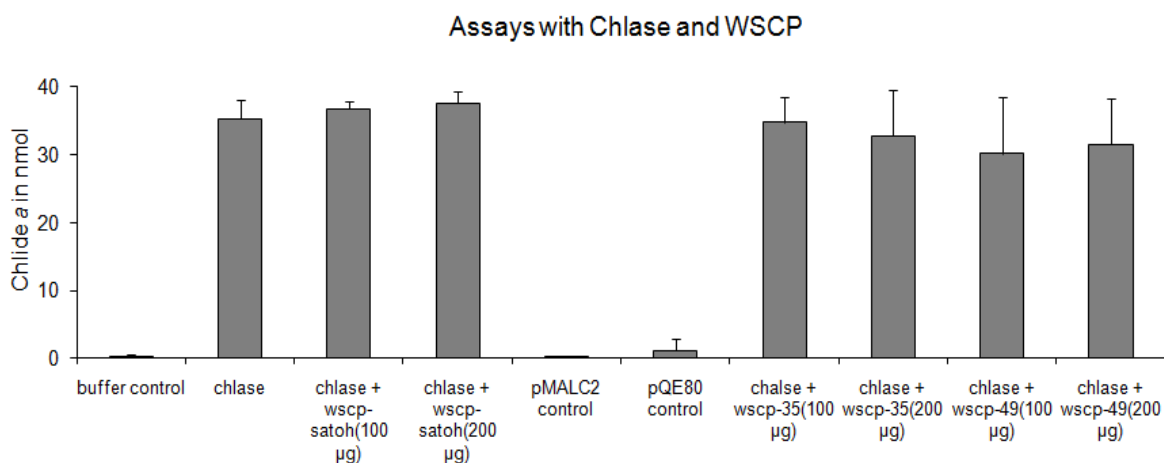


Fig. 40: Coupled assays performed using recombinant His-CcChlase and WSCP proteins with Chl to demonstrate the inability of WSCP to promote the functional activity of Chlase *in vitro*. The bacterial soluble extracts containing both MBP-Cau-WSCP-35/MBP-Cau-WSCP-49 were employed as source of WSCP and that of MBP-Cau-WSCP-Satoh as positive control for WSCP. The buffer control denotes absence of enzyme (Chlase or WSCP) and the soluble extracts of bacteria containing empty plasmids (pMALC2 or pQE80) were used as negative controls for the protein sequences. All the assays were performed thrice independently and the results stand for statistical proof.

Results from Fig. 40 showed that addition of MBP-Cau-WSCP-35 or MBP-Cau-WSCP-49 to the reaction did not affect the activity of His-CcChlase, and the amount of Chlide formed with or without WSCP was similar (Fig. 40). A similar effect was observed with the positive control of WSCP protein (Satoh plasmid clone). Plasmid controls (pQE80) and pMALC2 for WSCP served as negative controls for Chlase and WSCP as no Chlide was generated in both the instances. Even addition of twice the amount of WSCP protein did not influence the Chlase activity *in vitro*.

5.2.3 Production of transgenic tobacco plants overexpressing *Cau- WSCP-35*

Transgenic tobacco plants overexpressing *Cau-WSCP-35* (encoding protein with transit peptide) were produced to study the role of WSCP in plant metabolism. In total, 53 WSCP overexpressor lines were produced as described in section 4.8.2. Although, the transgene *Cau-WSCP-35* was constitutively expressed under the control of 35S promoter, the WSCP overexpressor plants did not show any characteristic phenotypic differences compared to WT tobacco plants (Fig. 41). One possible explanation could be that WSCP being a

transport protein, overexpression of this protein may not significantly affect the morphology of the plants.

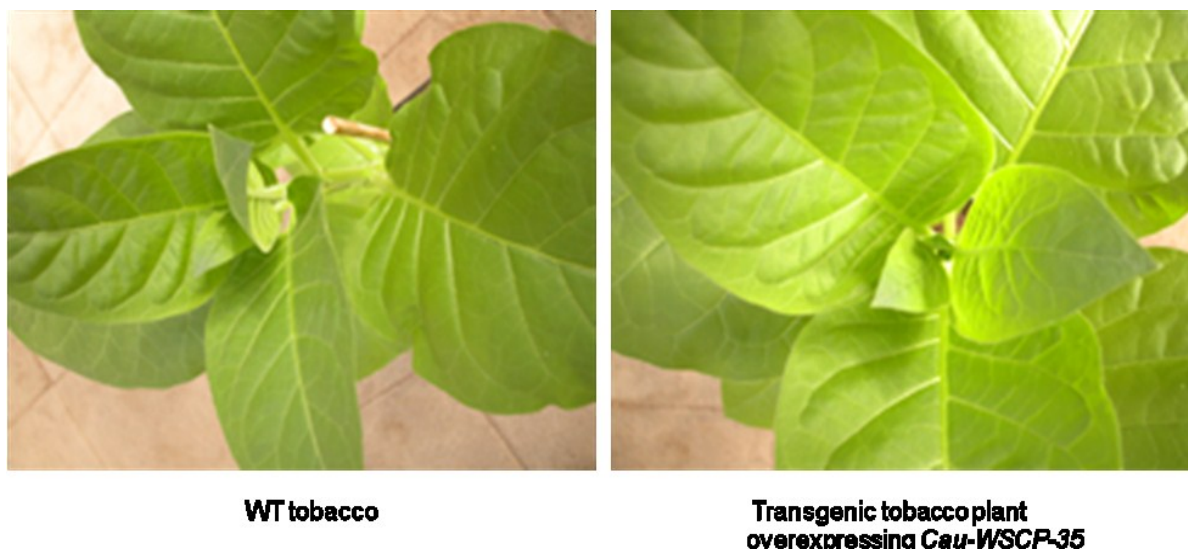


Fig. 41: Phenotypic representation of WSCP overexpressor plants compared to WT tobacco plants. The overexpressor lines did not show any change in leaf morphology and also in other aspects like plant height, number of leaves etc.

5.2.4 Selection of WSCP overexpressor candidate lines

As the *WSCP* overexpressing lines could not be distinguished from WT plants based on phenotypical differences, all *WSCP* overexpressor lines were screened by PCR and western blot to select candidate lines for maximum overexpression of *Cau-WSCP-35*.

PCR of the genomic DNAs isolated from *WSCP* overexpressor and WT tobacco plants

All *WSCP* overexpressor lines generated from section 5.2.3 were analysed by PCR using gene specific primers for *Cau-WSCP-35* (section 3.2). Expected size of the amplicon was 800 bp, and included the 3' end of the 35S promoter and the complete cDNA sequence of *Cau-WSCP-35*. Genomic DNA from WT leaf samples was used as negative control to rule out any non-specific amplification from tobacco genomic DNA. A non-template control was also used as a negative control. The positive control used was plasmid DNA of the binary vector pCAMBIA3301 containing the *Cau-WSCP-35* sequence. The resultant amplicons on agarose gel electrophoresis showed that 35 of 53 *WSCP* overexpressor lines showed the presence of the transgene (Fig. 42). The length of the amplicon matched with that of the positive control (Fig 42, +ve). Negative controls i.e., WT tobacco plant DNA and non-template DNA control (-ve) did not show any amplification.

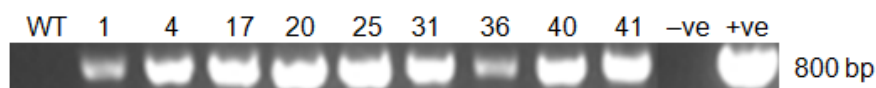


Fig. 42: Agarose gel electrophoresis of PCR amplified fragments of *Cau-WSCP-35* transgene of WSCP overexpressor lines. The samples WT and –ve water control did not show any amplification, while the overexpressor samples (1, 4, 17, 20, 25, 31, 36, 40 and 41) showed amplification similar to + ve control.

Western blot of WSCP overexpressor and WT tobacco plants

The PCR positive lines were tested for the presence of recombinant *Cau-WSCP-35* protein by western blot analysis of total soluble protein extracts from leaf material of both WT and WSCP overexpressor lines as per section 4.11.7.2. An immune-reacting protein of 22 kDa, representing WSCP protein was detected in soluble protein fractions of the overexpressor lines similar to that of the positive control i.e., cauliflower leaves. Western blot analysis for some of the tested overexpressor lines was shown in Fig. 43. WT tobacco protein samples served as negative control as the antibody did not show any cross-reactivity with any other plant proteins. Based on the results, the primary transformants (T0) with maximum protein expression (1, 2, 3, 4, 17, 25, 39, 40, 41, and 45) were selected for further analysis.

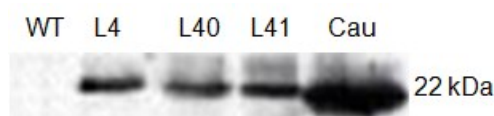


Fig. 43: Western blot analysis of total soluble protein fractions from WT and WSCP overexpressor lines. The protein extract from cauliflower was used as positive control. The WSCP protein was detected as 22 kDa protein in both overexpressor lines and cauliflower leaf samples.

5.2.5 Estimation of copy number of *WSCP* transgene in WSCP overexpressor lines

The copy number of *Cau-WSCP-35* transgene in the overexpressor lines was determined using Southern blot analysis. The selected T0 lines from the section 5.2.4 were analysed for the copy number of the transgene (i.e., number of insertions of T-DNA into the chromosomal DNA of tobacco).

Genomic DNA was isolated from all the selected 10 WSCP overexpressor lines (1, 2, 3, 4, 17, 25, 39, 40, 41, and 45) along with WT tobacco and digested with restriction enzyme *Xba*I (does not cut the transgene but once in the T-DNA). Hybridization was carried out with a radio-labelled PCR product of *Cau-WSCP-35* (obtained as per section 4.11.4 using pCAMBIA3301 vector construct containing *Cau-WSCP-35*). The results attained showed that the overexpressor lines varied with number of insertions of the transgene (Fig. 44).

The copy number of transgene *Cau-WSCP-35* was from 1 – 4 indicating the number of insertion sites of *Cau-WSCP-35* into the chromosomal DNA of transformed WT tobacco plants.

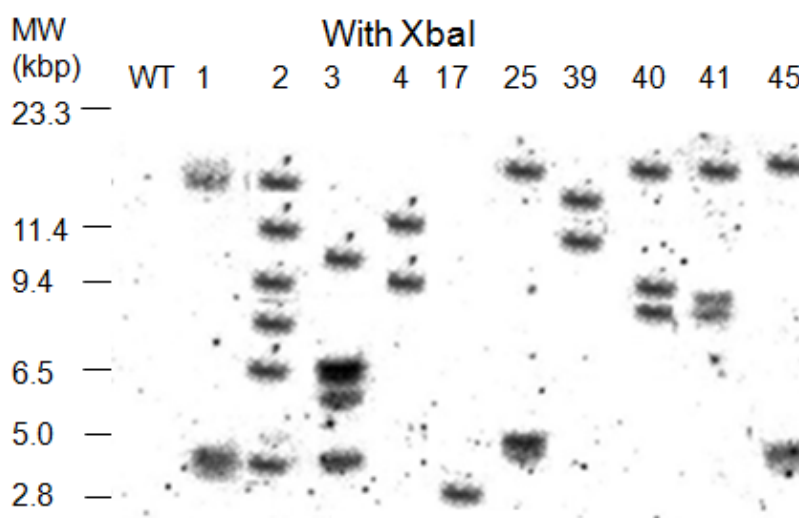


Fig. 44: Southern blot of genomic DNAs isolated from the selected 10 WSCP overexpressor and WT tobacco plants restriction digested with XbaI. The hybridization signals represent the copy number of the transgene *Cau-WSCP-35* in the overexpressor lines. Twenty μ g of XbaI digested tobacco genomic DNA was hybridized with *Cau-WSCP-35* radio-labelled probe. The negative control (WT) contained XbaI digested DNA isolated from untransformed plants.

The lines 40, 41, 1 and 45 had insertions of the transgene at similar positions in the genome, respectively. The WT plants served as negative controls which did not show any detection of a hybridising band. The probe used corresponded correctly to the *Cau-WSCP-35* transgene without any cross reactivity.

5.2.6 Analysis of T1 generation of WSCP overexpressor plants

Of the 10 WSCP overexpressor lines, three lines (4, 40 and 41) were selected for further analysis. The progenies of the above selected lines (T1 generation) along with WT, grown under normal light/dark conditions were used as experimental material.

5.2.6.1 Functional role of *Cau-WSCP-35* during Chl degradation seen as leaf senescence

The role of WSCP in the Chl catabolic pathway was studied by analysing its protein expression pattern during the course of leaf senescence. Both western blot and pigment measurements were done for *WSCP* overexpressing lines and compared with WT plants.

Protein expression profile of *Cau-WSCP-35* in the WSCP overexpressor plants

Total soluble protein extracts were derived from the leaves of different age i.e., from young to senescent, of the overexpressor lines 4, 40 and 41 and WT tobacco and analysed by western blot. The results demonstrated that protein expression of *Cau-WSCP-35* was abundant during the early stages of leaf development (young leaves) and decreased gradually with increase in leaf age (senescent leaves) following an order $y > m > s$ (Fig. 45). Positive control i.e., cauliflower leaves showed the presence of WSCP protein, but as expected the WT tobacco leaves did not contain *Cau-WSCP* protein (labelled as *Cau* and WT in Fig. 45).

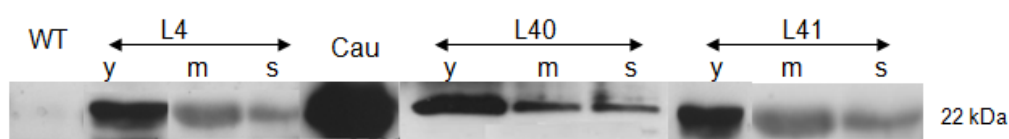


Fig. 45: Western blot analysis of young, mature and senescent leaf samples of the selected T1 WSCP overexpressor lines. y = young, m = mature, s = senescent. WT protein sample was used as negative control and that from cauliflower (denoted as *Cau*) as positive control.

The above result of a decreasing trend of WSCP protein expression from young to senescent leaves was further analysed by taking every leaf of line 40 i.e., from young to senescent. It was seen that accumulation of recombinant WSCP was higher in the youngest leaf (leaf 6 in Fig. 46) and diminished gradually with increasing age (leaves 2 and 1 in Fig. 46).

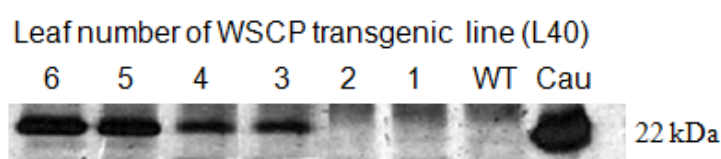


Fig. 46: Western blot of total soluble protein extracts containing recombinant *Cau-WSCP-35* from all leaves of line 40. The leaf number denotes the age of the leaf with ascending number representing the young leaf. Cauliflower protein extract (*Cau*) was used as positive control and that of WT as negative control.

Simultaneously, the expression profile of native WSCP protein was analysed during cauliflower leaf development. Greenhouse grown cauliflower plants were taken, total soluble protein was extracted from every leaf and the native WSCP protein was detected using the anti-*Cau-WSCP* antibody. The native WSCP protein showed the similar profile of protein expression as that of line 40 i.e., $y > m > s$ (Fig. 47). The protein expression of *Cau-WSCP* was higher in young leaves and decreased with leaf age (leaf 8 > leaf 1).

Sequential decrease in the amount of WSCP with increase in the age of leaf was clearly demonstrated.

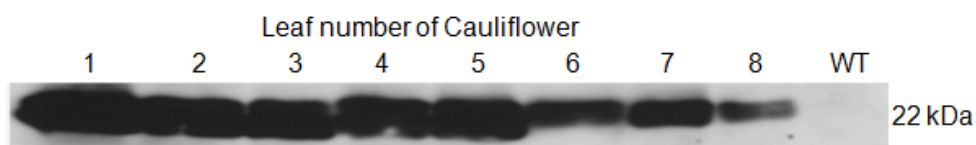


Fig. 47: Western blot analysis of native WSCP protein from cauliflower leaves. The leaf number indicates the age of the leaf in descending order. The protein was detected at 22 kDa band and was in agreement with the report of Satoh et al. (1998). The protein was not detected in WT tobacco leaves.

Measurement of Chl and Chlide *a* contents in the WSCP overexpressor plants

WSCP is considered to play a role in Chl catabolism by transferring the thylakoid bound Chl molecule to the site of action of Chlase (Matile et al., 1997). To verify this hypothesis, the transgenic plants overexpressing *Cau-WSCP-35* were screened for the contents of green coloured pigments in their leaves.

Accordingly, pigments were extracted using the following extraction methods to ascertain the effect of WSCP on Chl catabolism – a) using 99% acetone for measuring *in vivo* steady state levels of Chl and Chlide *a* and b) using 80% acetone for measuring *in vitro* accumulation of Chlide *a*.

Steady state levels of pigments

Total pigments were extracted from the leaves of both WT and WSCP overexpressor plants as per the method 4.10.12.1. Leaves chosen belonged to various developmental stages (young, mature and senescent). Steady state levels of both Chl and Chlide *a* were measured by HPLC from WT and three WSCP overexpressing lines (Fig. 48). It was found that line 40 showed significantly higher amounts of Chls compared to WT in the young leaf samples. But the amounts of Chls in the mature and senescent leaves of line 40 did not differ from the WT. In line 4, only the senescent leaf samples showed significantly lesser quantities of Chls which was not seen in young and mature leaves of line 4. The line 41 showed significantly lesser Chl amounts in both mature and senescent leaf samples but not in the young leaves.

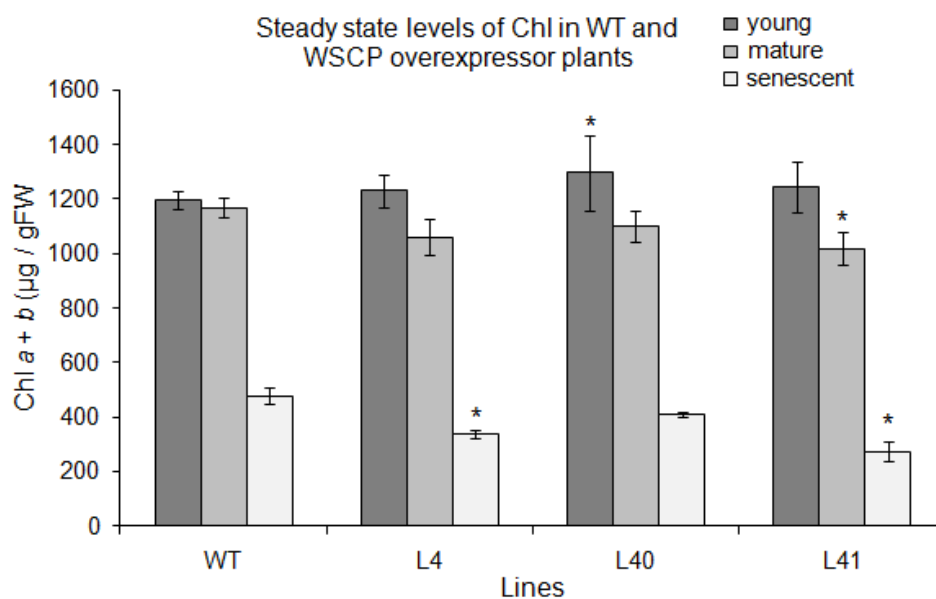


Fig. 48: Steady state levels of Chl ($a+b$) analysed from leaf pigment extracts of different age groups (young, mature and senescent) from WT and progenies of the T1 generation of the selected three WSCP overexpressor lines. Chl ($a + b$) amounts were given as $\mu\text{g/gFW}$. The calculated results represent mean values \pm SD from three independent experiments ($n = 3$). The difference between WT and overexpressor plants was given as * for $p < 0.05$ as calculated from F-test and T-test.

Steady state levels of Chlide a were not detectable in WSCP overexpressing lines and WT tobacco plants suggesting that presence of recombinant WSCP protein did not contribute to an enhanced Chl catabolic pathway *in vivo*.

***In vitro* accumulation of Chlide a during pigment extraction**

Another set of pigment extractions was performed using 80% acetone (section 4.11.12.4) from both WT and WSCP overexpressor tobacco lines. This *in vitro* estimation showed no significant differences in the levels of both Chl and Chlide a between WSCP overexpressor and WT leaf samples of any age group (Fig. 49). Presence of similar levels of Chlide a in both WT and overexpressor lines indicated that presence of Cau-WSCP-35 protein had no influence on *in vitro* Chlase activity.

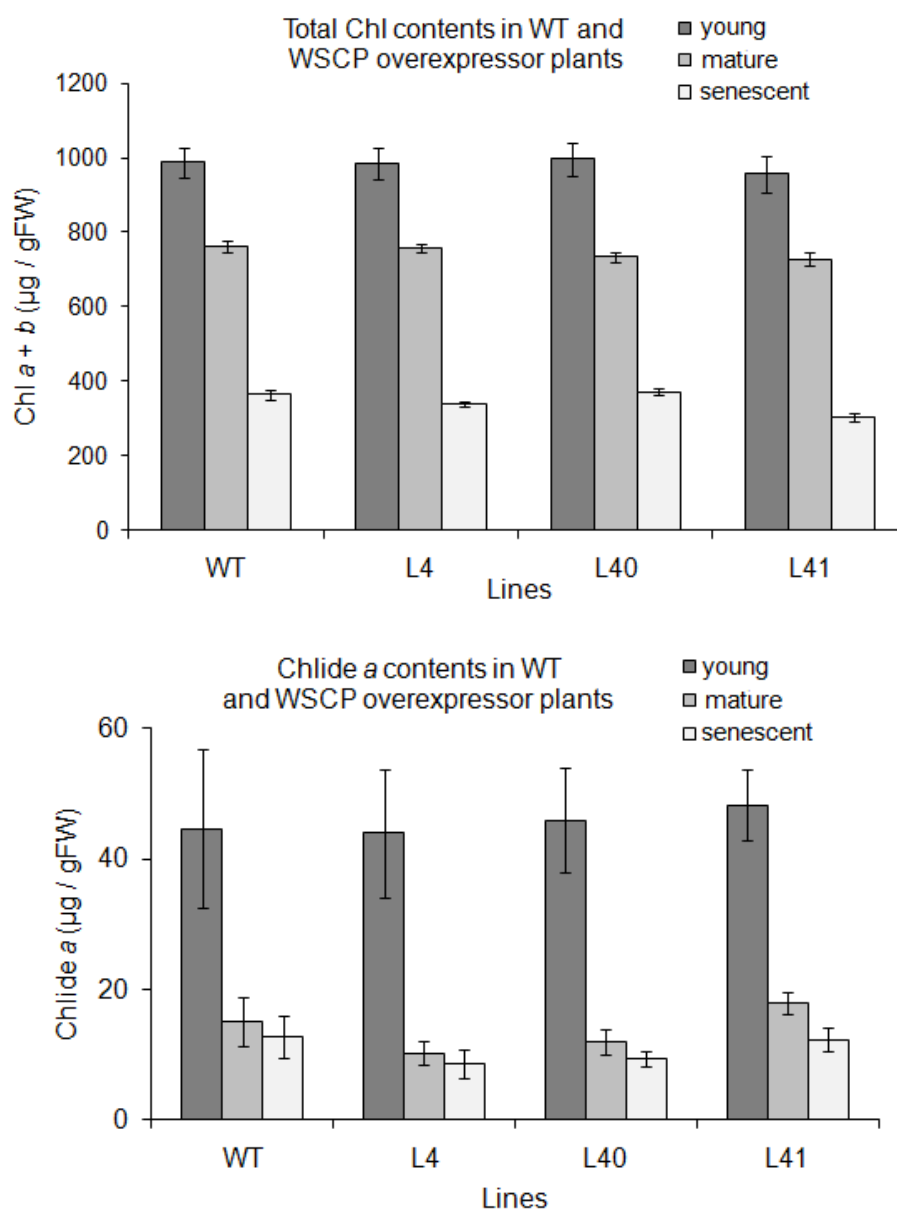


Fig. 49: Chl (*a + b*) and Chlide *a* amounts analyzed from pigment extracts of leaf material of different age groups (young, mature and senescent) of WT and T1 generation of the selected three WSCP overexpressor lines. The pigment amounts were given as $\mu\text{g/gFW}$ and the values represent mean \pm SD of three independent sample extractions.

5.2.6.2 Measurements of Chl precursors like Pchlide in WSCP overexpressor plants

To analyse the role of WSCP to act as a repository for Pchlide, ALA feeding experiments in addition to estimation of Pchlide levels in dark grown seedlings were performed on WSCP overexpressor lines.

Progenies of both WT and selected WSCP overexpressor tobacco lines (two-week-old and green house grown) were taken and ALA solution (5 mM and 10 mM) was sprayed on the selected leaves. Care was taken that leaves of approximately same age were selected from

every plant. After dark incubation of the plants for 3 days, Pchlide levels were determined as per section 4.11.12.3. Pchlide levels were higher in WSCP overexpressor lines compared to WT tobacco at both tested concentrations of ALA in comparison to absence of ALA (0 mM ALA) (Fig. 50). The 0 mM ALA samples were collected from leaves of plants incubated for O/N in dark prior to the application of ALA onto the leaves.

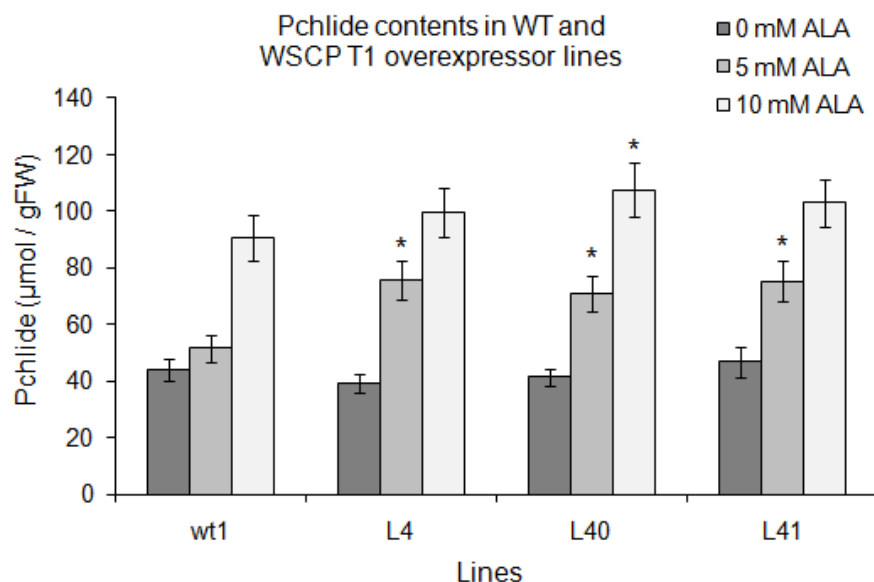


Fig. 50: Pchlide levels estimated in WT tobacco and WSCP overexpressor lines during the course of ALA feeding experiments. The bars represent the Pchlide contents after application of different ALA concentrations on leaves and incubation for three days in the dark room. The pigment amounts were given as $\mu\text{mol/gFW}$ and the values represent the means \pm SD of three independent experiments ($n = 3$). The difference between WT and WSCP overexpressor plants was given as * for $p < 0.05$ as calculated from F-test and T-test.

From the above results, it was evident that the amount of Pchlide deposited in the plant cells increased with exogenous application of increased ALA concentrations. Accumulation of Pchlide was observed in both WT and WSCP overexpressor lines at both the tested concentrations of ALA (5 mM and 10 mM) but higher in the overexpressor lines than the WT tobacco plants. Of the three overexpressor lines, line 40 showed significantly higher Pchlide levels at both 5 mM and 10 mM ALA concentrations in comparison to WT tobacco plants. The lines 4 and 41 showed significant accumulation of Pchlide only at 5 mM ALA concentration in comparison to WT tobacco plants.

The above result was further supported by the determination of Pchlide in one week old etiolated seedlings of both WT and WSCP overexpressor plants. The obtained results (Fig. 51) confirmed the presence of higher amounts of Pchlide in WSCP overexpressor

seedlings compared to WT. Both results (Fig. 50 and 51) revealed the accumulation of higher Pchlde amounts in the overexpressor plants in comparison to WT tobacco plants.

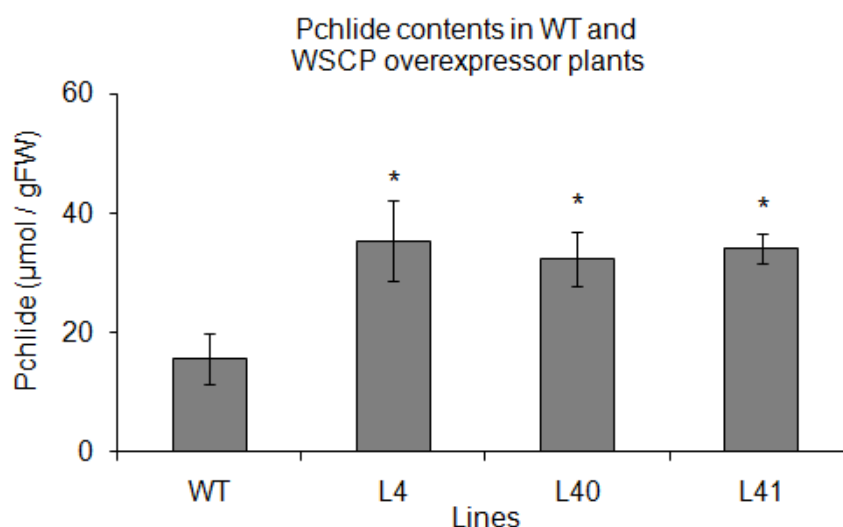


Fig. 51: Amounts of Pchlde in etiolated seedlings of WT and selected WSCP overexpressor lines. Respective seeds were grown in darkness and Pchlde contents were determined from one week old etiolated seedlings. The pigment amounts were given as $\mu\text{mol/gFW}$ and the values represent the means \pm SD of three independent experiments ($n = 3$). The difference between WT and overexpressor plants was given as * for $p < 0.05$ as calculated from F-test and T-test.

To verify if the increased levels of Pchlde in the WSCP overexpressor lines were due to changes in POR or WSCP protein levels, the protein extracts were analysed by western blot. The results demonstrated that expression of both POR and WSCP remained unaltered in the overexpressor lines and was comparable to that seen in WT tobacco plants (Fig. 52). The native POR protein was recognized at a band size of 30 kDa (Fig. 52a). The protein expression levels of recombinant WSCP were similar in all the overexpressor plants and was absent in WT tobacco plants (Fig. 52b).

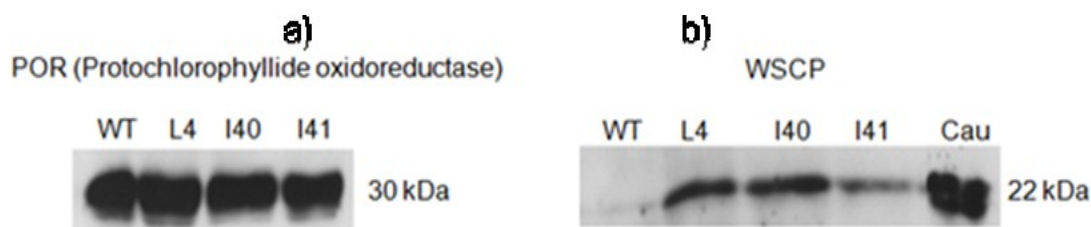


Fig. 52: a) Protein expression pattern of *POR* (protochlorophyllide oxidoreductase) in etiolated seedlings of WT tobacco and WSCP overexpressor plants. The *POR* protein was detected as a 30 kDa protein and was seen in similar amounts in all the tested samples. b) Protein expression pattern of Cau-WSCP-35 in etiolated seedlings of WSCP overexpressor plants. WT tobacco protein samples were used as a negative control and cauliflower protein extracts as positive control.

5.2.6.3 Expression levels of Cau-WSCP-35 protein during drought stress

A WSCP homolog from rapeseed was recently described as a drought induced protein, BnD22. This protein was highly expressed during leaf detachment and drought conditions (Ilami et al., 1997). Therefore, experiments were performed to assess the expression pattern of WSCP during water deficit conditions in the WSCP overexpressor plants.

Detached leaves were taken from both WT tobacco and selected lines (lines 4, 40 and 41) and subjected to drought stress conditions as listed in section 4.11.11. Presence of an immune-reacting band of WSCP of 22 kDa was visualised in overexpressor protein fractions similar to that of cauliflower protein extracts (positive control) (Fig. 53). No WSCP protein was detected in the WT tobacco leaf samples. Proof for equal loading of protein samples (each 20 µg) was shown in Fig. 54.

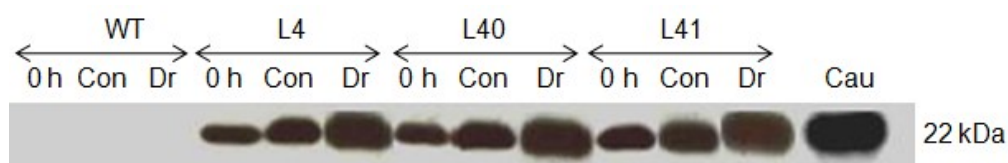


Fig. 53: Western blot analysis of soluble protein extracts of drought stressed leaf samples from WT tobacco and the WSCP overexpressor lines. Samples indicate 0 h (prior to start of the experiment), Con (30 h incubation of leaf in water) and Dr (30 h incubation of leaf without water). The protein extracts from cauliflower leaves was used as positive control.

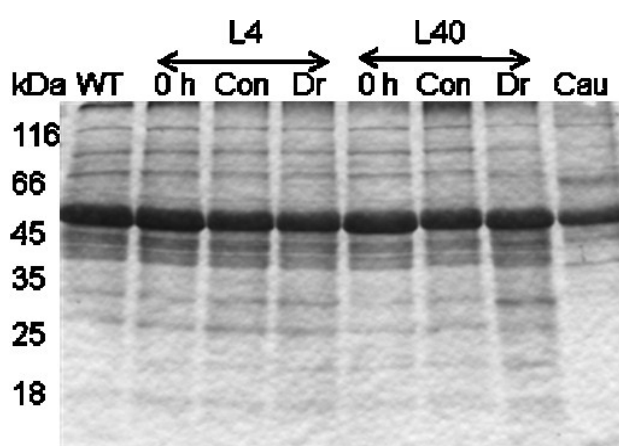


Fig. 54: SDS-PAGE analysis of soluble protein extracts of leaf samples from leaves exposed to drought stress from WT tobacco and the WSCP overexpressor lines. Samples indicate 0 h (prior to start of the experiment), Con (30 h incubation of leaf in water) and Dr (30 h incubation of leaf without water).

Fig. 53 clearly showed the accumulation of WSCP in the leaves subjected to drought stress compared to control and 0 h samples. In addition, the control samples showed increased

protein amounts than the 0 h which indicated the induction of protein expression due to leaf detachment accounting to wound stress.

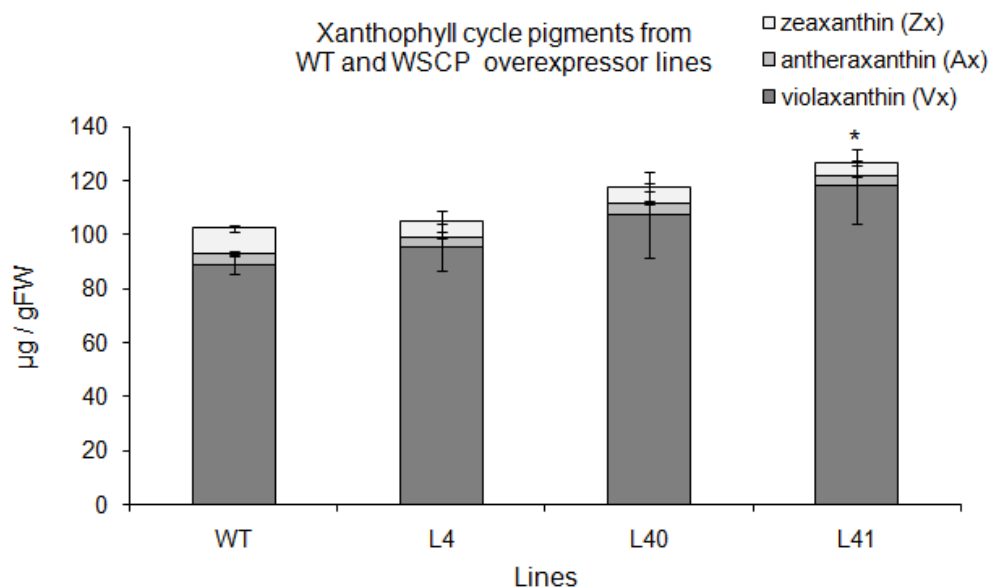
5.2.6.4 Determination of phototolerance mechanism in WSCP overexpressor plants

The inhibition of photooxidation of light exposed Chl-Cau-WSCP complexes in spite of the absence of carotenoids was shown *in vitro* by Schmidt et al. (2003). They reported that WSCP-Chl complexes exposed to high light evolved lower levels of ROS measured in comparison to unbound Chl molecules. To corroborate and confirm the possible participation of WSCP for tolerance to high light intensities *in vivo*, WSCP overexpressor lines were subjected to a series of high light stress experiments and analysed for altered levels of carotenoids and ROS. These data were supported by Chl fluorescence measurements of the WSCP overexpressor plants after their exposure to high light intensities.

Zeaxanthin levels in WSCP overexpressor plants

The conversion of violaxanthin to zeaxanthin in the de-epoxidation reaction of the xanthophyll cycle plays an important role in the protection of chloroplasts against photooxidative damage (Wehner et al., 2004). Hence, the levels of the xanthophyll cycle pigments (violaxanthin (Vx), zeaxanthin (Zx), and antheraxanthin (Ax)) were measured in both WT and WSCP overexpressor tobacco plants grown under normal growth conditions ($150 \mu\text{mol photons m}^{-2} \text{s}^{-1}$). The results showed that the Zx levels were lower in WSCP overexpressor lines in comparison to WT tobacco plants (Fig. 55).

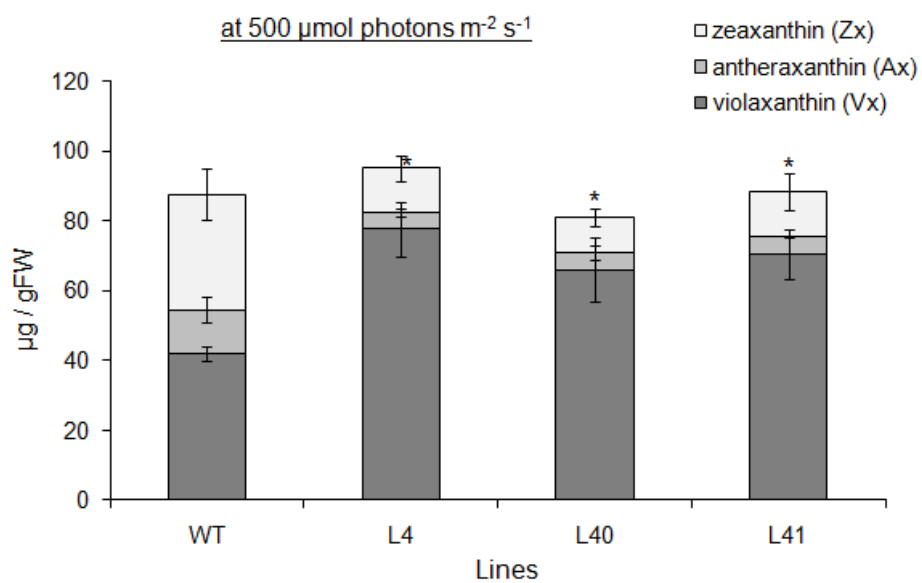
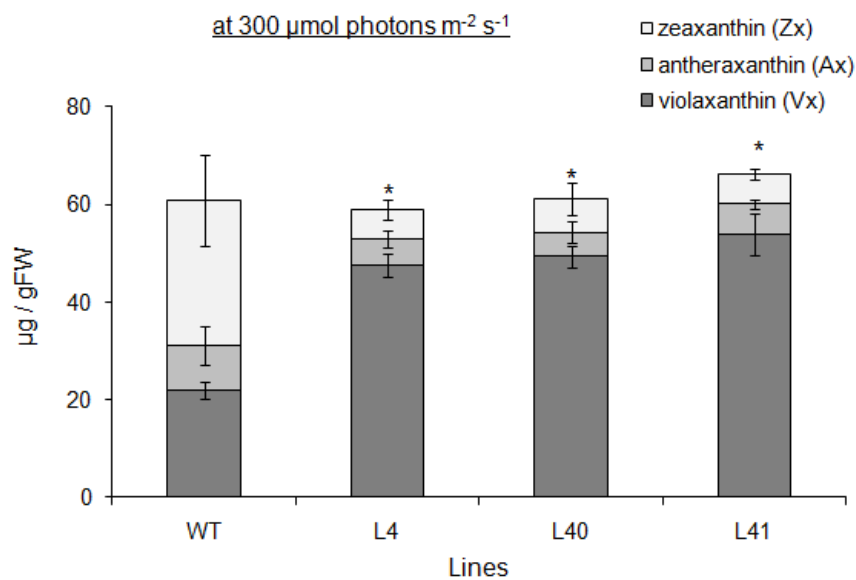
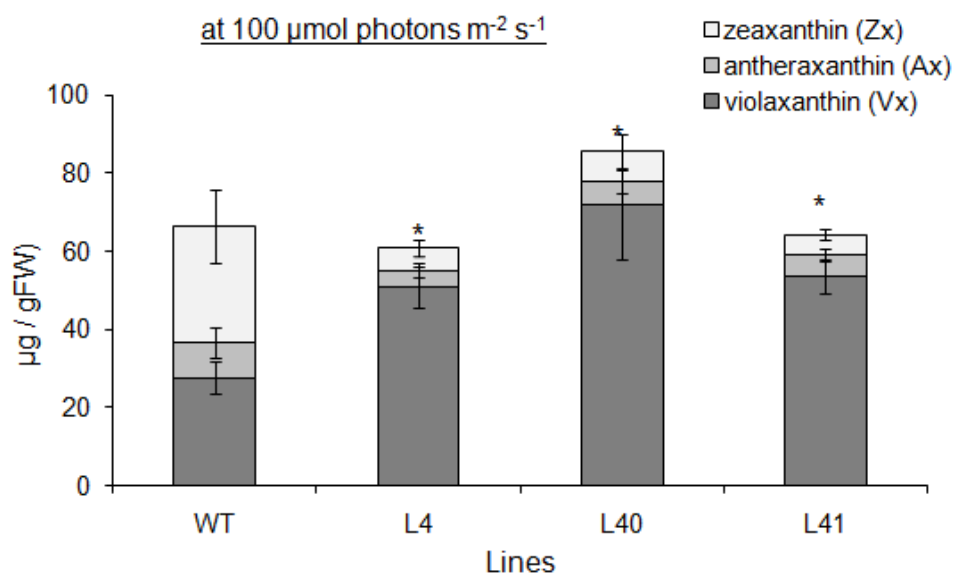
The total sum of Vx, Ax and Zx were higher in WSCP overexpressor plants in comparison to WT tobacco plants. The increased $\Sigma\text{Vx}+\text{Zx}+\text{Ax}/\text{Chl } a$ values in the WSCP overexpressor plants indicated a higher relative amount of xanthophyll cycle pigments in comparison to Chl. However, increased levels of xanthophylls were based on increased levels of violaxanthin relative to zeaxanthin. Thus, the ratios of Ax+Zx to total amounts of xanthophylls were lower in the overexpressor plants indicating the lower deepoxidation state of the xanthophyll cycle pool.



Lines	$\text{Ax} + \text{Zx} / \text{Ax} + \text{Zx} + \text{Vx}$	$\Sigma \text{Vx} + \text{Ax} + \text{Zx} / \text{Chl } a$
WT	0.11	0.16
L4	0.09	0.19
L40	0.09	0.21
L41	0.07	0.21

Fig. 55: Determination of xanthophyll cycle pigment levels: The WSCP overexpressor plants contained lower amounts of zeaxanthin compared to WT tobacco plants. The ratios of $\Sigma \text{Vx} + \text{Zx} + \text{Ax} / \text{Chl } a$ and $\text{Ax} + \text{Zx} / \text{Ax} + \text{Vx} + \text{Zx}$ (deepoxidation state) were calculated and given in adjacent table. The pigment amounts were given as $\mu\text{g/gFW}$ and the values represent the means \pm SD of three independent experiments ($n = 3$). The difference between WT and WSCP overexpressor tobacco plants was given as * for $p < 0.05$ as calculated from F-test and T-test.

To further verify the above results, detached leaves of both WT and WSCP overexpressor tobacco plants were subjected to different light intensities ranging from $100 \mu\text{mol photons m}^{-2} \text{ s}^{-1}$ to $1000 \mu\text{mol photons m}^{-2} \text{ s}^{-1}$ for 4 h. The xanthophyll cycle pigments were quantified from total pigment extracts by HPLC. The obtained results (Fig. 56) showed that all the selected WSCP overexpressor lines retained lower levels of Zx than the WT under all illumination (light stress) conditions. Though an increase in the amounts of Zx with increased light intensity (from 100 to $1000 \mu\text{mol photons m}^{-2} \text{ s}^{-1}$) was seen in both WT and WSCP overexpressor lines, the WSCP overexpressors contained lower Zx amounts than the WT tobacco plants.



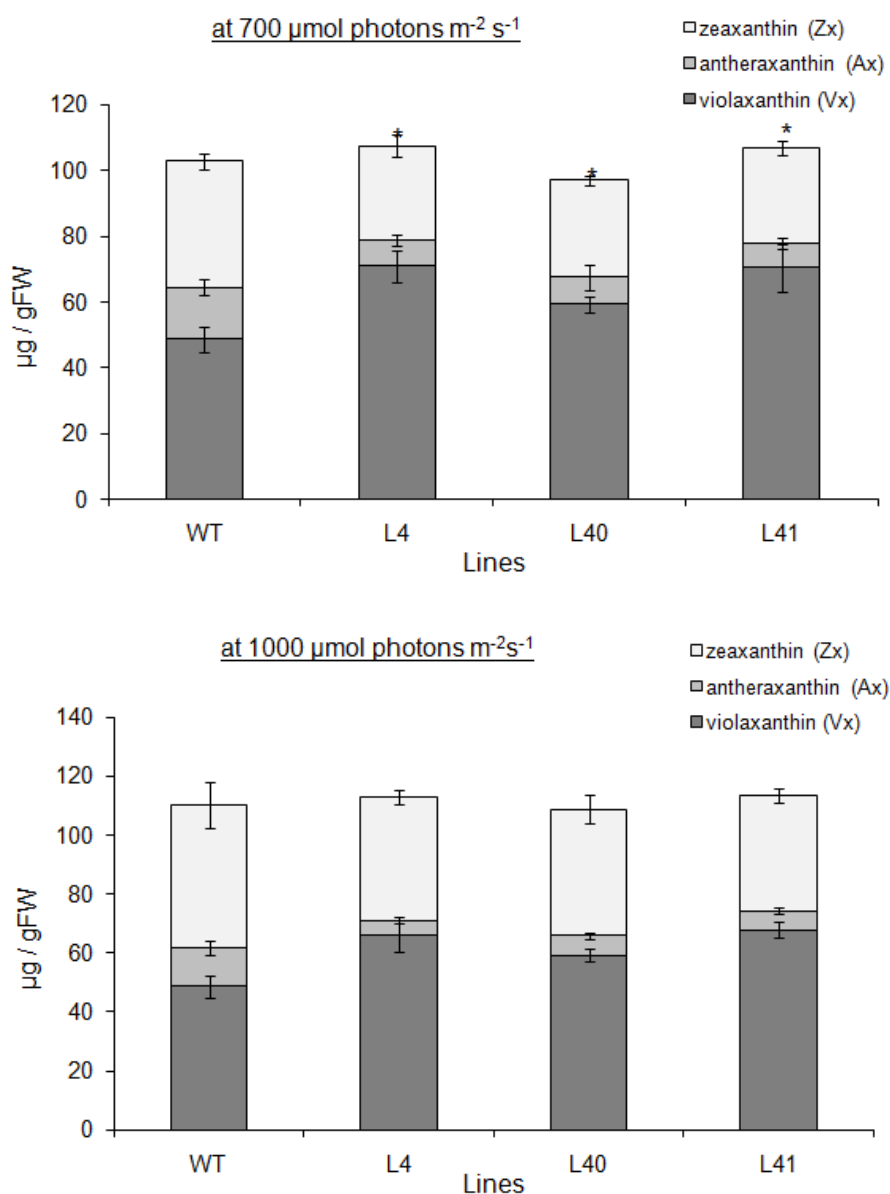


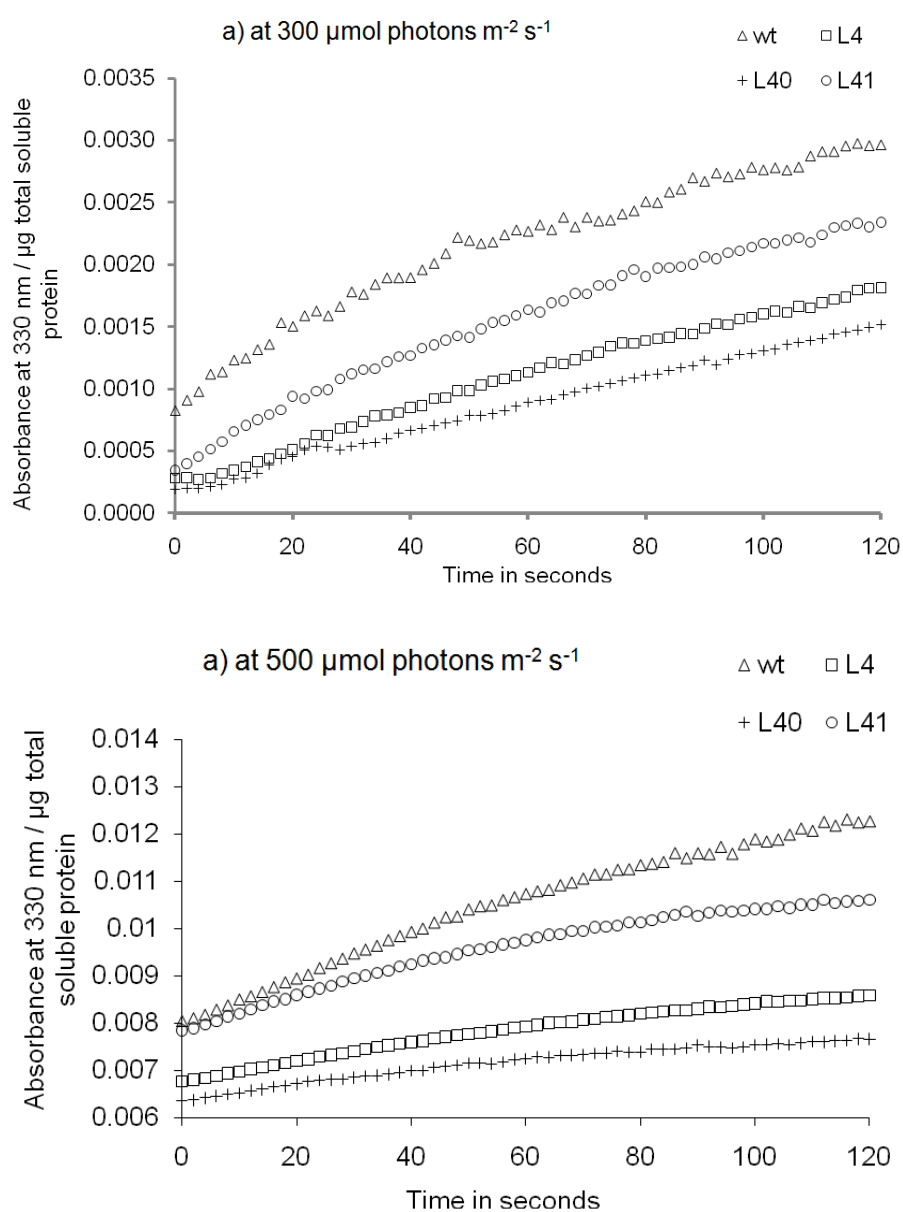
Fig. 56: Xanthophyll cycle pigments [violaxanthin (Vx), antheraxanthin (Ax) and zeaxanthin (Zx)] from both WT and WSCP overexpressor leaves exposed to different light intensities for 4 h. The range of light intensities used was 100 to 1000 $\mu\text{mol photons m}^{-2} \text{s}^{-1}$ with a gradient of 200 $\mu\text{mol photons m}^{-2} \text{s}^{-1}$. The pigment amounts were given as $\mu\text{g/gFW}$ and the values represent the means \pm SD of three independent experiments ($n = 3$). The difference between WT and WSCP overexpressor plants was given as * for $p < 0.05$ as calculated from F-test and T-test.

Measurements of ROS in terms of peroxidase activity in WSCP overexpressor plants

Although it has been reported that WSCP-Chl complexes do not contain any carotenoids (Kamimura, 1997), the mechanism of phototolerance of WSCP-Chl complexes remained unclear. Schmidt et al. (2003) proved this *in vitro* by measuring the rate of singlet oxygen formation in illuminated His-WSCP-Chl complexes. To examine this *in vivo*, the WSCP overexpressor plants were analysed for the production of ROS (peroxide free radicals) in

terms of peroxidase activity which explained the susceptibility of the plants to photooxidation.

Detached leaves from both WT and selected WSCP overexpressor tobacco lines were taken and exposed to various light intensities (300, 500 and 700 $\mu\text{mol photons m}^{-2} \text{s}^{-1}$) for 4 h. Total soluble protein extracts were isolated from the stress-exposed leaves and an *in vitro* estimation of the peroxidase activity was done as per section 4.11.15. Obtained results depicted in Fig. 57 clearly showed that the protein extracts from the WSCP overexpressor leaf samples exhibited less peroxidase activity (absorbance measured at 330 nm/ μg protein) on incubation with H_2O_2 .



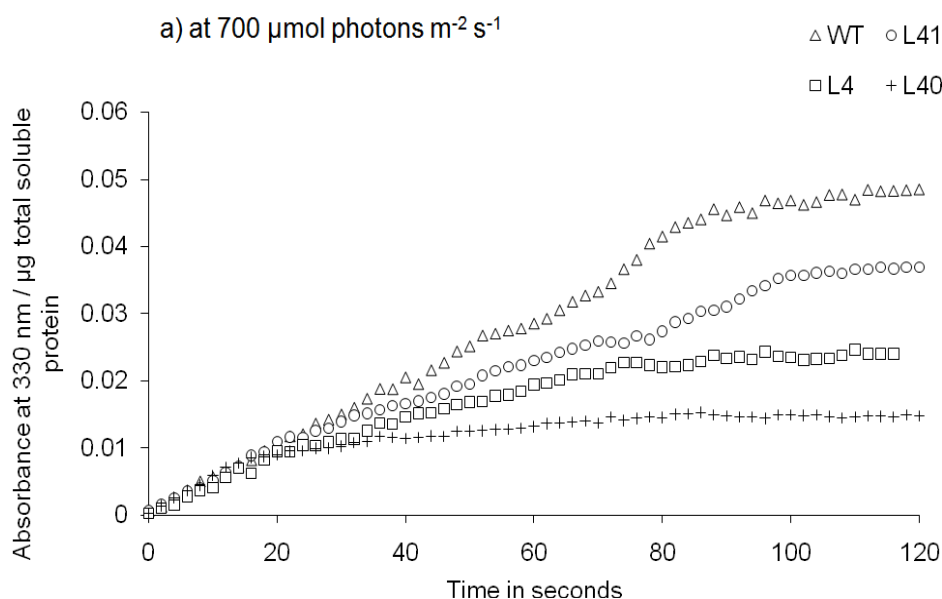


Fig. 57: Estimation of free peroxide radicals formed due to *in vitro* peroxidase activity in WT and WSCP overexpressor leaves on exposure for 4 h to high light intensities: a) 300 $\mu\text{mol photons m}^{-2} \text{s}^{-1}$ light, b) 500 $\mu\text{mol photons m}^{-2} \text{s}^{-1}$ and c) 700 $\mu\text{mol photons m}^{-2} \text{s}^{-1}$. Extent of free radical formation was given as absorbance measured at 330 nm/ μg protein.

The amount of peroxide radicals formed in the assay increased with increase in light intensity as indicated by absorbance at 330 nm (values on y-axis). In addition, the *in vivo* production of free radicals in both WT and WSCP overexpressor tobacco leaves was also ascertained. Incubation of the total soluble protein extracts with DAB without any additional supply of H_2O_2 indicated the amounts of peroxide radicals formed *in vivo*. It was observed that peroxide radical production in WSCP overexpressor plants was less than that seen in WT tobacco plants on illumination to high light (Fig. 58). However, the amounts of free radicals produced *in vivo* were lower in both WT and overexpressor tobacco plants compared to that seen with external supply of H_2O_2 (Fig. 57).

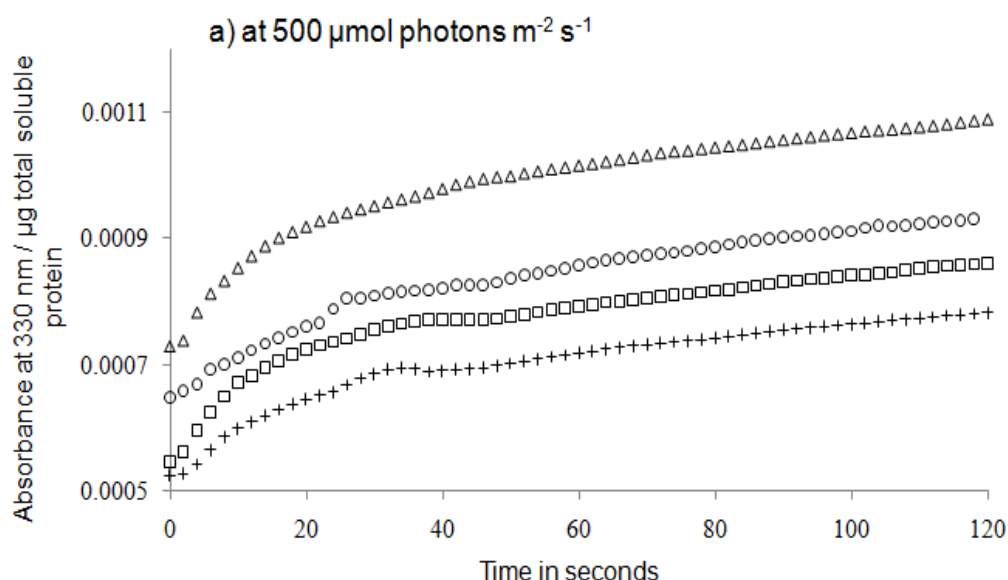


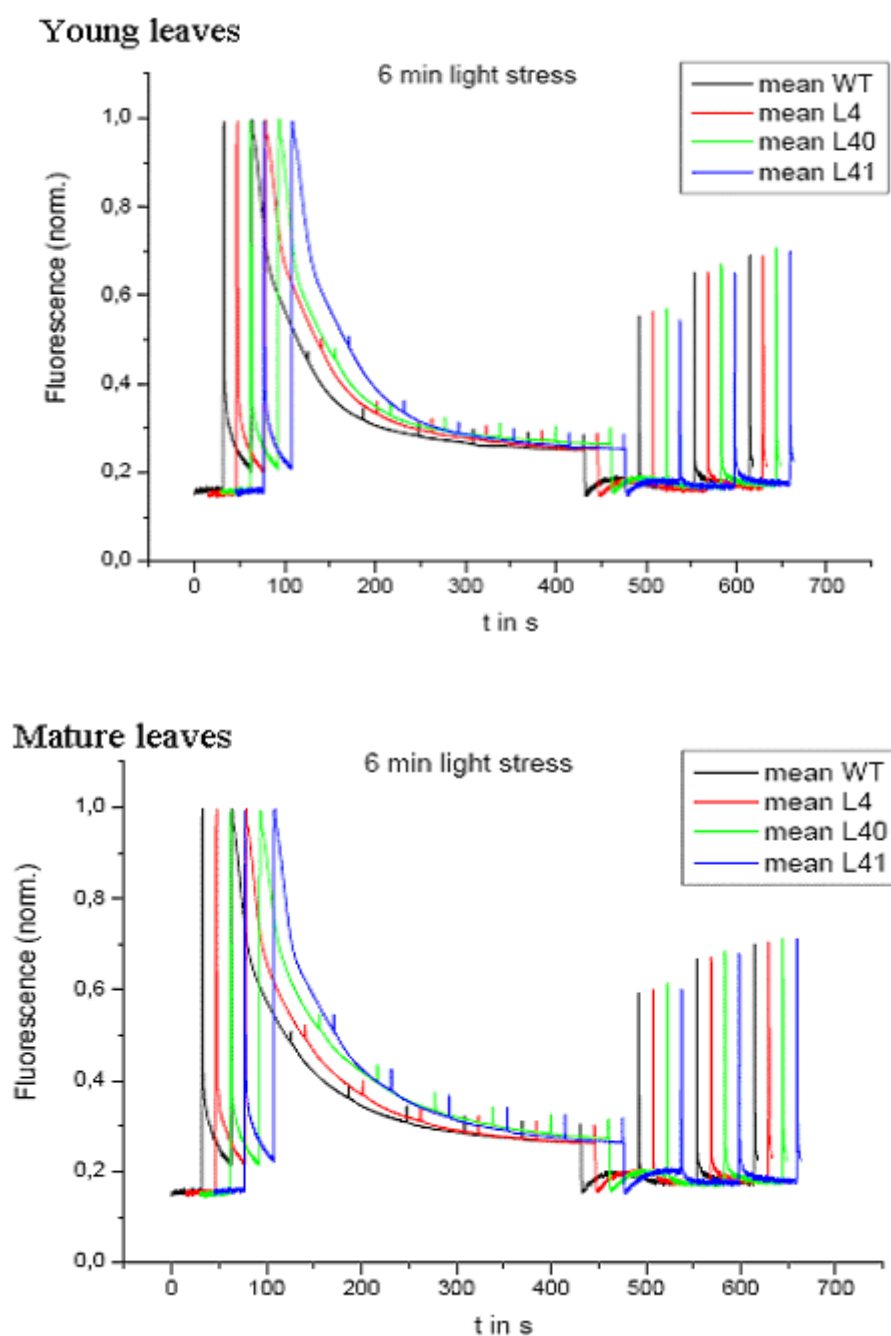
Fig. 58: Estimation of free peroxide radicals generated *in vivo* in WT and WSCP overexpressor plants. Free radical amounts were denoted as absorbance measured at 330 nm/ μg protein. The levels of peroxide radicals were lower in WSCP overexpressors than the WT tobacco plants.

Chl fluorescence measurements in WSCP overexpressor plants in response to high light stress

Decreased levels of zeaxanthin and peroxidase activity in WSCP overexpressor plants (Fig. 56 and Fig. 57) indicated the capacity of WSCP overexpressor plants to withstand high light stress. To further corroborate these observations, Chl fluorescence measurements were made on WT tobacco and WSCP overexpressing lines as described in section 4.11.14. A measure of Chl fluorescence during high light stress would give an account of non-photochemical processes, called as non-photochemical quenching (NPQ or q_N) that dissipate excitation energy of the excited Chls, resultant from excessive light absorption by photosynthetic reaction centres (Horton and Ruban, 1992; Horton et al., 1994).

Both WT and WSCP overexpressor tobacco plants were dark adapted and exposed to high-light treatment with an actinic light intensity of $900 \mu\text{mol photons m}^{-2} \text{s}^{-1}$. Chl fluorescence measurements were made with two different periods of light stress: short term (6 min) and long term (50 min) to differentiate between the various components of NPQ, i.e., q_E and q_I . The initial major and most rapid component of NPQ, which relaxes within seconds to minutes from high light stress is the pH or energy dependent quenching component termed as q_E . The other component, q_I is the photoinhibitory quenching and shows slowest relaxation kinetics in the range of long periods of time.

As the expression profile of the recombinant Cau-WSCP-35 protein followed the order young > mature > senescent in all the WSCP overexpressor plants (Fig. 45), fluorescence measurements were also performed taking the same age group leaves from both WT and overexpressor plants. No significant differences in qE were seen between WT and overexpressor tobacco plants in short term light-stress experiments (6 min) irrespective of leaf age (Fig. 59).



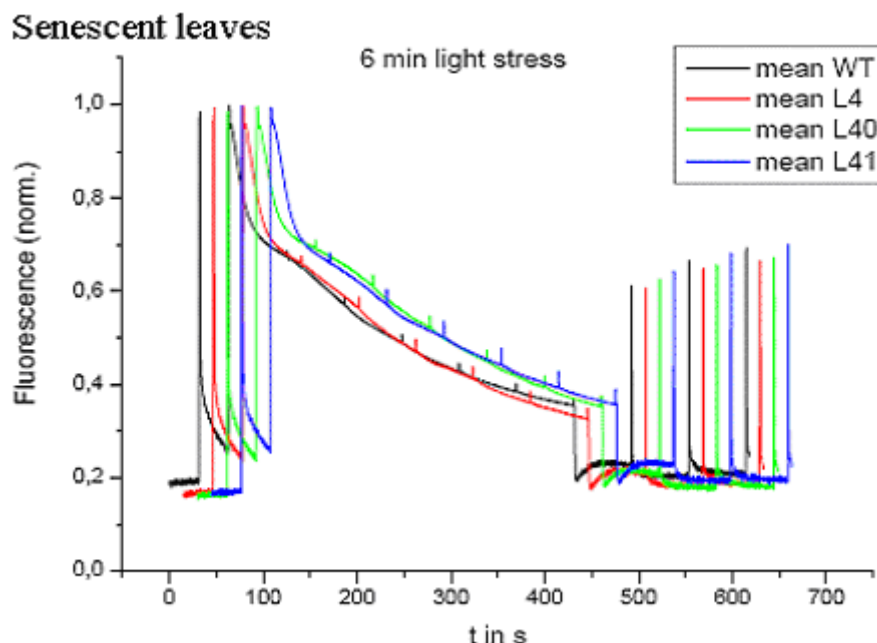
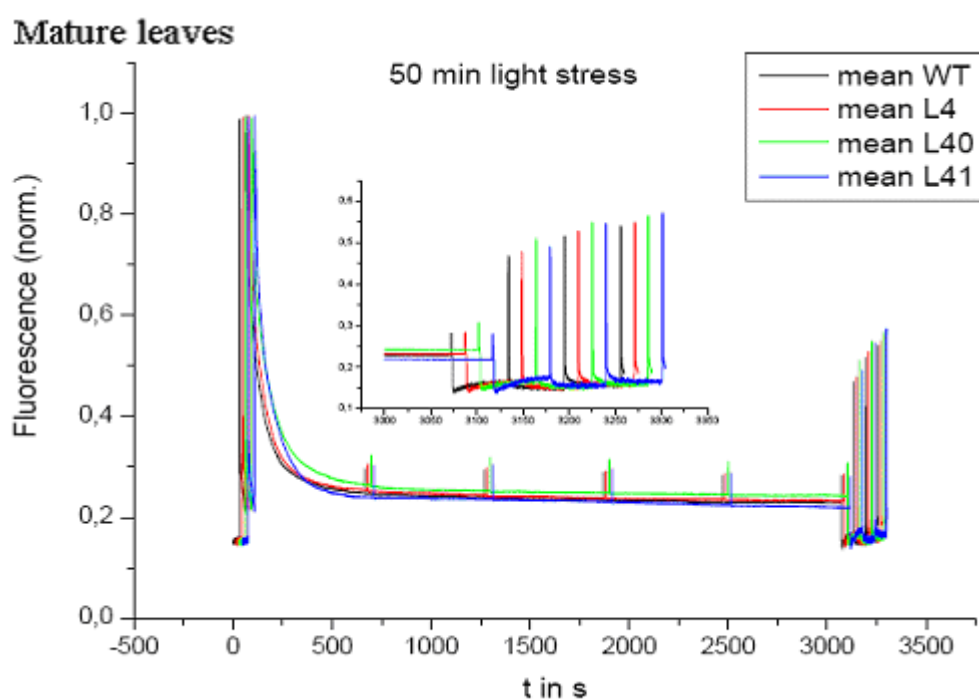
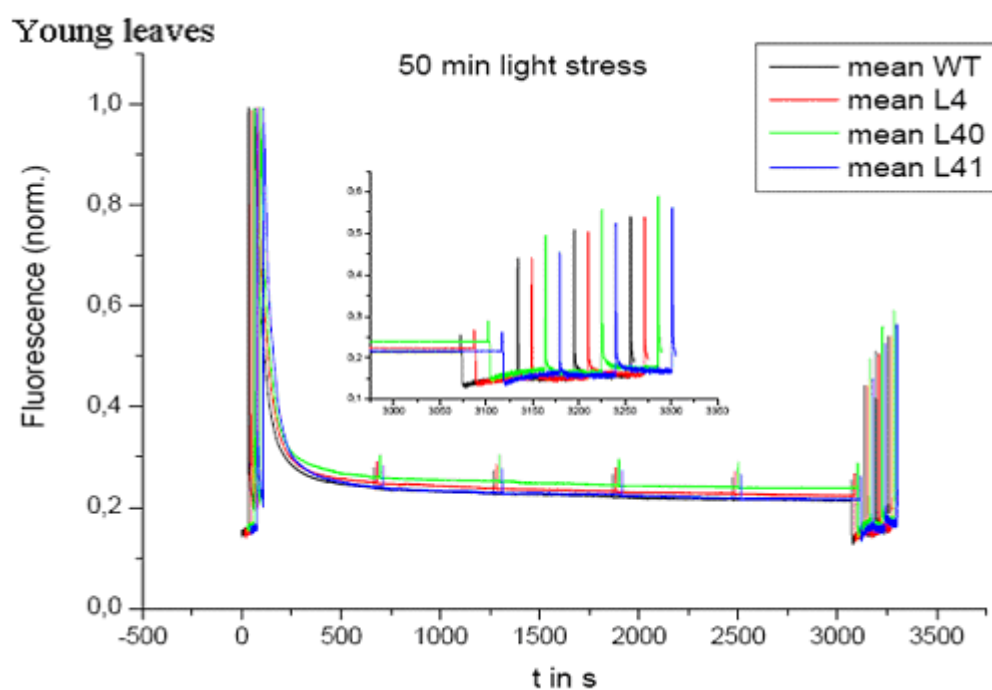


Fig. 59: Chl fluorescence measurements with WT and WSCP overexpressor plants - short-term light stress. Dark-adapted plants were taken, leaves of the same age were selected for respective measurements from all plants and subjected to actinic light of $900 \mu\text{mol photons m}^{-2} \text{s}^{-1}$ for 6 min with saturating pulses every minute. The data represent means of six independent measurements made on young, mature and senescent leaves of both WT and overexpressor plants.

It can be deduced from Fig. 59 that the short-term (6 min) light stress did not exert any influence on WSCP overexpressor plants in terms of faster induction or relaxation of non-photochemical quenching of Chl fluorescence (qE) as response to high light intensities. The results were similar with leaves of all ages and higher expression of WSCP in young leaves did not show any effect. This could be due to the fact that WSCP was not involved in short term photoprotective responses (such as the major, energization-dependent component, qE, of NPQ) in plants.

Long-term (50 min) light-stress experiments were performed to indicate the photoinhibitory component of NPQ (qI) more readily. These experiments showed faster relaxation of NPQ only in one progeny of overexpressor leaves (line 40) as compared to WT after prolonged exposure to high light intensity of $900 \mu\text{mol photons m}^{-2} \text{s}^{-1}$. The observation was more pronounced in the case of young leaves than the mature and senescent leaves of line 40 (Fig. 60).



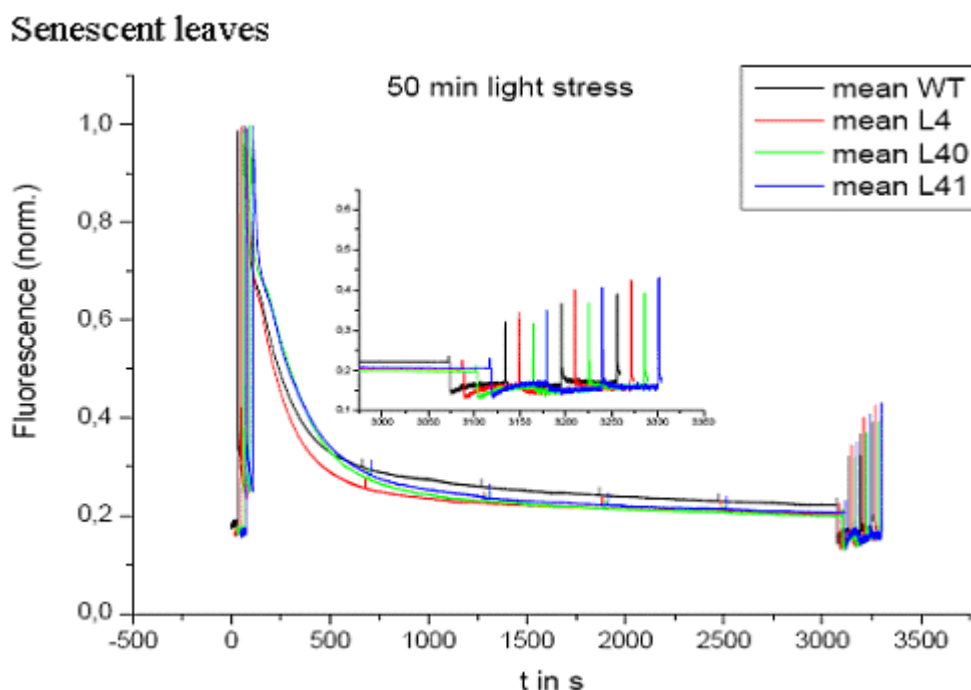


Fig. 60: Chl fluorescence measurements with WT and WSCP overexpressor plants - long-term light stress. Dark-adapted plants were taken, leaves of same age were selected for respective measurements from all plants and actinic light of $900 \mu\text{mol photons m}^{-2} \text{s}^{-1}$ was supplied for 50 min with saturating pulses every 10 minutes. The data represent means of six independent measurements made on young, mature and senescent leaves of both WT and overexpressor tobacco plants.

Derived from Fig. 60, it was obvious that young (and to some extent, mature) leaves of line 40 subjected to long-term light stress experiments (50 min of $900 \mu\text{mol photons m}^{-2} \text{s}^{-1}$) showed significant advantage (less photoinhibition, qI). The leaves of line 40 relaxed faster than the WT but this phenomenon was not seen in senescent leaves. The other two WSCP overexpressor lines, 4 and 41 showed slightly less qI than the WT or line 40. This could possibly be attributed to lower protein expression levels of Cau-WSCP-35 in the concerned leaves.

Of the three WSCP overexpressor lines analyzed, line 40 showed some consistency with regard to lower ROS and relaxation from high light stress.

6 DISCUSSION

Chl metabolism involves a coordinated regulation of Chl synthesis and degradation and thereby plays a distinct role in plant growth. It is widely assumed that the “Green seed problem” of oil rapeseed (*Brassica napus*) is due to delayed Chl breakdown during sub-lethal freezing stress conditions of autumn weather. In an effort to alleviate this problem, present work focussed on overexpression of Chlase and WSCP in transgenic tobacco and study the effect of the respective proteins under various stress conditions.

6.1 Choice of *Citrus* Chlase as transgene

EST database shows that most plants contain more than one Chlase homologue and only some of them were characterised (Table 1). Of these, *CHLASE1* from *Citrus* (Jacob-Wilk et al., 1999) was well studied in terms of chloroplast localisation (Trebitsh et al., 1993), and senescence (Shemer et al., 2008) confirming its significant role in Chl degradation pathway. Hence the present work favoured the *Chlase* gene from *Citrus clementii* (termed as *CcCHLASE*) as the transgene which was extracted from fruit peels and analysed for its enzymatic activities both *in vitro* and *in vivo*.

6.1.1 *CcCHLASE* was expressed as His-CcChlase and used for antibody production

The *CcCHLASE* cDNA sequence without its transit peptide sequence was expressed in BL21DE3pLysS strain of *E. coli* as His-tagged CcChlase protein. A protein band of 35 kDa, representing His-CcChlase was found after induction in the *E. coli* strains in total lysate, soluble and insoluble fractions (Fig. 9, lanes 3 - 5). Purification of His-CcChlase using Ni-NTA affinity chromatography showed a single protein band of 35 kDa (Fig. 9, lane 6) in line with the protein in the fractions of induced *E. coli* strains. Western blot analysis using anti-His antibody confirmed the presence of His-CcChlase in all the cellular fractions of *E. coli* (Fig. 9, lanes 9 - 11) and also the purified fraction (Fig. 9, lane 12). Identification of 35 kDa protein band (33 kDa without His-tag) was in concordance with the reports of purified Chlase from acetone powders of *Citrus* fruit peels (Trebitsh et al., 1993) and the Chlase protein from fruit peels of Valencia orange (Jacob-Wilk et al., 1999). Expression studies on other Chlase homologues i.e., *AtCLH1*, *CaCLH*, and *CHLASE1* in *E. coli* also showed similar molecular weight (Benedetti and Arruda, 2002; Tsuchiya et al., 1999; Jacob-Wilk et al., 1999). Anti-His antibody was used due to unavailability of a commercial CcChlase specific antibody. Keeping in view of the greater need for such a

specific antibody, induced soluble extracts of *E. coli* containing His-CcChlase were purified on a large scale and used as antigen for the production of a polyclonal antibody.

The serum collected after 60 days from rabbits immunized with His-CcChlase was used to probe total cell lysate, soluble fractions of *E. coli* and purified protein fraction containing the His-CcChlase protein (Fig. 10). Identification of a 35 kDa protein in all the fractions (Fig. 10, lanes 10 - 12) in line with the results from Fig. 9 confirmed the specificity of antibody against the His-CcChlase. Similarly, this antibody also detected a protein band of size 33 kDa in membrane protein extracts of *Citrus* leaves which corresponded to the calculated molecular weight of Chlase protein without transit peptide (Fig. 10, lane 13). The results were similar to those obtained by Jacob-Wilk et al. (1999) and Harpaz-Saad et al. (2007) who confirmed that the mature Chlase protein in the plant cells has 33 kDa molecular weight.

However, in a separate experiment during screening of transgenic tobacco plants overexpressing *CcCHLASE*, the antiserum cross-reacted with proteins of WT tobacco plants detecting a protein band with a molecular mass of 33 kDa similar to the expected size of mature Chlase protein (Fig. 10, lanes 14 - 16). This finding showed the inability of the antibody to distinguish between WT tobacco plants and transgenic plants containing overexpressed CcChlase protein. Hence the antiserum could not be used for further applications such as screening for selection of candidate Chlase overexpressor lines.

6.1.2 Enhanced *in vitro* Chl hydrolysis by His-CcChlase proved its Chlase activity

The recombinant His-CcChlase protein was tested *in vitro* for its functional activity. *In vitro* Chlase activity of recombinant *COR1* protein was reported by Tsuchiya et al. (1999) using total bacterial lysates as a source of enzyme. The present study adopted the same protocol. Assays were initially standardised for the determination of detergent (TX-100) and protease inhibitor (PMSF) composition as well as source of bacterial fraction to be used as enzyme (i.e., total lysate or soluble or membrane extract containing His-CcChlase).

All the assays were performed in a water-miscible organic solvent system as previous reports showed a higher hydrolytic activity of Chlase in water-miscible organic solvent system compared to water-immiscible organic solvent system (Khamessan et al., 1995). The assay system used comprised of a mixture of buffer and acetone as organic phase (easily miscible with buffer) providing a continuous phase system for Chlase. This system

was superior to the biphasic organic system where in both substrate and enzyme should come into contact with each other at the interphase. Enzyme activity of Chlase was measured as the amount of Chlide formed after Chl breakdown.

Crude cellular extracts from the induced bacterial cultures containing His-CcChlase exhibited Chlase activity by hydrolysing Chl to Chlide. This was visualized by the green coloured aqueous phase due to the formation of hydrophilic Chlide after removal of hydrophobic phytol side chain of Chl (Fig. 11). Similar results were obtained by Benedetti and Arruda, (2002) by performing Chlase assays with bacterial soluble extracts containing recombinant COR11 protein in which accumulation of Chlide was seen in the lower aqueous phases after extraction with a hexane/acetone mixture.

Addition of 0.1% TX-100 to the assay system enhanced Chlase activity by 2 - 3 fold, as seen in the form of higher amounts of Chlide formed in the reaction in comparison to the Chlide contents in the absence of detergent. Presence of TX-100 has dual functions; it releases the protein from the membrane fraction during protein extraction and when present in the reaction medium, can activate the enzyme by preventing the intramolecular aggregation and loosening the hydrophobic contacts. Another important component of the buffer, PMSF, a serine protease inhibitor, when present in higher concentration, can inhibit Chlase which has serine lipase motif. Hence, PMSF titration was needed to find the optimal concentration at which Chlase activity was not affected. The enzyme was not inhibited up to 1.5 mM PMSF, but was inactivated at more than 2 mM PMSF in the reaction. Thus 0.1% TX-100 and 1.2 mM PMSF were maintained in all enzyme assays of Chlase to ensure its maximum functional activity.

Chlase activity was analysed to select the appropriate bacterial fractions for subsequent enzyme assays. Induced bacterial cultures containing His-CcChlase were sonicated in an extraction buffer containing TX-100 (0.1% v/v) to ensure higher accumulation of proteins into soluble phase. All the three phases (total cellular lysate, soluble and insoluble – 100 µg each) were tested for enzyme activity *in vitro* and specific activities were calculated as nmol hydrolysed Chl protein mg⁻¹ min⁻¹ respectively. It was obvious that total cell lysate showed higher activity than the other two due to the presence of more His-CcChlase in an aliquot of 100 µg compared to the soluble and insoluble fraction (Fig. 12). Although similar amounts of His-CcChlase were seen in soluble and membrane fraction (seen from coomassie gel picture), the former showed relatively higher activity compared to the

membrane fraction (graph of Fig. 12). This could be due to the presence of His-CcChlase in a proper folded and enzymatically active form in soluble fraction than in the insoluble fraction. Similar observations were made by Yan et al. (2006) for Oligopeptidase B (OpdB) of *E. coli* which was present in enzymatically active form in the soluble fraction of the bacterial induced cultures. Hence, soluble fractions were employed in all subsequent enzyme assays.

Purified soluble His-CcChlase was also subjected to enzyme assays. This was done in an attempt to supply the purified protein for industrial purpose as enzyme source to degrade Chl in the process of refining rapeseed oil. Both bacterial soluble extracts containing His-CcChlase and pure His-CcChlase protein fraction were tested for their functional activity by measuring the amounts of Chlide formed in the reaction (Fig. 13). The amount of Chlide formed was higher in assays performed with bacterial soluble extracts containing His-CcChlase compared to aliquots of purified Chlase protein. The soluble extracts from bacterial cultures containing the pQEempty vector showed almost no Chlase activity, ruling out the possibility of enzymatic activity from other bacterial proteins. The possible reasons for lower activity of the purified His-CcChlase could be 1) partial aggregation and inactivation of the protein molecules due to the presence of high concentrations of imidazole in the buffer (250 mM) and 2) the Ni^{+2} ions present in the resin during purification procedure can precipitate proteins by salt bridge formation and damage the protein because of its nucleophilic properties. Additionally, purified Chlase could be less stable compared to crude protein, because the total protein extracts probably protect the enzyme against proteolytic degradation *in vitro*. Hence, crude soluble extracts containing His-CcChlase were chosen for its further characterization in terms of enzyme kinetics and optimization of the reaction parameters.

6.1.2.1 His-CcChlase exhibits an optimal activity at 40°C and pH 8.0

Typically activity of any enzyme depends on the incubation temperature, pH and the ionic content of the medium. Literature data shows that *in vitro* Chlase activity vary in different plant species with respect to pH and temperature: sugar beat (40°C, pH 7.1) (Bacon and Holden, 1970), *Citrus limon* (pH 7.8) (Fernandez-Lopez et al., 1992), *Capsicum annuum* L. fruits (50°C, pH 8.5) (Hornero-Me'ndez and Mi'nguez-Mosquera, 2001), greened rye seedlings (30°C, pH 7.0 - 8.5) (Tanaka et al., 1982), *C. sinensis* L. (45°C, pH 7.5) (Trebitsh et al., 1993), *C. album* (pH 7.0) (Tsuchiya et al., 1997), olive fruits (50°C, pH 8.5) (Mi'nguez-Mosquera et al., 1994) and algae such as *P. tricornutum* [31°C and 35°C (Gaffer

et al., 1999), pH 8.0 (Khalyfa et al., 1995)], *Chlorrella vulgaris* (pH 7.2 - 7.3) (Böger, 1965) and *Chlorella protothecoides* (45°C pH 6.0 - 8.5) (Tamai et al., 1979).

In the present study, activity and stability of His-CcChlase in relation to pH was determined by sonicating induced bacterial cultures using buffers of varying pH. Results from Fig. 14 show that activity of Chlase exhibited different temperature optima by varying the pH of extraction buffer. Activity of His-CcChlase recorded temperature optima of 40°C in the presence of high pH extraction buffer (> 7.0). The results were similar to Chlase isolated from *C. sinensis* leaves (pH 7.0 - 8.0 and 45°C; Amir-Shapira et al., 1986). Decreasing the pH to slightly acidic pH i.e., 6.0 and 6.6, shifted the temperature optimum to a higher temperature of 50°C. Overall, activity of His-CcChlase was better at alkaline pH (7.4 and 8.0) than in acidic pH (6.0 and 6.6). It was found that Chlase from *C. clementii* exhibited a pH optimum of 8.0 in a water-miscible organic solvent system. This result was in agreement with activity of partially purified Chlase from *P. tricornatum* in a similar reaction system (pH 8.0; Khamessan et al., 1995) and Chlase from *G. biloba* (*GbCLH*) (pH 7.5; Okazawa et al., 2006). This suggests that His-CcChlase works in slightly neutral or weakly basic environment such as in the cytoplasm or chloroplasts. In contrast, acidic optimum pH values were reported for Chlase from tea leaves [30-35°C, pH 5.8 (Ogura, 1972) and pH 5.5 (Kuroki et al., 1981)]. With the temperature optimum being 40°C at pH > 7.0, all assays were performed in extraction buffer of pH 7.4 as source of enzyme.

6.1.2.2 Effect of incubation time on His-CcChlase activity

Duration of incubation time for Chlase activity depends on the type of organic solvent used in the reaction system. The hydrolytic activity of Chlase requires more time in case of non-polar solvents like hexane compared to polar organic solvent like acetone (Khamessan et al., 1995). In the present study, Chl substrate was often dissolved in acetone solvent. It was observed that for the given amount of Chl substrate (250 µM) and bacterial soluble extract containing His-CcChlase (100 µg), Chl hydrolysis was higher in the first 5 min of the reaction (about 5%). Increasing the incubation time to 30 min resulted in overall Chl hydrolysis of 10%. No significant amount of Chl hydrolysis was observed after 30 min (only 1.4% of Chl hydrolysis after 30 min till 105 min) (Table 7). It was apparent that the limiting factor has been the amount of enzyme and could only hydrolyse 10% of Chl substrate in 30 min. The decrease in rate of hydrolysis during the time course after 30 min could be due to a) inaccessibility of Chl to Chlase b) lack of substrate in the reaction media, and hence the lower availability of the substrate for the enzyme c) decrease in the

stability of Chlase (Khamessan and Kermasha, 1995). As 10% of Chl was hydrolysed in 30 min, a reaction time of 30 min was followed for most of the enzyme assays. The specific activities of His-CcChlase decreased with increasing time of incubation of the reaction mixture, being highest in the initial 5 min.

6.1.2.3 Increased acetone concentration minimises the His-CcChlase activity

The hydrolytic activity of Chlase largely depends on nature of organic solvent present in the reaction mixture, showing higher activity in water-miscible organic solvent like acetone than in water-immiscible organic solvent like hexane (Khamessan et al., 1995). Activity of Chlase depends on acetone concentration and differs significantly in various plant species: snap beans – at 50% (Fang et al., 1998), *P. tricornatum* – at 17.5% and 30% (Khamessan et al., 1993) and green rye seedlings – at 30% of acetone (Tanaka et al., 1982).

In the present study, all enzyme assays of His-CcChlase were performed in a water-miscible organic solvent system, consisting of defined amounts of acetone and buffer. The amount of acetone added to the reaction mixtures was in addition to the amount of acetone present as solvent in the substrate aliquot used in the assays. Based on results in Fig. 15, it was found that the activity of His-CcChlase decreased with an increase in acetone concentration. The specific activity of His-CcChlase was highest with 10% of acetone and decreased by 1.5 fold at 38% of acetone concentration (Fig. 15). However, beyond 38 - 40%, a steep decrease in activity was noticed with almost no activity at concentrations of 80 - 98% acetone. This showed that His-CcChlase was tolerant in acetone concentrations of 38% and this result was comparable with previous findings, e.g. *CaCLH* at 20% acetone (Tsuchiya et al., 1997), *CHLASE1* at 9% (Jacob-Wilk et al., 1999), wheat Chlase at 20% (Arkus et al., 2005), *CORII* at 30% of acetone concentration (Benedetti and Arruda, 2002). While lower concentrations of acetone (below 20%) ideally increase the substrate (Chl) solubility leading to better hydrolysis, higher concentrations of acetone on the other hand could precipitate the protein (Chlase) inhibiting the hydrolysis (Mc Feeters, 1975). Also acetone could aid in dissociation of Chl dimers and oligomers into monomers (Kermasha et al., 1992).

6.1.2.4 Substrate – Enzyme interaction

Hydrolysis of Chl by Chlase follows first order kinetics (Garcia et al., 1980). An attempt was made to determine the threshold of His-CcChlase activity in the presence of saturating

amounts of Chl substrate, when the reaction follows a first order kinetics in a system containing acetone and buffer.

The kinetic parameters for His-CcChlase catalytic activity were determined in a water-miscible organic solvent system with substrate concentration in the range of 50 - 500 μM /700 μl . The results (Fig. 16a) showed that the relationship between Chlase activity and Chl concentration followed a hyperbolic curve at Chl concentrations lower than 350 μM in the reaction. The results indicated that the initial reaction rate increased with increasing substrate concentration but then remained almost stationary at higher concentrations of 400 to 500 μM /700 μl . This decrease in Chlase activity at higher substrate concentrations could be attributed to enzyme inhibition by the by-product phytol (Bitar et al., 2004).

Results in Fig. 16b also demonstrated that Chlase-Chl interactions in water-miscible organic solvent system obeyed Michaelis–Menten kinetics as indicated by the linearity of corresponding Lineweaver–Burk plot. The obtained high K_m value showed that the rate of product formation depended on substrate availability. These results were in agreement with observations of Khamessan et al. (1993). The K_m (272.3 nmol/ml) and V_{max} (39.6 nmol hydrolysed Chl mg protein⁻¹ min⁻¹) values represented higher affinity and solubility of Chl in a water-miscible organic solvent system. Also the Chlase isolated from *P. tricornutum* exhibited K_m and V_{max} values of 328 nmol/ml and 1.9 nmol hydrolysed Chl mg protein⁻¹ min⁻¹ in a water-miscible organic solvent system (with 400 μM of Chl and 200 μg enzyme) (Yi et al., 2006).

6.1.2.5 Effect of enzyme concentration on His-CcChlase activity

The optimum amount of Chlase protein required for hydrolysis of Chl depends on the nature of organic solvent used in the reaction media. Addition of polar solvent increases the solubility of both substrate and enzyme in the assay and would therefore require lower amounts of enzyme for hydrolysis (Khamessan et al., 1995). Hence, assays were done to study the effect of enzyme concentration (His-CcChlase) on hydrolytic activity of Chlase and bioconversion of Chl. With Chl as substrate, the hydrolytic activity (in terms of % of Chl hydrolysis) increased with increasing Chlase concentration in the reaction. Increasing the protein concentration from 50 μg to 400 μg showed an increase in Chl breakdown by approximately 14% (Table 8). The reaction kinetics followed first order kinetics and the K_m value was determined to be 242.3 nmol/ml of Chl which was required to achieve half of Chlase's maximum velocity (Fig. 17).

6.1.2.6 Specificity of His-CcChlase towards Chl *a* and Chl *b*

Chlase was found to be active on Chl *a* and also on Chl *b* (Mc Feeters et al., 1971). The interaction between Chl and Chlase is based up on stereo specificity of substrate which relates to the configuration around the C13 of tetrapyrrole ring of the Chl (Fiedor et al., 1992). Literature data shows contrasting K_m and V_{max} values for Chlase with Chl *a* and Chl *b*. Fernandez-Lopez et al. (1992) reported higher K_m for Chl *a* than Chl *b* and on the other hand lower K_m for Chl *a* than Chl *b* was reported by Shimokawa, (1982), Tsuchiya et al. (1997) and Trebitsh et al. (1993).

The activity of His-CcChlase was checked with both purified Chl *a* and Chl *b* as substrates in a water-miscible organic solvent system. With Chl *a* as substrate, His-CcChlase showed proportional increase in hydrolysis until 250 μM of substrate and then remained more or less stationary (with an enzyme concentration of 100 μg in all the reactions) (Fig. 18a) which could be due to saturation of all enzyme active sites at higher substrate concentrations. The interaction between Chl *a* and His-CcChlase in the reaction system obeyed Michaelis–Menten kinetics indicated by linearity of corresponding Lineweaver–Burk plot and the K_m and V_{max} values were calculated to be 148.9 nmol/ml of Chl and 25.9 nmol hydrolysed Chl $\text{mg protein}^{-1} \text{ min}^{-1}$ respectively (Fig. 18b).

When Chl *b* was used as substrate, His-CcChlase activity showed a steep increase at 50 μM substrate concentration, and subsequently a gradual increase up to 250 μM and eventually remained constant (Fig. 19a). The Lineweaver–Burk graph (Fig. 19b) showed a K_m value of 48.9 nmol/ml of Chl and V_{max} of 24.8 nmol hydrolysed Chl $\text{mg protein}^{-1} \text{ min}^{-1}$. Since His-CcChlase protein exhibited almost 3 times higher K_m value for Chl *a* than Chl *b*, it may be concluded that the enzyme exhibits higher affinity towards Chl *b* than Chl *a*. This can be attributed to the structural differences between Chl *a* and Chl *b* at the C3 carbon ($-\text{CH}_3$ and $-\text{CHO}$, respectively) indicating the involvement of a carbonyl group in the substrate recognition. Similarly, a slightly higher V_{max} value, denoting faster enzyme activity of Chlase for Chl *a* in comparison to Chl *b* was in agreement with the fact that Chl *a* is the natural substrate for Chlase. These results were similar to that obtained by Okazawa et al. (2006) on recombinant Chlase from *G. biloba* (*GbCLH*), which exhibited maximum affinity for Chl *b* by Chlase and hydrolysed Chl *b* more rapidly than Chl *a*. Similar results were also reported on olive (Minguez-Mosquera et al., 1994), Satsuma mandarin (Shimokawa, 1979) and *Capsicum* fruits (Hornero-Mendez and Minguez-Mosquera, 2001).

6.1.2.7 Inhibitory effect of Phytol on His-CcChlase activity

Phytol, an initial byproduct of Chl hydrolysis, is a non-competitive inhibitor of Chlase influencing the equilibrium state of hydrolysis of Chl and Phe into Chlide and Pheide (Khmaessan et al., 1993). The phytol molecule can competitively bind at the active site of Chlase, and inhibit its activity (Levadoux et al., 1987). Results from the present study in Fig. 20a, showed that an increase in phytol concentration from 2 to 8 μM in reaction inhibited the enzyme activity by 50 % and up to 95% activity at 10 μM . Lineweaver–Burk plot (Fig. 20b) showed the non-competitive inhibitory nature of phytol on Chlase activity with a K_i value of 5.4 μM . The results indicate that phytol could bind to enzyme-substrate complex yielding an inactive enzyme substrate inhibitor complex. Similar results were obtained by Khmaessan et al. (1995) for Chlase isolated and characterized from *P. tricornatum* to exhibit a K_i value of 1.9 μM for phytol in a water/acetone system (with 20 μM Chl, 10 μg enzyme and phytol from 0 – 3 μM).

6.1.2.8 His-CcChlase activity on thylakoid membranes clarifies how Chl was stabilized in thylakoid membranes

In higher plants, Chl is bound up in a couple of the large and complex protein complexes called photosystem I and photosystem II in thylakoid membranes of chloroplasts and has to be released from proteins before it can become substrate for Chlase catalysis. Additions of detergent like TX-100 or organic solvent like acetone facilitates the process of removal of pigment molecules from membranes into the reaction system (Shimokawa, 1981; Jacob-Wilk et al., 1999). To study the above phenomenon *in vitro*, thylakoid membranes were used in the assays based on their Chl contents. As both TX-100 and acetone were present in the reaction system; their influence on Chlase activity was studied. With increase in Chl contents of thylakoid membranes in the assays from 50 to 500 μM , there was a steady increase in Chlide amounts produced in the reaction (Fig. 21a). The formation of higher amounts of Chlide reflected an easier removal of membrane bound Chl into the aqueous phase of the reaction system *in vitro*. The reaction kinetics follow Michaelis–Menten law, indicated by linearity of corresponding Lineweaver–Burk plot with K_m and V_{max} values at 259.9 nmol of Chl/ml and 54.8 nmol hydrolysed Chl $\text{mg protein}^{-1} \text{ min}^{-1}$ respectively (Fig. 21b). The K_m value in the present case (with thylakoid membranes) was slightly lower than that obtained with purified Chl as substrate (272.3 nmol of Chl/ml) indicating relatively higher affinity of Chlase to membrane bound Chls compared to free purified Chls. But V_{max} values attained with purified Chl (V_{max} - 39.6 nmol hydrolysed Chl/mg

protein⁻¹ min⁻¹) was lower than that obtained with thylakoid membranes. This could be due to ready availability of free (or extracted) Chls as substrate compared to the one bound to membranes proteins, in which Chls have to be released by some mechanism for action of Chlase. Samaha and Kermasha, (1997 a & b) reported similar results using purified and partially purified Phe as substrates for Chlase. The enzyme showed higher affinity towards partially purified Phe compared to purified Phe.

6.1.2.9 Inactivation of His-CcChlase by metal ions

Chl, which is a tetrapyrrole with a central Mg⁺², is the substrate for Chlase. Literature data points that presence of Mg⁺² and other metal divalent cations (Hg⁺², Mn⁺², Cu⁺², Zn⁺², Co⁺², Fe⁺² and Fe⁺³) in the assay mix affects the Chlase activity. The activity of enzyme isolated from *P. tricornatum* was enhanced by addition of Mg⁺² combined with a reducing agent (Terpstra, 1980; Khalyfa et al., 1995). Wheat Chlase was inhibited to a different extent by all metal ions and largely by Hg⁺² and Fe⁺² (Arkus et al., 2006). Chlase from tea sprouts did not show any enhanced activity in the presence of divalent cation Mg⁺² (Kuroki et al., 1981).

Similar experiments with His-CcChlase were done to study the inhibitory effect of various divalent cations like Mg⁺², Mn⁺², Cu⁺², Zn⁺², Co⁺², Fe⁺² and Fe⁺³ in a water-miscible organic solvent system. The observed results demonstrated that of all ions tested, Mg²⁺ and Fe³⁺ showed lesser inhibitory effect on the enzyme compared to control (Table 9). The metal ions Mn⁺², Cu⁺², Zn⁺², Co⁺² and Fe⁺² showed higher levels of inhibition of Chlase compared to previously discussed metal ions. The obtained results were similar to those reported by Arkus et al. (2006) on recombinant wheat Chlase where the protein was inhibited to a large extent by Fe⁺² and to a lesser extent by Mg²⁺ and Fe³⁺. This could be due to the association of Mg²⁺ and Fe³⁺ metal ions to other enzymes in the Chl degradation pathway (reviewed in Takamiya et al., 2000; Matile et al., 1999) and the Chl biosynthetic pathway (Hornero-Mendez and Minguez-Mosquera, 2001). Therefore, they may be present in the *in vivo* environment of Chlase. The above observations were comparable to those obtained by Hornero-Mendez and Minguez-Mosquera, (2001), with higher inhibition of Chlase by metals such as Cu⁺², Fe⁺², Zn⁺² and Co⁺². This could be due to the possibility that these metal ions react with sulfhydryl groups of the aa residue cysteine, indicating the need for such groups in the reaction mechanism of the enzyme.

6.1.2.10 Functional groups involved

Effects of various functional groups on Chlase activity were reported by many research groups, using chemicals such as IAE, NEM, DTT, β -ME, p-HMB, MMTS. Tsuchiya et al. (2003) reported an inhibitory effect of IAE, NEM, DFP, and PCMB on recombinant Chlase from *C. album*. IAE and NEM showed smaller inhibitory effect, whereas DFP and PCMB inhibited the enzyme to large extent. The observed inhibitory effect was different among sulfhydryl reagents which could be due to differences in their molecular properties such as hydrophobicity and structure of reagent. Also the inhibitory effects depend on the amount of enzyme applied in the assays. However, Chlase from *C. protethecoides* was unaffected by presence of such functional groups (Shioi et al., 1980).

The present study determined the affect of DTT, β -ME, IAE and NEM on the activity of recombinant His-CcChlase in a water-miscible organic solvent system. The results in Table 10 show that DTT and β -ME enhanced the enzyme activity by 30 - 40% whereas IAE and NEM decreased the activity by 10 - 20%. Increased activity of His-CcChlase due to DTT and β -ME could be attributed to the reduction of –S-S- bonds to –SH groups in the active site of the Chlase. This leads to an increasing accessibility of substrate to active sites of the enzyme as indicated by enhanced activity. The inhibitory effect of IAE and NEM could be due to blockage of sulfhydryl groups of Chlase. The results obtained were similar to those reported by Arkus et al. (2006) on wheat Chlase. Wheat Chlase was inhibited to a lesser extent by IAE and NEM, whereas DTT enhanced its activity. Similarly, Chlase from *C. annuum* showed an increase in activity up to 10 - 15% with DTT and β -ME, while IAE and NEM decreased the activity by 5 - 15% (Hornero-Mendez and Minguez-Mosquera, 2001). DTT was also found to activate the Chlase from *Phaeodactylum* (Terpstra, 1978) but did not exert an influence on soluble tea Chlase (Kuroki et al., 1981).

6.1.2.11 Increase in oil concentration leads to reduced His-CcChlase activity

One aspect of the present study was to find the applicability of His-CcChlase in oil industry with an aim to remove the Chl from rapeseed oil during oil refining. This intention necessitates optimising the Chlase activity *in vitro* in the presence of varying oil concentrations in the reaction system. Work done by Khamessan and Kermasha, (1996a) and Bitar et al. (2004) using Chlase to remove green pigments from canola oil demonstrated this method as an alternative to the expensive adsorptive bleaching technique. However, addition of oil to Chlase assay mixtures decreased the enzyme activity. The hydrophilic by-products of Chl hydrolysis i.e., Chlide and Pheide, could be

removed easily from edible canola oil by extraction and/or centrifugation techniques (Drazkiewicz, 1994).

Hydrolytic activity of recombinant His-CcChlase was investigated in a refined bleached – rapeseed oil (Rapsol) model system. With defined amounts of substrate and enzyme in the reaction, assays were carried out at various temperatures ranging from 30°C to 60°C in a water-miscible organic solvent system, when the buffer phase was replaced by increasing amounts of oil from 0 to 71%. The results (Fig. 22) showed that even if there was an increase in oil proportion in the assay, Chlase was relatively stable to facilitate Chl hydrolysis. But, higher percentages of oil as 55% and 71% caused a decrease in specific activity of His-CcChlase by 26% and 34%. This could be due to lower affinity of both Chlase and Chl in oil, which might render both enzyme and substrate unsuitable and/or unavailable for enzymatic reaction. Still, with an increased oil amount in the assays, the enzyme His-CcChlase showed good activity at higher temperature than the optimal 40°C (55°C at 55% and 71% oil containing assays). Although there was a decline in enzymatic activity, the enzyme was functionally stable even at higher percentages of oil in the reaction. Hence, it was emphasised that providing Chlase to oil during refining procedures could successfully remove the extra pigment present in rapeseed oil.

Results obtained in the present study were superior to those reported by Khamessan and Kermasha, (1996a), on partially isolated Chlase from *P. tricornatum*, when the enzyme was not effective even at 20% oil in the system. Presence of 30% refined bleached canola oil in the reaction decreased the specific activity of the enzyme by 50 to 75% in various reaction media. Decreased specific activity of Chlase indicated a non-competitive inhibitory effect of oil on enzymatic activity (Khamessan and Kermasha, 1996a). Bitar et al. (2004) also reported similar observations. The hydrolytic activity of Chlase was reduced by 2.2 times with a presence of 20% refined bleached deodorised canola oil in the system. Addition of 20% oil to water-miscible organic solvent system decreased Chlase activity from 35 to 90% (Karboune et al., 2005).

6.1.2.12 Selection of different extraction solutions other than acetone to recover more Chlide during oil processing

Acetone has been used in the process of optimizing reaction conditions for Chlase in various reaction systems containing oil at different percentages. The Chlide generated in the reaction system was collected in aqueous acetone phases and removed easily by phase

separation (Bitar et al., 2004; Karboune et al., 2005). Acetone of 10 - 20% in any type of reaction system helps in easy recovery of Chlide.

As the present work was aimed at application of Chlase in oil industry on a large scale, acetone cannot be employed as a source of recovery of Chlide. Due to this limitation, it was necessary to develop alternative methods of using a solvent other than acetone for removing the Chlide formed in the reaction. In this direction, attempts were made to substitute acetone with hexane, linoleate and ethanol during phase separation.

Using hexane alone did not efficiently remove Chlide formed in assays compared to the mixture of hexane and acetone as seen from Fig. 23. This showed the inability of the hexane phase to retain hydrophilic Chlide and therefore use of hexane alone was ruled out for Chlide recovery. For further investigation, combination of fatty acids like sodium linoleate with water was employed to extract Chlide in the reaction. The mixture consisted of water and sodium linoleate in different concentrations. From the obtained results, it was clear that an increase in linoleate content in phase extraction mixture lead to increased extraction of Chlide (Table 11). Also, the amounts of Chlide accumulation using water-linoleate (1:4) was found comparable to that obtained using hexane/acetone (1:1) system. Hence, the buffer-fatty acid mixtures can be successfully employed in oil industry for easy removal of Chlide from oil-pigment mixture.

Alternatively, ethanol was also tested for its extraction capacity of Chlide. Buffers of various pH ranges (2 - 13) were used in combination of ethanol, to facilitate easy and increased accumulation of Chlide. It was observed that extraction of Chlide was maximum at pH 8 compared to other pH values (Fig. 24). This could be due to presence of similar pH environment as in plastids which provide increased stability of substrate and product in the assay.

Taking all these findings into consideration, it was evident that reagents like fatty acid solution or ethanol can successfully aid in the removal of Chl breakdown products like Chlide in these oil-containing assays. This finding has industrial importance since using acetone as the solvent results in formation of turbidity in oil during processing and storage (Liu et al., 1996).

6.1.2.13 His-CcChlase also hydrolyses Phe

Chl and Chl-type compounds in seeds are mostly converted to Phe during seed conditioning steps that occur before oil extraction. The presence of Chl derivatives, such as Phe *a* and *b*, pyropheophytins *a* and *b* and probably pheophytins *a'* and *b'*, were detected in crude and degummed edible oils (Endo et al., 1992; Suzuki and Nishioka, 1993).

In this context, experiments were performed to investigate the extent of hydrolytic activity of recombinant His-CcChlase towards Phe. Assays performed with 55% oil content in the reaction mixture confirmed the catalytic activity of Chlase protein towards Phe (Table 12; shown as Phe hydrolysed in nmol). Although the enzyme could successfully hydrolyse Phe, the results were not comparable to that observed with Chl. The reason for such a difference in activity might be due to the absence of a central Mg^{+2} ion in Phe, as it affects the binding of enzyme to substrate. Overall, it was clear that Chlase could use Phe as substrate for its activity even at such high oil concentration as 55%. Similar results were obtained by Samaha and Kermasha, (1997a & b) when Chlase isolated from *P. tricornutum* could mediate hydrolysis of Phe.

6.1.2.14 His-CcChlase activity in oils during different phases of oil processing

Based on the observed results of His-CcChlase activity in an oil containing assay system and the Chlide extraction capacity of different solvents, it was worthwhile to confirm the observations for industrial applications. Therefore, the efficiency of recombinant His-CcChlase to remove residual Chl during various stages of oil production was done on a pilot scale *in vitro*. For this, oil samples were collected from various oil processing steps and Chl was added externally to enrich pigment content in the oil. The oil samples were a generous gift from a company of the oil mill industry (PPM – Pilot Pflanzenöltechnologie Magdeburg e. V., Magdeburg, Germany). All assays were performed at 55% oil concentration and it was evident that recombinant Chlase could efficiently remove the pigment from oil samples (Fig. 25). Although a slight difference was observed in enzyme activity with the selected oil samples (filtered oil after seed pressing and refining), it was clear that His-CcChlase facilitated an easy removal of Chl from oil. Similar assays were performed on a batch scale at PPM – Pilot Pflanzenöltechnologie Magdeburg e. V. and confirmed the ability of Chlase in removal of residual Chl from oil. The results could be extended to application of soluble extracts of *E. coli* over expressing *CcCHLASE* on a large scale to save the user at oil mill companies from both commercial and industrial risks.

In conclusion it can be stated that recombinant CcChlase protein could be a better choice to that of partially isolated enzyme Chlase from alga like *P. tricornutum* and its use during oil extraction would decrease the Chl content from mature rapeseed. This gains credence from the observation that His-CcChlase was active at 71% oil in the reaction containing 250 μ M Chl and 100 μ g of total bacterial soluble protein extract in comparison to the reported activity of algal Chlase which was not active even at 20% oil in the reaction containing 640 μ M Chl and 200 μ g of protein (Bitar et al., 2004). In addition, largescale production of recombinant protein fractions will be easier compared to the extraction of Chlase from plants or algae for usage in oil industry. Hence the idea of application of recombinant Chlase to minimize “Green seed problem” is novel and when implemented the oil producers could benefit from this approach. Also production of high quality oil could potentially decrease the health risks which are otherwise associated with low quality rapeseed oil. In long term, this work could be a prelude for potential applications of Chlase in the removal of green colour from vegetable oil and protein concentrates in food industry.

6.1.3 Need for transgenic rape seed plants with increased *CcCHLASE* expression

In addition to the above discussed results of using recombinant His-CcChlase protein extracts in oil industry, development of new varieties of rapeseed plants is mandatory to curtail the “Green seed problem”. This could be possible by either a breeding or a transgenic approach which would bring features like higher yield, improved quality or tolerance to heat, cold and drought into the plant system and improve the possibilities to solve the problems associated with maturation of rapeseed.

Breeding is a conventional technique of raising newer varieties of crop plants with desirable characteristics, yet is a tedious process. The science of traditional plant breeding has been limited to artificially crossing plants with in the same species or with closely related species to give way to newer plant varieties. Advent of transgenic technology enabled plant breeders to bring together in one plant specific genes across the whole plant kingdom, not confining to closely related plants. Thereby it generates crop varieties with more agronomic traits by offering possibilities beyond limitations imposed by conventional techniques. The aim is to design plants with specific characteristics by artificial insertion of genes from other species into a selected model plant. Most commonly used model plants are *Arabidopsis*, tobacco etc.

In the present study, after confirming the *in vitro* functionality of His-CcChlase, *CcCHLASE* was chosen as transgene for transgenic studies. It was assumed that transgenic rapeseed plants with increased seed-specific expression of Chlase would remove residual Chl present in the mature *Brassica* seed. But, primarily, it was of paramount importance to explore whether overexpression of Chlase in plant system can affect Chl metabolism i.e., the processes of synthesis and regulation. As Chl is mainly accumulated in leaf tissue, the activity of the recombinant Chlase protein can be better studied taking leaves as experimental organs. For this purpose, the Chlase gene was constitutively expressed in the plant system to facilitate easy analysis of the protein in terms of its functionality *in vivo*.

6.1.4 Overexpression of *CcCHLASE* in tobacco did not impart phenotypic and morphological differences to the plants

Transgenic tobacco plants overexpressing *CcCHLASE* could provide a good tool to analyze the functional and regulatory aspects of Chlase *in vivo* during senescence and various stress conditions. The transgene *CcCHLASE* was inserted into tobacco plants by the *A. tumefaciens*-Ti system, using the C58C1 strain of the bacterial pathogen. The strain C58C1 has a highly sensitive chemotaxis system and responds to a range of sugars and aa (Loake et al., 1988). The full length *CcCHLASE* cDNA sequence containing signal peptide sequence was cloned into binary vector pCAMBIA3301, under the 35S promoter of Cauliflower mosaic virus (CaMV). This vector also contained a Basta resistance selection marker to select the transformants. The viral CaMV 35S promoter is a strong constitutive promoter with high levels of gene expression in almost any type of plant cells and tissues at any developmental stage.

The Chlase overexpressor plants were generated by the *Agrobacterium* (C58C1) mediated transformation of sterile hypocotyls (as source of plant material) due to their high regenerative capacity. Appropriate hormonal concentrations (BAP and NAA) led to efficient growth of shoots and roots. Addition of the Basta into the medium enabled easy selection of transformants against WT tobacco progeny. The mature plants produced from serial subcultures of regenerated calli were transferred to green house for further analysis.

The Chlase transgenic plants overexpressing *CcCHLASE* under the control of constitutive promoter were expected to produce higher amounts of Chlide in overexpressor plants than in WT plants. This excess free Chlide if not bound to Chl binding proteins of photosystem I and photosystem II, was expected to cause photodynamic damage on exposure to light,

resulting in phenotypic change in leaves of Chlase overexpressor plants. In contrast to the expectation, the overexpressor plants had a similar phenotype with WT tobacco plants (Fig. 26) which could be due to a) the immediate conversion of the accumulated photooxidatively toxic free Chlide *a* to subsequent breakdown products and prevention of the plants from photodynamic damage, b) even after overexpression of Chlase in the overexpressor lines, the enzyme might not find its access to Chl due to spatial latency and hence no increased Chl degradation to result in leaf colour. Hence, the extra Chlide produced in the leaves of Chlase overexpressor plants may not be phototoxic to result in visibly altered phenotype.

The Chlase overexpressor plants behaved perfectly normal like the WT tobacco plants in terms of development and morphological aspects (plant height, leaf pattern, onset of flowering and seed maturation). Similar observation was reported, for *coil* mutants of *Arabidopsis*, with transformed plants constitutively expressing sense and anti sense forms of *ATHCOR1* gene, failed to show any phenotypic difference from WT plants (Benedetti and Arruda, 2002).

6.1.5 PCR and *in vitro* enzyme activity measurements confirmed the presence of *CcCHLASE* transgene in the Chlase overexpressor plants

PCR provided a powerful tool to screen the overexpressor plants for the presence of *CcCHLASE* transgene and more than 92% of the transformants were found positive (Fig. 27). With the use of one gene specific reverse primer and another primer specific for the 3' end of the promoter region, the transgene could be identified from the genome of overexpressor plants. This was evident in the form of amplification of the transgene from the leaf genomic DNA samples of the Chlase overexpressor lines (such as 2, 3, 4, 5, 6, and 7, Fig. 27). The amplified fragment seen in the overexpressor samples was in accordance with the positive control (pCAMBIA3301 plasmid containing *CcCHLASE* cDNA coding for protein with transit peptide) which also showed a PCR band at ~1100 bp. WT tobacco plants served as negative controls as no amplification of the transgene was seen in their genomic DNA samples.

While PCR could only indicate the presence of intact gene, its protein product could only be confirmed by western blot. Although a polyclonal antibody using His-CcChlase was produced, this antibody cross-reacted with protein fractions of WT tobacco leaves and hence could not be used for detection of the CcChlase protein in the overexpressor plants

(Fig. 10). The focus of the present study was to validate the functional activity of recombinant CcChlase protein in Chlase overexpressor plants. Therefore, *in vitro* Chlase activity was measured in the leaves of overexpressor plants to select the candidate lines that show more Chlase activity. Data from the present study, tabulated in Table 13 showed that overall the Chlase overexpressor plants had 2 - 20 fold increase in the specific activity of the recombinant CcChlase than WT plants (Table 13). Comparing the Chlide *a* contents between WT and overexpressor plants, it was evident that the presence of extra amounts of Chlide *a* in the overexpressor lines could only be due to efficient activity of overexpressed CcChlase protein. However, the increase in Chlide *a* amounts was not uniform and the differences observed in the catabolite contents could be due to differences in intensity of expression and activity of CcChlase protein among various overexpressor lines. Most of the overexpressor lines exhibited low to moderate activity of the enzyme i.e., with a range of 2 - 6 folds increased activity than the WT plants. Very few lines were noticed to have higher activity of 8 - 20 times relative to the WT plants.

These data were comparable to the reports of Harpar-Saad et al. (2007) on *Citrus Chlase* gene overexpressed in squash plants grown both in normal and low light conditions. The accumulation of Chlide *a* was higher in transgenic squash plants due to increased Chlase activity compared to control plants. Benedetti and Arruda, (2002) reported higher levels of Chlide *a* in leaf pigment extracts of *Arabidopsis* WT and sense *coil* mutants overexpressing *ATHCOR1* (under the control of 35S promoter). The antisense *coil* mutants and the non-transformed *coil* lines had lower Chlase activities compared to WT and even lesser activity than the sense mutants.

6.1.6 Southern blot confirmed the stable integration of *CcCHLASE* transgene in the Chlase overexpressor plants

Stability and expression profile of *CcCHLASE* transgene in the Chlase overexpressor lines can sometimes be correlated with the number of its insertion sites in the chromosomal DNA of the plant. Evidence for transgenic nature of the selected 15 putative Chlase overexpressor lines (T0) was provided by Southern blot analysis of genomic DNA isolated from leaf material of the overexpressor lines. Presence of a hybridisation signal corresponding to *CcCHLASE* gene confirmed a successful integration of the transgene into the genome of tobacco (Fig. 28). Based on the size of the hybridization band resulting from EcoRV restriction digestion of the genomic DNA samples, it was plausible to conclude that *CcCHLASE* gene was integrated at different sites in the respective plant genome. Only

line 13 showed multiple insertion of the transgene. The Chlase overexpressor lines 7, 36, 38, 46, 52 and 56 showed the same integration pattern of *CcCHLASE*, indicating their origin from the same Basta-resistant callus line. Similarly, lines 9, 17, 34, 48, 49, 51 and 58 were probably regenerated from the same callus. The other two lines 11 and 13 might have produced from different calli (Fig. 28).

Presence of a single insertion site of the transgene is superior to multiple insertion sites as it would lead to uniform and predictable expression of gene when they received a single copy of gene. Multiple insertion of the GUS transgene into tobacco was shown to have reduced expression than that seen with a single copy insertion of the gene (Hobbs et al., 1990). Similarly, Linn et al. (1990) working on transgenic petunia plants, reported no gene expression due to gene silencing and promoter methylation in plants with multiple insertions of the transgene. Possible other other post-transcriptional gene silencing modifications may also contribute to lowered gene expression due to insertion of multiple copies of transgene.

6.1.7 Characterization of T1 generation of Chlase overexpressor plants

Presence of higher Chlide *a* levels indicated enhanced *CcCHLASE* expression in the overexpressor plants (Table 13). Therefore, subsequent analysis was done to evaluate functional activity of CcChlase protein during various courses of senescence and abiotic stress conditions. Three Chlase overexpressor lines (46, 51 and 52) having higher Chlase specific activities were selected and progenies of their T1 generation were used to study the functional aspects of recombinant CcChlase protein.

6.1.7.1 Northern blot analysis confirmed the presence of *CcCHLASE* transcripts only in the overexpressor lines

Transcript levels of the transgene form crucial part of gene expression study and their quantification is best done by northern hybridisation. It was evident from Fig. 29b that *CcCHLASE* transcripts were detected only in the Chlase overexpressor lines. Moreover, the presence of *CcCHLASE* transgene did not affect the transcriptional activity of the native Chlase gene from tobacco. The transcript levels of the native *NtCHLASE* gene remained similar irrespective of the leaf developmental stage (Fig. 30b).

6.1.7.2 CcChlase activity was retained in the membrane fraction of chloroplasts

The existence of Chlase activity in chloroplast fractions demonstrated its intracellular localization in the membrane fraction of chloroplasts. This was proved in many plants through Chlase activity measurements: in barley (Matile et al., 1997), *Citrus* fruit (Trebitsh et al., 1993), *Citrus* leaves (Garcia and Galindo, 1991), and *Ginkgo* leaves (Okazawa et al., 2006). The Chlase activity was specifically associated with the plastid membrane fraction (Harpaz-Saad et al., 2007) or specifically with thylakoids (Okazawa et al., 2006). Presence of Chlase activity in the membrane fraction of chloroplasts isolated from *C. sinensis* leaves confirmed the distribution of the protein in chloroplasts membranes (Brandis et al., 1996). Similarly, the presence of CcChlase protein in the overexpressor plants was confined to the membrane fractions of the chloroplasts. Higher Chlase activity was seen in the chloroplast membrane fractions in comparison to the soluble fraction of the chloroplasts in both WT and Chlase overexpressor tobacco plants. The activity measured with overexpressor plant samples was approximately 6 - 8 times than the WT samples. Of the three lines, line 52 showed maximum activity (Table 14). Hence, the presence of higher Chlase activity in chloroplastic membrane fractions of the overexpressor plants proved that *Citrus* Chlase was located in the plastid membranes. The present results were in agreement with *in situ* immuno-fluorescence on ethylene treated fruit peel (flavedo) tissue showing the localisation of Chlase protein in membrane fractions of plastids (Shemer et al., 2008). These findings were in contrast to the reports of Schenk et al. (2007) that *Arabidopsis* Chlases were localised in cytoplasm.

6.1.7.3 Young leaves of the Chlase overexpressor lines retained higher *in vitro* CcChlase activity

Degradation of Chl and disintegration of the photosynthetic apparatus mostly occurs during leaf senescence. Chlase takes part in the initial step of Chl breakdown in senescing plant tissues (Matile et al., 1999). Therefore, it was of interest to examine the changes in Chlase activity during the course of leaf senescence. Normally, an increased Chlase activity was expected during leaf senescence due to enhancement of Chl degradation. But the chances of Chlase degradation in the senescing chloroplasts along with other components of the photosynthetic system cannot be ruled out (Matile et al., 1997). The changes in Chlase activity during the course of leaf senescence were studied in various plant species. A senescence-associated increase in Chlase activity was reported in barley (Sabater and Rodriguez, 1978; Rodriguez et al., 1987), spinach (Yamauchi and Watada,

1991), and sunflower (Purohit, 1982). On the other hand, an opposite trend of higher Chlase activity in freshly harvested non-senescent leaves and decreased Chlase activity in the course of senescence was observed in bean leaves (Fang et al., 1998).

Likewise, the present study tested the Chlase activity during the course of senescence by *in vitro* activity assays using total membrane protein extracts of leaves taken from both WT and Chlase overexpressor lines. Enzyme activity was monitored both under dark and normal growth conditions. Recombinant CcChlase activity was analysed in leaves of all developmental stages i.e., young, mature and senescent. Results from Fig. 31a showed a 5-fold increase in the specific activity of Chlase in the overexpressor lines compared to WT plant samples. Protein extracts of young leaves exhibited maximum activity compared to mature and senescent leaves which could be due to the presence of non-degraded Chlase protein in young leaves. In senescent leaves, the degeneration of the chloroplasts would degrade the Chlase protein resulting in reduced activity of the enzyme.

Compared to the light/dark growth conditions, all the three Chlase overexpressor lines showed similar Chlase activity profile i.e., $y > m > s$ in dark growth conditions (Fig. 31 a and b). Differences in Chlase activity were observed among the lines only during normal light/dark growth conditions (line 46; $y > m \sim s$, line 51; $y > s > m$ and line 52 $y > m > s$). The variation in the calculated Chlase activity in lines 46 and 51 could be due to changes in the expression levels of the *CcCHLASE* transgene in the respective leaf samples. Of the three lines studied, lines 46 and 52 showed maximum Chlase activity irrespective of the leaf age which could be due to enhanced expression of the *CcCHLASE* transgene in these lines. However, about 25% reduction in Chlase activity was seen in dark grown samples in comparison to the light/dark grown samples. The possible reasons could be decreased Chl and protein synthesis and reduced Chl turnover in dark conditions than in the normal growth conditions. Overall, the Chlase overexpressor plants retained higher Chlase activity than the WT plants which was attributed to the presence of recombinant *CcCHLASE* in the overexpressor plants. These results were in agreement with the following previous reports. Ben-Yaarkov et al. (2006) reported a decrease in Chlase activity with a decrease in Chl levels in the order of $y > m > s$ in tobacco plants both under normal day light and dark incubation conditions. Similarly, a decrease in Chlase activity with senescence was reported in spinach (Yamauchi and Watada, 1991), soybean primary leaves (Majumdar et al., 1991), olive (Minguez-Mosquera and Gallardo-Guerrero, 1996) and snap bean (Fang et al., 1998). Chen et al. (2008) reported that in broccoli, the expression and activity of

BoCLHI was high at younger stages and fresh harvest and declined gradually with a prolonged senescence period.

6.1.7.4 Recombinant CcChlase protein remains active in 80% acetone seen as higher amounts of Chl catabolites in the leaf pigment extracts

Many research groups have provided evidence for the production of Chlide *a* in response to overexpression of Chlase genes in plant system: in *Arabidopsis* (Benedetti and Arruda, 2002; Schenk et al., 2007; Zhou et al., 2008), *Ginkgo* (Okazawa et al., 2006) and *Citrus* (Harpar-Saad et al., 2007). Most of the pigment extractions were done using acetone in the range of 70 - 80% and activity of the Chlase was determined based on the amounts of Chlide *a* produced in the leaf samples.

Based on the above reports, 80% acetone was used in the present study for pigment extraction from both WT and Chlase overexpressor tobacco plants. But the persistence of *Citrus* Chlase activity during 80% acetone extraction led to a deposition of elevated Chlide *a* in the leaf extracts of the overexpressor lines in comparison to the WT plants (Fig. 32). In both WT and Chlase overexpressors, the Chl and Chlide *a* amounts followed the order of $y > m > s$. More than 50% of Chl was converted to Chlide *a* and nearly 10% of this resultant Chlide *a* was converted to Pheide *a* during the process of extraction in the overexpressor leaf samples. A similar rate of conversion of Chlide *a* to Pheide *a* (about 9%) was also seen in WT samples, but the presence of higher amounts of Pheide *a* in overexpressor samples was due to the initial increased levels of Chlide *a* (Fig. 32).

The amounts of pigments (Chl, Chlide *a* and Pheide *a*) were higher in young leaf samples than in the mature and senescent samples calculated on the fresh weight basis (Fig. 32). Senescent leaves have an increasing cell size with enlarged vacuoles resulting in less pigment per gram fresh weight. This explains the decreasing levels of catabolite with decreasing levels of Chl. Therefore, decrease in the amount of Chlide and Pheide was apparent in the senescent leaf samples compared to the young leaf samples in the overexpressor plants. Also, the active cell regeneration and Chl biosynthesis result in higher amounts of Chl in young leaves than in the mature and senescent leaves. Subsequently, the active protein synthesis machinery in young leaves would result in increased breakdown of Chl (as seen from Fig. 31a).

Higher amounts of Chlide *a* detected during extraction with 80% acetone indicated a persistent activity of CcChlase in the solution which do not reflect *in vivo* production of the pigment in the plant cells. This was mainly because the *in vitro* activity assays involve destruction of the chloroplastic compartments due to freeze-thaw process and also the presence of organic solvent facilitates easy accessibility of Chl to Chlase. These cause more activity of Chlase *in vitro* compared to *in vivo*. Hence, an alternative extraction method was developed to estimate the steady state levels of Chlide *a* produced in the overexpressor leaf samples.

6.1.7.5 Absolute acetone minimised the extent of *in vitro* production of Chlide *a*

Strict assessment of the intact *in vivo* Chlase activity was made by rapid extraction of pigments using absolute acetone (> 99%) and the steady state levels of both Chl and Chlide *a* were measured by HPLC. Absolute acetone precipitates all the proteins present in the leaf samples thereby inhibiting any of CcChlase enzyme activity during the extraction process. This method gave a better picture on the extent of Chl catabolism in Chlase overexpressor plants compared to WT plants. Pigment analysis proved the overexpression of Chlase in the transgenic plants displaying the presence of steady state levels of Chlide *a* only in overexpressor plants and not in WT plants (Fig. 33). The results were similar to the observations made by Harpar-Saad et al. (2007) in squash overexpressing *Citrus* Chlase, in which 100% acetone was used to extract pigments from control and transgenic squash plants.

6.1.7.6 Steady state levels of Chl and Chlide *a* and NCC contents in Chlase overexpressor lines during senescence

CcCHLASE was expressed constitutively under the control of a constitutive 35S promoter in the overexpressor plants and supposed to result in uniform expression of the transgene during all stages of leaf development. But, enhanced expression of *CcCHLASE* alone would not lead to enhanced Chl breakdown. The important factors that drive the Chl breakdown process in plants are a) increased association between Chl and Chlase for an increased Chlide *a* production and other subsequent catabolites and b) the degradation of LHCII (light harvesting complex II) for proper degeneration of the thylakoid membrane (Kusaba et al., 2007) to release the Chl molecule from pigment-proteolipid complexes. These two factors will be activated during programmed leaf senescence that results in leaf yellowing.

In addition to the above, Chl degradation also occurs in response to various external environmental factors like darkness, stress and response to hormones (reviewed in Vicky Buchanan-Wollaston, 1997). Few types of stress that result in induced or artificial senescence in plants are drought and high salt concentration that cause changes in the chloroplast structures leading to enhancement of senescence. Of various types of hormones that promote senescence, methyl jasmonate and ethylene are the most widely used (Benedetti and Arruda, 2000; Jacob-Wilk et al., 1999).

As the present work focuses on analysis of changes in steady state levels of Chl and Chlide *a* in the Chlase overexpressing plants, it was worthwhile to study the aspects of Chlide *a* production in plants during various courses of senescence. This would give a measure of enhanced Chl breakdown in the Chlase overexpressor lines that can be attributed to CcChlase activity in comparison to nontransformed WT plants.

Natural senescence: The phenomenon of leaf yellowing during aging is a naturally occurring process, involving various enzymatic steps of Chl breakdown and there by produce non-fluorescent Chl catabolites, resulting in changes of leaf colour.

Considering the active participation of Chlase during natural senescence process in plants, steady state levels of Chl and Chlide *a* were determined from the leaves belonging to all developmental stages (young, mature and senescent). The amounts of Chls deposited in both WT and the overexpressor lines followed the order $y > m > s$ (Fig. 33) which could be explained by larger cell size and high water content in the senescent leaves resulting in lower accumulation of the pigment for given fresh weight. The total Chl contents in the overexpressors were lower by about 5% in comparison to the WT tobacco plants. Significant differences in the Chl contents were seen in young and senescent leaves of lines 51 and 52 when compared to the WT plants (Fig. 33). On the other hand, such effect was perceived only in senescent leaves of line 46. The variations in the total Chl contents between the WT tobacco and Chlase overexpressor plants could be explained by the presence of steady state levels of Chlide *a* in the latter (Fig. 33). This confirmed the active role of CcCHLASE in Chl degradation which is otherwise not seen in WT tobacco plants.

However, Chlide *a* amounts deposited in the leaves followed a reverse order to Chl i.e., $y < m < s$ (Fig. 33). The affect was consistent in all the three Chlase overexpressor lines and of them, lines 46 and 51 showed higher deposition of Chlide *a* compared to line 52. The

reason could be presence of more Chlase activity in senescent leaves of lines 46 and 51 than in line 52 (from Fig. 31a).

The *in vitro* measurements of recombinant CcChlase activity in terms of specific activity of the protein (using protein extracts from WT and Chlase overexpressor lines, Fig. 31a) and accumulation of Chlide *a* using 80% acetone extraction procedure showed higher enzyme activity in young leaf samples (Fig. 32). But in the case of estimation of *in vivo* accumulation of Chlide *a*, the amounts of catabolite was minimal in young leaves compared to mature and senescent leaves (Fig. 33). This could be explained by the following reasons: a) faster and continuous use of Chlide *a* formed in the formation of Chl *b* by Chl *b* synthesis pathway in the young leaves and b) presence of intact chloroplast structures in the young leaves when compared to senescent leaves that makes it impossible for Chl to be easily accessible to the enzyme Chlase. On the other hand, changes in the chloroplast structures associated with onset of leaf ageing disrupt the thylakoid membranes and makes Chl easily accessible to Chlase. Hence, a higher deposition of Chlide *a* in the concerned senescent leaf tissues was observed. Also the enzymes down stream of Chlase like PAO were senescence inducible and convert the extra Chlide *a* rapidly into subsequent end products. In addition, the degenerated chloroplasts were transformed into gerontoplasts which are sites for enzymes involved in Chl degradation resulting deposition of its end products (NCCs) in vacuoles (Kräutler and Matile, 1999).

The ratio of Chlide *a*/Chl measurable in the overexpressor lines (Fig. 34) increased in the order of $y < m < s$. As the amounts of steady state levels of Chlide *a* increased with leaf age ($m < s$) (Fig. 33), the ratio of Chlide *a*/Chl also increased (Fig. 34). Because of the absence of steady state levels of Chlide *a* in WT samples, the ratio of Chlide *a*/Chl was not possible.

The amounts of NCCs deposited were higher in the senescent leaf samples compared to the young leaves of overexpressor lines and as well as WT (Fig. 35). This was in accordance with the expected result that NCC deposition was higher during leaf yellowing (reviewed in Hörtensteiner, 2006). But no significant differences were seen in the NCC contents between WT and Chlase overexpressor lines due to very minute levels of extra end products formed from Chlide *a*.

With respect to Pheide *a*, *in vitro* studies showed accumulation of the pigment (Fig. 32), however were not detected during extraction with 99% acetone. The plausible reason could be the lower amounts of steady state levels of Chlide *a* (< 1%) detected during the process compared to the 80% extraction procedure. Although, these lower amounts of Chlide *a* were expected to be degraded to Pheide *a*, the catabolite levels would be so negligible that they were not detected by HPLC. The same applies for NCCs which were produced from Pheide *a*, though present in higher levels in the overexpressor plants in comparison to WT were not detected by HPLC (Fig. 35).

The observations in the present study were consistent with the reports of Fang et al. (1998) on WT and non-yellowing mutants of snap bean. The WT snap beans though accumulated higher Chlide *a* levels did not show any presence of Pheide *a* in HPLC measurements due to the reason that the production of Pheide *a* was so rapid that they could not be detected in the pigment extracts.

Induced senescence

Dark incubation of detached leaves

Induction of artificial senescence was achieved by dark incubation of detached leaves from both WT and selected Chlase overexpressor lines. On detaching a leaf from a plant, first sign of senescence will be a rapid fall in protein content and on dark incubation, the Chl amounts begins to fall at an increasing rate.

From Table 15, it was seen that the Chl contents were lower in the detached leaves of overexpressor plants than the WT leaves at all tested treatment conditions. This was related to the presence of steady state levels of Chlide *a* in the overexpressors. Normally, both detachment and incubation of the leaves in water in light/dark or complete dark promoted senescence mechanism in the leaves, increasing the accessibility of Chl to Chlase. Because of this, an increased Chlide *a* production was expected in both WT and overexpressor lines, but the presence of recombinant CcChlase protein resulted in the generation of extra amounts of Chlide *a* in the overexpressor lines.

Incubation of the detached leaves in light/dark (12 h/12 h) resulted in increased Chl degradation in the overexpressor leaves than the WT as was evident from the amounts of decreased Chl contents. Subsequently, the Chlide *a* amounts increased by 10 – 20% in the overexpressor leaves after incubation of the leaves for 5 days (12 h/12 d). On contrary, the

difference in residual Chl amounts between WT and the overexpressor leaves (only 1%) was not so prominent on continuous dark incubation for 5 days. Also the Chlide *a* amounts were lower upon dark treatment in the overexpressors in comparison to the light/dark conditions (Table 15). This could be explained by a) decreased Chl synthesis in the dark would result in lower availability of Chl as substrate b) continuous degradation of Chlide *a* to the subsequent catabolites by senescence induced genes like *PAO* c) the dark treatment results in pseudosenescence by delaying the degreening process (Ougham et al., 2008).

The measurements of Chl/Chlide *a* ratios showed that only the Chlase overexpressors possessed such ratios due to the presence of steady state levels of Chlide *a* in contrast to the WT plants. From Table 15, it was clear that the Chl/Chlide *a* ratios decreased with increased generation of Chlide *a* steady state levels after light/dark incubation of the leaves of Chlase overexpressor lines in comparison to the ratios calculated at the beginning of the experiment (0 h). Further, it was expected that the ratios would be much lowered in the leaves of overexpressor lines after continuous dark incubation, but no such effect was observed. This might be due to the presence of lower steady state levels of both Chl and Chlide *a* in dark treated samples than the light/dark treated samples.

The end products of Chl degradation (NCCs) were seen in higher amounts in mature and senescent leaves compared to young leaf samples in both WT and overexpressor lines (Fig. 36). In comparison to the NCCs produced in normal light/dark conditions (Fig. 35), the NCCs increased by 1.5 fold in senescent leaves and 2 fold in mature leaves. Thus dark incubation of plants induced senescence associated PAO activity and other processes resulting in higher catabolite contents in the plants. Even though, there was increased production of NCCs in the overexpressor leaf samples from the extra Chlide *a*, the differential amounts were so negligible that no statistical significant differences were seen between WT and overexpressor lines on HPLC detection.

Role of methyl jasmonate and ACC in enhancing the process of senescence in the Chlase overexpressor lines

Methyl jasmonate and ethylene were well known to accelerate leaf senescence and fruit ripening by accelerating the Chlase activity (Creelman and Mullet, 1994; Smart, 1994; Drazkiewicz, 1994). Treatment with methyl jasmonate markedly increased the expression of *AtCLH1* but not *AtCLH2* in the rosette leaves of *Arabidopsis* (Tsuchiya et al., 1999). Ethylene treatment enhanced *de novo* synthesis of Chlase enabling increase of its activity

leading to Chl destruction (Trebitsh et al., 1993). *Citrus CHLASE1* mRNA levels were increased by ethylene treatment of the mature green fruits (Jacob-Wilk et al., 1999). Besides, enhancement of ethylene production during senescence and unfavourable growth conditions was studied (Johnson-Flanagan and Spencer, 1996).

The Chlase overexpressor plants exhibited increased steady state levels of Chlide *a* in the leaf discs in response to both methyl jasmonate and ACC. The decrease in Chl amounts in both WT and Chlase overexpressors was higher in the case of treatment of the leaf discs with ACC than methyl jasmonate for 24 h after start-up of the experiment (Table 16). This suggested that ACC was a better senescence promoting agent in comparison to methyl jasmonate. The increase in the amount of Chlide *a* steady state levels generated with both ACC and methyl jasmonate were in the range of 75 – 85% in the overexpressor leaves after 24 h (Table 16). Although a higher production of Chlide *a* was expected in response to ACC in combination with endogenous ethylene resultant of mechanical stress, only a difference of about 5% in Chlide *a* levels was seen in comparison to that of methyl jasmonate treatment. This indicated that both ACC and methyl jasmonate had similar effect on overexpressed Chlase for the generation of Chlide *a in vivo*. Further incubation of the leaf discs up to 48 h resulted in a higher decline in Chl amounts in WT than the Chlase overexpressors with both the reagents. In addition, the Chlide *a* steady state levels were decreased in the overexpressor samples after 48 h in the case of both ACC and methyl jasmonate treatments. Consequently, the changes in pigment contents also affected the Chl/Chlide *a* ratios in the overexpressors, being lower after 24 h and higher at 48 h in response to both the reagents (Table 16).

The above phenomenon suggests that both ACC and methyl jasmoante were able to initiate and enhance senescence in the leaf samples in the initial 24 h by increasing the accessibility of substrate to the enzyme. Hence, an initial rise in catabolite contents was observed. But the later decrease in both Chl and Chlide *a* levels were possible due to a) no persistent effect of the reagents to enhance senescence mechanism b) rapid conversion of Chlide *a* to subsequent catabolites by senescence induced enzymes like PAO downstream of Chlase in the catabolic pathway c) conversion of the Chlide *a* produced in the cells to Chl *b* via the Chl *b* synthesis pathway and regeneration of the Chl *b* into Chl cycle to maintain the Chl *a/b* ratio in the plant cells.

The perceived effect of increased Chlide *a* levels in response to methyl jasmonate was in accordance with that seen in the case of *Arabidopsis* sense *coil* mutants overexpressing *ATHCOR1* in response to methyl jasmonate relative to WT control (Benedetti and Arruda, 2002). The results also concur with the elucidations of Trebitsch et al. (1993) and Jacob-Wilk et al. (1999) who noted increased Chlase expression and activity in *Citrus* fruits in response to ethylene treatment and presence of Chlase in plastid membrane fractions (Shemer et al., 2008).

An insight into the NCC contents show that the amounts of end products of Chl breakdown were slightly higher after 24 h in comparison to those measured at beginning of the experiment (Table 17). But the amounts remained more or less similar after 48 h which might be due to faster recycling of the Chl breakdown products as a source of nitrogen and carbon to be recycled into other metabolic processes like Chl and protein synthesis. The differences observed in the amounts of NCCs between the samples treated with ACC and methyl jasmonate depends on the age of the leaf chosen for the experiment.

In all, the increased Chlide *a* levels in Chlase overexpressor lines were solely attributed to the presence and activity of overexpressed *CcCHLASE* in the Chlase overexpressing plants.

Recombinant Chlase (encoded by *CcCHLASE*) withstands various unfavourable conditions

Chlase activity was reported to fall in concert with Chl degradation in maize seedlings exposed to osmotic stress (Garcia et al., 1987). Sunflower plants exposed to different salt concentrations (NaCl) showed decreased Chl contents due to impaired ALA synthesis rather than Chlase mediated Chl breakdown (Santos, 2004). Decrease in water content of soybean leaves increased Chlase activity (Majumdar et al., 1991). In a similar way, the transgenic plants overexpressing *CcCHLASE* were analyzed for their ability to cope up with different unfavourable conditions, like salt and drought stress conditions. The stability of the overexpressed CcChlase protein was assessed in terms of efficient production of Chlide *a* *in vivo*.

A decrease in Chl contents was observed with incubation of the detached leaves in salt solution in both WT and Chlase overexpressor plants. The reduction in Chl contents was prominent in the salt stressed leaves than the water control leaves when compared to the

start-up of experiment (0 h). The large variation in the pigment contents could be due to enhanced chloroplasts degeneration as a result of osmotic stress in the salt stressed leaves. The higher decrease in Chl amounts in the overexpressor leaf samples than the WT could be accounted for the extra Chlide *a* amounts in the overexpressors (Table 18). The reduction in the amounts of Chlide *a* in the salt stressed leaves (by 20 – 60%) compared to the water control leaves of the overexpressors might be due to faster conversion of Chlide *a* to NCCs. However, the presence of Chlide *a* levels also in the salt stressed leaves suggested that the accessibility of Chl to Chlase was increased during salt stress. It may be concluded that the overexpressed Chlase was quite stable to bring about the process of Chl breakdown.

The Chl/Chlide *a* ratios were found to be lower in the water control leaves than the salt stressed leaves. This might be due to the continuous turn over of Chl in the water control leaves. On the other hand, in the salt stressed leaves, though there was rapid disruption of the chloroplast membranes releasing the Chl molecules, the enzyme machinery would not be so active to take part in Chl breakdown process. Hence, a higher Chl/Chlide *a* ratios could be observed.

Though there was an increase in the amounts of NCCs during salt stress, the difference in their contents was not significant between WT and the Chlase overexpressor plants (Table 20).

Decreased Chl contents were observed in both WT and the Chlase overexpressor plants in response to water deficit stress (Table 19) for 30 h. The decline in residual Chl amounts was more or less similar in both Chlase overexpressor and WT leaves during water deficit stress. On the other hand, the water control leaves of overexpressor plants showed slightly higher loss of Chl than the WT control leaves in comparison to the beginning of the experiment. The generation of Chlide *a* levels in the overexpressor leaves was due to increased accessibility of the Chl to Chlase under induced stress conditions. However, the presence of higher Chlide *a* levels in water control leaves of the overexpressors indicated a continuous recycling of the Chl molecules to be available for Chlase activity. This was reflected in the form of lower Chl/Chlide *a* ratios in samples collected from leaves incubated in water for 30 h than the drought stressed leaves. Comparable amounts of Chlide *a* (about 50 – 75%) were seen in the drought stressed leaves with those detected in the water control leaves. The decreased catabolite levels in the water deficit leaves

indicated a faster conversion of Chlide *a* to end products of Chl catabolism. The presence of Chlide *a* levels even at such extreme drought conditions in the Chlase overexpressor plants indicated the stability and activity of the overexpressed Chlase protein.

The amounts of NCCs detected during water deficit stress were higher than the water control leaves (Table 20) in both WT and Chlase overexpressor plants. Though, the overexpressor leaves possessed slightly higher levels of NCCs than the WT, the differences were not statistically significant. The extra amounts of Chlide *a* present in the overexpressor samples under water deficit conditions though converted into final end products could not make any significant differences with respect to WT.

6.1.7.7 Chlase overexpressor plants did not show any differences in ALA synthesizing capacity

D-Aminolevulinic acid (δ -ALA) is the first compound in the porphyrin synthesis pathway, leading to Chl in plants. The production of δ -ALA is the step on that the speed of synthesis Chl is regulated. The synthesis of ALA has been confirmed as the rate-limiting step in Chl synthesis (Kannangara and Gough, 1979; Kruse et al., 1997). Since Chlase overexpressor plants showed less Chl contents compared to WT (and higher Chlide levels), experiments were performed to analyse differences in ALA synthesizing capacity in the plants. The obtained results showed that no differences were seen in the ALA synthesizing capacity between the Chlase overexpressor and WT plants (Fig. 37). The young leaves exhibited higher ALA synthesizing rates than the mature leaves which could be attributed to higher Chl synthetic rate in the former ones. Therefore it can be concluded that decreased Chl contents and increased Chlide levels in the overexpressor plants does not influence the ALA synthesizing rate in the Chlase overexpressor lines.

6.2 Importance of WSCP in plant metabolism

WSCP is a chloroplastic soluble protein that has been hypothesized to mediate the transfer of Chl molecules from thylakoid membranes to the site of action of Chlase, i.e., the inner envelope membrane of chloroplasts (Matile et al., 1997). Researchers have also reported the phototolerance capacity of irradiated WSCP-Chl complexes *in vitro* (Schmidt et al., 2003) and the association of WSCP with Chl precursors during light-induced chloroplast development (Reinbothe et al., 2004).

To ascertain the exact role of WSCP in plant system, transgenic tobacco plants overexpressing the WSCP protein were produced by insertion of the selected WSCP cDNA into the genome of the model plant tobacco. Moreover, the expression of the gene in a prokaryotic system would show its activity *in vitro*. All these would ultimately give a better insight into the functional role of WSCP during regulation of Chl metabolism and in response to different kinds of stress.

6.2.1 *Cau-WSCP* as transgene

Until to date, various groups reported sequencing and characterization of WSCPs from many plant species but most of the research was performed with the cauliflower WSCP. Hence, the gene sequence for *Cau-WSCP* (Satoh et al., 1998) was selected for the present study. In the current work, evidence was provided for some of the aspects of the *in vitro* and *in vivo* functions of WSCP isolated from cauliflower leaves. In addition, the effects of WSCP accumulation were analyzed on processes of Chl degradation, storage of Chl derivatives and phototolerance mechanisms in WSCP overexpressing tobacco plants.

6.2.2 Isolation and expression of WSCP from cauliflower

The *WSCP* gene sequence from cauliflower (*Brassica oleracea* var *botrys*) was taken as reference (Satoh et al., 1998) having an open reading frame of 654 bp and encoding a protein of 218 aa which includes a 19 aa long transit peptide sequence.

Cloning and characterisation of cDNA for *Cau-WSCP* (coding for protein without transit peptide) by *E. coli* expression was performed by Dr. Ulrich Eckhardt. The isolated *WSCP* gene showed 98% homology to the reference sequence (Satoh et al., 1998). Among many isolated cDNAs, two were selected which had high homology to the reference sequence and were termed as *Cau-WSCP-35* and *Cau-WSCP-49*. The latter cDNA sequence had a single point mutation by which a nucleotide substitution resulted in glycine (G) in the place of glutamic acid (E) (E108G). Deduced amino acid sequences of both *Cau-WSCP-35* and *Cau-WSCP-49* retained the signature motif for Kunitz type protease inhibitor family (Fig. 38).

In vitro expression studies using both the gene constructs (*Cau-WSCP-35* and *Cau-WSCP-49*) resulted in a 66 kDa protein product (MBP fusion protein) (lanes 2 – 5, Fig. 39) and was in agreement with the positive control i.e., MBP-Cau-WSCP from Satoh et al. (1998) (lane 6, Fig. 39). Western blot analysis using anti-Cau-WSCP antibody (Satoh et al., 1998)

specifically detected the 66 kDa protein in both soluble and membrane fractions of *E. coli* sonicates containing either Cau-WSCP-35 (lanes 8 & 9, Fig. 39) or Cau-WSCP-49 (lanes 10 & 11, Fig. 39). The size of the immune-reacting band was in agreement with that obtained by using the expressed protein derived from the reference *Cau-WSCP* gene (lane 12, Fig. 39). The results were in agreement with the reports of Satoh et al. (1998) that MBP-Cau-WSCP was a 66 kDa protein.

6.2.3 WSCP did not aid in enhanced Chlase mediated Chl hydrolysis *in vitro*

The focus of the present work was to validate the function of WSCP as a Chl carrier protein (represented as \otimes in Fig. 3 of section 1.4) to the site of Chlase during Chl breakdown in plants. Therefore, *in vitro* Chlase assays were performed by addition of soluble extracts containing recombinant WSCP (MBP-Cau-WSCP-35 / MBP-Cau-WSCP-49 / MBP-Cau-WSCP-Satoh) into the reaction mixtures containing His-CcChlase and Chl.

The coupled assays of Chlase and WSCP were conducted in a water-miscible organic solvent system and the capacity of WSCP in promoting the Chlase activity was studied (Fig. 40). It was evident that WSCP (both MBP-Cau-WSCP-35 and MBP-Cau-WSCP-49) protein did not exert any influence on Chlase activity. It was visible in the form of presence of similar Chlide amounts in the assays performed with or without the addition of WSCP. Even the addition of double amount of recombinant WSCP, Chlase activity remained unaltered. Likewise, assays done using recombinant WSCP from Satoh also showed no increase in Chlase activity *in vitro*. Thus, it was obvious that WSCP does not affect the process of Chl breakdown. But, it is a soluble Chl carrier protein and possibly exhibits other functions.

6.2.4 WSCP overexpressor plants did not show any phenotypical differences with respect to WT tobacco

As the *in vitro* activity assays did not provide substantial information about the Chlase promoting activity of WSCP, transgenic plants overexpressing *Cau-WSCP-35* were produced to validate *in vivo* functionality of WSCP. This would contribute to verify its role in Chl degradation pathway as well as in other plant metabolic processes.

Transgenic tobacco plants overexpressing *Cau-WSCP-35* were produced using *A. tumefaciens* system and the advantages of using such bacterial system were discussed in section 6.1.4. The bacterial hosts (*Agrobacterium* C58C1) contained the binary vector

constructs of pCAMBIA3301 with the *Cau-WSCP-35* cDNA sequence (coding for protein with transit peptide) under the control of 35S CaMV promoter. This promoter leads to constitutive expression of the gene in all plant cells irrespective of developmental stage. Use of sterile young leaves for the transformation to generate the WSCP overexpressor plants was advantageous as they contained active RNA and protein synthetic machinery required for faster regeneration of callus from the tissues. Hormonal concentrations (BAP and NAA) were optimised for progressive shoot and root formation. The WSCP overexpressor plants did not show any phenotypic differences compared to WT plants (Fig. 41) as mere expression of a carrier protein in plants apparently may not induce any structural and morphological changes in the plants. The WSCP overexpressor plants behaved like normal WT tobacco plants in all aspects of growth like, leaf number, height of the stem, leaf colour, and also flowering.

6.2.5 Presence of *Cau-WSCP-35* in WSCP overexpressor plants was confirmed by PCR and western blot

PCR screening (using gene specific reverse primer and the one specific for 3' end of promoter region) of Basta resistant WSCP overexpressor lines showed that about 66% of the screened lines were positive for the presence of *Cau-WSCP-35* transgene. This was evident in the form of amplification of the transgene from genomic DNA samples of some of the WSCP overexpressor lines (samples 1, 4, 17, 20, 25, 31, 36, 40 and 41, Fig. 42). The size of the amplicon was in agreement with the PCR amplification obtained from positive control (pCAMBIA3301 plasmid containing *Cau-WSCP-35*) which also showed a PCR band at ~800 bp. WT plants served as good negative controls as they did not show any amplification of the transgene in their genomic DNA samples.

Further, protein expression of the *Cau-WSCP-35* transgene in the PCR positive lines was confirmed by western blot. Presence of recombinant *Cau-WSCP-35* protein as a 22 kDa protein in the soluble fraction of plant protein extracts (Fig. 43) was in agreement with known fact that *Cau-WSCP* was a soluble protein 22 kDa protein (Sato et al., 1998). Also WSCP from barley exist as a 22 kDa protein in its mature form (Reinbothe et al., 2004). Absence of any immune-reacting band in WT samples proves that the antibody does not exhibit any cross reactivity.

6.2.6 Copy number of *Cau-WSCP-35* transgene in WSCP overexpressor plants

Southern blot analysis helps to determine the copy number and the degree of homoplasmy of the integrated transgene. Presence of a hybridisation signal corresponding to *Cau-WSCP-35* gene confirmed successful integration of transgene into the genome of tobacco (Fig. 44). Based on the size of the hybridization band from XbaI digestion, it may be concluded that the transgene was integrated at different sites in their genome. The transgene copy number in most of the plants was >1 and varied from 2 to 6. Only line 17 showed single insertion of the transgene. The WSCP overexpressor lines 1, 25 and 45 showed the same integration pattern of *Cau-WSCP-35*, indicating their origin from the same Basta-resistant callus. Similarly, lines 40 and 41 would have been regenerated from the same callus. Lines 2 and 3 showed higher number of transgene insertions of 6 and 4 respectively. Although lines 4 and 39, showed similar number of insertions, their position in the genome was different as seen from the size of the hybridization signals. The WT genomic DNA samples served as good negative controls as they showed no transgene detection even after restriction digestion and radio-labelling.

6.2.7 Presence of recombinant *Cau-WSCP* did not enhance the Chl breakdown pathway *in vivo*

Chl breakdown is virtually seen during leaf senescence in plants. Hence, to elucidate the role of WSCP during Chl degradation, the protein expression pattern of the recombinant *Cau-WSCP-35* was studied at different stages of leaf development. As the WSCP transgene was expressed under the control of a constitutive 35S promoter, a uniform protein expression pattern was expected in the overexpressor plants independent of stage of development. But, a different phenomenon was observed with the expression of recombinant WSCP protein being maximum in young leaves and declined gradually with increase in leaf age (Fig. 45). This could be due to active protein expression of *Cau-WSCP-35* during leaf development (active Chl synthesis) but not during leaf senescence (diminished Chl synthesis).

The above result was confirmed when total soluble protein extracts from every leaf of one the WSCP overexpressor line (line 41) were screened. Accumulation of protein in terms of the immune-reacting band intensity decreased with an increase in leaf age (Fig. 46). In very old leaves, almost no WSCP was detectable, but was clearly seen up to leaf maturing stage. Analysis of cauliflower leaves in similar manner (from young to senescent leaves) produced equal results. Reduced accumulation of native WSCP followed the order $y > m >$

s (Fig. 47). Hence it could be concluded that WSCP was present in more quantities during Chl synthesis but may be fastly degraded during chloroplast degeneration with onset of leaf ageing.

Further, the *in vivo* steady state levels of Chls and Chlide *a* were assessed to predict the role of WSCP during increasing Chlase activity in intact leaf tissue. The amounts of Chls decreased from young to senescent leaves (Fig. 48). The differences in Chl amounts ($y > m > s$) were explained by active Chl synthesis in the tender leaves in comparison to senescent leaves. Also the presence of large vacuoles in the senescent leaves would decrease the net amount of Chls extracted when it was related to fresh weights. In case of young leaves, only line 40 showed significantly higher Chl levels than the WT. Both lines 4 and 41 showed significant differences in Chl levels in senescent leaves while line 41 also differed with respect to mature leaves. But this did not result in enhanced accumulation of Chlide *a* levels in the leaves. The results were consistent at all leaf developmental stages and hence confirm the inability of WSCP to enhance Chl breakdown *in vivo*.

The observations were substantiated with another set of results which showed that no extra Chlide *a* was generated *in vitro* in the overexpressor leaf samples (Fig. 49). No significant variations were observed in Chl amounts of both WT and WSCP overexpressor plants (Fig. 49). The amounts of Chlide *a* generated were in the order $y > m > s$ which was explained by degenerated protein synthesis and higher water content in senescent leaves. Comparison of the present results with those discussed for *in vitro* activity assays of recombinant plant Chlase, (section 6.1.7.4) clarifies that WSCP did not accelerate Chlase activity. All the data discussed together with that in section 6.2.3 conclude that WSCP does not play any active role during Chl degradation and functions as a mere Chl carrier and binding protein *in vivo*. Also the protein could majorly contribute in nitrogen recycling and may play a role in protecting the younger tissues from adverse conditions by maintaining protein integrity and photosynthesis (Desclos et al., 2008).

6.2.8 WSCP acts as a repository for Chl precursors *in vivo*

WSCP isolated from barley (*h_v-WSCP*) was reported as a 22 kDa protein in etioplasts and served as a putative carrier protein of Chl derivatives during light-induced chloroplast development and Chl biogenesis (Reinbothe et al., 2004). ALA feeding experiments of intact leaves and analysis of Pchlide levels after dark incubation produced similar results in WSCP overexpressor plants. Though the deposition of Pchide was seen in O/N dark

incubated plants, there was a significant rise in pigment levels after exogenous ALA application. Prolonged dark incubation of plants (for 3 days) contributed to the rise in Pchl_{ide} in leaf tissues. The effect was similar in both WT and WSCP overexpressor plants but significantly higher levels of Pchl_{ide} were seen in the WSCP overexpressor lines (Fig. 50). Line 40 showed significant accumulation of Pchl_{ide} at both the tested concentrations of ALA (5 mM and 10 mM) compared to WT plants treated with same concentrations of ALA. But in lines 4 and 41 the Pchl_{ide} levels showed significant differences at 5 mM ALA concentration, but not at 10 mM ALA concentration when compared to WT. However, the higher Pchl_{ide} amounts in the overexpressor plants would support the notion that WSCP helps in storage of Chl precursor molecules in dark rather than Chl degradation.

To corroborate the above discussed result, Pchl_{ide} levels from etiolated tobacco seedlings (WT and WSCP overexpressor plants) were determined. Also, the expression of POR protein was monitored to rule out the expected result that elevated Pchl_{ide} synthesis was due to enhanced POR accumulation (Reinbothe et al., 1995). Dark germination of WSCP transgenic seed and their subsequent growth in dark led to higher deposition of Pchl_{ide} (Fig. 51) than the WT. The significant rise in Pchl_{ide} amounts was certainly not due to accumulated POR enzyme levels as was evident from Fig. 52a. The immune-reacting band of POR recognized as a 30 kDa protein by anti-POR antibody showed equal signal intensities in both WT and the selected T1 WSCP progeny. Also the expression of recombinant Cau-WSCP-35 protein was not affected as seen from Fig. 52b demonstrating similar protein expression profile in the WSCP overexpressor lines. As expected, the WT tobacco plants did not show presence of WSCP protein.

Based on all observations, it was evident that presence of recombinant WSCP in plants leads to higher deposition of Chl precursors *in vivo* and that the proteins acts as a storage molecule for the Chl precursors.

6.2.9 WSCP: A stress induced protein in plants

The aa sequence of Cau-WSCP shows homology to drought and salt stress induced proteins, BnD22 – oil seed rape and P22 – radish, (Satoh et al., 2001). Protein expression of WSCP was induced by drought (Downing et al., 1992), leaf detachment (Nishio and Satoh, 1997) and heat stress (Annamalai and Yannagihara, 1999).

The abundance of WSCP in detached leaves of the WSCP overexpressor lines was shown in Fig. 53. The levels of WSCP in the detached leaves drastically increased after 30 h of detachment in both control and water stressed leaves. The WSCP levels increased during incubation of the detached leaves in water shown by presence of intense immune-reacting band compared to start-up of the experiments (0 h). Nevertheless, the protein accumulation was also higher in the water deficient leaves. Presence of recombinant WSCP during the tested stress conditions was similar in all the three selected WSCP overexpressor lines. Leaf detachment also caused wounding as well as water stress on the leaf. In conclusion, water deficit and wounding were considered to account for WSCP accumulation.

Similar results were reported by Nishio and Satoh, (1997). They showed that WSCP from cauliflower was induced by drought and wound stresses. Also Ilami et al. (1997) showed same affects for BnD22 from rapeseed.

6.2.10 Photoprotective function of recombinant Cau-WSCP-35 protein

Though light is the primary source for photochemical reactions like photosynthesis, it can also act as one of the most deleterious environmental factors causing photooxidative stress (Baroli et al., 2003). Exposure of the plants to higher irradiance that could not be utilized during photosynthesis or not dissipated through harmless processes leads to damage of the photosynthetic apparatus termed as photoinhibition (qI) (Krause, 1998). At high photon flux densities (PFDs), the accumulation of excitation energy in the light-harvesting chlorophyll antennae (LHC) of the photosystems may lead to the production of triplet excited chlorophyll molecules (^3Chl) that can interact with O_2 to generate reactive singlet oxygen ($^1\text{O}_2$). Overreduction of the photosynthetic electron carrier chain may also favor the direct reduction of O_2 by photosystem I (PSI) and the subsequent production of damaging ROS, such as superoxide (O_2^-), hydrogen peroxide (H_2O_2), and the hydroxyl radical ($^{\bullet}\text{OH}$). In addition, many environmental stress conditions limit the ability of a plant to utilize light energy through photosynthesis so that excess excitation of the photosystems can also occur at moderate light intensities (Demming-Adams and Adams, 1992). Consequently, photooxidative damage, especially to PSII (Prasil et al., 1992), appears to be an unavoidable consequence of the photosynthetic activity and can be a major factor that causes sustained depressions in photosynthetic efficiency (photoinhibition).

Hence, to overcome the imbalance between the absorption of the excitation energy and its use, plants use a series of antioxidant molecules and enzymes to detoxify the ROS and free

radicals (Niyogi, 1999). Carotenoids including xanthophylls are membrane bound antioxidants that quench the ^3Chl and $^1\text{O}_2$, inhibit lipid peroxidation, and stabilize membranes (Havaux, 1998). In particular, zeaxanthin and lutein are essential for the transition of LHCs of PSII from a conformation that favors thermal dissipation of the part of the excess excitation energy under high light stress (Niyogi et al., 2001). This thermal dissipation of excess light energy which involves direct quenching of excess $^1\text{Chl}^*$, can be measured and often referred to as nonphotochemical quenching (NPQ or q_N) of Chl fluorescence (Horton et al., 1996; Müller et al., 2001).

Therefore measuring the levels of individual xanthophyll cycle pigments, ROS and changes in Chl fluorescence gave an account of either sensitivity or tolerance of plants to high light intensities. As it was successfully demonstrated *in vitro* that WSCP-Chl complexes were prone to less photoinhibition in spite of absence of carotenoids (Schmidt et al., 2003), the WSCP overexpressor plants were analyzed for their capacity to withstand high light stress.

WSCP overexpressor plants accumulate lower levels of zeaxanthin

Xanthophylls (O-derivatives of carotenes), found in all Chl or BChl containing pigment-protein-complexes play a key role in the protection of photosynthetic organisms against the toxic effects of light by quenching the ^3Chl and $^1\text{O}_2$ states in the PSII complexes (Frank and Cogdell, 1996; Müller et al., 2001; Horton et al., 2005). In plants, under excess light conditions, an increase in thylakoid pH causes a rapid change in the composition of xanthophyll pigments of the LHCs; the diepoxide xanthophyll violaxanthin (Vx) rapidly and reversibly converts to epoxide-free zeaxanthin (Zx) via the intermediate antheraxanthin (Ax) under the action of the enzyme Vx-deepoxidase (Pfündel and Bilger, 1994). The chemical transformation of Vx is involved in the conversion of PSII from a state of efficient light harvesting to a state of high thermal energy dissipation and low Chl fluorescence emission. It was suggested that Zx could quench directly the singlet excited state of chlorophylls (^1Chl) (Demming-Adams and Adams, 1996; Gilmore, 1997) or could favor proton-induced aggregation of the LHCs of PSII leading to energy dissipation (Horton et al., 1996). This energy dissipation can be measured as a nonphotochemical quenching (NPQ) of Chl fluorescence. An increase in thermal deactivation of ^1Chl is potentially beneficial because it can protect the PSII reaction centers from overexcitation and subsequent photoinhibition and it also can reduce the probability of ^3Chl and $^1\text{O}_2$ formation in the LHCs. It must be noted, however, that the protective function of the Vx

cycle was probably not restricted to PSII, because the cycle takes place in both PSII and PSI (Thayer and Björkman, 1992).

Similar to all Chl binding protein complexes, the WSCP-Chl complexes were expected to contain carotenoids. However, a contrast phenomenon was observed in which the WSCP-Chl complexes did not contain any carotenoids (Kamimura et al., 1997). But the absence of carotenoids did not exert any influence on photoresistance capacity of high light illuminated WSCP-Chl complexes and this was proved *in vitro* by Schmidt et al. (2003). In the present study, evidence for the above observation was provided by measurement of the levels of the xanthophyll cycle pigments from both WT and WSCP overexpressor leaves exposed to a range of high light intensities.

Preliminary results confirmed the presence of lower deepoxidized xanthophyll (Zx and Ax) levels in WSCP overexpressor plants than the WT (Fig. 55) under normal growth conditions. A slight increase in $\Sigma Vx+Zx+Ax/Chl\ a$ values was observed in WSCP overexpressor plants in comparison to WT, however, the amounts of Zx were lower in the WSCP overexpressor leaves. This might be due to faster reconversion of Zx to Vx in the WSCP overexpressor plants. Also the ratio of $Ax+Zx/Ax+Vx+Zx$ was lower in the WSCP overexpressor lines in comparison to WT leaves.

In addition, various high light stress experiments performed on the WSCP overexpressor leaves also revealed the presence of significantly lower amounts of Zx (Fig. 56) in comparison to that seen in WT. Though production of Zx increased as a stress response with rise in light intensity (100 to 1000 $\mu\text{mol photons m}^{-2} \text{s}^{-1}$) in both WT and WSCP overexpressor plants, the latter always showed relatively lower amounts of the pigment at all tested conditions. At lower and moderately higher light intensities (100, 300 and 500 $\mu\text{mol photons m}^{-2} \text{s}^{-1}$), the WSCP overexpressor leaves had only about 50% of Zx compared to WT. But at higher intensities (700 and 1000 $\mu\text{mol photons m}^{-2} \text{s}^{-1}$), the difference in Zx of WSCP overexpressor plants was only about 20% to 30% relative to WT. Overall, it was evident that WSCP overexpressor plants exhibit phototolerance as seen in the form of lower amounts of de-epoxidised xanthophylls (Zx + Ax).

The observations in the present study were different from the normal phenomenon of increased zeaxanthin levels under high light stress to quench the triplet and singlet oxygen states (reviewed in Baroli et al., 2004 and Havaux et al., 2004). Though the pigments of

xanthophyll cycle pool were higher in WSCP overexpressor plants compared to WT (Fig. 55), the levels of zeaxanthin were lower in WSCP overexpressor plants. The same effect was seen even under high light intensities which show the ability of the WSCP overexpressor plants to cope up the stress conditions.

Decreased peroxidase activity in WSCP overexpressor plants than the WT

Increased production of ROS in plants in response to high light stress is a well-known fact (Grace and Logan, 1996). This is due to excitation of Chl binding protein complexes on illumination and the production of Chl triplet and the oxygen singlet excited states (Asada and Takahashi, 1987). Of the various types of ROS generated in plants due to stress responses, one is superoxide (O_2^- - non radical form – H_2O_2) as a result of peroxidase activity (Barry Halliwell, 2006).

As it was proven *in vitro* that reconstituted WSCP-Chl complexes produced lower amounts of ROS on illumination (Schmidt et al., 2003), the same was analysed in WSCP overexpressor plants. The results from Fig. 57 (a, b and c) show that the extent of ROS formation by *in vitro* peroxidase activity was lower in WSCP overexpressor leaves compared to WT. Of the three WSCP overexpressor lines, line 40 showed lower peroxidase activity than the other two lines (lines 4 and 41). Even though, elevated peroxidase activity (in terms of absorbance measured/ μg of protein) was witnessed with increased illumination (from 500 to 700 μmol photons $m^{-2} s^{-1}$), the WSCP overexpressor lines retained minimal accumulation of the free radicals. Similar data were obtained regarding the *in vivo* superoxide formation in the plant cells after high light stress at 500 μmol photons $m^{-2} s^{-1}$ as evident in Fig. 58 (no external supply of H_2O_2). From all these, it was clear that even after such high light illumination, the WSCP overexpressor leaves did not result in enhanced peroxidase activity compared to WT. The results were in agreement with those reported by Schmidt et al. (2003), that reconstituted His-tagged WSCP-Chl complexes on illumination (500 μmol photons $m^{-2} s^{-1}$, 60 min) showed only 25% of ROS formation of that seen for free Chls. Thus, the WSCP overexpressor plants are relatively photostable than the WT tobacco plants.

Chl fluorescence measurements indicated faster relaxation of line 40 in comparison to other WSCP overexpressor lines

As it is known that exposure of the leaves to high light intensities leads to photoinhibition, the excess energy is dissipated nonphotochemically which is detected as quenching of Chl

fluorescence referred to as nonphotochemical quenching, qN (reviewed in Demmig-Adams and Adams, 1992; Horton and Ruban, 1992; Horton et al., 1994). The heterogeneous nature of qN has been revealed by a study of its relaxation in darkness (Horton and Hague, 1988; Walters and Horton, 1991). Therefore the degree of photoinhibition can be monitored via measurements of the Chl fluorescence recovery kinetics in a dark period following high light treatment and depends on the photon flux density of the high-light stress (Lichtenthaler and Burkart, 1999). The quenching of the excited Chls solely due to NPQ can be determined by measuring the fluorescence during a brief (0.8 s) pulse of light that saturates photochemistry (qP) so that there is no quenching anymore due to qP. In this context, Chl fluorescence induction (and recovery) kinetics were measured with intact leaves of both WT and WSCP overexpressor plants in response to high light intensities.

Using a pulse modulated fluorometer, it was possible to measure both, short term (6 min) and long term (50 min) stress responses of dark adapted plants irradiated with high photon flux densities ($900 \mu\text{mol photons m}^{-2} \text{s}^{-1}$). Exposure of the leaves to high light for short time period gives a measure of the most rapid component of NPQ, the qE (pH or energy dependent quenching) which relaxes within seconds to minutes (Müller et al., 2001). With long term exposure, qI (photoinhibitory quenching component) which shows slowest relaxation in range of hours could be measured. With the help of qI the extent of photoinhibition of photosynthesis can be assessed.

The results given in Fig. 59 showed that short-term (6 min) exposure of WSCP overexpressor plants to high light did not show any significant differences in terms of Chl fluorescence after the cut off from light source. This was obvious from similar Chl fluorescence peaks seen for WT as well as WSCP overexpressor plants. The observations were similar for all the three selected overexpressor lines. On giving saturating pulses after light stress in dark period, the peaks of Chl fluorescence remained similar in all plants irrespective of leaf age (young, mature and senescent). This indicated that no differences were noticed in rapid quenching or faster relaxation that was observed within minutes of high light exposure.

Exposure of the plants to long term radiation caused a different effect (Fig. 60). It was seen that, of the three WSCP overexpressor lines tested, line 40 showed relatively faster relaxation i.e., less photoinhibitory quenching (qI) which was evident from the slightly

higher peaks of Chl fluorescence in comparison to other lines. The other two lines 4 and 41, along with WT did not show any less qI, as seen by lower Chl fluorescence peaks irrespective of leaf age. The phenomenon was observed only in the case of young and mature leaves of line 40 but not in senescent leaves which could be explained by lower expression levels of WSCP in senescent leaves (Fig. 45). Based on the results, it could be emphasized that WSCP was involved during photoprotection of plants during long term responses (qI) to high light stress but not short term photoprotective responses (qE).

Of the three WSCP overexpressor lines analyzed, line 40 showed some consistency with regard to lower peroxide radical levels and relaxation from high light stress.

In overview, presence of lower zeaxanthin levels and decreased peroxidase activity indicated the efficiency of WSCP to participate in photoprotection mechanism of plants which could be explained by the elucidations of Horigome et al. (2007) on crystal structure of *Lepidium* WSCP-Chl complexes. The formation of lower ROS could be due to absence of direct contact between Chl and molecular oxygen in the WSCP-Chl tetramer that inhibits the generation of ROS in the WSCP overexpressor plants. Also the quenching of the excitation energy was favored by a sequence of electron exchanges between the Chl molecules and the nearby aromatic residues, Trp-90 and Trp-154 similar to riboflavin binding proteins (Zhong and Zewail, 2001). Also the energy transfer between the Chl molecules could aid in photoprotective mechanism of WSCP.

7 CONCLUSIONS

7.1 Chlorophyllase

1. The various *in vitro* enzyme assays performed using soluble extracts of *E. coli* containing His-CcChlase proved the functional activity of CcChlase. It was found that CcChlase protein had an optimum activity at 40°C and pH 8.0. Enzyme activity of CcChlase protein was also observed in the presence of higher proportions of oil in the assays (71%).
2. Addition of soluble extracts of CcChlase during oil refining considerably decreased the residual Chl amounts in oil and the resultant catabolites were removed by modified extraction methods.
3. Production of transgenic plants overexpressing *CcCHLASE* led to assess the functional activity of the protein *in vivo*. Most of the Chlase overexpressor plants showed higher Chlide *a* levels in their leaves compared to WT leaves.
4. Quantification of Chlide *a* by using 99% acetone extraction method confirmed the functional activity of CcChlase in the overexpressor plants.
5. Presence of higher Chlase activity in chloroplastic membrane fractions confirmed the localisation of *CcCHLASE* in chloroplasts unlike the Chlase proteins previously proposed for *Arabidopsis* (Schenk et al., 2007). Also the Chlase activity could be due to the presence of other candidate genes encoding for esterase like proteins related to Chlase.
6. The constitutive expression of *CcCHLASE* led to higher content of steady state levels of Chlide *a* in senescent leaf samples confirming the active participation of Chlase during senescence.
7. Presence of steady state levels of Chlide *a* under induced senescence proved the significance of CcChlase protein from *Citrus* in Chl catabolism, in contrast to the observations made by Schelbert et al. (2009) in *Arabidopsis*. This was confirmed by the absence of Phe in the leaf pigment extracts.
8. Induction of stress response (high salt and drought) in the Chlase overexpressor plants led to increased accessibility of the substrate (Chl) to Chlase making possible the generation of higher amounts of Chlide *a* during extremely unfavourable conditions.
9. The Chlase overexpressor plants contained about 15 – 20% lesser Chl levels than the WT plants, but no differences in ALA synthesising capacity were noticed.

10. Although high amounts of Chlide *a* were seen in the Chlase overexpressor plants, the amounts of subsequent catabolites were so little to be detected by HPLC. Hence, no changes in NCC contents could be observed.

7.2 Water Soluble Chlorophyll Protein

1. *In vitro* coupled assays of recombinant WSCP and Chlase did not show any enhanced Chlase activity in the presence of WSCP.
2. Chlide *a* levels were not enhanced during *in vitro* extraction conditions of the pigments from the WSCP overexpressor plants. Also the absence of steady state levels of Chlide *a* in the WSCP overexpressor plants similar to the WT confirmed its lack of activity in Chl degradation.
3. Accumulation of higher amounts of Pchlade in WSCP overexpressor plants compared to WT confirmed the role of WSCP as a repository for Chl precursor molecules.
4. The WSCP protein was highly expressed during drought conditions confirmed its activity during stress response.
5. Photoprotective role of WSCP could be demonstrated by the decreased zeaxanthin levels, reduced ROS levels and Chl fluorescence measurements of the WSCP overexpressor plants.

REFERENCES

1. Adachi M., Tsuzuki E. and Shimokawa K. (1996) Effect of ethylene on degreening of intact radish (*Raphanus satinus* L.) cotyledons. *Sci. Hortic.*, *65*, 1-9.
2. Amir-Shapira D., Goldschmidt E. E., and Altman A. (1987) Chlorophyll catabolism in senescing plant tissues: in vitro breakdown intermediates suggest different degradative pathways for Citrus fruit and parsley leaves. *Proc Natl Acad Sci.* *84*, 1901-1905.
3. Annamalai P., and Yanagihara S. (1999) Identification and characterization of a heat-stress induced gene in cabbage encodes a Kunitz type protease inhibitor. *J Plant Physiol.* *155*, 226–233.
4. Andersson B., and Barber J. (1996) Mechanisms of photodamage and protein degradation during photoinhibition of photosystem II. In *Photosynthesis and the Environment*, N.R. Baker, Ed (Dordrecht, The Netherlands: Kluwer Academic Publishers), pp. 101–121.
5. Ardao C., and Vennesland B. (1960) Chlorophyllase Activity of Spinach Chloroplastin. *Plant Physiol.* *35*(3), 368-71.
6. Arkus K. A., Cahoon E. B., and Jez J. M. (2005) Mechanistic analysis of wheat chlorophyllase. *Arch Biochem Biophys.* *438*(2), 146-55.
7. Arkus K. A., and Jez J. M. (2006) Development of a high-throughput purification method and a continuous assay system for chlorophyllase. *Anal Biochem.* *353*(1), 93-8.
8. Arriagada-Strodtloff P., Karboune S., Neufeld R. J., and Kermasha S. (2007) Optimization of chlorophyllase-catalyzed hydrolysis of chlorophyll in monophasic organic solvent media. *Appl Biochem Biotechnol.* *142*(3), 263-75.
9. Asada K., and Takahashi M. (1987) Production and scavenging of active oxygen in photosynthesis. In D. J. Kyle, C. B. Osmond, and C. J. Arntzen (eds.), *Photoinhibition*, Elsevier, Amsterdam. pp. 227-287.
10. Bacon M. F., and Holden M. (1970) Chlorophyllase of sugar-beet leaves. *Phytochemistry.* *9*, 115-125.
11. Bahmaei M., Sabbaghian E. S., and Farzadkish E. (2005) Development of a method for chlorophyll removal from canola oil using mineral acids. *Journal of the American Oil Chemists' Society* *82*(9), 679–684.
12. Barrett J., and Jeffrey S. W. (1964) Chlorophyllase and formation of an atypical chlorophyllide in marine algae. *Plant Physiol.* *39*(1), 44-7.

13. Baroli I., Do A. D., Yamane T., and Niyogi K. K (2003) Zeaxanthin accumulation in the absence of a functional xanthophyll cycle protects *Chlamydomonas reinhardtii* from photooxidative stress. *Plant Cell*. *15*, 992–1008.
14. Baroli I., Gutman B. L., Ledford H. K., Shin J. W., Chin B. L., Havaux M., and Niyogi K. K. (2004) Photo-oxidative stress in a xanthophyll-deficient mutant of *Chlamydomonas*. *J Biol Chem*. *279*(8), 6337-44.
15. Barry H. (2006) Reactive species and antioxidants. Redox biology is a fundamental theme of aerobic life. *Plant physiology*. *141*(2), 312-22.
16. Ben-Yaakov E., Harpaz-Saad S., Galili D., Eyal Y., and Goldschmidt E. (2006) The relationship between chlorophyllase activity and chlorophyll degradation during the course of leaf senescence in various plant species *Israel Journal of Plant Sciences* *54*, 129–135.
17. Benedetti C. E., Costa C. L., Turcinelli S. R., and Arruda P. (1998) Differential expression of a novel gene in response to coronatine, methyl jasmonate, and wounding in the *coi1* mutant of *Arabidopsis*. *Plant Physiol*. *116*, 1037–1042.
18. Benedetti C. E., and Arruda P. (2002) Altering the expression of the chlorophyllase gene *ATHCOR1* in transgenic *Arabidopsis* caused changes in the chlorophyll-to-chlorophyllide ratio. *Plant Physiol*. *128*(4), 1255-63.
19. Berghold J., Eichmüller C., Hörtensteiner S., and Kräutler B. (2004) Chlorophyll breakdown in tobacco: on the structure of two nonfluorescent chlorophyll catabolites. *Chem Biodivers*. *1*, 657-668.
20. Bitar M., Karboune S., Bisakowski B., and Kermasha S. (2004) Chlorophyllase biocatalysis in an aqueous/miscible organic medium containing canola oil. *J. Am. Oil Chem. Soc.* *81*, 927–932.
21. Bonham-Smith P. C., Gilmer S., Zhou R., Galka M., and Abrams S. R. (2006) Non-lethal freezing effects on seed degreening in *Brassica napus*. *Planta*. *224*, 145-154.
22. Böger P. (1965) Chlorophyllase of *Chlorella vulgaris* Beijerinck. *Phytochemistry*. *4*, 435-443.
23. Brandis A., Vainstein A., and Goldschmidt E. E. (1996) Distribution of chlorophyllase among components of chloroplast membranes in *Citrus sinensis* organs. *Plant Physiol Biochem*. *34*, 49-54.
24. Bradford M. M. (1976) A rapid and sensitive method for quantitation of microgram quantities of protein utilizing the principle of protein-dye-binding. *Anal Biochem*. *72*, 248-54.
25. Brown S. B., Houghton J. D., and Hendry G. A. F. (1991) Chlorophyll breakdown. In *Chlorophylls*, (Scheer H., ed.), CRC Press, Boca Raton, FL, 465-489.

26. Chen O. L-F., Lin C-H., Kelkar M. S., Chang Y-M., and Shawa J-F. (2008) Transgenic broccoli (*Brassica oleracea* var. *italica*) with antisense chlorophyllase (BoCLH1) delays postharvest yellowing. *Plant Science*. 174, 25–31.
27. Chomczynski P. (1993) A reagent for the single-step simultaneous isolation of RNA, DNA and proteins from cell and tissue samples. *Biotechniques (Band 5)*. 3, 532-4, 536-7.
28. Creelman R. A., and Mullet J. E. (1995) Jasmonic acid distribution and action in plants: regulation during development and response to biotic and abiotic stress. *Proc Natl Acad Sci*. 92(10), 4114–4119.
29. Damaraju S. (2003) Expression and activity of recombinant enzymes of chlorophyll catabolism. Dissertation work submitted at Faculty of Mathematics and Nature Sciences I, Humboldt University, Berlin.
30. De Block M., De Brouwer D., and Tenning P. (1989) Transformation of *Brassica napus* and *Brassica oleracea* Using *Agrobacterium tumefaciens* and the expression of the bar and neo genes in the transgenic plants. *Plant Physiol*. 91(2), 694-701.
31. Demmig-Adams B., and Adams W. W. (1992) Photoprotection and other responses of plants to high light stress. *Annu Rev Plant Physiol Plant Mol Biol*. 43, 599-626.
32. Demmig-Adams B., and Adams W.W. III (1996) Chlorophyll and carotenoid composition in leaves of *Euonymus kiautschovicus* acclimated to different degree of light stress in the field. *Australian Journal of Plant Physiology*. 23, 649–659.
33. Desclos M., Dubousset L., Etienne P., Le Caherec F., Satoh H., Bonnefoy J., Ourry A., and Avice J. C. (2008) A proteomic profiling approach to reveal a novel role of *Brassica napus* drought 22 kD/water-soluble chlorophyll-binding protein in young leaves during nitrogen remobilization induced by stressful conditions. *Plant Physiol*. 147(4), 1830-44.
34. Downing W. L., Mauxion F., Fauvarque M-O., Reviron M-P., de Vienne D., Vartanian N., and Giraudat J. (1992) A *Brassica napus* transcript encoding a protein related to the Kunitz proteaseinhibitor family accumulates upon water stress in leaves, not in seeds. *Plant J*. 2, 685-693.
35. Drazkiewicz M. (1994) Chlorophyllase: occurrence, functions, mechanisms of action, effects of external and internal factors. *Phytosynthetica*. 30, 321–331.
36. Drzewiecka-Matuszek A., Skalna A., Karocki A., Stochel G., and Fiedor L. (2005) Effects of heavy central metal on the ground and excited states of chlorophyll. *J. Biol. Inorg. Chem*. 10, 453–462.
37. Doyle J., and Doyle L. (1990) Isolation of plant DNA from fresh tissue. *Focus* 12, 13-15.

38. Eckhardt U., Grimm B., and Hörtensteiner S. (2004) Recent advances in chlorophyll biosynthesis and breakdown in higher plants. *Plant Molecular Biology*. 56, 1–14.
39. Endo Y., Thorsteinson C. T., and Daun J. K. (1992) Characterization of chlorophyll pigments present in canola seed, meal and oil. *J. Am. Oil Chem. Soc.* 69, 564–568.
40. Fang L. Z., Bouwkamp J., and Solomos T. (1998) Chlorophyllase activities and chlorophyll degradation during leaf senescence in non-yellowing mutant and wild type of *Phaseolus vulgaris*. *Journal of Experimental Botany*. 49, 503–510.
41. Fernandez-Lopez J. A., Almela L., Almansa M. S., and Lopez-Roca J. M. (1992) Partial purification and properties of chlorophyllase from chlorotic Citrus limon leaves. *Phytochemistry*. 31, 447–449.
42. Fiedor L., Rosenbach-Belkin V., and Scherz A. (1992) The stereospecific interaction between chlorophylls and chlorophyllase. Possible implication for chlorophyll biosynthesis and degradation. *J Biol Chem*. 267(31), 22043–7.
43. Folly P., and Engel N. (1999) Chlorophyll b to chlorophyll a conversion precedes chlorophyll degradation in *Hordeum vulgare* L. *J. Biol. Chem.* 274, 21811–21816.
44. Frank H. A., and Cogdell R. J. (1996) Carotenoids in photosynthesis. *Photochem Photobiol.* 63(3), 257–264.
45. Gaffer R., Kermasha S., and Bisakowski B. (1999) Biocatalysis of immobilized chlorophyllase in a ternary micellar system. *J. Biotechnol.* 75, 45–55.
46. Garcia A. L., Galindo L., and Navarro S. (1980) Chlorophyllase in Citrus Leaves. Kinetic aspects of the reaction. *Biologia Plantarum*. 22(4), 255—264.
47. García A. L., Torrecillas A., León A. and Sánchez-Blanco M. J. (1987) Biochemical indicators of water stress in sunflower seedlings. *Biologia Plantarum*. 29, 473–475.
48. Garcia A. L., and Galindo L. (1991) Chlorophyllase in Citrus leaves. Localization and partial purification of the enzyme. *Photosynthetica*. 25, 105–111.
49. Gilmore A. M. (1997) Mechanistic aspects of xanthophyll cycle-dependent photoprotection in higher plant chloroplasts and leaves. *Physiol Plant*. 99, 197–209.
50. Goldschmidt E. E. (2001) Chlorophyll decomposition in senescing leaves and ripening fruits: Functional and evolutionary perspectives. *Acta Hort.* 553, 331–335.
51. Gong Y., and Mattheis J. P. (2003) Effects of ethylene and 1-methylcyclopropene on chlorophyll catabolism of broccoli florets. *Plant growth regul.* 40, 33–38.

52. Grace S. C., and Logan B. A. (1996) Acclimation of foliar antioxidant systems to growth irradiance in three broadleaved evergreen species. *Plant Physiol.* *112*, 1631–1640.
53. Gray G. D., Yamauchi N., Akiyama Y., Kako S., and Hashinaga F. (1997) Chlorophyll degradation in Wase satsuma mandarin (*Citrus unshiu* Marc.) fruit with on-tree maturation and ethylene treatment. *Scientia Horticulturae.* *71*, 35-42.
54. Gray J., Janick-Bruckner D., Bruckner B., Close P. S., and Johal G. S. (2002) Light-dependent death of maize lls1 cells is mediated by mature chloroplasts. *Plant Physiol.* *130*, 1894–907.
55. Gray J., Wardzala E., Yang M., Reinbothe S., Haller S., and Pauli F. (2004) A small family of LLS1-related non-heme oxygenases in plants with an origin amongst oxygenic photosynthesizers. *Plant Mol. Biol.* *54*, 39–54.
56. Gualberto J. M., Handa H., and Grienemberger J. M. (1995) Isolation and fractionation of plant mitochondria and chloroplasts: Specific examples. *Methods of cell biology.* *50*, 161-173.
57. Harpaz-Saad S., Azoulay T., Arazi T., Ben-Yaakov E., Mett A., Shibolet Y. M., Hörtensteiner S., Gidoni D., Gal-On A., Goldschmidt E. E., and Eyal Y. (2007) Chlorophyllase Is a rate-limiting enzyme in chlorophyll catabolism and is posttranslationally regulated. *Plant Cell.* *19*(3), 1007–1022.
58. Havaux M. (1998) Carotenoids as membrane stabilizers in chloroplasts. *Trends Plant Sci.* *3*, 147-151.
59. Havaux M., Dall'Osto L., Cuine' S., Giuliano G., and Bassi R (2004) The effect of zeaxanthin as the only xanthophyll on the structure and function of the photosynthetic apparatus in *Arabidopsis thaliana*. *J Biol Chem.* *279*, 13878–13888.
60. Hinder B., Schellenberg M., Rodoni S., Ginsburg S., and Vogt E. (1996) How plants dispose of chlorophyll catabolites. Directly energized uptake of tetrapyrrolic breakdown products into isolated vacuoles. *J. Biol. Chem.* *271*, 27233–36.
61. Hobbs S. L. A., Kpodar P., and DeLong C. M. O. (1990) The effect of T-DNA copy number, position and methylation on reporter gene expression in tobacco transformants. *Plant Mol. Biol.* *15*, 851-864.
62. Holden M. (1961) The breakdown of chlorophyll by chlorophyllase. *Biochem J.* *78*, 359-64.
63. Hörtensteiner S. (2004) The loss of green color during chlorophyll degradation - a prerequisite to prevent cell death? *Planta* *219*, 191–94.
64. Hörtensteiner S. (2006) Chlorophyll degradation during senescence. *Annu Rev Plant Biol.* *57*, 55-77.

65. Hornero-Méndez D., and Mínguez-Mosquera M. I. (2001) Properties of chlorophyllase from *Capsicum annuum* L. fruits. *Z Naturforsch [C]*. 56(11-12), 1015-21.
66. Hornero-Méndez D., and Mínguez-Mosquera M. I. (2002) Chlorophyll disappearance and chlorophyllase activity during ripening of *Capsicum annuum* L. fruits. *Journal of the Science of Food and Agriculture*. 82(13), 1564-1570.
67. Horigome D., Satoh H., and Uchida A. (2003) Purification, crystallization and preliminary X-ray analysis of a water-soluble chlorophyll protein from *Brassica oleracea* L. var. *acephala* (kale) *Acta Cryst. D*59, 2283-2285.
68. Horigome D., Satoh H., Itoh N., Mitsunaga K., Oonishi I., Nakagawa A., and Uchida A. (2007) Structural mechanism and photoprotective function of water-soluble chlorophyll-binding protein. *J Biol Chem*. 282(9), 6525-31.
69. Horsch R. B., Fraley R. T., Rogers S. G., Sanders P. R., and Lloyd A. (1985) A simple and general method for transferring genes into plants. *Science* 227, 1229-1231.
70. Horton P., and Hague A. (1988) Studies on the induction of chlorophyll fluorescence in isolated barley chloroplasts. IV. Resolution of non-photochemical quenching. *Biochim. Biophys. Acta*. 932, 107–115.
71. Horton P., Ruban A. V., Rees D., Pascal A. A., Noctor G., and Young A. J. (1991) Control of the light-harvesting function of chloroplast membranes by aggregation of the LHCII chlorophyll-protein complex. *FEBS Lett*. 292, 1–4.
72. Horton P., and Ruban A. V. (1992) Regulation of photosystem 11. *Photosynth Res*. 34, 375-385.
73. Horton P., Ruban A. V., and Walters R. G. (1994) Regulation of light harvesting in green plants: indication by nonphotochemical quenching of chlorophyll fluorescence. *Plant Physiol*. 106, 415–420.
74. Horton P., Ruban A. V., and Walters R. G. (1996). Regulation of light harvesting in green plants. *Annu. Rev. Plant Physiol. Plant Mol. Biol*. 47, 655-684.
75. Horton P., Wentworth M., and Ruban A. (2005) Control of the light-harvesting function of chloroplast membranes: the LHCII-aggregation model for non-photochemical quenching. *FEBS Lett*. 579, 4201–4206.
76. Hudák J., Gálová E., and Zemanová L. (2005) Plastid morphogenesis – Handbook of Photosynthesis. 2, 221-245.

77. Ilami G., Nespoulous C., Huet J-C., Vartanian N., and Pernollet J-C. (1997) Characterization of BnD22, a drought-induced protein expressed in *Brassica napus* leaves. *Phytochemistry*. *45*, 1-8.
78. Itoh R., Itoh S., Sugawa M., Oishi O., Tabata K., Okada M., Nishimura M., and Yakushiji E. (1982) Isolation of crystalline Water-soluble Chlorophyll Proteins with different chlorophyll a and b Contents from Stems and Leaves of *Lepidium virginicum* Plant Cell Physiology. *23*(3), 557-560.
79. Jacob-Wilk D., Holland D., Goldschmidt E. E., Riov J., and Eyal Y. (1999) Chlorophyll breakdown by chlorophyllase: Isolation and functional expression of the Chlase1 gene from ethylene-treated Citrus fruit and its regulation during development. *Plant J.* *20*(6), 653-61.
80. Johnson-Flanagan A., Singh J., and Thiagarajah M. (1990) The impact of sublethal freezing during maturation of pigment content in seeds of *Brassica napus*. *J. Plant Physiol.* *136*, 385-390.
81. Johnson-Flanagan A. M., and Spencer M. (1994) Ethylene production during degreening of maturing seeds of mustard and canola. *Plant Physiol.* *106*, 601–606.
82. Johnson-Flanagan A. M., and Spencer M. S. (1996) Chlorophyllase and peroxidase activity during degreening of mature canola (*Brassica napus*) and mustard (*Brassica juncea*) seed. *Physiologia Plantarum* *97*, 353–359.
83. Johnson-Flanagan A. M., Go N., Sun F., Singh J., Robert L., and Konschuh M. N. (1999) Antisense RNA to decrease the green seed problem in canola. In: *New horizons for an old crop*, Proceedings of the 10th International Rapeseed Congress, Canberra, Australia.
84. Kalmokoff M. L., Pickard M. D., and GrootWassink J. W. D. (1988) Resistance of green pigments in commercial canola to enzymatic hydrolysis. *Can. Inst. Food. Sci. technol. J.* *21*, 534-536.
85. Kamimura Y. (1997) Proceedings of the 61st annual meeting of the botanical society of Japan p: 112.
86. Kamimura Y., Mori T., Yamasaki T., and Katoh S. (1997) Isolation, properties and a possible function of a water-soluble chlorophyll a/b-protein from brussels sprouts. *Plant Cell Physiol.* *38*(2), 133-8.
87. Kannangara C. G., and Gough S. P. (1979) Biosynthesis of a-aminolevulinate in greening barley leaves II: Induction of enzyme synthesis by light. *Carlsberg Res. Commun.* *44*, 11-20.

88. Karboune S., Neufeld R. J., and Kermasha S. (2005) Immobilization and biocatalysis of chlorophyllase in selected organic solvent systems. *J. Biotechnol.* *120*, 273-283.
89. Kariola T., Brader G., Li J., and Palva E. T. (2005) Chlorophyllase 1, a damage control enzyme, affects the balance between defense pathways in plants. *Plant Cell.* *17(1)*, 282-94.
90. Kermasha S., Khalyfa A., Marsot P., Alli I., and Fournier R. (1992) Biomass production, purification and characterization of chlorophyllase from algae *Phaeodactylum tricornutum*. *Biotechnol. Appl. Biochem.* *14*, 142-159.
91. Kermasha S., and Khamessan A. (2001) Application of chlorophyllase to the removal of chlorophylls from canola oil: Department of Food Science and Agricultural Chemistry, McGill University.
92. Khamessan A., Kermasha S., and Marsot P. (1993) Biocatalysis of chlorophyllase from algae *Phaeodactylum tricornutum* in water:miscible-organic-solvent system. *Biotechnol. Appl. Biochem.* *18*, 285-298.
93. Khamessan A., Kermasha S., Marsot P., and Ismail, A. A. (1994) Biocatalysis of chlorophyllase from algae *Phaeodactylum tricornutum* in biphasic organic system. *J. Chem. Technol. Biotechnol.* *60*, 73-81.
94. Khamessan A., Kermasha S. and Marsot P. (1995) Biocatalysis of chlorophyllase from *Phaeodactylum tricornutum* in organic solvent media. *Process Biochem.* *30*, 159-68.
95. Khamessan A., Kermasha S., and Mollimard L. (1995b) Optimization of chlorophyllase-catalyzed hydrolytic activity in a micellar ternary system. *Biotechnol. Appl. Biochem.* *22*, 327-343.
96. Khamessan A., and Kermasha S. (1996) Biocatalysis of chlorophyllase from *Phaeodactylum tricornutum* in micellar ternary system containing Spans. *J. Biotechnol.* *45*, 253-264.
97. Khamessan A., and Kermasha S. (1996a) Biocatalysis of chlorophyllase in canola oil using organic solvent systems. *J. Food Biochem.* *20*, 73-81.
98. Khalyfa A., Kermasha S., Marsot P. and Goetghebeur M. (1995) Purification and characterization of chlorophyllase from alga *Phaeodactylum tricornutum* by preparative native electrophoresis. *Appl. Biochem. Biotechnol.* *53*, 11-27.
99. Klein A. O., and Vishniac W. (1961) Activity and partial purification of chlorophyllase in aqueous systems. *J Biol Chem.* *236*, 2544-7.
100. Kräutler B. (2003) Chlorophyll breakdown and chlorophyll catabolites. In *The Porphyrin Handbook*, Vol. 13, ed. KM Kadish, KM Smith, R Guilard, pp. 183-209.

101. Kräutler B. and Matile P. (1999) Solving the riddle of chlorophyll breakdown. *Acc Chem Res* 32, 35–43.
102. Krause G. H. (1988) Photoinhibition of photosynthesis. An evaluation of damaging and protective processes. *Physiol Plant.* 74, 566-574.
103. Kreuz K., Tommasini R., and Martinoia E. (1996) Old enzymes for a new job. Herbicide detoxification in plants. *Plant Physiology.* 111, 349–353.
104. Kruse E., Grimm B., Beator J., and Kloppstech K. (1997) Developmental and circadian control of the capacity for σ -aminolevulinic acid synthesis in green barley. *Planta.* 202, 235-241.
105. Kura-Hotta M., Satoh K., and Katoh S. (1987) Relationship between photosynthesis and chlorophyll content during leaf senescence of rice seedlings. *Plant Cell Physiol.* 28, 1321-1329.
106. Kuroki M., Shioi Y., and Sasa T. (1981) Purification and properties of soluble chlorophyllase from tea leaf sprouts. *Plant Cell Physiol.* 22, 717-725.
107. Kusaba M., Ito H., Morita R., Iida S., Sato Y., Fujimoto M., Kawasaki S., Tanaka R., Hirochika H., Nishimura M., and Tanaka A. (2007) Rice NON-YELLOW COLORING1 is involved in light-harvesting complex II and grana degradation during leaf senescence. *Plant Cell.* 19, 1362–1375.
108. Lambers J. W., and Terpstra W. (1985) Inactivation of chlorophyllase by negatively charged plant membrane lipids. *Biochim Biophys Acta.* 831(2), 225-35.
109. Levadoux W. L., Kalmokoff M. L., Pickard M. D., and GrootWassink J. W. D. (1987) Pigment removal from canola oil using chlorophyllase. *J. Am. Oil Chem. Soc.* 64, 139-144.
110. Liao Y., An K., Zhou X., Chen W-J., and Kuai B-K. (2007) AtCLH2, a Typical but Possibly Distinctive Chlorophyllase Gene in Arabidopsis. *Journal of Integrative Plant Biology.* 49(4), 531–539.
111. Lichtenthaler H. K., and Wellburn A. R. (1983) Determination of total carotenoids and chlorophylls a and b of leaf extracts in different solvents. *Biochemical Society Transactions.* 591-603.
112. Lichtenthaler H. K. (1987) Chlorophylls and carotenoids, the pigments of photosynthetic biomembranes. *Methods Enzymol.* 148, 350-382.
113. Lichtenthaler H. K., and Burkart S. (1999) Photosynthesis and high light stress. *Bulg. J. Plant Physiol.* 25(3–4), 3–16.

114. Linn F., Heidmann I., Saedler H., and Meyer P. (1990) Epigenetic changes in the expression of the maize A1 gene in petunia: role of numbers of integrated gene copies and state of methylation. *Mol. Gen. Genet.* 222, 320–336.
115. Liu H., Przybylski R., and Michael Eskin N. A. (1996) Turbidimetric measurement of haze in canola oil by acetone precipitation. *Journal of the American Oil Chemists' Society.* 73, 1557-1560.
116. Loake G. J., Ashby A. M., and Shaw C. H. (1988) Attraction of *Agrobacterium tumefaciens* C58C1 towards sugars involves a highly sensitive chemotaxis system. *J. Gen. Microbiol.* 134, 1427–1432.
117. Mach J. M., Castillo A. R., Hoogstraten R., and Greenberg J. T. (2001) The Arabidopsis accelerated cell death gene ACD2 encodes red chlorophyll catabolite reductase and suppresses the spread of disease symptoms. *Proc. Natl. Acad. Sci.* 98, 771–76.
118. Majumdar S., Ghosh S., Glick B. R., Erwin B., and Dumbrof T. (1991) Activities of chlorophyllase, phosphoenolpyruvate carboxylase and ribulose-1, 5-bisphosphate carboxylase in the primary leaves of soybean during senescence and drought *Physiologia Plantarum.* 81, 473-480.
119. Matile P., Hörtensteiner S., Thomas H., and Kräutler, B. (1996) Chlorophyll breakdown in senescent leaves. *Plant Physiol.* 112, 1403-1409.
120. Matile P., Schellenberg M., and Vicentini F. (1997) Localization of chlorophyllase in the chloroplast envelope. *Planta.* 201, 96-99.
121. Matile P., Hörtensteiner S., and Thomas H. (1999) Chlorophyll degradation. *Annu. Rev. Plant Physiol. Plant Mol. Biol.* 50, 67–95.
122. Mauzerall D., and Granick S. (1956) The occurrence and determination of d-aminolevulinic acid and porphobilinogen in urine. *J. Bio. Chem.* 219, 435-446.
123. McGregor I., Das S., Miki B., Keller W., and Fu P. (1999) Enhancement of chlorophyll clearing in maturing canola seed by overexpressing invertase during seed maturation. “New Horizons for an old crop”, Proceedings of the 10 th International Rapeseed Congress, Canberra, Australia.
124. McFeeters R. F., Chichester C. O., and Whitaker J. R. (1971) Purification and Properties of chlorophyllase from *Ailanthus altissima* (Tree-of-Heaven). *Plant Physiol.* 47(5), 609-618.
125. McFeeters R. F. (1975) Substrate Specificity of Chlorophyllase. *Plant Physiol.* 55(2), 377-381.

126. Michalski T. J., Hunt J. E., Bradshaw C., Wagner A. M., Norris J. R. and Katz J. J. (1988) Enzyme-catalyzed organic syntheses: transesterification reactions of chlorophyll a, bacteriochlorophyll a, and derivatives with chlorophyllase. *J. Amer. Chem. Soc.* *110*, 5888–5891.
127. Mihailovic N., Lazarevic M., Dzeletovic Z., Vuckovic M., and Durdevic M. (1997) Chlorophyllase activity in wheat, *Triticum aestivum* L. leaves during drought and its dependence on the nitrogen ion form applied. *Plant Science.* *129*, 141-146.
128. Mínguez-Mosquera M. I., Gandul-Rojas B., and Gallardo-Guerrero L. (1994) Measurement of chlorophyllase activity in olive fruit (*Olea europaea*). *J Biochem.* *116*(2), 263-8.
129. Mínguez-Mosquera I., and Gallardo-Guerrero L. (1996) Role of Chlorophyllase in chlorophyll metabolism in olives cv. Gordal Ma. *Phytochemistry*, *41*(3), 691-97.
130. Müller T., Moser S., Ongania K-H., Pruz'inska A., Hörtensteiner S., and Kräutler B. (2006) A divergent path of chlorophyll breakdown in the model plant *Arabidopsis thaliana*. *Chem BioChem* *7*, 40–42.
131. Müller P., Li X., and Niyogi K. (2001) Non-photochemical quenching. A response to excess light energy. *Plant Physiol.* *125*, 1558–1566.
132. Murata T., Toda F., Uchino K., and Yakushiji E. (1971) Water-soluble chlorophyll protein of *Brassica oleracea* var. Botrys (cauliflower). *Biochim Biophys Acta.* *245*, 208-215.
133. Murata T., and Murata N. (1971) Water-soluble chlorophyll proteins from *Brassica nigra* and *Lepidium virginicum* L. *Carnegie Inst. Wash. Year Book* *70*, 504-507.
134. Murata T., Itoh R., and Yakushiji E. (1980) Crystallization of water-soluble chlorophyll-proteins from *Lepidium virginicum*. *Biochim Biophys Acta.* *593*(1), 167-70.
135. Murata T., and Ishikawa C. (1981) Chemical, physicochemical and spectrophotometric properties of crystalline chlorophyll-protein complexes from *Lepidium virginicum* L. *Biochim Biophys Acta.* *635*(2), 341-7.
136. Nishio N., and Satoh H. (1997) A water-soluble chlorophyll protein in cauliflower may be identical to BnD22, a drought-induced, 22-kilodalton protein in rapeseed. *Plant Physiol.* *115*(2), 841-6.
137. Niyogi K. K. (1999) Photoprotection revisited: genetic and molecular approaches. *Annu. Rev. Plant Physiol. Plant Mol. Biol.* *50*, 333–359.
138. Niyogi K. K., Shih C., Chow W. S., Pogson B. J., DellaPenna D., and Björkman O. (2001) Photoprotection in a zeaxanthin and lutein-deficient double mutant of *Arabidopsis*. *Photosyn Res.* *67*, 139–145.

139. Oberhuber M., Berghold J., Breuker K., Hörtensteiner S., and Kräutler B. (2003) Breakdown of chlorophyll: A nonenzymatic reaction accounts for the formation of the colorless “nonfluorescent” chlorophyll catabolites. *Proc. Natl. Acad. Sci.* *100*, 6910–15.
140. Ogura N. (1972) Studies on chlorophyllase in tea leaves III. Properties of soluble and insoluble chlorophyllases. *Plant Cell Physiol.* *13*, 971-979.
141. Ougham H., Hörtensteiner S., Armstead I., Donnison I., King I., Thomas H. and Mur L. (2008) The control of chlorophyll catabolism and the status of yellowing as a biomarker of leaf senescence. *Plant Biology.* *10*, 4–14.
142. Okazawa A., Tango L., Itoh Y., Fukusaki E., and Kobayashi A. (2006) Characterization and subcellular localization of chlorophyllase from *Ginkgo biloba*. *Z Naturforsch [C]*. *61(1-2)*, 111-7.
143. Oku T., and Tomita G. (1975) The reversible photoconversion of *Chenopodium* chlorophyll protein and its control by the apoprotein structure. *Plant Cell Physiol.* *16*, 1009-1016.
144. Prasil O., Adir N., and Ohad I (1992) Dynamics of photosystem II: Mechanism of photoinhibition and recovery process. In *Topics in Photosynthesis: The Photosystem Structure, Function and Molecular Biology*, *11*, 295–384.
145. Pfandl E., and Bilger W. (1994) Regulation and possible function of the violaxanthin cycle. *Photosynth Res.* *42*, 89-109.
146. Průžinská A., Anders I., Tanner G., Roca M., and Hörtensteiner S (2003) Chlorophyll breakdown: pheophorbide a oxygenase is a Rieske-type iron-sulfur protein, encoded by the accelerated cell death 1 gene. *Proc. Natl. Acad. Sci.* *100*, 15259–64.
147. Průžinská A., Tanner G., Aubry S., Anders I., and Moser S. (2005) Chlorophyll breakdown in senescent *Arabidopsis* leaves: characterization of chlorophyll catabolites and of chlorophyll catabolic enzymes involved in the de-greening reaction. *Plant Physiol.* *139*, 52–63.
148. Průžinská A., Anders I., Aubry S., Schenk N., Tapernoux-Lüthi E., Müller T., Kräutler B., and Hörtensteiner S. (2007) In vivo participation of red chlorophyll catabolite reductase in chlorophyll breakdown. *Plant Cell.* *19*, 369–387.
149. Purvis A. C. (1980) Sequence of Chloroplast Degreening in Calamondin Fruit as Influenced by Ethylene and AgNO₃. *Plant Physiol.* *66(4)*, 624-627.
150. Purohit S. S. (1982) Monocarpic senescence in *Helianthus annuus* L. Relation of fruit induced senescence, chlorophyll and chlorophyllase activity. *Photosynthetica.* *16*, 542-545.

151. Rammurthy S., and Low N. H. (1995) Effect of possible chlorophyll breakdown products on canola oil stability. *J. Agric. Food Chem.* *43*(6), 1479–1483.
152. Reinbothe C., Satoh H., Alcaraz J. P., and Reinbothe S. (2004) A novel role of water-soluble chlorophyll proteins in the transitory storage of chlorophyllide. *Plant Physiol.* *134*(4), 1355-65.
153. Roca M., and Mínguez-Mosquera M. I. (2003) Involvement of chlorophyllase in chlorophyll metabolism in olive varieties with high and low chlorophyll content. *Physiol Plant.* *117*(4), 459-466.
154. Rodoni S., Mühlecker W., Anderl M., Kräutler B., and Moser D. (1997) Chlorophyll breakdown in senescent chloroplasts. Cleavage of pheophorbide a in two enzymic steps. *Plant Physiol.* *115*, 669–76.
155. Rodri'guez M. T., Gonza'lez M. P., and Linares J. M. (1987) Degradation of chlorophyll and chlorophyllase activity in senescing barley leaves. *J. Plant Physiol.* *129*, 369-374.
156. Sabater B., and Rodriguez M. T. (1978) Control of chlorophyll degradation in detached leaves of barley and oat through effect of kinetin on chlorophyllase levels. *Physiol. Plant.* *43*, 274-276.
157. Samaha H., and Kermasha S. (1997a) Biocatalysis of chlorophyllase in ternary micellar systems using Pheophytins as substrates *Journal of Chemical Technology and Biotechnology.* *68*(3), 315-323.
158. Samaha H., and Kermasha S. (1997b) Biocatalysis of chlorophyllase in ternary micellar system containing Span 85 using purified and oxidized pheophytins as substrates. *Journal Biotechnology.* *55*, 181-191.
159. Sambrook and Russell (2001) *Molecular Cloning: A laboratory manual.*
160. Sambrook J., Fritsch E. F., and Maniatis T. (1989) *Molecular Cloning - A Laboratory Manual, 2nd Edition.* Cold Spring Harbour Laboratory Press, New York.
161. Santos V. C. (2004) Regulation of chlorophyll biosynthesis and degradation by salt stress in sunflower leaves. *Scientia horticulturae.* *103*, 93-99.
162. Satoh H., Nakayama K., and Okada M. (1998) Molecular cloning and functional expression of a water-soluble chlorophyll protein, a putative carrier of chlorophyll molecules in cauliflower. *J Biol Chem.* *273*(46), 30568-75.
163. Satoh H., Uchida A., Nakayama K., and Okada M. (2001) Water-soluble chlorophyll protein in Brassicaceae plants is a stress-induced chlorophyll-binding protein. *Plant Cell Physiol.* *42*(9), 906-11.

164. Satoh H., Zanma A., and Shinashi K. (2002) Molecular cloning and sequence analysis of a water-soluble chlorophyll protein cDNA from Japanese radish. *J. Plant Physiol.* *159*, 325–327.
165. Schenk N., Schelbert S., Kanwischer M., Goldschmidt E. E., Dörmann P., and Hörtensteiner S. (2007) The chlorophyllases AtCLH1 and AtCLH2 are not essential for senescence-related chlorophyll breakdown in *Arabidopsis thaliana*. *FEBS.* *581(28)*, 5517-25.
166. Schelbert S., Aubry S., Burla B., Agne B., Kessler F., Krupinska K., and Hörtensteiner S. (2009) Pheophytin Pheophorbide Hydrolase (Pheophytinase) is involved in chlorophyll breakdown during leaf senescence in *Arabidopsis*. *Plant cell.* *21(3)*, 767-85.
167. Schmidt K., Fufezan C., Krieger-Liszkay A., Satoh H., and Paulsen H. (2003) Recombinant water-soluble chlorophyll protein from *Brassica oleracea* var. botrys binds various chlorophyll derivatives. *Biochemistry.* *42(24)*, 7427-33
168. Scheumann V. V., Schoch S., and Rudiger W. (1999) Chlorophyll b reduction during senescence of barley seedlings. *Planta.* *209(3)*, 364-70.
169. Shemer T. A., Harpaz-Saad S., Belausov E., Lovat N., Krokhn O., Spicer V., Standing G. K., Goldschmidt E. E., and Eyal Y. (2008) Citrus Chlorophyllase dynamics at ethylene-induced fruit color-break: A study of Chlorophyllase expression, posttranslational processing kinetics, and in situ intracellular localization *Plant Physiology.* *148*, 108-118.
170. Shioi Y., Tamai H., and Sasa T. (1980) A simple purification method for the preparation of solubilized chlorophyllase from *Chlorella protothecoides*. *Anal Biochem.* *105(1)*, 74-9.
171. Shioi, Y., Tatsumi, Y. and Shimokawa, K. (1991) Enzymatic degradation of chlorophyll in *Chenopodium album*. *Plant Cell Physiol.* *32*, 87–93.
172. Shimokawa K., and Uchida Y. (1992) A chlorophyllide a degrading enzyme (H₂O₂-DCP requiring) of Citrus unshiu fruits. *J. Japan Soc. Hort. Sci.* *61*, 175–181.
173. Shimokawa K. (1979) Preferential degradation of chlorophyll b in ethylene-treated fruits of ‘Satsuma’ mandarin. *Scientia Hort.* *11*, 253-256.
174. Shimokawa K. (1981) Purification of ethylene-enhanced chlorophyllase from Citrus unshiu fruits. *Agric. Biol. Chem.* *45*, 2357–2359.
175. Shimokawa K. (1982) Hydrophobic chromatographic purification of ethylene-enhanced chlorophyllase from Citrus unshiu fruits. *Phytochemistry.* *21*, 543-545.
176. Shinashi K., Satoh H., Uchida A., Nakayama K., Okada M., and Oonishi I. (2000) Molecular characterization of a water-soluble chlorophyll protein from main veins of Japanese radish. *J. Plant Physiol.* *157*, 255-262.

177. Singh R. D., and Chuaqui C. A. (1991) Development of a continuous process to remove chlorophylls from canola oil. Ninth project report: Research on canola seed oil and meal. pp. 449-472.
178. Smart C. M. (1994) Gene expression during leaf senescence. *New Phytol.* 126, 419–448.
179. Sodergreen E., Gustafsson I. B., Basu S., Nourooz-Zadeh J., Nalsen C., Turpeinen A., Berglund L., and Vessby B. (2001) A diet containing rapeseed oil-based fats does not increase lipid peroxidation in humans when compared to a diet rich in saturated fatty acids. *Eur J Clin Nutr.* 55(11), 922-31.
180. Southern E. M. (1975) Detection of specific sequences among DNA fragments separated by gel electrophoresis. *J. Mol. Biol.* 98, 503-517.
181. Sugiyama K. I., and Murata N. (1978) Analyses of absorption and fluorescence spectra of water-soluble chlorophyll proteins, pigment system II particles and chlorophyll a in diethylether solution by the curve-fitting method. *Biochim Biophys Acta.* 503(1), 107-19.
182. Suzuki T., and Shioi Y. (2002) Re-examination of Mg-dechelation reaction in the degradation of chlorophylls using chlorophyllin a as substrate. *Photosynth. Res.* 74, 217–23.
183. Suzuki N., and Nishioka A. (1993) Behavior of chlorophyll derivatives in canola oil processing. *J. Am. Chem. Soc.* 70, 837–841.
184. Takamiya A., Obata H., Yakushiji E., Kok B., and Jagendorf A. T. (1963) Photosynthetic mechanisms of Green Plants, 1143, 479.
185. Takamiya A., Kamimura Y., Kira A., Shibata K., Takamiya A., Jagendorf A. T., and Fuller R. C. (1968) Comparative Biochemistry and Biophysics of Photosynthesis, University of Tokyo Press, Tokyo. p. 229
186. Takamiya A. (1973) *Carnegie Inst. Wash. Yearbook* 72, 330-336.
187. Takamiya K. I., Tsuchiya T., and Ohta H. (2000) Degradation pathway(s) of chlorophyll: what has gene cloning revealed? *Trends Plant Sci.* 5(10), 426-31.
188. Tamai H., Shioi Y., and Sasa T. (1979) Studies on chlorophyllase of *Chlorella protothecoides* IV. Some properties of the purified enzyme. *Plant Cell Physiol.* 20, 1141-1145.
189. Tanaka K., Kakuno T., Yamashita J., and Horio T. (1982) Purification and properties of chlorophyllase from greened rye seedlings. *J Biochem.* 92(6), 1763-73.
190. Tang L., Okazawa A., Itoh Y., Fukusaki E., and Kobayashi A. (2003) Expression of chlorophyllase is not induced during autumnal yellowing in *Ginkgo biloba* Z. *Naturforsch.* 59c, 415-420.

191. Tautorus C. L., and Low N. H. (1993) Chemical aspects of chlorophyll breakdown products and their relevance to canola oil stability. *J. Am. Oil. Chem. Soc.* *70*, 843-847.
192. Terpstra W. (1978) Chlorophyllase in *Phaeodactylum tricomutum* Photosynthetic Membranes. Extractability, Small-Scale Purification and Molecular Weight Determination by SDS-Gel-Electrophoresis. *Physiol. Plant.* *44*: 329-334.
193. Terpstra W. (1980) Influence of lecithin liposomes on chlorophyllase-catalyzed chlorophyll hydrolysis: comparison of intramembraneous and solubilized *Phaeodactylum* chlorophyllase. *Biochim Biophys Acta.* *600(1)*, 36-47.
194. Terpstra W. (1981) Identification of chlorophyllase as a glycoprotein. *FEBS* *126*, 231-235.
195. Thayer S. S., and Björkman O. (1992) Carotenoid distribution and deepoxidation in thylakoid pigment-protein complexes from cotton leaves and bundle sheath cells of maize. *Photosynth. Res.* *33*, 213-225.
196. Todorov D. T., Karanov E. N., Smith A. R., and Hall M. A. (2003a) Chlorophyllase activity and Chlorophyll contents in wild and mutant plants of *Arabidopsis thaliana*. *Biologia plantarum.* *46 (1)*, 125-127.
197. Trebitsh T., Goldschmidt E. E., and Riov J. (1993) Ethylene induces de novo synthesis of chlorophyllase, a chlorophyll degrading enzyme, in Citrus fruit peel. *Proc Natl Acad Sci* *90*, 9441-9445.
198. Tsang E. W., Yang J., Chang Q., Nowak G., Kolenovsky A., McGregor D. I., and Keller W. A. (2003) Chlorophyll reduction in the seed of *Brassica napus* with a glutamate 1-semialdehyde aminotransferase antisense gene. *Plant Mol Biol.* *51(2)*, 191-201.
199. Tsuchiya T., Ohta H., Masuda T., Mikami B., Kita N., Shioi Y., and Takamiya K. (1997) Purification and characterization of two isozymes of chlorophyllase from mature leaves of *Chenopodium album*. *Plant Cell Physiol.* *38*, 1026-1031.
200. Tsuchiya T., Ohta H., Okawa K., Iwamatsu A., Shimada H., Masuda T., and Takamiya K. (1999) Cloning of chlorophyllase, the key enzyme in chlorophyll degradation: Finding of a lipase motif and the induction by methyl jasmonate *Proc Natl Acad Sci.* *96*, 2615362–15367.
201. Tsuchiya T., Suzuki T., Yamada T., Shimada H., Masuda T., Ohta H., and Takamiya K. (2003) Chlorophyllase as a serine hydrolase: identification of a putative catalytic triad. *Plant Cell Physiol.* *44(1)*, 96-101.
202. Vicentini F., Iten F., and Matile P. (1995) Development of an assay for Mg-dechelatase of oilseed rape cotyledons, using chlorophyllin as the substrate. *Physiol. Plant.* *94*, 57–63.

203. Vicky Buchanan-Wollaston (1997) The molecular biology of leaf senescence. *Journal of Experimental Botany*. 48(2), 181-199.
204. Walters R. G., and Horton P. (1991) Resolution of components of non-photochemical chlorophyll fluorescence quenching in barley leaves. *Photosynth. Res.* 27, 121–133.
205. Wehner A., Storf S., Jahns P., and Schmid V. H. R. (2004) De-epoxidation of violaxanthin in light-harvesting complex I proteins. *J Biol Chem*. 279, 26823–26829.
206. Willstätter R., and Stoll A. (1913) Die Wirkungen der Chlorophyllase. In *Untersuchungen über Chlorophyll*. pp. 172–187. Springer, Berlin.
207. Wüthrich K. L., Bovet L., Hunziker P. E., Donnison I. S., and Hörtensteiner S. (2000) Molecular cloning, functional expression and characterisation of RCCreductase involved in chlorophyll catabolism. *Plant J*. 21, 189–98.
208. Yakushiji E., Uchino K., Sugimura Y., Shiratori I., and Takamiya F. (1963) Isolation of water soluble chlorophyll protein from the leaves of *Chenopodium album*. *Biochim Biophys Acta*. 75, 293-8.
209. Yamauchi N., and Watada A. E. (1991) Regulated chlorophyll degradation in spinach leaves during storage. *J. Am. Soc. Hort. Sci.* 116, 58-62.
210. Yamauchi N., Funamoto Y., and Shigyo M. (2004) Peroxidase-mediated chlorophyll degradation in horticultural crops. *Phytochemistry reviews*. 3(1-2), 221-228.
211. Yan J-B., Wang G-Q., Du P., Zhu D-X., Wang M-W., and Jiang X-Y. (2006) High-level expression and purification of *Escherichia coli* oligopeptidase B. *Protein Expression and Purification*. 47(2), 645-650.
212. Yao N., Eisfelder B. J., Marvin J., and Greenberg J. T. (2004) The mitochondrion - an organelle commonly involved in programmed cell death in *Arabidopsis thaliana*. *Plant J*. 40, 596–610.
213. Yao N., and Greenberg J. T. (2006) *Arabidopsis* ACCELERATED CELL DEATH2 modulates programmed cell death. *Plant Cell*, 18, 397–411.
214. Yi Y., Kermasha S., and Neufeld R. (2006) Characterization of sol-gel entrapped chlorophyllase. *Biotechnol Bioeng*. 95(5), 840-9.
215. Zhou X., Liao Y., Ren G. D., Zhang Y. Y., Chen W. J., and Kuai B. K. (2008) Repression of *AtCLH1* expression results in a decrease in the ratio of chlorophyll a/b but doesnot affect the rate of chlorophyll degradation during leaf senescence. *Zhi Wu Sheng Li Yu Fen Zi Sheng Wu Xue Xue Bao*. 33(6), 596-606.

216. Zhong D., and Zewail A. H. (2001) Femtosecond dynamics of flavoproteins: Charge separation and recombination in riboflavine (vitamin B2)-binding protein and in glucose oxidase enzyme. *Proc. Natl. Acad. Sci.* 98, 11867–11872.

ACKNOWLEDGEMENTS

This work was done at the Department of Plant Physiology, Institute of Biology, Humboldt University, Berlin.

At the outset, I wish to express my profound thanks to my employer and supervisor Prof. Dr. Bernhard Grimm for offering me a research position to conduct my Doctoral thesis work. He has been a great support for me through out my research work. His observations and critical suggestions have paved way into finding new ways to deal with the research.

I am also thankful to Dr. Ulrich Eckhardt, for his valuable guidance during my experimental work and helpful discussions in research related problems. I also extend my thanks for providing me the gene constructs for the generation of transgenic plants.

My sincere thanks to Dr. rer. nat. Thomas Krause and Dr.-Ing. Frank Pudel, Pilot Pflanzenöltechnologie Magdeburg e. V. (PPM) for their valuable suggestions regarding the optimization of different extraction procedures for Chlide recovery process during oil refining.

I am grateful to PD. Dr. Heiko Lokstein, Institute of Biochemistry and Biology/Plant Physiology, University of Potsdam, for his kind help and guidance in planning, conducting and analyzing the results from high light stress experiments on WSCP overexpressor plants. I also thank his students, Stephanie Schlede and Saskia Rheinhardt for carrying out PAM measurements on WSCP overexpressor plants and especially Stephanie for her helpful discussions in interpreting the data.

I would like to thank Mrs. Barbara Hickel for HPLC analysis of plant pigment extracts. I also thank Mrs. Kerstin Träder for her excellent technical assistance during the course of my work. I also acknowledge the technical assistance of Mrs. Alexandra Hackel and Mrs. Renate Kraft during northern blot experiments. Thanks are also due for Mrs. Angelika Pötter without whose help propagation of the transgenic plants would have been very difficult.

I am also very much thankful to Dr. Yvonne Pörs for having spent her valuable time on analysis of Chlase overexpressor plants.

I extend my sincere thanks to the Institute of Molecular Biophysics for providing me space to conduct my radioactivity experiments and using phosphoimager.

I express my gratitude to Prof. Hiroyuki Satoh, Department of Biomolecular science, Toho University, Chiba, Japan for providing me the gene construct of *Cau-WSCP* for *E. coli* expression studies and also for the anti-WSCP antibody.

My warm thanks to all the staff at Department of plant physiology, who have created a friendly milieu in the group and have supported me in so many ways. I am particularly grateful for Dieter Hackenberg, Enrico Peter, Immo Rheinhardt, Olaf Czarnecki, Hagen Schlicke, Hongxia He, Izabella Chincinska, Yangfang Wu, Angelika Mustroph, Undine Krügel and Maxi Rothbart for making my stay very memorable. My warmest thanks are due for Hye-Jung Lee, for her sisterly affection.

My special thanks to Mrs. Susanne El-Badawi secretary to Prof. Grimm and Mrs. Frauke Weiss (former secretary) and for helping me to get over all the bureaucracy matters.

I would like to thank Dr. Boris Hedtke, Dr. Ali Alawady and PD. Dr. Christina Kühn for their valuable suggestions in the need of hour.

I am indebted to various funding agencies like BMBF, NaFöG, Humboldt Innovation and DFG for providing me the financial help for my subsistence during my research period.

Friends have always been my strength and it is a delight to acknowledge all those who have been with me for various periods of time. I take this opportunity to acknowledge one and all.

Finally, my fondest appreciations go to my parents, brother, and husband. It is their love and encouragement for what I am today.

SELBSTÄNDIGKEITSERKLÄRUNG

Hiermit erkläre ich, die vorliegende Arbeit selbständig ohne fremde Hilfe verfasst zu haben und nur die angegebene Literatur verwendet zu haben.

Ich besitze keinen entsprechenden Doktorgrad und habe mich anderwärts nicht um einen Doktorgrad beworben.

Die dem Promotionsverfahren zugrunde liegende Promotionsordnung vom 01.10.2003 ist mir bekannt.

Sridevi Damaraju

20.12.2009.